

# Development of oleophilic membranes for VOC/N<sub>2</sub> separation

by

Xuezhen Wang

A thesis  
presented to the University of Waterloo  
in fulfillment of the  
thesis requirement for the degree of  
Doctor of Philosophy  
in  
Chemical Engineering

Waterloo, Ontario, Canada, 2021

©Xuezhen Wang 2021

## **Author's Declaration**

I hereby declare that I am the sole author of this thesis. This is a true copy of the thesis, including any required final revisions, as accepted by my examiners.

I understand that my thesis may be made electronically available to the public.

## Abstract

Volatile organic compounds (VOCs) are the foremost hazardous pollutants in the air. VOC emissions have significant effects on the environment and human health. Membrane separation, as an excellent technology for VOC removal and recovery, has advantages in low energy consumption, compact size, and easy operation. The membranes with efficient separation performance are required for the membrane separation process. This study focuses on developing the oleophilic membrane on VOC/N<sub>2</sub> separation. 15 VOCs such as MTBE, acetone, DMC, methanol, ethanol, propanol, butanol, pentane, hexane, cyclohexane, isooctane, heptane, benzene, toluene, and xylene were selected for membrane performance evaluation.

The oleo gel membrane was developed by immobilizing bis (2-ethylhexyl) phthalate (DEHP) oil in the PEBA matrix. Multiple PEBA/DEHP oleo gel membranes were prepared, and the content of DEHP in the membranes varied from 15 to 75wt.%. The properties of the prepared PEBA/DEHP oleo gel membrane were comprehensively investigated. The physical properties, structures, and morphologies of the PEBA/DEHP membranes were characterized by Fourier-transform infrared spectroscopy (FTIR), differential scanning calorimeter (DSC), thermogravimetric analysis (TGA), and scanning electron microscope (SEM). The gas permeation properties of the prepared PEBA/DEHP membranes were also investigated. DEHP content in the membranes was demonstrated to have significant effects on their VOC permeabilities and VOC/N<sub>2</sub> selectivities, and the prepared membranes showed significantly higher VOC permeabilities than the traditional PEBA membrane in binary VOC/N<sub>2</sub> separation test. The effects of feed VOC concentration and operating temperature on the VOC/N<sub>2</sub> separation performance of the PEBA/DEHP membranes were evaluated with selected VOCs. The membrane showed excellent VOC/N<sub>2</sub> separation performance under all conditions with good stability.

Furthermore, the bis (2-ethylhexyl) adipate (DEHA) oil, of which the VOC solubility is higher than that of DEHP oil, was adopted to improve the VOC permeability of the oleo gel membrane. Newly developed PEBA/DEHA membrane showed drastic VOC/N<sub>2</sub> performance improvement compared to the PEBA membrane and previously reported PEBA/DEHP oleo gel membranes. The VOC permeability in the membrane was found to follow the miscible blending rules, which enable the acquirement of VOC permeability of the oil by calculation. The effects of feed VOC concentration and operating temperature on membrane VOC/N<sub>2</sub> separation performance were comprehensively investigated on various VOCs. Semi-empirical correlations were developed to relate the membrane VOC permeability to operation parameters, which include feed VOC composition and operating

pressures. PEBA/DEHA oleo gel membrane showed excellent VOC permeability and VOC/N<sub>2</sub> selectivity under all testing conditions. And the effect of the operation condition of the high VOC concentration and high temperature on the VOC/N<sub>2</sub> separation performance of PEBA/DEHA oleo gel membrane was less than the pristine PEBA membrane. The membrane was stable during the 35 days test under various conditions.

Another new oleo gel membrane (OLGM) was developed by gelling the DEHA oil in the crosslinked poly dimethyl siloxane (PDMS) matrix. A series of dense membranes were successfully fabricated. PDMS, as the "oil holder", differs from the PEBA in its adjustable and manipulated crosslinking degree. The effects of the crosslinked degree of the PDMS on the content of the oil immobilized in the membrane and membrane VOC/N<sub>2</sub> separation performance were investigated. The VOC permeability of the PDMS/DEHA membrane was further improved than the PEBA/DEHA membrane, which is attributed to the better VOC permeabilities in the PDMS than the PEBA. The systematic assessments of membrane separation performance on VOC/N<sub>2</sub> were performed with respect to temperature and feed VOC concentration. The VOC permeation in the membrane was proved to follow the sorption-diffusion mechanism. The membrane showed significantly higher VOC permeability and VOC/N<sub>2</sub> selectivity than the traditional PDMS membrane and the other previously reported OLGMs.

In the end, two types of the supported liquid membrane were developed in this work for VOC/N<sub>2</sub> separation. One is the silicone oil (SO) based supported liquid membrane, which was made by using SO to wet the surface of the Polysulfone (PS) membrane. The as-prepared membranes showed good stability when using pure gas as the feed at elevated pressure. And its VOC/N<sub>2</sub> selectivity was higher compared to silicone rubber membranes for VOCs selected from the alcohol group. However, the membrane was unstable in certain VOCs (e.g., DMC, benzene, hexane), which could be attributed to the instability of PS in specific VOCs, and the instability of PS further weakens the immobilization of SO in the pores of the PS membrane. The other type of membrane, supported PDMS/SO oleo gel membrane, was further developed to improve the stability of the membrane in a variable VOCs environment. The PDMS/SO oleo gel was reinforced in the PTFE membrane substrate, which was believed to have better chemical resistance than the PS membrane. It should be noted that the intrinsic property of the PDMS/SO oleo gel on VOC/N<sub>2</sub> separation performance was investigated by testing the PDMS/SO oleo gel membranes (OLGMs) preprepared at different PDMS/SO weight ratios. The experiment results showed that the membranes had better VOC/N<sub>2</sub> perm-selectivity than the pristine PDMS. After that, the supported PDMS/SO oleo gel membrane showed competitive VOC/N<sub>2</sub>

separation performance to pristine PDMS, and the membrane was demonstrated stable in a long-term test for over 100 hours.

## Acknowledgements

I would like to express my sincere appreciation to my supervisor, Prof. Xianshe Feng, for giving me a great opportunity to study at the University of Waterloo. His diligent guidance and advice are like the light in the dark and encourage me to overcome the difficulties in my PhD study. His generous support is invaluable to me to pass the courses, design the experiments, and prepare the thesis. His passion for research will continue to inspire me on the research road in the future.

I would also like to thank all the members of the Membrane Research Lab in the Department of Chemical Engineering, the University of Waterloo, for their help and friendship in my PhD study. Special thanks are given to my former colleagues at Membrane Technology and Research, Inc (MTR), US, and my current colleagues at Imtex Membranes, Corp (Imtex), Canada, for their mentoring and friendship over the past years.

I would like to sincerely thank my PhD Thesis Examination Committee members, Prof. Christopher Lan, Prof. John Wen, Prof. Boxin Zhao, and Prof. Leonardo Simon, who have provided valuable suggestions regarding my research.

I would also like to extend my sincere gratitude to the University of Waterloo for providing the research scholar for the whole duration of my PhD study. The financial support by the Natural Science and Engineering Research Council (NSERC) of Canada is acknowledged here. My thanks also go to all the staff in the Department of Chemical Engineering, who have helped me in material characterization, laboratory services and administrative matters.

Last but not least, my appreciation also goes to my parents and friends for their companion, love, encouragement, and support. Hope there will be a place where the people I miss are together!

## Table of Contents

Author's Declaration .....	ii
Abstract .....	iii
Acknowledgements .....	vi
List of Figures .....	x
List of Tables.....	xvi
Chapter 1 Introduction.....	1
1.1 Background .....	1
1.2 Research objective.....	4
1.3 Scope of the thesis .....	5
Chapter 2 Literature review .....	8
2.1 Background of VOC emissions .....	8
2.2 VOC treatment technology .....	10
2.2.1 VOC destruction.....	11
2.2.2 VOC recovery.....	11
2.3 Gas transport in the membrane .....	13
2.3.1 Mechanism of gas permeation.....	13
2.3.2 Gas transport in the composite membrane .....	18
2.3.3 VOC and nitrogen permeation in the membrane .....	19
2.4 The membrane used in VOC treatment .....	22
2.4.1 Rubbery polymeric membrane .....	22
2.4.2 Glassy polymeric membrane .....	25
2.4.3 Supported ionic liquid membrane.....	26
2.5 Membrane vapor/gas separation process.....	27
Chapter 3 PEBA/DEHP oleo gel membrane for VOC/N <sub>2</sub> separation .....	30
3.1 Introduction .....	30
3.2 Experiment .....	32
3.2.1 Material .....	32
3.2.2 Membrane preparation.....	32
3.2.3 Membrane characterization .....	32
3.2.4 Permeation experiment.....	33
3.2.5 Pure gas permeance measurement.....	34
3.2.6 VOC/N <sub>2</sub> separation performance characterization .....	34
3.3 Results and discussion.....	35

3.3.1 Characterization of oil content in the membrane .....	35
3.3.2 Physical properties of OLGMs .....	38
3.3.3 Morphology studies of OLGm .....	42
3.3.4 Mechanical property study .....	43
3.3.5 Effect of oil content in the membrane on gas permeation .....	45
3.3.6 Effect of VOC concentration on VOCs permeation .....	50
3.3.7 Effect of temperature on VOCs permeation.....	54
3.3.8 Membrane stability .....	58
3.4 Conclusion .....	58
Chapter 4 PEBA/DEHA oleo gel membrane for VOC/N <sub>2</sub> Separation.....	60
4.1 Introduction.....	60
4.2 Experiment.....	61
4.2.1 Material .....	61
4.2.2 Membrane preparation .....	62
4.2.3 Permeation experiment .....	62
4.2.4 Gas permeance measurement.....	62
4.2.5 VOC/N <sub>2</sub> separation performance characterization.....	62
4.3 Result and discussion.....	63
4.3.1 Characterization of oil content in the membrane .....	63
4.3.2 Gas permeation properties in the membrane.....	65
4.3.3 Effect of VOC concentration .....	72
4.3.4 Effect of temperature .....	83
4.3.5 Membrane stability .....	89
4.4 Conclusion .....	89
Chapter 5 PDMS/DEHA oleo gel membrane for VOC/N <sub>2</sub> separation.....	91
5.1 Introduction.....	91
5.2 Experiment.....	92
5.2.1 Material .....	92
5.2.2 Membrane preparation .....	92
5.2.3 Contact angle, SEM, microscope, and mechanical properties .....	93
5.2.4 Permeation experiment .....	93
5.2.5 Nitrogen permeance measurement.....	94
5.2.6 VOC/N <sub>2</sub> separation performance characterization.....	94
5.3 Result and discussion.....	94



5.3.1 Membrane characterization .....	95
5.3.2 Effect of oil content in membranes on gas permeation .....	101
5.3.3 Effect of oil content in membranes on VOC permeation .....	102
5.3.4 Effects of base/curing ratio (A: B) on vapor permeation .....	106
5.3.5 Effect of feed VOC concentration .....	109
5.3.6 Effect of temperature .....	116
5.3.7 Membrane stability .....	121
5.4 Conclusion .....	122
Chapter 6 Supported liquid membrane for VOC/N <sub>2</sub> separation .....	123
6.1 Introduction .....	123
6.2 Experiment .....	125
6.2.1 Materials .....	125
6.2.2 Membrane preparation .....	125
6.2.3 Membrane characterization .....	127
6.2.4 Permeation experiment .....	127
6.3 Result and discussion .....	127
6.3.1 SO based supported liquid membrane .....	127
6.3.2 PDMS/SO oleo gel membrane .....	135
6.3.3 PDMS/SO based supported oleo gel membrane .....	148
6.4 Conclusion .....	153
Chapter 7 General conclusion, contributions and recommendations .....	155
7.1 General conclusions and contributions .....	155
7.2 Recommendations for future work .....	156
7.2.1 Investigation of VOC diffusivity and solubility in the membrane .....	156
7.2.2 Development of supported oleo gel membrane .....	157
7.2.3 Development of oleo gel hollow fiber membranes .....	157
7.2.4 Separation at the high stage cut (recovery) .....	158
Bibliography .....	159
Appendix A Sample calculation .....	166
A.1 Sample calculations for pure gas permeation .....	166
A.2 Sample calculations for mixed gas permeation .....	167
A.3 Sample calculations for experimental errors .....	168

## List of Figures

<b>Figure 1.1</b> Thesis structure in term of chapters and content relevance .....	7
<b>Figure 2.1</b> Oil and gas production compared to emissions of VOCs, NO <sub>x</sub> , and greenhouse gases from the petroleum and natural gas supply chains (2002–2011); all data were normalized to 2002 levels [9]. .....	9
<b>Figure 2.2</b> A schematic overview of VOC in the troposphere [12]. .....	10
<b>Figure 2.3</b> Classification of VOC control techniques [13]. .....	11
<b>Figure 2.4</b> Operation condition of various techniques for recovering VOCs [18]. .....	12
<b>Figure 2.5</b> Schematic diagram of gas permeation in the porous membrane. ....	14
<b>Figure 2.6</b> Schematic diagram of gas permeation in the non-porous membrane by sorption diffusion mechanism. ....	16
<b>Figure 2.7</b> Gas permeation in the composite membrane [2]. .....	18
<b>Figure 2.8</b> Permeability and selectivity for toluene in various rubber membranes [7]. .....	23
<b>Figure 2.9</b> A hybrid membrane process to recover propylene in propylene/nitrogen mixture from vent line in polypropylene plant [2]. .....	27
<b>Figure 2.10</b> A hybrid membrane process to remove the VOC from the off-gas [51]. .....	28
<b>Figure 3.1</b> Schematic diagram of the experimental setup used for the VOC permeability test. (1) nitrogen cylinder, (2) mass flow controller, (3) VOC liquid reservoir, (4) porous gas diffuser, (5) thermal bath, (6) pressure gauge, (7) vapor/gas mixer, (8) water bath, (9) membrane cell, (10) bubble flow meter, (11) temperature gauge, (12) vacuum pressure gauge, (13) cold trap, (14) vacuum pump. .....	33
<b>Figure 3.2</b> The content of PEBA and DEHP in the membrane casting solution (wt.%) vs. the content of PEBA and DEHP in the membrane (wt.%); membranes are named as PEBA/DEHP content in the membrane and labeled on the left of the Figure. ....	35
<b>Figure 3.3</b> Image of transparent membranes: (A) PEBA, (B) 85PEBA/15DEHP, (C) 75PEBA/25DEHP, (D) 50PEBA/50DEHP, (E) 26PEBA/74DEHP and (F) 17PEBA/83DEHP.....	36
<b>Figure 3.4</b> FTIR spectra of PEBA/DEHP oleo gel membranes. ....	37
<b>Figure 3.5</b> DSC measurement on PEBA/DEHP OLGMs. (A) DSC thermograms: (a) PEBA, (b) 85PEBA/15DEHP, (c) 75PEBA/25DEHP, (d) 50PEBA/50DEHP (e) 26PEBA/74DEHP and (f) 17PEBA/83DEHP; (B) The crystallinities of PA in OLGMs. ....	39
<b>Figure 3.6</b> Thermal property analysis of the OLGMs. (A) thermogravimetric analysis(TGA) curves, (B) derivative thermogravimetric (DTG) curves. ....	40

<b>Figure 3.7</b> The cross-section SEM image of PEBA/DEHP OLGMs. (A) PEBA, (B) 85PEBA/15DEHP, (C) 75PEBA/25DEHP, (D) 50PEBA/50DEHP, (E) 26PEBA/74DEHP, and (F) 17 PEBA/83DEHP. ....	42
<b>Figure 3.8</b> Mechanical properties of the PEBA/DEHP OLGMs. ....	43
<b>Figure 3.9</b> The effect of DEHP content in the membrane on pure gas perm-selectivity. (A) Gas permeability vs. DEHP content, (B) Gas/N <sub>2</sub> selectivity vs. DEHP content. ....	45
<b>Figure 3.10</b> The effect of DEHA content in the membrane on the VOC permeability of the membrane. (A) fuels additives, (B) alcohols, (C) paraffin, (D) aromatic compounds. ....	46
<b>Figure 3.11</b> The effect of DEHP content in the membrane on VOC/N <sub>2</sub> selectivity of the membrane. (A) fuel additives, (B) alcohols, (C) paraffin, (D) aromatic compounds. ....	48
<b>Figure 3.12</b> Effect relative vapor pressure ( $P/P^0$ ) on VOC permeability. VOCs permeabilities of 26PEAB/74DEHP membrane are in solid line, VOCs are (A) alcohols and (C) paraffin. VOCs permeabilities of PEBA membrane are in the dashed line, VOCs are (B) alcohols and (D) paraffin. .	50
<b>Figure 3.13</b> Permeate flux of VOC vs feed VOC concentration, (A) alcohols, and (B) paraffin. ....	52
<b>Figure 3.14</b> Permeate VOC concentration vs feed VOC concentration, (A) alcohols, and (B) paraffin. ....	53
<b>Figure 3.15</b> Effect of temperature ( $1000/T$ ) on VOC permeability. VOCs permeabilities of 26PEBA/74DEHPmembrane are in solid line, VOCs are (A) alcohols and (C) paraffin. VOCs permeabilities of PEBA membrane are in the dashed line, VOCs are (B) alcohols and (D) paraffin. .	54
<b>Figure 3.16</b> Effect of temperature ( $1000/T$ ) on N <sub>2</sub> permeability. The solid line is for the 26PEBA/74DEHPmembrane, and the dashed line is for the PEBA membrane. ....	56
<b>Figure 3.17</b> Effect of temperature ( $1000/T$ ) on VOC/N <sub>2</sub> selectivity. VOC/N <sub>2</sub> selectivity of 26PEBA/74DEHPmembrane is in solid line, VOCs are (A) alcohols and (C) paraffin. VOC/N <sub>2</sub> selectivity of PEBA membrane are in the dashed line, VOCs are (B) alcohols and (D) paraffin. ....	57
<b>Figure 3.18</b> Pure gas permeability of 26PEBA/74DEHP membrane. ....	58
<b>Figure 4.1</b> The content of PEBA and DEHA in the membrane casting solution and membranes; PEBA and DEHA content in the membrane are used to name membranes, and names were labeled on the left side of the Figure. ....	63
<b>Figure 4.2</b> FTIR spectra of PEBA/DEHA oleo gel membranes. (a) PEBA, (b)73PEBA/27DEHA, (c) 40PEBA/60DEHA, (d) 25PEBA/75DEHA and (e) DEHA oil. ....	64
<b>Figure 4.3</b> The effect of DEHA content in the membrane on pure gas perm-selectivity. (A) permeability vs. DEHA content, (B) Gas/N <sub>2</sub> selectivity (pure gas permeability ratio) vs. DEHA content. ....	65

<b>Figure 4.4</b> Pure gas permeability of membranes vs. critical temperature of gases. The pure gas permeability of 26PEBA/74DEHP is from Chapter 3. ....	66
<b>Figure 4.5</b> The effect of DEHA oil volumetric content on VOC permeability in the membrane (A) fuel additives, (B) alcohols, (C) paraffin, (D) aromatic compounds.....	68
<b>Figure 4.6</b> VOC permeability vs. critical temperature of VOCs. VOC permeabilities of 26PEBA /74DEHP membrane are from Chapter 3. ....	71
<b>Figure 4.7</b> VOC permeate flux vs. feed VOC concentration. (A) fuel additives, (B) alcohols, (C) paraffin, and (D) aromatic compounds. ....	72
<b>Figure 4.8</b> VOC permeability vs. feed VOC concentration. (A) fuel additives, (B) alcohols, (C) paraffin, (D) aromatic compounds. The solid lines are obtained from the equation correlation, and the symbols are experimental data. ....	75
<b>Figure 4.9</b> Permeate VOC concentration vs. feed VOC concentration. (A) fuel additives, (B) alcohols, (C) paraffin, and (D) aromatic compounds.....	76
<b>Figure 4.10</b> VOC permeability comparison between 25PEBA/75DEHA and PEBA membranes. $P/P^0$ (VOC relative volatility) is defined as VOC vapor pressure to its saturation vapor pressure. Fuel additives: (A)&(B); Alcohols:(C)&(D); Paraffins:(E)&(F); Aromatic compounds:(G)&(H). ....	77
<b>Figure 4.11</b> $N_2$ permeability in 25PEBA/75DEHA and PEBA membranes. $P/P^0$ is VOC relative pressure. ....	80
<b>Figure 4.12</b> VOC/ $N_2$ comparison between 25PEBA/75DEHA and PEBA membranes. $P/P^0$ is VOC relative volatility. Fuel additives: (A)&(B); Alcohols:(C)&(D); Paraffins:(E)&(F); Aromatic compounds:(G)&(H). ....	82
<b>Figure 4.13</b> Effect of temperature ( $1000/T$ ) on VOC permeability. VOCs permeabilities of 25PEAB/75DEHA membrane and PEBA membrane are in solid line and dashed line, respectively. Fuel additives: (A)&(B); Alcohols:(C)&(D); Paraffins:(E)&(F); Aromatic compounds:(G)&(H). ....	85
<b>Figure 4.14</b> $N_2$ Permeability at different temperatures. ....	86
<b>Figure 4.15</b> Effect of temperature ( $1000/T$ ) on VOC/ $N_2$ selectivity. VOC/ $N_2$ selectivity of 25PEAB/75DEHA membrane and PEBA membrane are in solid line and dashed line, respectively. Fuel additives: (A)&(B); Alcohols:(C)&(D); Paraffin:(E)&(F); Aromatic compounds:(G)&(H). ....	88
<b>Figure 4.16</b> Membrane stability evaluation by measuring the pure gas performance of the membrane in the 60 days. ....	89
<b>Figure 5.1</b> Schematic diagram of DEHA oil randomly dispersed in the PDMS matrix. ....	94
<b>Figure 5.2</b> Image of standard crosslinked PDMS/DEHA membranes and the papers underneath: (A) PDMS(SC), (B) PDMS(SC)-95/DEHA-5, (C) PDMS(SC)-90/DEHA-10, (D) PDMS(SC)-75/DEHA-25, (E) PDMS(SC)-60/DEHA-40. ....	95

**Figure 5.3** Membrane surface image scanned under Microscopic: (A) PDMS(SC), (B) PDMS(SC)-90/DEHA-10, (C) PDMS(SC)-75/DEHA-25, (D) PDMS(SC)-60/DEHA-40(non-dripping area), (E) PDMS(SC)-60/DEHA-40(dripping area), (F) enlarged scan of the DEHA liquid droplet on image (E). ..... 96

**Figure 5.4** (A) membrane weight loss after oil removal vs. DEHA content in PDMS/DEHA mixture in the membrane casting solution. (B) DEHA oil content in the membrane vs. DEHA content in PDMS/DEHA mixture in the membrane casting solution. The membrane weight loss after oil removal is normalized by the initial membrane weight before oil removal. .... 98

**Figure 5.5** FTIR spectra of PDMS and PDMS/DEHA OLGMs. The blue dash line indicates the peaks from the PDMS, and the black dash line shows the peaks from the DEHA. .... 99

**Figure 5.6** Mechanical properties of the PDMS/DEHA OLGMs..... 100

**Figure 5.7** The effect of DEHA oil content in the standard cross-linked OLGMs on pure gas permeability and pure gas permeability ratio (selectivity). .... 101

**Figure 5.8** The effect of DEHA content in the standard cross-linked membrane on membrane VOC permeability. (A) fuel additives, (B) alcohols, (C) paraffin, (D) aromatic compounds. Top X-axis: DEHA oil content is in wt.%. Bottom X-axis: DEHA oil content is in vol%. .... 102

**Figure 5.9** The VOC permeability of PDMS and DEHA. The VOC permeabilities of PDMS (curve fitting) and DEHA oil (curve fitting) were generated from the maxwell equation correlation. The VOC permeabilities of the PDMS (experiment) were measured in work. The VOC permeabilities of DEHA oil (reported) were generated from the miscible blending equation and reported in Chapter 4. .... 105

**Figure 5.10** Membrane perm selectivity vs VOC critical temperature. ■ : membrane PDMS(SC)-60/DEHA-40; ● : membrane PDMS(LC)-60/DEHA-40..... 107

**Figure 5.11** VOC permeability comparison among the membranes. The data of PDMS and PDMS(SC)-60/DEHA-40 are from this work. The data of PEBA and PEBA-25/DEHA-75 are from Chapter 4. .... 108

**Figure 5.12** SEM images of membrane PDMS(SC)-60/DEHA-40. (A) Cross-section, (B) Enlarged cross-section. .... 109

**Figure 5.13** VOC permeate flux vs feed VOC concentration. (A) fuel additives, (B) alcohols, (C) paraffin, (D) aromatic compounds. .... 110

**Figure 5.14** The relationship of Parameters (  $D_{00}$  ) and (  $\phi_{\omega}$  ) to mole volume and critical temperatures of the VOCs. Four types of VOCs are color-coded, as shown in above Figure and Table 5.4. .... 112

<b>Figure 5.15</b> VOC permeability vs. feed VOC concentration. (A) fuel additives, (B) alcohols, (C) paraffin, (D) aromatic compounds. The solid lines are obtained from the equation correlation. The symbols are experimental data. ....	114
<b>Figure 5.16</b> Permeate VOC concentration vs. feed VOC concentration. (A) fuel additives, (B) alcohols, (C) paraffin, (D) aromatic compounds. ....	115
<b>Figure 5.17</b> Permeability of VOCs vs. 1000/T. (A) fuel additives, (B) alcohols, (C) paraffin, (D) aromatic compounds. ....	117
<b>Figure 5.18</b> N <sub>2</sub> Permeability at different temperatures. ....	118
<b>Figure 5.19</b> VOC/N <sub>2</sub> selectivity vs. 1000/T. (A) fuel additives, (B) alcohols, (C) paraffin, (D) aromatic compounds. ....	120
<b>Figure 5.20</b> Membrane stability evaluation by measuring the pure gas performance of the membrane in the 60 days. ....	121
<b>Figure 6.1</b> The process of making SO based supported liquid membrane. ....	125
<b>Figure 6.2</b> Schematic diagram of SO-based supported liquid membrane: (A) oil-filled membrane; (B) membrane under the gas flow. ....	128
<b>Figure 6.3</b> The surface SEM image of PS membrane (image A and B) and SO-based supported liquid membrane (image C & D), which was scanned at different magnification: (A) and (C) were at 22KX; (C) and (D) were at 115KX. ....	129
<b>Figure 6.4</b> The cross-section SEM image of PS membrane (image A, B &C) and SO-based supported liquid membrane (image D, E & F), which was scanned at different magnification: (A) and (D) were at 500X; (B) and (E) were at 1500X;(C) and (F) were at 20,000X.....	130
<b>Figure 6.5</b> SEM-EDX analysis performed on the cross-section of PS membrane. The SEM image with the EDX scanning area is on the left, and the corresponding EDX spectra are on the right hand. (A)PS membrane and (B) SO-based supported liquid membrane. EDX analysis was performed at an accelerating voltage of 20.0 kV using a silicon drift detector.....	131
<b>Figure 6.6</b> Pure gas permeance of SO based supported liquid membrane. ....	132
<b>Figure 6.7</b> The stability of SO-supported liquid membrane in long-term VOCs permeation test. ...	134
<b>Figure 6.8</b> The image of PDMS/SO oleo gel membrane. (A) PDMS, (B) PDMS-90/SO-10, (C) PDMS-75/SO-25, (D) PDMS-60/SO-40.....	135
<b>Figure 6.9</b> Microscopic images of SO oleo gel membrane at different magnifications. PDMS-90/SO-10 membrane:(A) and (D); PDMS-75/SO-25 membrane:(B) and (E); PDMS-60/SO-40 membrane: (C) and (F). ....	136
<b>Figure 6.10</b> The cross-section SEM image of PDMS/SO OLGs: (A) PDMS, (B) PDMS-90/SO-10, (C) PDMS-75/SO-25 and (D) PDMS-60/SO-40. ....	137

<b>Figure 6.11</b> (A) The membrane weight vs. SO content in PDMS/SO mixture in the membrane casting solution. (B) SO content in the membrane vs. SO content in PDMS/SO mixture in the membrane casting solution. The membrane weight in Figure (A) is the membrane weight after oil removal on the membrane surface to the membrane weight before oil removal.....	138
<b>Figure 6.12</b> Mechanical properties of PDMS/SO OLGMs. ....	139
<b>Figure 6.13</b> The effect of SO content on membrane perm-selectivity.....	140
<b>Figure 6.14</b> The effect of SO content in the membrane on VOCs permeability of the membrane. (A) fuel additives, (B) alcohols, (C) paraffin, (D) aromatic compounds. ....	141
<b>Figure 6.15</b> VOC permeate flux vs feed VOC concentration. (A) fuel additives, (B) alcohols, (C) paraffin, (D) aromatic compounds. ....	142
<b>Figure 6.16</b> Relationship between parameters and VOC physical properties. (A) parameters ( $D_0/\phi$ ) - critical temperature of VOCs, (B) parameters ( $\phi\omega$ ) -boiling points.....	145
<b>Figure 6.17</b> VOC permeability vs. feed VOC concentration. (A) fuel additives, (B) alcohols, (C) paraffin, (D) aromatic compounds. ....	146
<b>Figure 6.18</b> Permeate VOC concentration vs feed VOC concentration. (A) fuel additives, (B) alcohols, (C) paraffin, (D) aromatic compounds.....	147
<b>Figure 6.19</b> The pure gas permeability of PDMS-75/SO-25 membrane measured over 27 days. ....	148
<b>Figure 6.20</b> The schematic diagram of the PDMS/SO supported oleo gel membrane. ....	149
Figure 6.21 The surface SEM image of PTFE membrane (image A and B) and PDMS-50/SO-50 supported oleo gel membrane (image C & D), which was scanned at different magnification: (A) and (C) were at 500X; (B) and (D) were at 3000X. ....	150
Figure 6.22 The cross-section SEM image of PTFE membrane (image A and B ) and PDMS-50/SO-50 supported oleo gel membrane (image C and D), which was scanned at different magnification: (A) and (C) were at 200X; (B) and (D) were at 20,000X. ....	151
<b>Figure 6.23</b> The comparison of VOC/N <sub>2</sub> separation performance between SO-SOLGM (supported oleo gel membrane) and PDMS dense membrane. The comparison is in terms of VOC/N <sub>2</sub> selectivity vs VOCs' critical temperature. VOCs in different categories are labeled with different colors: fuel additive-black, alcohol-orange, paraffin-green, aromatic-blue. ■ PDMS dense membrane; ● : PDMS-50/SO-50 supported oleo gel membrane (SO-SOLGM). ....	152
<b>Figure 6.24</b> The stability of PDMS-50/SO-50 supported oleo gel membrane. ....	153

## List of Tables

Table 1.1 Milestone of the membrane applications on gas separation [2].	2
<b>Table 2.1</b> Comparison of techniques of VOC recovery	13
<b>Table 2.2</b> Properties of VOCs and nitrogen [23].	21
<b>Table 2.3</b> Polymer composition in different PEBAAs [31].	24
<b>Table 2.4</b> Glassy polymer used for VOC permeation.	26
<b>Table 3.1</b> Results of thermal analysis for OLGMs.	41
<b>Table 3.2</b> Membrane performance in the literature.	49
<b>Table 3.3</b> Saturated vapor pressure at 22°C and molar volume of VOCs at STP.	51
<b>Table 3.4</b> Activation energy for permeation of VOC and N <sub>2</sub>	56
<b>Table 4.1</b> Solubility parameters for components in the membrane and VOCs.	69
<b>Table 4.2</b> Parameters from the correlation between permeate VOC flux and the feed VOC concentration.	73
<b>Table 4.3</b> Saturated vapor pressure at 22°C and molar volume of VOCs at STP.	79
<b>Table 4.4</b> Feed VOC concentrations in feed stream with binary VOC/N <sub>2</sub> .	83
<b>Table 4.5</b> Activation energy for permeation of VOC and N <sub>2</sub> .	87
<b>Table 5.1</b> The composition of the membrane casting solution.	93
<b>Table 5.2</b> fitting coefficient in maxwell equation correlation.	104
<b>Table 5.3</b> Parameters from the correlation between permeate VOC flux and the feed VOC concentration.	111
<b>Table 5.4</b> The supplementary table for Figure 5.14.	113
<b>Table 5.5</b> Feed VOC concentrations used in determining temperature effects on VOC/N <sub>2</sub> separation performance of the membrane.	116
<b>Table 5.6</b> Activation energy for permeation of VOC and N <sub>2</sub>	119
<b>Table 6.1</b> The composition of the membrane casting solution.	126
<b>Table 6.2</b> The composition of the membrane casting solution.	127
<b>Table 6.3</b> pure gas separation performance of SO based supported liquid membrane.	132
<b>Table 6.4</b> VOCs/N <sub>2</sub> selectivity of SO-based supported liquid membrane vs. PDMS membrane.	133
<b>Table 6.5</b> Parameters from the correlation between the permeate VOC flux and the feed VOC concentration.	143
Table 6.6 Mechanical properties of membranes	149



# Chapter 1 Introduction

## 1.1 Background

Membrane is a selective barrier with the ability to permeate chemical species at different rates, achieving the separation of one or several species from the others. The advantages of the membrane process include energy-saving, compact size, ease of maintenance and operation, and environmental friendliness.

The concept relevant to the membrane was proposed by Nolet in 1748 to describe the permeation of the water through a diaphragm [1]. Before the early twentieth century, there was no industrial or commercial use of membranes, and membranes were only used as a laboratory tool for research. The first application of membranes was at the end of World War II. The research was sponsored by the US Army. It was later exploited by the Millipore Corporation to solve the problem of drinking water supply breakdown by purifying and supplying drinking water to communities in Germany and elsewhere in Europe [2]. However, the membranes suffered various problems, such as unreliable, unselective, expensive, and having low permeability. Thus, extensive research over the past 50 years has been devoted to developing membranes and membrane processes. Gradually, membranes have become progressively important in chemical technology for broad applications, including water treatment, gas separation, pervaporation, pharmaceutical product separation, fuel cells, etc. The global market was increasing as the application of the membrane technology expanded. The size of the global membrane market was around \$4 billion US dollars in 1998 and grew by five times in 20 years. In 2017, the global demand for membrane modules in water treatment and industrial use combined was valued at approximately \$20.8 billion US dollars. Driven by innovation in membrane development, the market is expected to grow at 7% annually and reach \$32.7 US billion dollars by 2023 [3, 4]. Now, the goal is to work towards increasing membrane reliability and perm-selectivity while reducing costs to make membrane technology mature and competitive to replace other technologies in the market.

Gas separation is one of the fastest-growing membrane applications. The industrial membrane application on gas separation includes hydrogen separation, oxygen/nitrogen separation, natural gas separation, carbon dioxide separation, vapor separation, dehydration of air, and vapor/vapor separation. In gas separation, the gas mixture under high pressure contacts one side of the membrane, which is the membrane feed or residue side. The other side of the membrane is under low pressure and is called the permeate side. The pressure difference across the membrane provides the driving force for gas permeation. The component with a high permeation rate is enriched in the membrane

permeate side, and the slow component is enriched in the membrane residue side. In most applications, including hydrogen separation, oxygen/nitrogen separation, natural gas separation, and carbon dioxide separation, high pressure is applied at the membrane feed side because the gas in applications is already at high pressure. In vapor/gas separation and air dehydration, the membrane feed side is usually at atmospheric pressure, and the permeate side is at the vacuum or flushed in the purging gas. This is to ensure the permeate vapor pressure is lower than the saturated vapor pressure at the feed.

The membrane and process development for gas separation began in the 1970s. The first commercial gas separation product was Monsanto Prism membrane for hydrogen separation, launched by Air Product in 1980. Since then, several major milestones have been achieved, as outlined in Table 1.1. The market growth of membrane on gas separation is around \$150 million US dollars per year [5]. However, more than 90% of the application on membrane gas separation is to separate non-condensable gases. Therefore, the development of membranes for the separation of condensable gases could have a lot of potentials. An example of the application is vapor/gas separation.

**Table 1.1** Milestone of the membrane applications on gas separation [2].

<b>Membrane applications</b>	<b>Company</b>	<b>Year</b>
N <sub>2</sub> /air separation	Dow(Generon)	1982
Natural gas separation	Separex, Cynara and Grace	1983
N <sub>2</sub> /O <sub>2</sub> , H <sub>2</sub> /N <sub>2</sub> and H <sub>2</sub> /CH <sub>4</sub>	Ube, Dupont and Dow	1987
Vapor/gas separation	MTR, GKSS and Nitto Denko	1988
N <sub>2</sub> /O <sub>2</sub> , H <sub>2</sub> /N <sub>2</sub> and H <sub>2</sub> /CH <sub>4</sub>	Ube, Dupont and Dow	1987
C <sub>3</sub> H <sub>6</sub> /N <sub>2</sub>	MTR	1996

Vapor/gas separation is the recovery of light hydrocarbons and volatile organic compounds (VOCs) from various light gases. The first plant for this process was installed in the early 1990s. The application was used to recover vapors from the vent of the gasoline terminal or chlorofluorocarbon (CFC) vapor from the vent of refrigeration plants. The application for vapor separation was then expanded to recover hydrocarbons and solvents from the off-gas in the petrochemical plant. Depending on the production capacity of plants, one vapor/gas separation membrane unit could

recover a value of \$2 to \$5 million US dollars per year from the off-gas, and the required membrane area in each unit is significant. Hence, it is desirable to improve the vapor permeation in membranes to reduce the required membrane area and thus realize economic benefits by reducing costs.

Membranes used for vapor/gas separation are usually made in glassy polymer and rubbery polymer. The glassy polymer (e.g., polyimide) is usually used to permeate the light gas, while the rubbery polymer (e.g., silicon rubber) is usually used to permeate the condensable gas. Theoretically, either glassy or rubber polymer could be used on vapor/gas separation. However, almost all the membranes used in commercial applications are made in rubbery polymers for two reasons: i) the rubbery polymer tends to have higher vapor permeability than the glassy polymer, sharply reducing the required membrane area in applications; ii) the glassy polymer is highly dependent on vapor composition in the feed stream, and the polymer gets plasticized at a high VOC concentration, resulting in limited applications.

Silicon rubber (also known as PDMS) is one of the most widely used rubbery polymers to make vapor-permeable membranes. This polymer is made from a hydrophobic rubbery material and preferentially sorbs condensable organic compounds. Vapor and gas permeate membranes following the sorption-diffusion mechanism, and the sorption term dominates over the diffusion term for gas permeation in rubbery polymers. The permeation of non-condensable or light gas in PDMS membranes is favored by the diffusion term. Meanwhile, the permeation of condensable gas (e.g., VOCs) in PDMS membranes is favored by the sorption term. Therefore, the silicon rubber membrane has better permeability for condensable gas (e.g., VOC) than non-condensable gas (e.g., N<sub>2</sub>).

Poly (ether block amide) (PEBA) is another widely investigated polymer used in vapor/gas separation. This material is a copolymer consisting of polyamide and polyether segments. PEBA 2533 comprises of 80wt.% poly (tetramethylene oxide) which represents the rubbery part in the polymer. And the remainder 20wt.% consists of polyamide segments, which endow an excellent mechanical property to the membrane. The good chemical-resistant, thermal and mechanical properties make it a good alternative polymer for silicone rubber.

This work aims to develop a membrane with higher vapor permeability and vapor/gas selectivity to the silicon rubber or PEBA membranes. VOCs as represented vapors, which are the hazards in the air, were selected to evaluate the vapor gas separation performance of the membrane in this work. The oils (DEHP and DEHA) have been proved to have high boiling points, low volatility, and both high diffusion and sorption coefficients for VOCs, which are favorable to VOCs/N<sub>2</sub> separation. However, researches in applying these oils into membrane separation for VOCs are scarce. To develop a membrane with better VOC permeation property than the silicon rubber, the oils (DEHP and DEHA)

were innovatively applied to incorporate with the polymer for the first time in this work to fabricate the membrane. The so-prepared membrane is named the oleophilic membrane.

The intrinsic VOC permeation property was investigated for the prepared oleophilic membrane. As one type of oleophilic membrane, the oleo gel membranes were in the form of films and made in different polymers and oils. PEBA/DEHP and PEBA/DEHA oleo gel membranes were made to investigate the effect of the oil on membrane VOC/N<sub>2</sub> separation performance. Moreover, PEBA/DEHA and PDMS/DEHA oleo gel membranes were fabricated to explore the impact of the polymers on membrane VOC/N<sub>2</sub> separation performance. All oleo gel membranes were made with polymers and oils at different ratios. The effect of oil content on VOC/N<sub>2</sub> separation performance was investigated. The evaluations of temperature dependence and feed VOC composition dependence of VOC permeability were also performed, and the VOC permeation in the membrane was proved to be sorption-dominated. Additionally, material properties, including physical properties, structures, and morphologies of oleo gel membranes, were comprehensively analyzed to explain the VOC and N<sub>2</sub> permeation in the membrane.

Since the prepared oleo gel membrane is weak in terms of mechanical strength and this weakness will limit its applications in the industry, so two composite oleophilic membranes were developed by coating the oil or oleo gel into membrane substrates. The membrane's mechanical property was then improved with the help of the membrane substrate. Two types of the supported liquid membrane were developed for VOC/N<sub>2</sub> separation in this work. One is the silicone oil (SO) based supported liquid membrane, which was made by using SO to wet the surface of the Polysulfone (PS) membrane, and the other is the supported PDMS/SO oleo gel membrane which was further developed to solve the instability issues of the SO based supported liquid membrane in a variable VOC environment. Both membranes were evaluated in a certain period and proved to be stable in the environment within selected VOCs.

## 1.2 Research objective

The research objectives have been derived in light of the discussion as mentioned above and are presented below.

Overall objective:

Develop the oleophilic membrane for VOC/N<sub>2</sub> separation. The membrane is expected to have higher VOC permeability than the widely industrial used silicon rubber membrane

Sub objectives:

Fabricating oleophilic membranes in the form of homogenous film (oleo gel membrane) to investigate the intrinsic VOC permeation properties in the membrane.

- Explore the effect of oils and polymers on VOC/N<sub>2</sub> separation performance of the membrane. Different oleo gel membranes including PEBA/DEHP, PEBA/DEHA and PDMS/DEHA were fabricated. The effects of the oil content in the membrane and crosslink agent ratio in the PDMS on VOC permeation in the membrane were investigated;
- Investigate the effect of operating parameters such as feed gas composition, operating temperature, and pressure on the VOC/N<sub>2</sub> separation performance of the membrane.

Fabricating the composite oleophilic membrane with the corporation of the suitable substrate to endow the prepared membrane with a strong mechanical strength for the feasible application in industry.

- Develop a simple way to fabricate the composite oleophilic membrane;
- Explore the substrates for composite oleophilic membrane fabrication;
- Investigate the VOC/N<sub>2</sub> separation performance of the composite oleophilic membranes.

The membrane films (oleo gel membranes) were fabricated to mainly investigate the intrinsic property of VOC permeation in the oleo gel. The composite membrane was developed afterward by coating the oleo gel in the substrate to make the membrane suitable for industrial application. The VOC/N<sub>2</sub> separation performance of the membrane is the overall performance of combined membrane films and substrate.

### **1.3 Scope of the thesis**

The thesis structure is illustrated in Figure 1.1 for a brief overview of the research. The thesis consists of seven chapters, and a summary for each chapter is presented below. It should be noted that the oleo gel membranes developed from Chapters 3 to 5 were the films, which aim to investigate the intrinsic VOC permeation property in the membrane. The effect of oils (e.g., DEHP and DEHA) and polymers (e.g., PEBA and PDMS) on VOC permeation and VOC/N<sub>2</sub> separation in the membrane was investigated and discussed in these Chapters. Based on that, PDMS was chosen as the polymer to immobilize the oil in the membrane substrate, and the composite oleophilic membrane was therefore developed in Chapter 6. Two types of composite membranes were fabricated, making the oleophilic membrane more applicable in the industry.

Chapter 1 introduces the background of this study, including the history of membrane development, the current status of membrane development, the membrane used in VOC/N<sub>2</sub> separation, and the objective of this study.

Chapter 2 presents the literature review of membrane for VOC/N<sub>2</sub> separation and introduces the technology used in the VOC treatment. The transport mechanism and material of membrane on VOC/N<sub>2</sub> separation are also described.

The PEBA/DEHP oleo gel membrane was developed and introduced in Chapter 3. The physical properties, structures, and morphologies of the oleo gel membrane were studied along with the vapor and gas permeation properties. The oil content in the membranes was demonstrated to have significant effects on their VOC permeability and VOC/N<sub>2</sub> selectivity, and the prepared membranes showed remarkably higher VOC permeability than the PEBA membrane in VOC/N<sub>2</sub> separation test.

In Chapter 4, the oleo gel membrane was further developed by introducing DEHA oil in the membrane, and the PEBA/DEHA oleo gel membrane was accordingly fabricated. DEHA oil showed better sorption to VOC than DEHP oil. The VOC/N<sub>2</sub> separation performance of the PEBA/DEHA membrane was investigated, and the membrane VOC permeability was compared with that of the PEBA/DEHP membrane. In this Chapter, the VOC permeability in the PEBA/DEHA membrane was found to follow the miscible blending rules, and the VOC permeability of the DEHA oil could be obtained from the calculation. Semi-empirical correlations were developed to relate the membrane VOC permeability to operation parameters, including feed VOC concentrations and operating pressures.

PDMS was used to replace PEBA to make PDMS/DEHA oleo gel membrane in Chapter 5. The membrane showed even better VOC permeability than both PEBA/DEHP and PEBA/DEHA membranes. By comparing the VOC permeabilities of the three membranes introduced in Chapter 3 to 5, the VOC/N<sub>2</sub> separation performance of the oleo gel membrane was proved to be affected not only by the oil (e.g., DEHA and DEHP) but also the oil holder (e.g., PEBA and PDMS). The effects of the crosslink in PDMS on the oil immobilization and membrane VOC/N<sub>2</sub> separation performance were investigated. The gas and vapor permeation in the oleo gel membranes follows the sorption-diffusion model. The VOC permeation was sorption-dominated, while the N<sub>2</sub> permeation was diffusion-dominated.

In Chapter 6, two types of supported liquid membrane were developed. One is the silicone oil (SO) based supported liquid membrane. The membrane was evaluated in a certain period and proved stable in the environment within the selected VOCs and pure gas. And the VOC/N<sub>2</sub> selectivity of the

membrane was comparable with the silicone rubber membrane. However, the SO based supported liquid membrane was not stable in other VOC/N<sub>2</sub> mixtures (e.g., DMC and Benzene). The PDMS/SO supported oleo gel membrane was further developed to solve the instability issues of the membrane in a variable VOC environment. The membrane showed competitive VOC/N<sub>2</sub> separation performance compared to PDMS membranes. Both SO supported liquid membrane and PDMS/SO supported oleo gel membranes have the substrate, which provided the membrane with the mechanical strength to be applicable in the membrane process.

Chapter 7 concludes and summarizes the findings in this study and recommends future work based on the research and analysis in previous chapters.

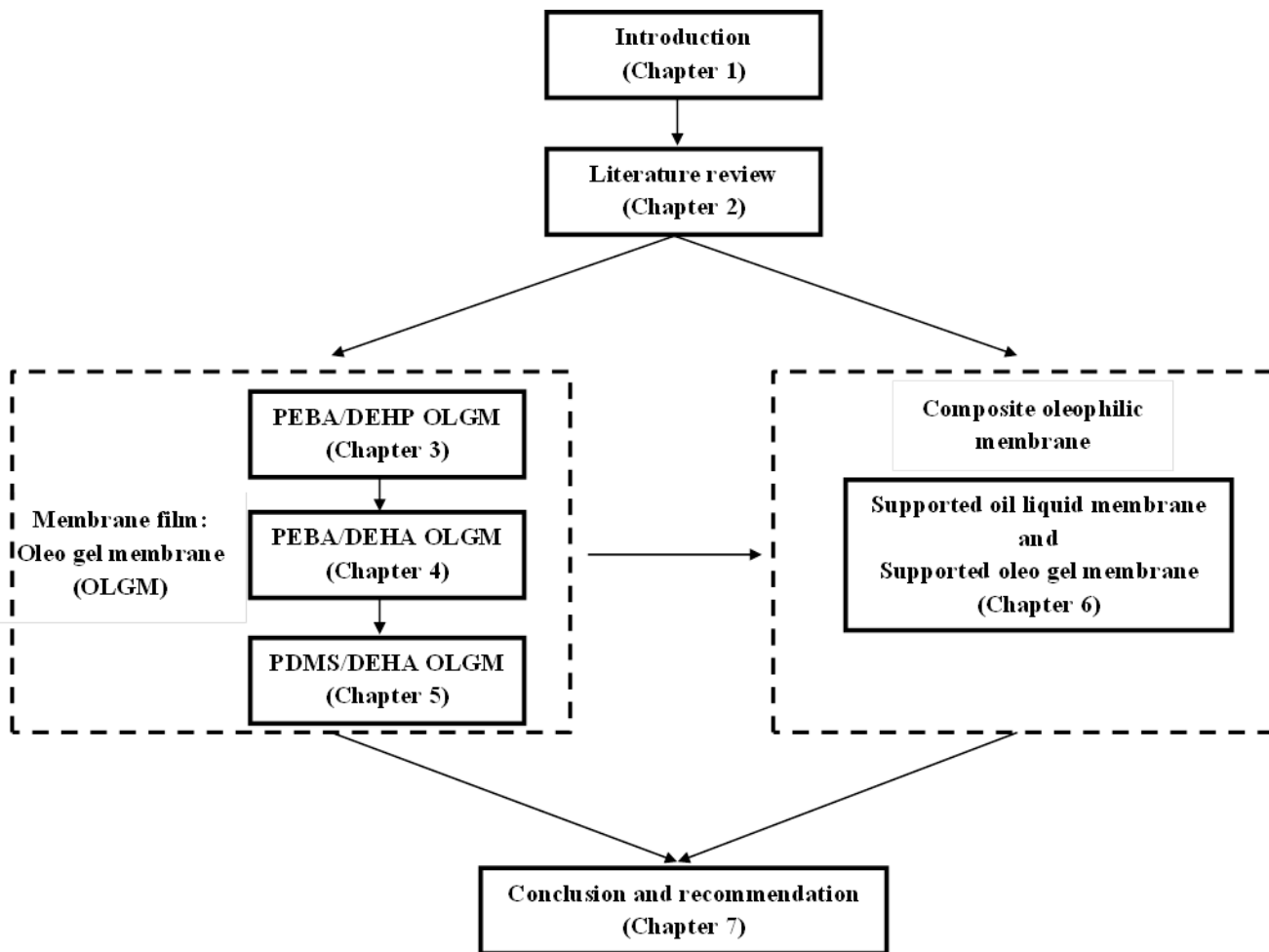


**Figure 1.1** Thesis structure in term of chapters and content relevance

## **Chapter 2**

### **Literature review**

This chapter attempts to review the literature related to VOC/N<sub>2</sub> separation membrane. The VOC treatment background, gas transport mechanism, the membrane development on VOC/N<sub>2</sub> separation, and the membrane process development are introduced in this chapter. More specific literature reviews about this work are presented in later relevant chapters.

#### **2.1 Background of VOC emissions**

Volatile organic compounds (VOCs) are organic chemicals in the form of carbon-containing gases and vapors, such as gasoline fumes and solvents (carbon dioxide, carbon monoxide, methane, and chlorofluorocarbons are excluded). There are thousands of organic compounds in the natural and polluted troposphere that meet the definition of VOCs, but most measurements usually define VOCs as hydrocarbons that have less than 12 carbons in their formulas.

The low boiling points and high vapor pressures at room temperature of the VOCs make them easily evaporate into the air. There are two sources of VOC emissions as pollutants in the air. One is a biogenic volatile organic compound (BVOC) that can be emitted by vegetation, microorganism, or other types of life in the biosphere. The other is from human activities, from emissions related to fuel production, industrial and domestic combustion (fossil fuel and biofuel), transportation (road, rail, air and ships), waste disposal, industrial processes, solvent production and use, and agriculture [6].

As the economy develops and resource consumption increases, VOC emissions have surged in recent years, mainly due to emissions from the oil and gas industry. Based on a report from the US Environmental Protection Agency (EPA), petroleum refining and related storage/transfer are the largest contributors to VOC emissions [7]. The total storage capacity of 30,000 lbs. of petroleum has the potential to emit VOCs to the air at a rate of over 100 tons/year. The national emissions inventories indicate that volatile organic compound (VOC) emissions from the oil and gas supply chains in the US have been increasing significantly in recent years [8]. Figure 2.1 shows that the oil and gas production in the US has increased by 1.3 times from 2005 to 2015, while VOC emissions from petroleum and related industries have increased by almost 400% during that same timeframe.



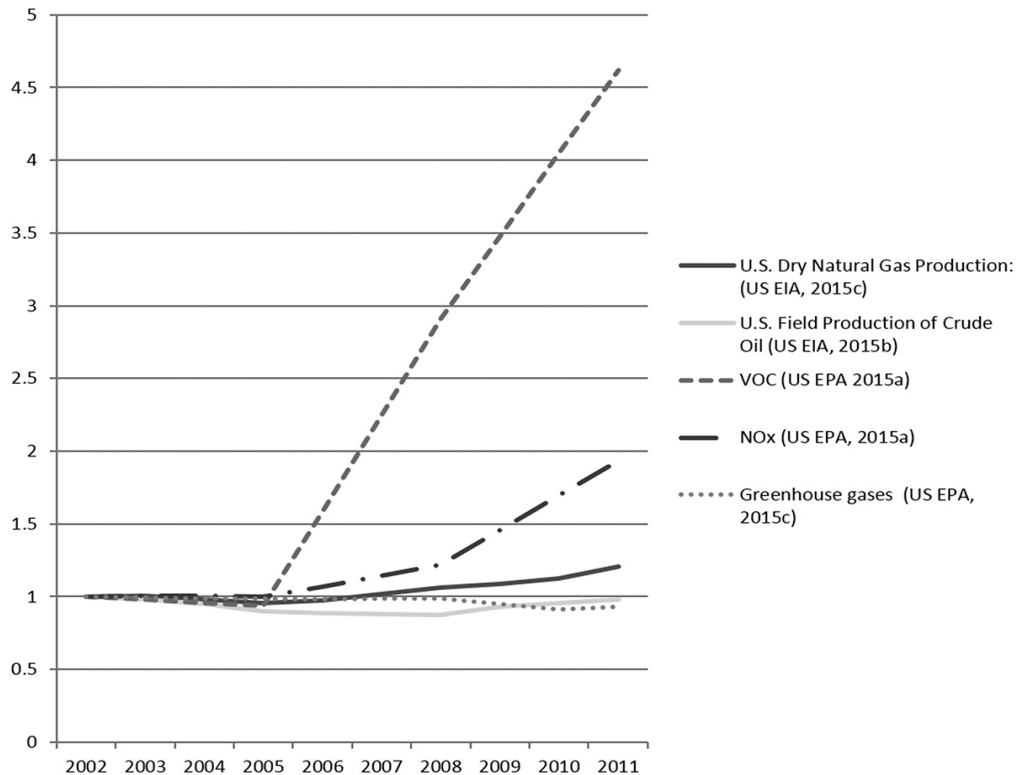


**Figure 2.1** Oil and gas production compared to emissions of VOCs, NO<sub>x</sub>, and greenhouse gases from the petroleum and natural gas supply chains (2002–2011); all data were normalized to 2002 levels [9].

Figure 2.2 shows an overview of VOCs emitted to the atmosphere. Since most VOCs are photochemically sensitive, VOCs react with nitrogen oxide under the illumination of sunshine. Ozone and other chemical compounds are created and can be digested by self-cleaning of nature (e.g. air advection, rain washout, and biological uptake by oceans and plants) at low concentrations. Otherwise, aerosols are formed by the nucleation of VOC and deposition of multiple chemical compounds, causing the ozonosphere and carcinogenic smog to form on the ground level. The hazardous origins of VOCs across various spatiotemporal scales make their presence in the air an issue.

Polluted air has various health effects on human beings, especially for individuals who have susceptible health issues. Even a low level of air pollution could cause them severe health problems. For most people, short-term exposure to air pollutants could cause chronic obstructive pulmonary disease, cough, shortness of breath, wheezing, asthma, respiratory disease, and high hospitalization rates. If the exposure to the air pollutant is long-term, it can cause chronic asthma, diabetes, pulmonary insufficiency, cardiovascular diseases, and cardiovascular mortality [10]. The World

Health Organization estimates that 2.4 million people die each year due to air pollution issues [11], which warns actions must be taken to control the VOC emissions.

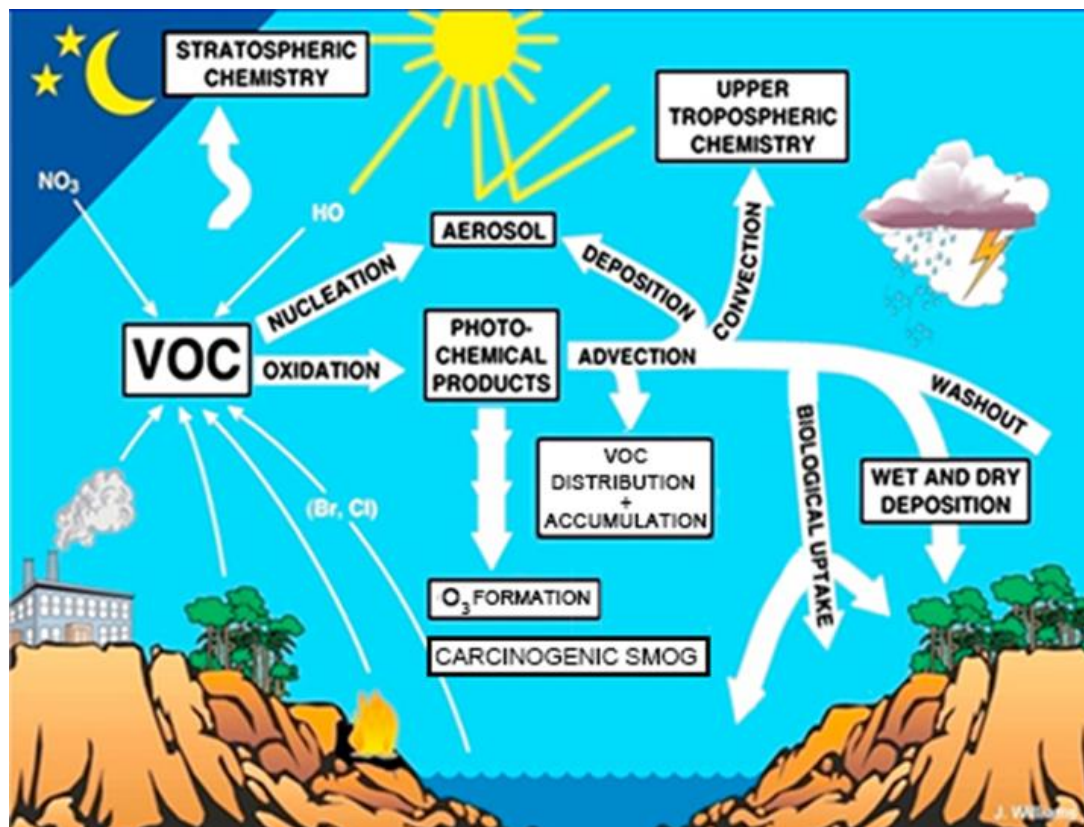
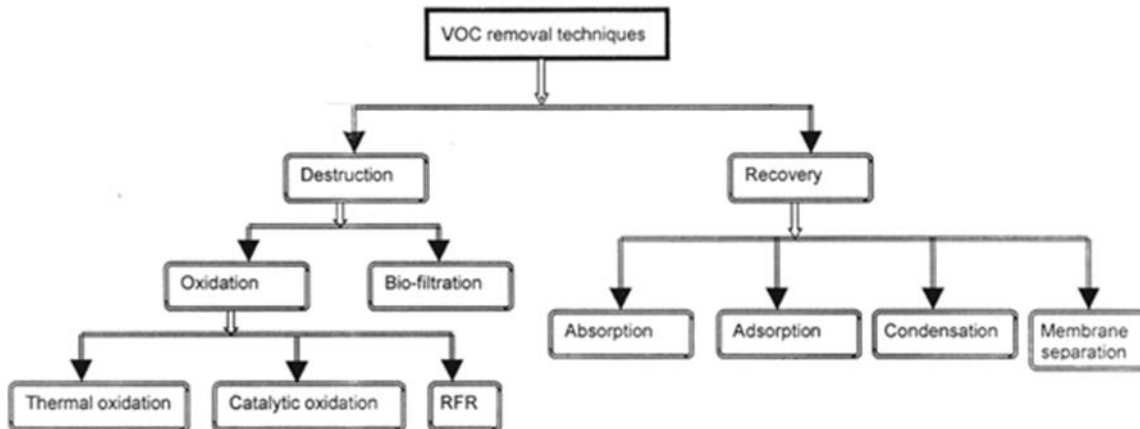


Figure 2.2 A schematic overview of VOC in the troposphere [12].

## 2.2 VOC treatment technology

To reduce the VOC emission in the air, many technologies have been used over the past 30 years, and a number of options are available. Based on the fate of VOCs after the treatment, the techniques can be classified as VOC destruction and VOC recovery, as shown in Figure 2.3.

The VOC destruction typically decomposes VOCs into CO<sub>2</sub> and H<sub>2</sub>O through the physical and chemical processes. These technologies typically involve thermal oxidation, catalytic oxidation and reverse flow reactors. VOC recovery could recover the VOCs from the off-gas, and the concentrated VOC could be either recycled back to the process to save the feedstock or used as fuel to save the cost in process operation. The standard technology in VOC recovery includes adsorption, absorption, condensation, and membrane separation.



**Figure 2.3** Classification of VOC control techniques [13].

## 2.2.1 VOC destruction

### Thermal oxidation

In VOC destruction, thermal oxidation has been widely adopted because it can handle a capacity of 1,000 to 500,000 cfm gases with feed VOC concentrations ranges from 100 to 2,000 ppm. The high operation temperature (1,300–1,800°F) can easily achieve the desired destruction removal while operating costs can also be reduced by recovering some thermal energy [14].

### Catalytic oxidation

With the implementation of catalysts, oxidation requires less energy and thus can operate at a lower temperature—typically about 700–900°F. A disadvantage with this application is that the treatment capacity is generally low (1,000 to 100,000 cfm) [15].

### Reverse flow reactor

The reverse flow reactor is an adiabatic reactor for VOC destruction. Its unsteady-state operation can make the process more profitable. However, it is not always easy to meet the adiabatic operation conditions.

## 2.2.2 VOC recovery

The conventional methods (condensation, adsorption, and absorption) and the alternative new method (membrane separation) for VOC recovery have been commercialized currently.

## Adsorption

Adsorption is a method to recover VOCs by trapping the VOCs on porous material. The Adsorbents are materials that usually have a large effective surface for adsorption, such as zeolite, carbon materials, and metal-organic framework (MOF) [16]. The balance between the cost and adsorption performance is the factor for adsorbent selection. Comparing the three adsorbents mentioned above, carbon material has a lower cost than the zeolite; MOF could be chemically modified to fit the application; however, the high price may limit its application in the industry [17]. The complexity of adsorbent regeneration also impacts the adsorbent selection. The adsorbent requires regeneration when it is saturated by adsorbate. And further treatment may be needed, depending on whether the adsorbate is contaminated. Sometimes, if the adsorbates cannot be regenerated, it would be difficult to dispose of the adsorbate.

## Absorption

Absorption works on VOC recovery and is based on the physical or chemical absorption of VOCs in the absorbent liquid. Absorption has a good performance to recover the VOC under certain conditions, but the operating cost and energy consumption are high. Similar to adsorption, the regeneration step is required.

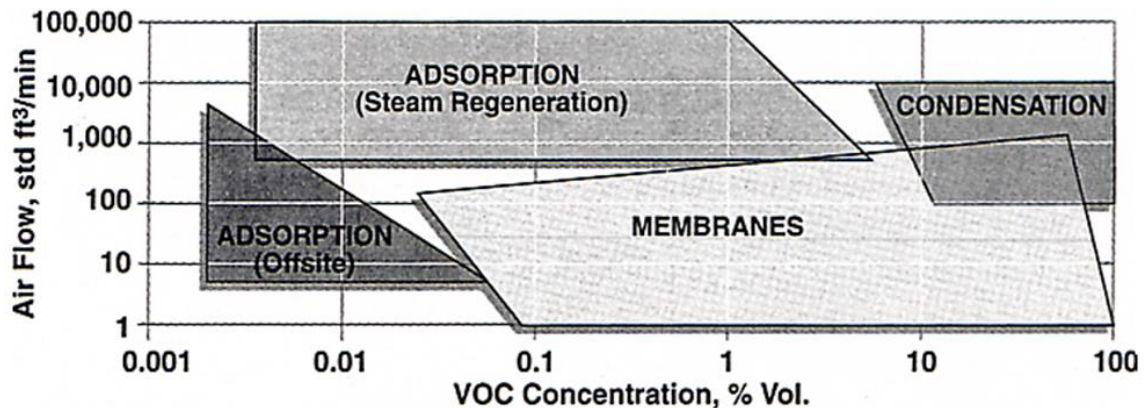


**Figure 2.4** Operation condition of various techniques for recovering VOCs [18].

Figure 2.4 shows the proper operating conditions for different technologies. The advantages and disadvantages of these technologies in VOC recovery are summarized in Table 2.1. There is no technology that is the best for operation under all conditions. The advantages and disadvantages are compared in terms of safety, performance, operating cost, and facility space. Sometimes, the combination of different technologies is designed to achieve better VOC recovery performance.

Compared with other VOC recovery processes, membrane separation is characterized by no regeneration, easy setup, and flexible module design. It is considered an economical technology alternative. Since the first VOC recovery membrane unit was installed on large refrigerators to recover CFC and HCFC halocarbons from vent streams, many units were installed to recover hydrocarbon vapors from air streams produced in gasoline loading and unloading operations. The cost of the processes can be justified by the value of the recovered vapors [19].

**Table 2.1** Comparison of techniques of VOC recovery

Methods	Advantages	Weaknesses
Condensation	<ul style="list-style-type: none"> <li>• Effective at high boiling point VOC removal.</li> <li>• Effective removal at high VOC concentration.</li> </ul>	<ul style="list-style-type: none"> <li>• Energy cost</li> </ul>
Absorption or adsorption	<ul style="list-style-type: none"> <li>• Effective removal at low VOC concentration</li> </ul>	<ul style="list-style-type: none"> <li>• Energy cost</li> <li>• Absorbent leakage</li> <li>• Complicated operation</li> <li>• Steam is required for the regeneration of the adsorbent.</li> </ul>
Membrane separation	<ul style="list-style-type: none"> <li>• Energy-efficient.</li> <li>• Compact size.</li> </ul>	<ul style="list-style-type: none"> <li>• Less efficient at low VOC concentration</li> </ul>

## 2.3 Gas transport in the membrane

### 2.3.1 Mechanism of gas permeation

The gas permeation through the membrane could be categorized into two scenarios, gas permeation through the porous membrane and gas permeation through the non-porous membrane. The porous membrane is usually used as the membrane substrate for mechanical support in gas separation. The non-porous membrane could be used as the selective layer for gas separation. The mechanisms for gas permeation in porous membranes and non-porous membranes are described below.

#### Gas permeation through the porous membrane

Figure 2.5 illustrates the mechanism of gas separation in porous membranes. The mechanism could be classified into five cases: viscous flow, Knudsen diffusion, surface diffusion, capillary condensation, and molecular sieving. The gas permeation through the membrane is strongly dependent on the pore size in the membrane. The gas stream through the membrane is the viscous

flow when the pore size in the membrane is larger than the mean free path of the gas molecule. When the pore size is smaller than the mean free path, the gas molecule permeates the membrane by Knudsen diffusion. If the gas molecules have a strong affinity to the walls in membrane pores, the gas permeation could be called surface diffusion. When the pore size becomes even smaller than previously mentioned permeation, the capillary condensation happens, and the large molecules could be restricted by the interaction between each other to permeate through the membrane pores. The pores of membranes used in molecular sieving are designed in specific diameters that the molecules with the size are smaller than the diameter of the membrane pores could permeate, and the big molecules are sieved by the membrane. Typically, the pore size in viscous flow is more than 1000 angstrom; the range of pore size for Knudson diffusion is between 100 to 1000 angstrom, and the range of pore size in molecular sieving is between 5 to 100 angstrom [2].

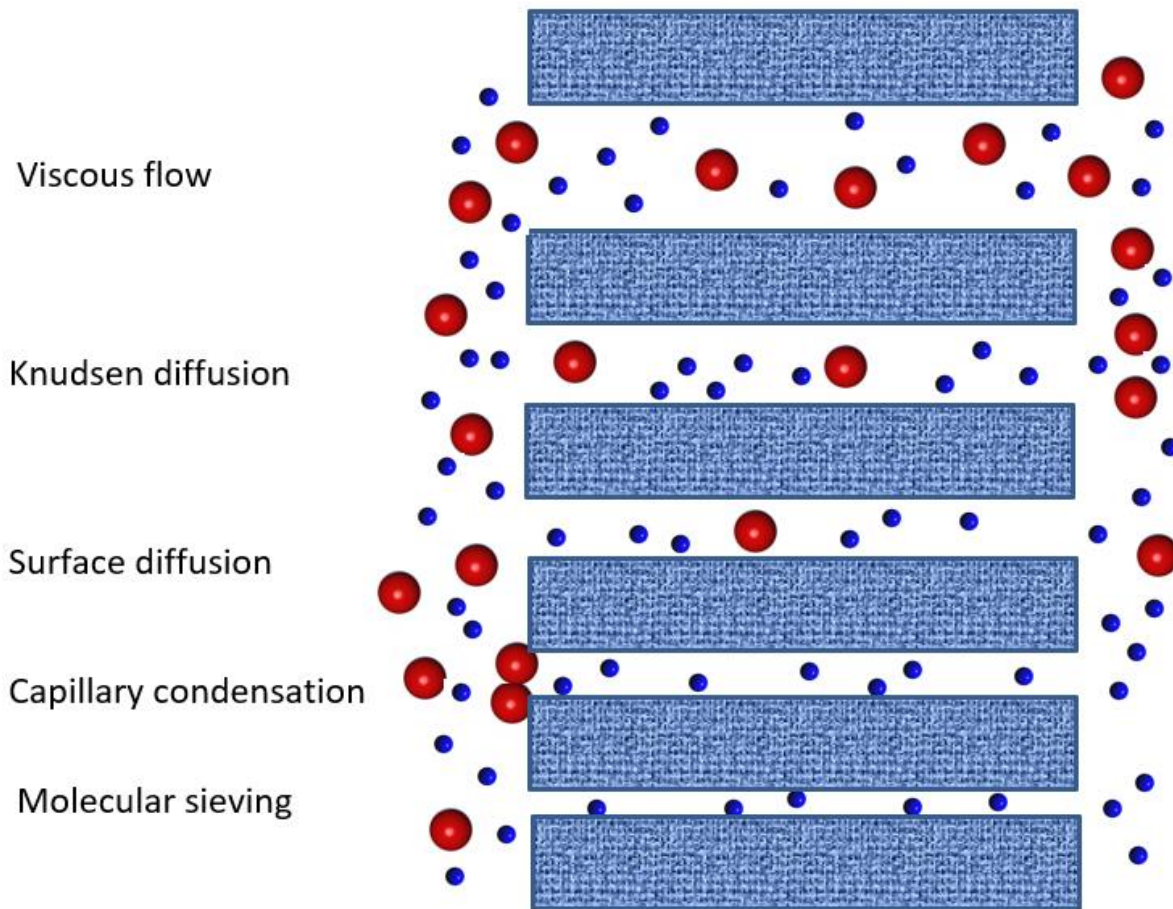
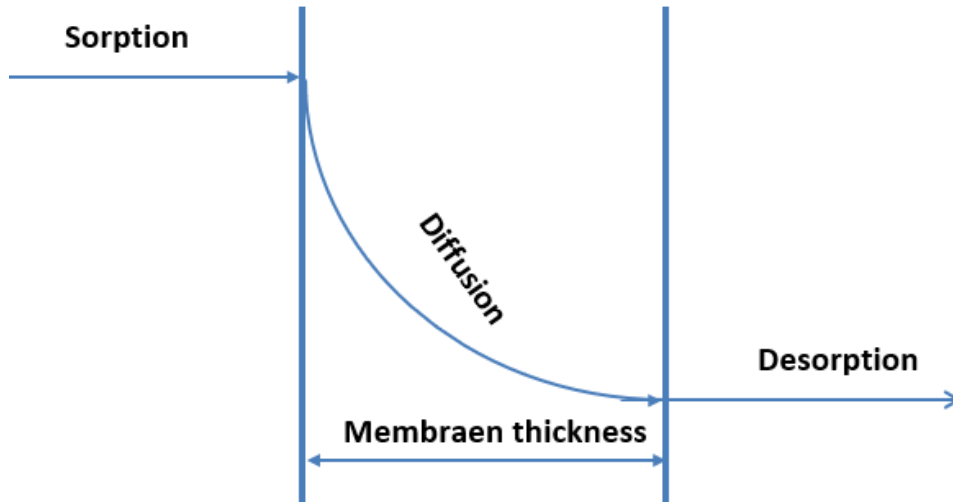


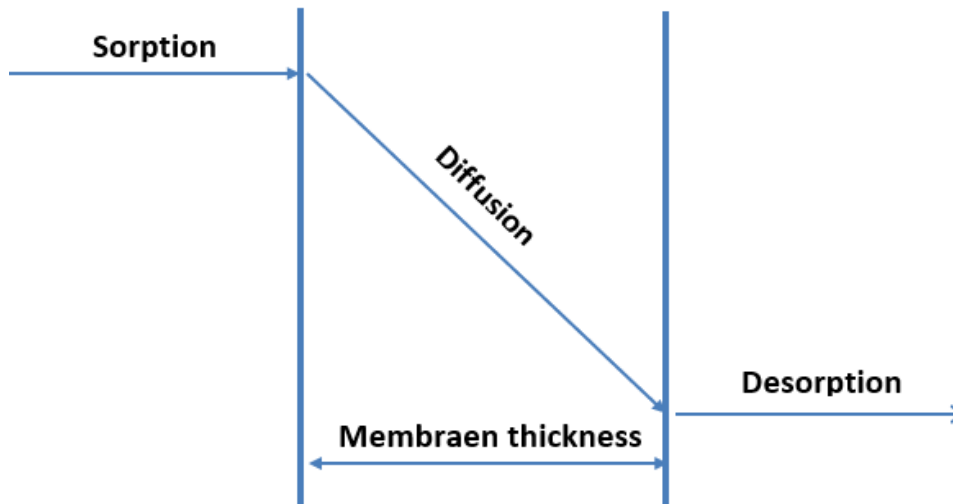
**Figure 2.5** Schematic diagram of gas permeation in the porous membrane.

### **Gas permeation through the non-porous membrane**

The solution diffusion mechanism is usually used to describe the gas permeation through the non-porous membrane [20]. In gas permeation, the feed gas is introduced to one side of the membrane, and the other side is maintained at a vacuum or atmosphere to induce the gas permeation. According to the solution diffusion mechanism, gas permeation generally involves three sequential steps (Figure 2.6). In the first step, gas molecules contact and dissolve in the membrane. In the second step, the dissolved gas molecules diffuse through the membrane under the concentration difference across the membrane. Figure 2.6 (a) shows that the concentration gradient is a non-linear curve at the beginning of the second step, which means the diffusion is at an unsteady state. When the gas diffusion reaches a steady state in Figure 2.6 (b), the concentration gradient across the membrane becomes linear. In the third step, gas molecules desorb from the membrane. The different molecules permeate through the membrane at different rates, resulting in separated gases.



(a) Unsteady state



(b) Steady state

**Figure 2.6** Schematic diagram of gas permeation in the non-porous membrane by sorption diffusion mechanism.

In the sorption diffusion mechanism, Both the sorption (first step) and desorption (third step) occur fast; equilibrium is reached instantaneously on both sides of the membrane. And diffusion is the rate-controlling step in gas permeation, which Fick's law could be used to describe the process:

$$Q_i = -D_i \frac{dc_i}{dz} \quad (2.1)$$

where  $Q_i$  is the permeation flux of component  $i$ .  $D_i$  is the diffusion coefficient, which is usually treated as the constant that is independent of gas composition. However,  $D$  could be affected by the



condensable gas or vapor in VOC/N<sub>2</sub> separation due to the swelling or plasticization effect from the permeant to the membrane.  $Z$  is the position of gas molecules crossing the membrane,  $C_i$  is the concentration of component  $a$  in the membrane,  $\frac{dC_i}{dZ}$  is the concentration gradient across the membrane, and the negative sign means that the gas permeation direction is opposite to the direction of the concentration gradient.

The concentration of component  $i$  in the membrane can be described by Henry's law:

$$C_i = S_i \times p_i \quad (2.2)$$

where  $S_i$  is Henry's solubility coefficient, and  $p_i$  is the partial vapor pressure of component  $i$  in equilibrium with the solution. If Henry's solubility coefficient is independent of concentration, by combining Equation (2.1) and (2.2), Equation (2.3) is obtained

$$J_i = -D_i \times S_i \frac{dp_i}{dZ} \quad (2.3)$$

Integrating Equation (2.3) over the cross-section of the membrane gives

$$J_i = D_i \times S_i \times \frac{p_{i,o} - p_{i,L}}{L} = P_i \times \frac{p_{i,o} - p_{i,L}}{L} \quad (2.4)$$

where  $P_i$  is defined as the permeability coefficient of component  $i$ .  $L$  is the membrane thickness. The subscripts  $o$  and  $L$  represent the positions at the feed and permeate of the membrane.

In Equation 2.4, The permeability coefficient could be related to the diffusion coefficient  $D_i$  and solubility coefficient  $S_i$ , as shown in Equation (2.5)

$$P_i = D_i \times S_i \quad (2.5)$$

The temperature dependence of  $D_i$  and  $S_i$  could be generally described by

$$D_i = D_{0i} \exp\left(-\frac{E_{Di}}{RT}\right) \quad (2.6)$$

$$S_i = S_{0i} \exp\left(-\frac{\Delta H_i}{RT}\right) \quad (2.7)$$

And thus

$$P_i = P_{0i} \exp\left(-\frac{E_{Pi}}{RT}\right) \quad (2.8)$$

Where  $E_P = E_D + \Delta H$ , and  $E_P$  is the activation energy of permeability, which is the combination of the activation energy of diffusion ( $E_D$ ) and the enthalpy of dissolution of the permeant in the membrane ( $\Delta H$ ).  $D_{0i}$ ,  $S_{0i}$  and  $P_{0i}$  are the pre-exponential factors, and  $P_{0i} = D_{0i} \times S_{0i}$ .  $E_P$  could be obtained from the plot of the slope of  $\ln(P_i)$  vs.  $(1/T)$ .

Generally,  $E_D$  is positive, while the heat of dissolution  $\Delta H$  is negative for the exothermic sorption process. When the dissolution process is over the diffusion process, a negative  $E_P$  value will derive, suggesting the gas permeability of the membrane is reversely dependent on the temperature.

### 2.3.2 Gas transport in the composite membrane

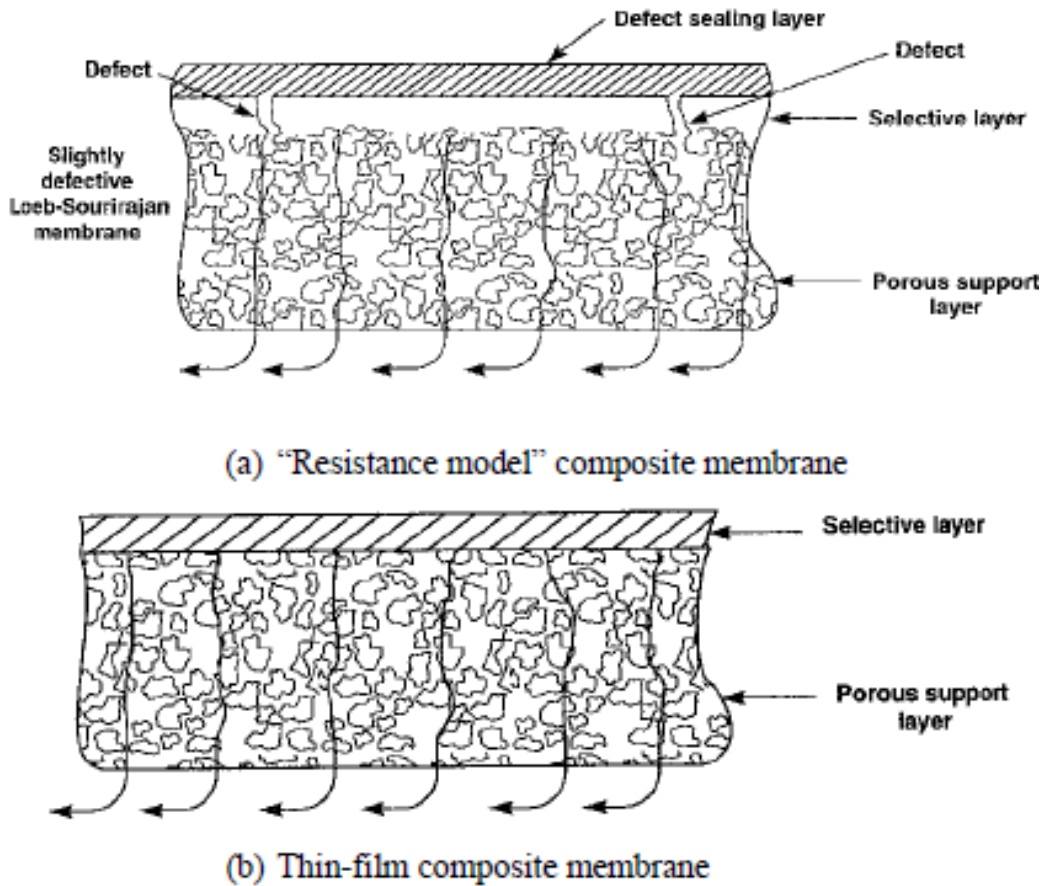


**Figure 2.7** Gas permeation in the composite membrane [2].

Membranes could be divided into the dense membrane or composite membranes by their structures. A dense membrane is manufactured by the same material, and the membrane is dense and homogeneous. The dense membrane is thick without any defects, therefore shows high selectivity, and could be used to measure the intrinsic separation performance of the membrane. In this work, the newly developed oleo gel membranes were made into dense membranes to investigate their intrinsic membrane separation performance for VOC/N<sub>2</sub>.

However, the dense membrane shows weak mechanical strength and low gas permeance, making the membrane hard to operate independently in industrial applications. Therefore, the thin membrane film is coated on the substrate to make the composite membrane. The composite membrane shows

good mechanical strength and good gas separation performance, which is then fabricated to membrane elements and widely used in an industrial membrane process.

The composite membrane could be classified into two types, resistance model composite membrane and thin-film composite membrane (shown in Figure 2.7). Both membranes have a thin dense layer sitting on the porous substrate. The thin dense layer is for selective gas permeation, and the porous substrate is for mechanical support.

In the resistance model composite membrane (shown in Figure 2.7 a), the selective layer and the substrate are formed from the same polymer by phase inversion technique. The thin selective layer in the Figure separates different gases, and the pores in the support layer serve the free channel to gas permeation, simultaneously offer support for the selective layer. Some defects may form on the selective layer during the membrane fabrication, the defect sealing layer will be coated on top of the selective layer to make the membrane defect-free.

In the thin-film composite membrane (shown in Figure 2.6 b), the materials in the selective layer and porous support layer are different. The thin selective layer is coated on the porous support layer. Compared to the resistance model composite membrane, the thin film membrane has many advantages and is attracted in recent years. The thin-film membrane is easier to be fabricated than the resistance model membrane. The consumption of material for thin-film membrane fabrication is much lower than the resistance model membrane, and the resistance model membrane requires 40 – 60 g polymer per membrane area, but the thin film membrane only requires 1 g polymer per membrane area [5]. However, there are some drawbacks for the thin-film membrane in the application. For example, the large pore size and porosity in the substrate of the thin-film composite membrane limit the membrane to be used under a pressure of more than 20 bar. Fortunately, the pressure for membrane applied in VOC/N<sub>2</sub> separation is low and usually less than 20 bar, which means that the pressure issue for thin-film membrane will not be considered.

In this work, two new types of composite membranes have been developed: the SO-based oil liquid membrane and the PDMS/SO supported oleo gel membrane. Both membranes have their support layer, but their selective layers are in the pores of support layers by filling the oil and oleo gel in the membrane substrate (porous support layer). By doing so, the membrane fabrication becomes even simpler than the thin-film composite membrane.

### **2.3.3 VOC and nitrogen permeation in the membrane**

The VOC and nitrogen permeation could be characterized by permeance and permeability. The permeance is usually used to indicate the gas permeation in the composite membrane, and the unit is gpu, 1gpu is equal to  $10^{-6}$  (STP)  $\text{cm}^{-2} \text{s}^{-1} \text{cm Hg}^{-1}$ . The permeability could be used to describe the

intrinsic gas permeation property of the membrane film, and the unit is barrer, 1 barrer equal to  $10^{-10}$  (STP)cm cm<sup>-2</sup> s<sup>-1</sup> cm Hg<sup>-1</sup>. The pure gas permeance and permeability could be calculated by equations as below,

$$Permeance = \frac{J}{\Delta P X A} = \frac{J}{(p_{feed} - p_{perm}) \times A} \quad (2.10)$$

$$Permeability = \frac{J \times L}{\Delta P X A} = \frac{J \times L}{(p_{feed} - p_{perm}) \times A} \quad (2.11)$$

where A is membrane area (cm<sup>2</sup>).  $\Delta P$  is the pressure difference across the membrane,  $p_{feed}$  is the pressure at the feed side of the membrane,  $p_{perm}$  is the pressure at the permeate side of the membrane, and the unit of the pressure here is cmHg.

The permeability and permeance of gas components in a binary mixture of VOC/N<sub>2</sub> could be expressed as the equations below. The Equation for VOC is used as an example here.

$$permeance_{VOC} = \frac{J_{VOC}}{\Delta P_{VOC} X A} = \frac{J \times x_{VOC}}{(p_{feedVOC} - p_{permVOC}) \times A} \quad (2.12)$$

$$permeability_{VOC} = \frac{J_{VOC} \times L}{\Delta P_{VOC} X A} = \frac{J \times x_{VOC} \times L}{(p_{feedVOC} - p_{permVOC}) \times A} \quad (2.13)$$

where  $x_{VOC}$  is the mole fraction of VOC in binary VOC/N<sub>2</sub> mixture.  $p_{feedVOC}$  is the VOC partial pressure in the feed stream,  $p_{permVOC}$  is the VOC partial pressure in the permeate stream.

The permeability or permeance ratio for VOC and nitrogen could be defined as the Equation below, and the ratio could be called selectivity. If permeability or permeance ratio is calculated by the data from the pure gas, it is usually called ideal gas selectivity.

$$Permeability \text{ ratio: } \alpha_{VOC/N_2} = \frac{Permeability_{VOC}}{Permeability_{N_2}} = \frac{D_{VOC}}{D_{N_2}} \times \frac{S_{N_2}}{S_{VOC}} \quad (2.14)$$

$$Permeance \text{ ratio: } \alpha_{VOC/N_2} = \frac{Permeance_{VOC}}{Permeance_{N_2}} \quad (2.15)$$

where  $\frac{D_{VOC}}{D_{N_2}}$  and  $\frac{S_{N_2}}{S_{VOC}}$  respectively represent diffusivity selectivity and solubility selectivity for VOC/N<sub>2</sub>. Those two ratios indicate the contribution of the diffusion and sorption process to overall selectivity.

In this work, S indicates the solubility of the VOCs and nitrogen in the membrane. The VOCs have higher boiling points than the nitrogen, which means the VOCs could dissolve in the membrane more than the nitrogen. The sorption of the gas in the membrane could also be indicated by the critical temperature. The higher the critical temperature of the gas molecule, the more condensable the gas is, and the gas is more easily dissolved in the membrane [21]. The analysis for VOC permeation dependent on the VOC physical properties is discussed in detail in later Chapters. The physical properties of gas molecules, including critical temperature and boiling point, which could be used as indicators for gas absorbed in the membrane, are listed in Table 2.2.

D could describe the mobility of gas molecules traveling in free volume between polymer chains. The size and shape of molecules affect gas diffusion in the membrane. Generally, the diffusion of the gas molecules is faster if the free volume of the polymer is higher [22], and the diffusion of small gas molecules in the membrane is faster than big molecules. In VOC/N<sub>2</sub> separation, the polymer chain in the membrane could become flexible when presented in the VOCs, which is called membrane plasticization. The membrane plasticization could enhance the diffusion of gas molecules through the membrane, but on the other hand, it could cause the instability of the membrane in the application.

**Table 2.2** Properties of VOCs and nitrogen [23].

Gas molecule	Molecular weight (g/mol)	Critical temperature (K)	Boiling point (°C)	Molar volume (cm <sup>3</sup> /mole)
MTBE	88	497	55	119
Acetone	58	508	56	73
DMC	90	539	90	61
Methanol	32	513	65	41
Ethanol	46	514	78	57
N-propanol	60	537	97	75
Iso-propanol	60	236	83	77
Butanol	58	662	118	92
Pentane	72	469	36	115
N-hexane	86	507	69	131
Cyclohexane	84	554	81	109
Heptane	100	540	98	149
Isooctane	114	544	99	165
Benzene	78	562	80	89
Toluene	92	593	111	107
Xylene	106	616	139	124

The VOC and nitrogen permeation are determined by the sorption and diffusion of their molecules in the membrane. In the oleo gel membrane fabricated in this work, the sorption is demonstrated to dominate over diffusion when separating VOCs/N<sub>2</sub> mixtures, and analysis was made in later Chapters.

## 2.4 The membrane used in VOC treatment

Currently, polymeric membranes are widely used in VOC recovery. The key factor in determining the separation performance of the membrane is the material used to fabricate the selective layer of the membrane. Based on the material used in the selective layer, they can be classified into glassy or rubbery polymeric membranes. The ionic liquid membrane as the other type of membrane is also introduced in this section.

### 2.4.1 Rubbery polymeric membrane

In rubbery polymers, the gas or vapor permeation is similar to permeation in liquids because of the soft polymer chain. The gas permeation in the rubbery polymer is often dominated by sorption. Though the solubility coefficient of the gas in polymers is not a strong function of gas pressure, the solubility coefficient of a VOC in rubbery polymers often increases with pressure due to swelling.

Figure 2.8 shows the result of ten rubbery polymeric membranes on toluene/N<sub>2</sub> separation. The formula and the supplier of the polymer are listed in the table below Figure 2.8. Toluene permeability and toluene/N<sub>2</sub> selectivity at different pressures for these membranes are shown in the Figure as well. The increasing trend of toluene permeability and toluene/N<sub>2</sub> selectivity shown in the Figure is due to the increasing pressure operation. Silicone rubber, Fluorel, Hypalon, and Neoprene have relatively good VOC selectivity for VOC recovery. However, the membrane made by Hypalon is sticky and difficult to make defect-free. The Fluorel and Neoprene show better toluene permeability and toluene/N<sub>2</sub> selectivity than silicone rubber, but it is hard to make the thin film membrane. Therefore, silicone rubber becomes the first choice to make VOC recovery membranes.

Various VOCs (including acetone, 1-1- trichloroethane(TCA), trichloroethane (TCE), toluene, and xylene) have been selected to evaluate the VOC/N<sub>2</sub> or VOC/air separation performance of the silicone rubber membrane in lab studies. The membrane showed good separation performance for different VOCs [24-26]. Later, further studies were performed on silicone rubber membranes to improve their performance. Liu et al. coated poly dimethyl silicone (PDMS) on an Al<sub>2</sub>O<sub>3</sub> hollow fiber substrate and

then made the membrane modules [27]. Majumdar et al. performed plasma treatment of PDMS, and a very high chloroform recovery was achieved by the membrane. The PDMS membrane was later used to make the hollow fiber modules and module tests showed an overall 95% VOC removal from off-gas in a pharmaceutical plant and a paint booth [28, 29].

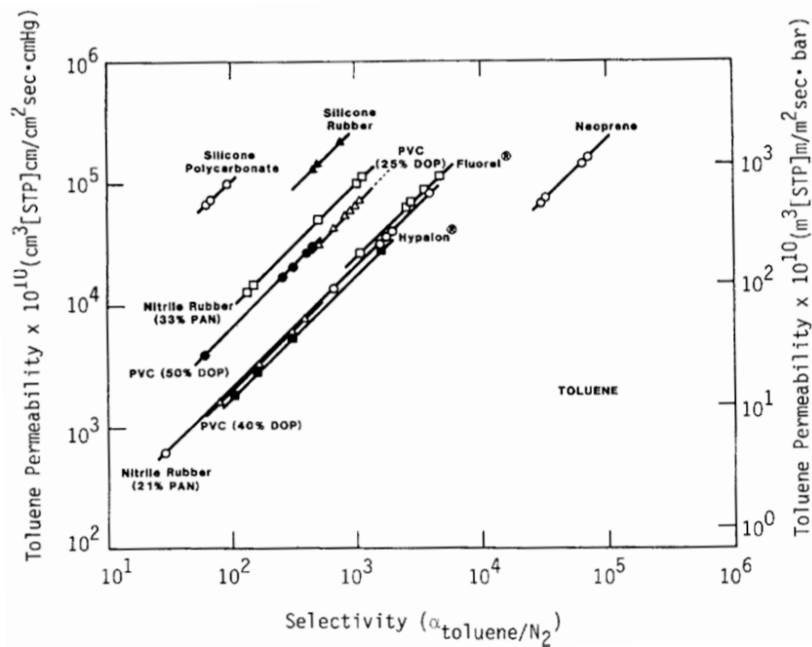
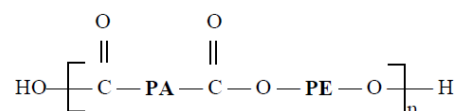


Figure notes		
Polymer	Polymer	Formula Supplier
Neoprene	$\left[ \text{CH}_2 - \underset{\text{Cl}}{\text{C}} = \text{CH} - \text{CH}_2 \right]_n$	Dupont
Hypalon	$\left[ \text{-(CH}_2\text{-CH)}_x\text{-(CH}_2\text{-CH)}_y\text{-(CH}_2\text{-CH}_2\text{)}_z\text{-} \right]_n$ $\begin{array}{c} \text{SO}_2\text{Cl} \\   \\ \text{CH} \\   \\ \text{Cl} \end{array}$	Dupont
Fluorel	$\left[ \text{-(CF}_2\text{-CF)}_x\text{-(CH}_2\text{-CF}_2\text{)}_y\text{-} \right]_n$ $\begin{array}{c} \text{CF}_3 \\   \\ \text{CF} \end{array}$	3M
Polydimethyl siloxane	$\left[ \text{Si} \begin{array}{c} \text{CH}_3 \\   \\ \text{O} \\   \\ \text{CH}_3 \end{array} \right]_n$	Dow Corning
Polyvinyl chloride (PVC)	$\left[ \text{CH}_2 - \underset{\text{Cl}}{\text{CH}} \right]_n$	Goodrich
Nitrile rubber	$\left[ \text{-(CH}_2\text{-CH)}_x\text{-(CH}_2\text{-CH=CH-CH}_2\text{)}_y\text{-} \right]$ $\begin{array}{c} \text{CN} \\   \\ \text{CH} \end{array}$	Chem Samples
Silicone polycarbonate	$\left[ \text{Si} \begin{array}{c} \text{CH}_3 \\   \\ \text{O} \\   \\ \text{CH}_3 \end{array} \right]_m \left[ \text{C} \begin{array}{c} \text{CH}_3 \\   \\ \text{O} \\   \\ \text{O} \\   \\ \text{O} \end{array} \right]_n$	General Electric

Figure 2.8 Permeability and selectivity for toluene in various rubber membranes [7].

Currently, the silicone rubber membrane has wide applications in the industry. Some applications include off-gas purification in polyolefin plants, ethylene recovery in ethylene oxide, vinyl acetate monomer production, fuel gas recovery, vapor recovery in polyvinyl chloride production, and LPG recovery in a refinery plant. More than hundreds of membrane systems equipped with silicone rubber membranes have been deployed all around the world. However, based on the permeabilities of pure gases, the VOC/N<sub>2</sub> or VOC/air selectivity of silicone rubber is often lower than its ideal gas selectivity. That is because the VOCs absorbed in the membrane tend to swell the membrane [30].

PEBA is a thermoplastic elastomer and shows better persistence than silicone rubber for VOCs absorbed in the membrane. This is because PEBA as a copolymer consists of two blocks: the polyamide block (PA) (e.g., nylon-6 and nylon-12) and the polyether block (PE) (e.g., poly(tetramethylene oxide) and poly(ethylene oxide)). The chemical formula of PEBA is as below:



The polyamide crystalline block provides mechanical strength to the polymer and makes it more rigid than the silicone rubber to prevent the membrane from getting swollen in the VOCs. Additionally, the soft polyether amorphous block offers a high permeability due to the high chain mobility of the ether linkage. Depending on the content of polyether and polyamide in the polymer, PEBA is produced in different grades which are shown in Table 2.2. The low glass transition temperature of PEBA reveals its overall rubbery features.

**Table 2.3** Polymer composition in different PEBA's [31].

Commercial name	Polymer configuration	PE content (wt.%)	Tg (°C)
PEBA 2533	Poly (tetramethylene oxide)/ Nylon12	80	-77
PEBA4033	Poly (tetramethylene oxide)/ Nylon12	53	-78
PEBA 5533	Poly (tetramethylene oxide)/ Nylon12	30	-
PEBA 1074	Poly (ethylene oxide)/ Nylon12	55	-55
PEBA 4011	Poly (ethylene oxide)/ Nylon6	57	-53

Rezac et al. [32] evaluated a series of PEBA polymers for separating methanol from the air, and PEBA 2533 was found to be the most promising in all PEBA polymers. Chen et al. [33] studied the permeation of propylene and propane in PEBA 2533 membrane, and the membrane showed high



permeability for both components. Liu et al. [34, 35] made a hollow fiber membrane comprising a PEBA 2533 skin layer supported on a microporous poly(vinylidene fluoride) substrate, confirming that PEBA 2533 is effective for recovering gasoline vapors from nitrogen and can be used as an alternative polymer to PDMS for VOC/gas separation.

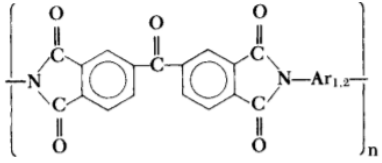
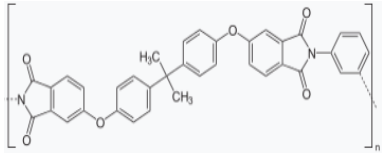
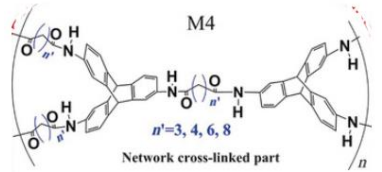
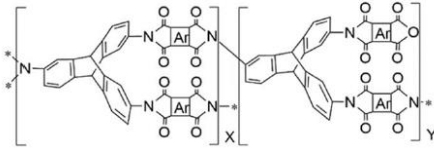
In conclusion, the membrane made of silicon rubber and PEBA 2533 showed excellent VOC permeability, and the membranes were verified to be stable in multiple test conditions with various VOCs presence. Therefore, PEBA 2533 and PDMS were the polymers selected to fabricate the oily liquid membrane for VOC/N<sub>2</sub> separation in this work. More analysis and references are shown in later chapters.

#### **2.4.2 Glassy polymeric membrane**

In glassy polymers, the chain mobility is less flexible because of the restriction of the polymer backbone. Therefore, gas perm selectivity in glassy membranes is dominated by diffusion selectivity. Glassy polymers, such as polyimide [5], intrinsic microporosity (PIMs) [36], thermally rearranged (TR) polymers [37], etc., have recently been widely studied because of their unique microstructure and excellent performance for gas separation [38]. However, glassy polymeric membranes are rarely used to separate the VOC from the stream.

There are only a few membranes based on glassy polymers for VOC separation, as shown in Table 2.4. As the backbone becomes more contorted, membranes showed more size-selective characteristics for VOC permeation. For VOC permeation in triptycene-based polyamide, as VOC molecular dimensions increase (acetone < heptane  $\approx$  hexane < cyclohexane), the VOC rejection rate increase as well. Moreover, the VOC permeation in glassy polymers is not only determined by the shape and size of molecules. For polymer PI 2080, the VOC/N<sub>2</sub> selectivity increases with VOC cohesive energy, indicating that VOC permeation through the membrane is affected by the interactions between the permeant and the membrane. The same phenomena can also be seen on aromatic polyimides and polyetherimides reported in other studies [39, 40]. Most of the polyimides mentioned above used for membrane fabrication possess a linear structure, which could limit the membrane microporosity and further impact VOC permeation. The Tri-BTDA-polyimide was synthesized and used for membrane fabrication. The microporous polymer with network structures makes the membrane show a high rejection rate for cyclohexane with a permeability of more than 2000 barrer. Currently, the glassy polymer fabricated membrane is at research stage for VOC/N<sub>2</sub> separation because the glassy polymer is used to permeate the small gas molecules and only has a few applications (e.g., H<sub>2</sub>/N<sub>2</sub> separation).

**Table 2.4** Glassy polymer used for VOC permeation.

#	Polymer structure	Polymer name	VOC/N <sub>2</sub> separation performance	Ref
1		PI 2080	VOC/N <sub>2</sub> selectivity @ 23 °C Methanol: 221 Ethanol: 196 Acetone: 41.7 Benzene: 50.5 Toluene: 179.9 Xylene: 480 Hexane: 32.4	[41]
2		PEI	VOC/N <sub>2</sub> selectivity @ 48 °C Pentane: 72.9 Pentanol: 1820	[40]
3		Triptycene-based polyamide	Rejection rate @ 24 °C Cyclohexane:99.2% Hexane: 99.1% Heptane:99 % Acetone:92.5%	[42]
4		Trip-BTDA based polyamide	Rejection rate @ 24 °C Cyclohexane:99.2% Cyclohexane permeability: 2000 ~ 2600 barrer	[43]



### 2.4.3 Supported ionic liquid membrane

By impregnating microporous support membranes with ionic liquids (IL), the supported ionic liquid membranes (SILM) are developed. Depending on the method and the membrane support selected to immobilize the IL phase, the membranes can be divided into polymeric ionic liquid membranes (PILM), hollow fiber supported ionic liquid membranes (HFSILM), and gel supported ionic liquid membrane (GSILM). They have been demonstrated to have promising performance on VOC recovery.

The imidazolium-based SILMs were extensively studied for the separation of benzene, toluene, ethylbenzene, and xylene (BETEX) from n-heptane. The total aromatic removal in the range of 40% to 70% was achieved by the membrane [44, 45]. However, SILM has one main drawback, that is, instability of IL in the pores [46]. To overcome this problem, hollow fiber-supported ionic liquid membranes (HFSILM) have been developed. Zhang et al. [47] made an HFSILM using polyvinylidene fluoride (PVDF) hollow fiber substrate. PVDF has excellent chemical stability to aromatic compounds and a good affinity to ionic liquids. The membrane was tested for 100 hrs, without instability issues. The other types of SILMs were also developed to improve IL stability in the support membrane. By mixing the IL with the dope solution during membrane formation, the IL is well dispersed and immobilized into the polymeric matrix, resulting in a homogeneous membrane. Depending on the composition of membrane solution, polymeric ionic liquid membranes (PILM) and gel supported ionic liquid membranes (GSILM) can be fabricated.

Ionic liquids are considered an alternative to organic solvents for VOC sorption or VOC separation because they have negligible vapor pressure, adaptability to the membrane substrate, and high selectivity to selected VOCs. However, they still pose many risks to aquatic and terrestrial environments. Further development and widespread use of ionic liquid could raise the risk of accidental discharge and contamination. Several works have proved the toxicity of ionic liquids to organisms and trophic levels, so they are still not being used at an industrial scale for VOC separation [48]. ILs only have a good selective separation to specific compounds; thus, modification for ionic salts is required by varying the anion and cation in their structure to achieve good selectivity to specific VOCs. The high price for those materials is the main limitation for the ionic liquid to be widely used [49]. The complexity of membrane solution preparation is the other drawback of the use of ILs for membrane application. The two of the most common cations present in ionic salt and ILs used for VOC recovery are imidazolium and pyridinium. Salt synthesis requires multiple steps,

including the quaternization reaction, anion exchange reaction, filtration, pre-treatment and post-treatment for the materials, which easily take a few days to complete [49, 50].

In this work, ILs are replaced by oils to develop the supported liquid membranes. The oils are cheap and easy to purchase from the market, which overcomes the shortcoming of high cost, difficult synthesis and environment unfriendly aspects in ILs. Various oleophilic membranes, including oleo gel dense membrane, supported oil liquid membrane and supported oleo gel membrane, were developed in this work.

## 2.5 Membrane vapor/gas separation process

Both glassy polymer and rubbery polymer have been used to fabricate the membrane for vapor gas separation. Because of the low flux for glassy polymeric membranes, the membrane made in the rubbery polymer is more widely used in the vapor/gas separation process. Membranes designed in multiple stages and incorporated with other technologies are widely adopted in the vapor/gas separation process.

### Membrane separation process on light hydrocarbon treatment

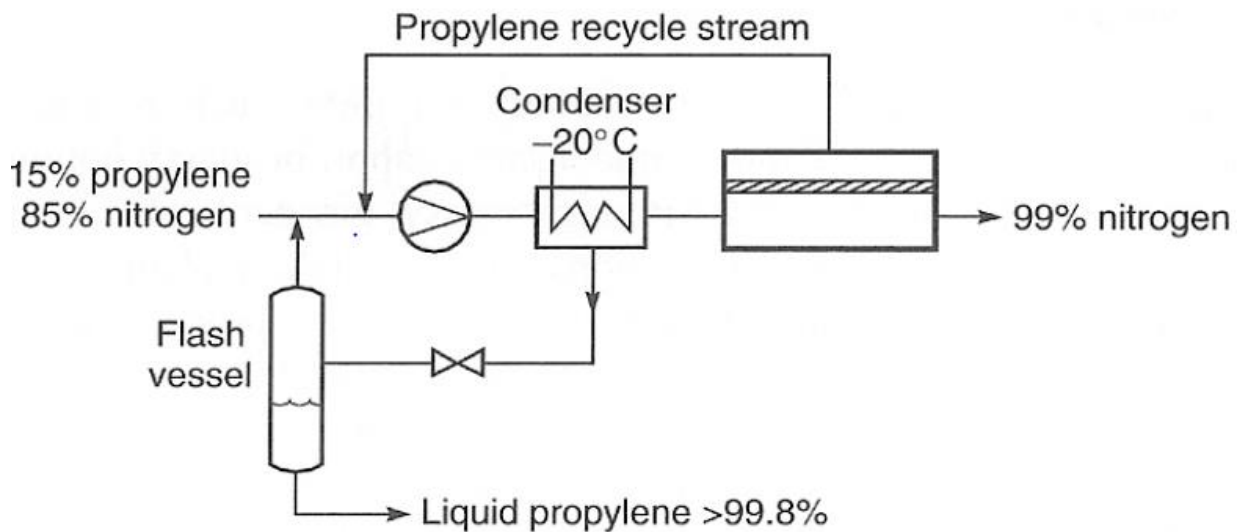


**Figure 2.9** A hybrid membrane process to recover propylene in propylene/nitrogen mixture from vent line in polypropylene plant [2].

The hydride membrane process to recover the olefin from the venting line is one of the most successful membrane applications. The olefins recovered here are mainly light hydrocarbons like ethylene, propylene, and butene, which is the feedstock for the polyolefin plant. Figure 2.9 shows the

process to recover the propylene from the vent gas in the polypropylene plant. The compression and condensation are incorporated in the process.

The composition of the feed gas to membrane process contains 15% propylene and 85% nitrogen. The stream is compressed after the compressor and most of the propylene is condensed at a low temperature in the flash vessel. The nitrogen and remaining propylene mixture feed into the membrane, and then the propylene is separated from nitrogen. Silicone rubber is the membrane used in the process in which the condensable gas permeates faster than the non-condensable gas, and the nitrogen is collected in the residue side at high pressure with purity at 99%. The pure recycled nitrogen is sent to the purge bin to flash the polypropylene particles, which could significantly help the plant save on nitrogen consumption in the purging process. The olefin in the permeate is recycled back to the suction side of the compressor to enrich the propylene concentration in the stream as it travels to the compressor and condenser. By enhancing the hydrocarbon concentration in the stream, the cost of the compressor and condenser could significantly decrease.

### Membrane separation process on heavy hydrocarbon (VOC) treatment

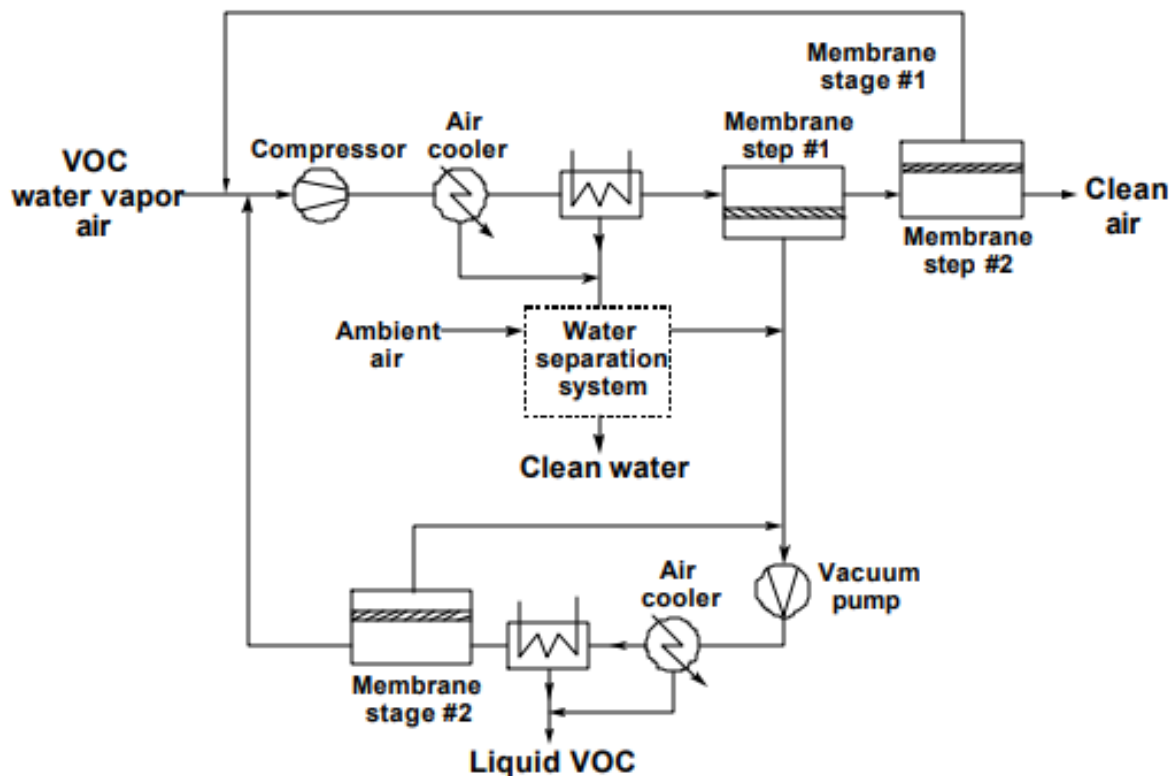


Figure 2.10 A hybrid membrane process to remove the VOC from the off-gas [51].

When hydrocarbon becomes heavy, it becomes a liquid phase at room temperature and atmospheric pressure. Those hydrocarbons are called VOC, and the carbon number in its chemical formula is usually more than five. Figure 2.10 shows the hybrid membrane process to remove the VOC from the off gas. The off gas as the feedstock to hybrid membrane process contains 1% to 2% water vapor, 0% to 2% VOCs, and the rest of the gas in the stream is air.

The membrane process has two steps and two stages. At the first stage, the mixture is compressed to 190 psia, and the water and VOC are condensed after the air cools. A small air stripper removes the VOCs from the condensed water, and the air and VOC mixture is sent and mixed with the permeate stream from the membrane at the first step. The mixture from two streams is recompressed to 80 psia after the vacuum pump. After the cooling, the VOC, as the liquid, is condensed out, and the remaining mixture is sent to the membrane at the second stage. The permeate stream from the membrane at the second stage enriches the VOCs and returns it to the suction side of the vacuum pump. The residue stream from the membrane at the second stage is air enriched and returned to the beginning of the process to do further VOC removal. The feed stream for the membrane at the second step contains a few amounts of VOCs. After the VOCs are further removed by the second step membrane, the VOC enriched permeate stream is recycled back to the suction side of the compressor to redo the VOC cooling and condensing process. The residue stream at the second step is the clean air.

The membrane with higher VOC permeability and VOC/air selectivity is required by the above process. The product purity in the permeate stream is high in the membrane with good selectivity, which makes the product meet the purity requirement; thus, the compressor will be not required in the process to compress the permeate for further purification. Hence, it could help save one step in membrane process design or decrease the size of the compressor and condenser in design.

## Chapter 3

### PEBA/DEHP oleo gel membrane for VOC/N<sub>2</sub> separation

#### 3.1 Introduction

Volatile organic compounds (VOCs) are hazardous air pollutants recognized by the United States Environmental Protection Agency (US-EPA) [52]. VOC emissions have been a severe problem to the environment and human health in the past few decades [49]. Various technologies, i.e., carbon adsorption, condensation, and incineration, have been developed to capture and recover VOCs from the off-gas. As an alternative technology, membrane separation has attracted increasing attention due to its low power consumption, environmental friendliness, and good VOC recovery performance, especially at relatively high VOC concentration (> 0.1 vol%) [5, 19, 53].

Non-porous membranes, the typical membrane used in VOC/N<sub>2</sub> separation, are made of rubbery polymer and glassy polymer (e.g., PDMS and polyimide) [2, 34, 42, 54, 55]. There may be a significant mass transfer resistance in the non-porous membrane, and an elevated pressure is required for the adequate removal efficiency for VOCs [44, 56]. Moreover, the trade-off relation between permeability and selectivity is also recognized in polymeric non-porous membranes. In other words, polymers that are more permeable for gases generally have less selectivity and vice versa [57, 58]. Polymers with high gas permeability and selectivity are desirable in the industry. This is because high permeability could decrease the membrane area required by the process, while high selectivity could result in high purity. The fabrication of supported liquid membrane by incorporating liquid into a polymer matrix or micropores of a support membrane has been recognized as a good strategy to improve both VOC permeability and selectivity simultaneously [46, 59]. Ionic liquid (IL), a group of salts that exist in liquid form at relatively low temperature (<100°C) [60], is an extensively studied incorporating liquid used in supported liquid membranes [59, 61, 62]. The anion and cation in IL could be varied in different combinations to modify the structure of IL to achieve both expected permeabilities and selectivities to VOCs. However, each given combination of cation and anion in IL can only help to improve the separation performance for specific VOC. For example, 1-butyl-3-methyl imidazolium, [bmin][PF<sub>6</sub>], and [Et<sub>2</sub>MeMeON][Ntf<sub>2</sub>] have a high solubility to aromatic hydrocarbons, but a low solubility to heptane and hexane [44]. Besides, the materials for making the IL are usually expensive [49], and the process for salt synthesis is complicated and time-consuming,



which normally takes a few days [49, 50]. In addition, the toxic and biodegradability of the IL also limit its use as a membrane material at an industrial scale [48]. Oil, another commonly used liquid in membrane fabrication, has become attractive to researchers. Ozturk et al. [63] developed a supported oil liquid membrane by impregnating vegetable oil and lubricating oil in cellulose acetate. However, limited VOC/N<sub>2</sub> separation data was reported as only benzene, tetracarbon chloride, and methanol were tested and a short test period of only 36 hrs was applied. Ito et al. [56] immobilized triethylene glycol (TEG) in microporous support with double layers of polytetrafluoroethylene (PTFE) and Durapel membrane (Millipore), but the membrane barely shows VOC/air separation performance that is competitive to the traditional silicon rubber membrane.

Bis (2-ethylhexyl) phthalate (DEHP) is a colorless viscous liquid that is soluble in oil. It has the following properties that make it more attractive than previously reported oil adopted to make oil liquid membrane on VOC /N<sub>2</sub> separation: (i) high boiling points and low volatility, (ii) high diffusion and sorption coefficient [64] (iii) a common plasticizer used in the plastic industry which may improve the gas diffusion [65]. Poly(ether block amide) (PEBA 2533), a block copolymer, which combines the advantages of rubbery and glassy polymers, has been widely and systematically evaluated for VOC/N<sub>2</sub> separation [34, 35]. The PEBA membrane shows comparable VOC/N<sub>2</sub> separation performance to PDMS and good stability. Even though VOC permeation in PEBA was refrained by rigid glassy polyamide, PEBA was still treated as an alternative to silicon rubber for VOC/N<sub>2</sub> separation.

In this study, DEHP oil was gelled in the PEBA network to make oleo gel membranes. The amine and hydroxyl groups are hydrogen bond donors, and carboxyl groups are hydrogen bond acceptors in PEBA [66, 67]. Those intermolecular hydrogen bonds in PEBA allow it to have a torsional structure to retain the DEHP oil. The carboxyl group in the DEHP oil could also form hydrogen bonds with the amine and hydroxyl group in PEBA, and the ether group in DEHP oil may form hydrogen bonds with the hydroxyl group in PEBA, leading to good oil dispersion and stable immobilization in the polymer matrix at the molecular level [68]. Moreover, the aromatic rings in the DEHP may improve its affinity to PEBA and thus, enhance its immobilization in the PEBA matrix [69].

VOCs are a wide variety of organic compounds, and VOCs emitted into the air are mainly naphtha and other compounds with complex compositions based on EPA's reports [7, 70]. To compare membrane performance for VOC/N<sub>2</sub> separation, 16 common VOCs from four groups were used in this study: alcohols (methanol, ethanol, propanol, isopropanol, and butanol); paraffin (pentane, hexane, cyclohexane, isooctane, and heptane); aromatic compounds (benzene, toluene, and xylene); and fuel additives (methyl tert-butyl ether (MTBE), dimethyl carbonate (DMC), and acetone).

Membranes with different DEHP oil content were fabricated and tested for VOC permeability and VOC/N<sub>2</sub> selectivity. All of the prepared membranes showed better performance than PEBA membranes, and it was demonstrated that the higher the DEHP content in the membrane, the better the VOC/N<sub>2</sub> separation performance. The effects of feed VOC concentration and temperature on the membrane performance for VOC/N<sub>2</sub> separation were also investigated. All prepared membranes were stable in long-period tests for VOC separation from nitrogen.

## **3.2 Experiment**

### **3.2.1 Material**

Poly (ether block amide) (PEBA 2533) was provided by Arkema Inc. (Philadelphia, PA) and comprised of 80 wt.% poly (tetramethylene oxide) (PTMO) and 20 wt.% polyamide-12 (PA-12). Bis (2-ethylhexyl) phthalate (DEHP) was purchased from Sigma Aldrich. All solvents used in membrane preparation and VOC separation experiment were reagent grade. N, N-dimethylacetamide (DMAc), methyl tert-butyl ether (MTBE), dimethyl carbonate (DMC), n-hexane, cyclohexane, and xylenes (mixed isomers) were obtained from Sigma-Aldrich (St. Louis, MO). N-Pentane and n-heptane were acquired from VWR international LLC (West Chester, PA); while Acetone, methanol, ethanol, n-propanol, isopropanol, butanol, isooctane, benzene, and toluene were provided by Fisher scientific (Billerica, MA). The purity of all gases used in the permeation experiment was at least 99.9%; Nitrogen, oxygen, methane, and carbon dioxide were purchased from Praxair Specialty Gases and Equipment.

### **3.2.2 Membrane preparation**

The membranes were prepared by the solvent casting method. PEBA 2533 and DEHP at desired ratio were dissolved in DMAc to prepare the membrane casting solutions. The homogeneous solution was obtained by stirring vigorously at 80°C for 10 hr and was then placed in the oven at 70°C for 12hrs to remove gas bubbles. Finally, the solution was cast onto a glass plate and kept at 70°C for 48 hrs to allow the solvent to evaporate completely.

### **3.2.3 Membrane characterization**

The surface of membranes was characterized by a scanning electron microscope (FEI Quanta Feg 250 ESEM). The melting point of membranes was determined by a differential scanning calorimeter (DSC-Q2000 with RCS90 refrigeration system) by heating the samples from -80 to 200°C at a heating rate of 10°C/min in N<sub>2</sub> atmosphere. The thermal characterizations were conducted on a thermal gravity analyzer (SDT-Q600) by heating the samples from room temperature (RT) to 800 °C

with a heating rate of 10°C/min in the N<sub>2</sub>. The fourier transformation infrared spectra (FTIR) were measured by the Bruker-VERTEX 70. Membrane structure characterizations were performed by X-ray powder diffraction measurement (Bruker-D8) with Cu K $\alpha$  radiation ( $\lambda = 0.15406$  nm). Lastly, mechanical properties determinations of membranes were carried out by Instron 4465 tensile and compression tester equipped with Bluehill software.

### 3.2.4 Permeation experiment

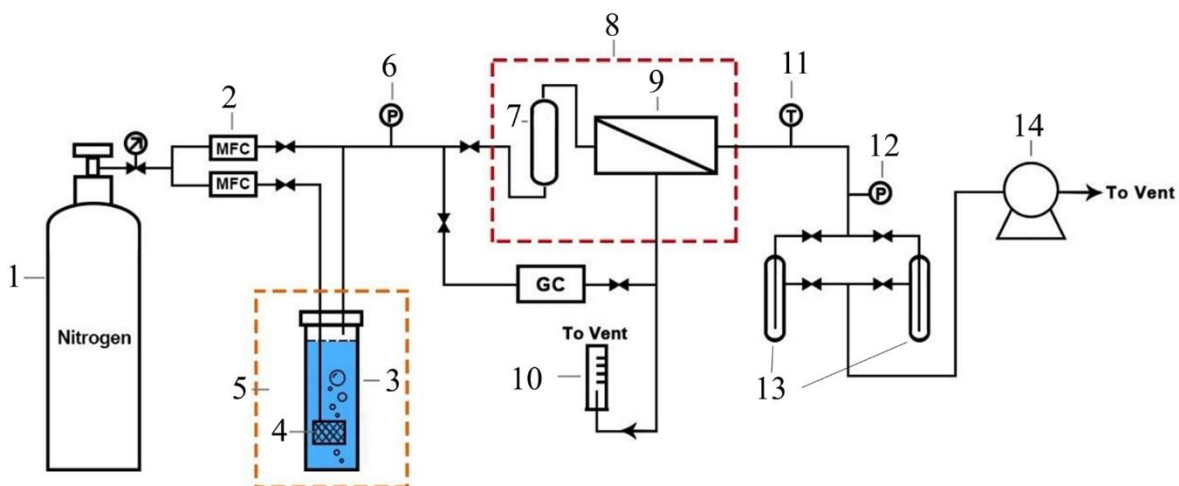


**Figure 3.1** Schematic diagram of the experimental setup used for the VOC permeability test. (1) nitrogen cylinder, (2) mass flow controller, (3) VOC liquid reservoir, (4) porous gas diffuser, (5) thermal bath, (6) pressure gauge, (7) vapor/gas mixer, (8) water bath, (9) membrane cell, (10) bubble flow meter, (11) temperature gauge, (12) vacuum pressure gauge, (13) cold trap, (14) vacuum pump.

The setup used to evaluate the membrane VOC/N<sub>2</sub> separation performance is illustrated in Figure 3.1. The VOC/N<sub>2</sub> mixture was generated by bubbling nitrogen through a porous gas diffuser made in stainless steel and immersed in the VOC liquid. The VOC liquid was in the reservoir placed in a thermal bath to maintain the VOC/N<sub>2</sub> mixture at a specific temperature. By adjusting the flow rates of two mass flow controllers, the streams with the mixture of VOC/N<sub>2</sub> at different ratios could be obtained. Before the mixture was supplied to the membrane cell, it was sent to a vapor/gas mixer to ensure the VOC and N<sub>2</sub> were well mixed. The vapor/gas mixer and membrane cells were also thermal-regulated with an accuracy of  $\pm 0.5^\circ\text{C}$ . The feed flow rate was recorded by the mass flow controller. The gas rejected by the membrane was on the residue side of the membrane, and the residue stream was sent to the bubble flow meter to measure the flow rate before venting. The compositions of VOC in the feed and residue streams were measured by a Varian CP 3800 gas

chromatograph equipped with a thermal conductivity detector and a 60-m long capillary column. A vacuum pump was applied at the permeate side of the membrane. The permeate pressure was monitored using a vacuum gauge (Supco V664), and the pressure was measured to be below 0.5 kPa. The gas/vapor mixture permeated through the membrane was condensed and collected in cold traps and then weighted to calculate the permeate flux. The membranes were tested under different operation conditions. The tests at each condition were carried out at least three times. A test period of more than 20 minutes was applied for each experiment to ensure the data was collected at a steady state. The average values were presented as the test result.

### 3.2.5 Pure gas permeance measurement

Pure nitrogen permeance was measured at a feed gauge pressure of 0.4MPa and keeping permeate pressure at 1atm. Permeate flow rate was measured by the bubble flow meter. The detailed calculation was introduced in Section 2.33. The pure gas permeance for O<sub>2</sub>, H<sub>2</sub>, CH<sub>4</sub>, and CO<sub>2</sub> was also determined.

### 3.2.6 VOC/N<sub>2</sub> separation performance characterization

The VOC/N<sub>2</sub> separation performance of the membranes was calculated as below [34, 35]. The flux of VOC through the membrane,  $Q_{VOC}$ , is determined by:

$$Q_{VOC} = \frac{W_{voc}}{tS} \quad (3.1)$$

where  $W_{voc}$  is the weight of the VOC collected in the permeate over a period of t, and S is the effective area of the membrane, which was 15.9 cm<sup>2</sup>.

The set of equations (3.2) to (3.4) need to be solved to determine the permeability of the VOC ( $P_{voc}$ ) and N<sub>2</sub> ( $P_{N_2}$ ):

$$P_{VOC} = \frac{Q_{voc}L}{M_{VOC}(P_F X - P_P Y)} \quad (3.2)$$

$$Y = \frac{Q_{voc} M_{N_2}}{Q_{voc} M_{N_2} + Q_{N_2} M_{VOC}} \quad (3.3)$$

$$P_{N_2} = \frac{Q_{N_2} L}{M_{N_2} [P_F (1-X) - P_P (1-Y)]} \quad (3.4)$$

where L is the membrane thickness, X and Y are mole fractions of the VOC in the feed and permeate, respectively.  $P_F$  and  $P_P$  are the feed and permeate pressure.  $Q_{voc}$  and  $Q_{N_2}$  are the permeate flux of VOC and nitrogen.  $M_{N_2}$  and  $M_{VOC}$  are the molecular weight of VOC and nitrogen, respectively. The differences in nitrogen permeability in the presence of different VOCs are considerably small, and they are close to pure nitrogen permeability [41]. Therefore, pure nitrogen permeability was used in

the calculations. Nitrogen flux, VOC permeate concentration, and VOC permeability are unknown values that can be obtained by solving the above equations.

All calculated results for VOC/N<sub>2</sub> separation performance evaluation were presented in average. The detailed calculation and error analysis were discussed in Section A.2 Sample calculations for mixed gas permeation.

### 3.3 Results and discussion

#### 3.3.1 Characterization of oil content in the membrane

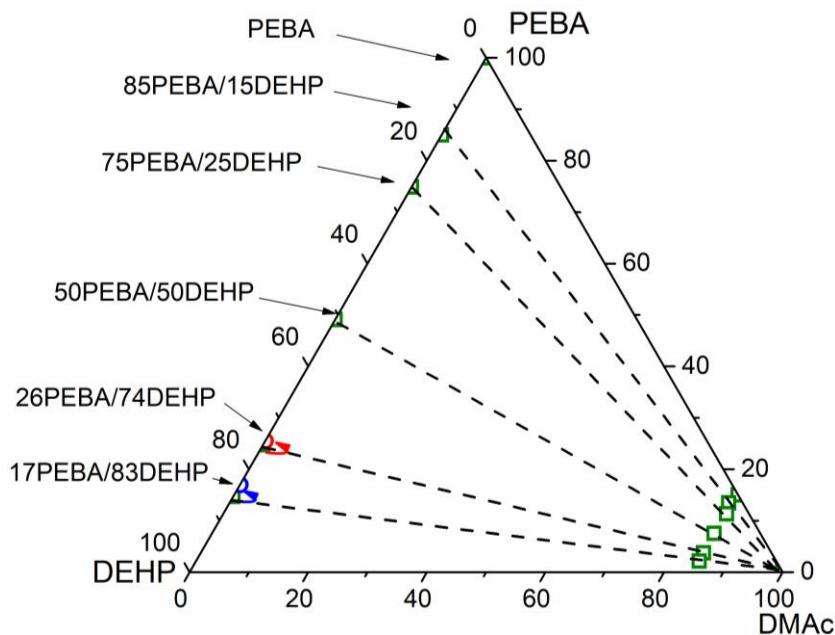


**Figure 3.2** The content of PEBA and DEHP in the membrane casting solution (wt.%) vs. the content of PEBA and DEHP in the membrane (wt.%); membranes are named as PEBA/DEHP content in the membrane and labeled on the left of the Figure.

Before the membrane fabrication, the weight of the components in the membrane casting solutions, including PEBA, DEHP, and DMAc, were measured along with the weight of the membranes after removing the saturated oil on the surface. The content of the DEHP oil immobilized in the membrane could be calculated based on the membrane weight and the total weight of PEBA and DEHP added in the membrane casting solutions. Figure 3.2 shows the component weights in the membranes and membrane casting solutions in the unit of wt.%. The green points at the right side of the Figure show that PEBA and DEHP were blended at different ratios and the total amount of PEBA and DEHP were kept at 15 wt.% in the casting solution. After the DMAc is evaporated during the membrane

formation, the points move along with the dashed lines to the left side boundary of the Figure to signify a DMAc concentration in the solution of 0%. In other words, the points on the left boundary indicate the PEBA and DEHP content in the resultant membranes. Moreover, some oil was saturated out during the solvent evaporation and membrane formation for the membranes with high DEHP content. As a result, the amount of DEHP in these membranes is smaller than what was dissolved in the casting solution. The amount of DEHP content in the casting solution is the total amount of DHEP oil used in membrane fabrication, including the oil-saturated out. The resultant points on the left boundary shift toward a higher PEBA content, as shown by the red and blue arrows in Figure 3.2.

The membranes were named according to the contents of PEBA and immobilized DEHP oil in the membrane. For example, 26PEBA/74DEHP has 26wt.% PEBA and 74wt.% DEHP in the membrane. The amount of oil saturated out from the membrane was then calculated. The oil saturated out from membranes 26PEBA/74DEHP and 17PEBA/83DEHP are respectively 0.6 wt.% and 2.5 wt.% out of the total oil used in membrane fabrication.



**Figure 3.3** Image of transparent membranes: (A) PEBA, (B) 85PEBA/15DEHP, (C) 75PEBA/25DEHP, (D) 50PEBA/50DEHP, (E) 26PEBA/74DEHP and (F) 17PEBA/83DEHP.

Figure 3.3 shows that all membranes are homogeneous and transparent, and the saturated oil wiped from 26PEBA/74DEHP and 17PEBA/83DEHP is observable on papers, as can be seen in Figure (E) and (H).

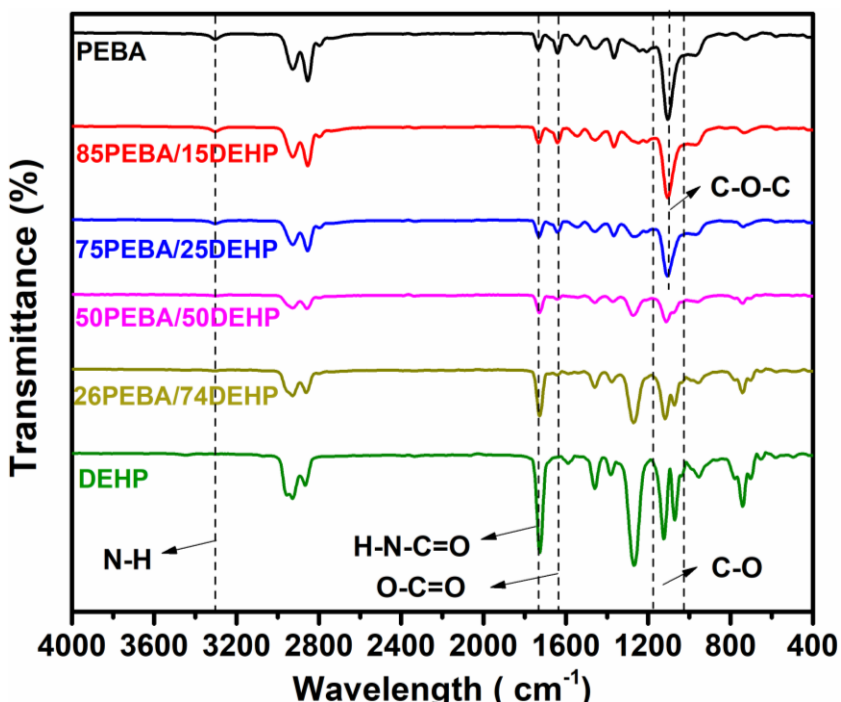


Figure 3.4 FTIR spectra of PEBA/DEHP oleo gel membranes.

PEBA/DEHP oleo gel membranes were characterized by FTIR to confirm that oil was successfully immobilized in the membrane. References such as PEBA membrane and DEHP oil were characterized as well. The adsorption peaks observed at  $3290\text{ cm}^{-1}$  and  $1640\text{ cm}^{-1}$  correspond to the stretching vibration peak of N-H and C=O (in O-C=O) in the PA group of PEBA [71, 72]. C=O (in H-N-C=O) is at the end of the PEBA polymer chain and its peaked is at  $1735\text{ cm}^{-1}$  [73]. The peak at  $1106\text{ cm}^{-1}$  is the stretching vibration of the ether bond (C-O-C) corresponding to the PTMO group in PEBA [74]. The hydrogen bond forms between the C-O group in DEHP oil and O-H group in PEBA [68], resulting in the peak of C-O shifting in spectra from PEBA to the DEHP oil. The aromatic ester in the DEHP molecule makes a signified C-O band [75] in a range of  $1072\sim 1250\text{ cm}^{-1}$ . As the oil content of 0% in PEBA increases to 100% in DEHP oil (from spectra PEBA to DEHP), the peaks of N-H and C=O (in H-N-C=O) in the PA group of PEBA become smaller until they gradually disappear, the peak of C-O (in O-C=O) in DEHP oil becomes stronger, and the peak of C-O in PEBA at  $1106\text{ cm}^{-1}$  gradually moves to the spectra range of  $1072\sim 1250\text{ cm}^{-1}$  for DEHP. Therefore, the

spectra changes in the PEBA/DEHP oleo gel membranes (OLGMs) are affected by oil content in the membrane and further indicate that the DEHP oil was successfully imobilized in the PEBA matrix

### 3.3.2 Physical properties of OLGMs

The second scan of DSC thermograms for PEBA/DEHP OLGMs is shown in Figure 3.5 (A), and all tested OLGMs showed two melting peaks. The peak at the lower melting point could be ascribed to the PTMO block, while the high-temperature peak could be ascribed to the PA block. As can be seen from the figure, the melting temperatures for both PTMO and PA decrease as the oil content in OLGMs increases. Pure PEBA membrane was characterized as a reference showed similar melting temperatures (10°C for PTMO and 139°C for PA) with reported literature [76].

As an indication of the degree of long-range order in material, crystallinity is regarded as an important factor in characterizing a membrane. The membrane with a higher crystallinity tends to have a more regular and ordered structure, thus possessing stronger hardness. The results shown in Figure 3.5 (A) could be utilized to calculate the membrane crystallinity based on Equation 3.5 below. As the permeation measurement was conducted at 22 °C, which is well above the melting point of the PTMO block, only the crystallinity of the PA-12 was included in the calculation

$$X_c = \frac{\Delta H_f}{\omega_{PA} \Delta H_f^0} \quad (3.5)$$

where  $X_c$  is the crystallinity of membrane,  $\Delta H_f$  is the enthalpy fusion of the PA phase in OLGMs (J/g), which could be integrated from Figure 3.5 (A).  $\Delta H_f^0$  is the enthalpy of fusion of PA-12 (PA-12=246 J/g) [77], and  $\omega_{PA}$  is the weight percent of PA presenting in the OLGMs. The calculated results of the crystallinity and enthalpy fusion of PA ( $\Delta H_f$ ) are shown in Figure 3.5 (B). As can be seen from the figure, the crystallinity of OLGM decreases with the increase of oil content. As a result, the OLGMs are expected to show a weaker hardness than the PEBA membrane, which will be elaborated on later in the mechanical property study.



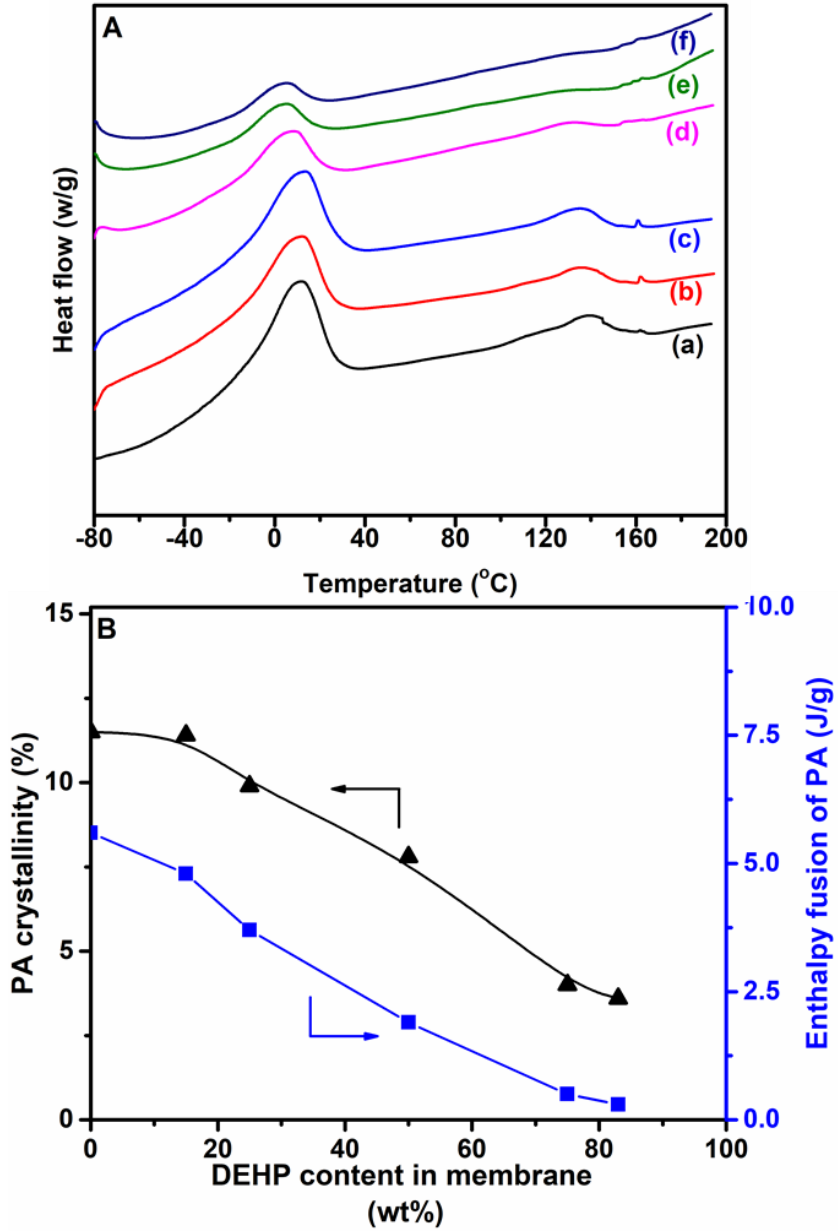


**Figure 3.5** DSC measurement on PEBA/DEHP OLGMs. (A) DSC thermograms: (a) PEBA, (b) 85PEBA/15DEHP, (c) 75PEBA/25DEHP, (d) 50PEBA/50DEHP (e) 26PEBA/74DEHP and (f) 17 PEBA/83DEHP; (B) The crystallinities of PA in OLGMs.

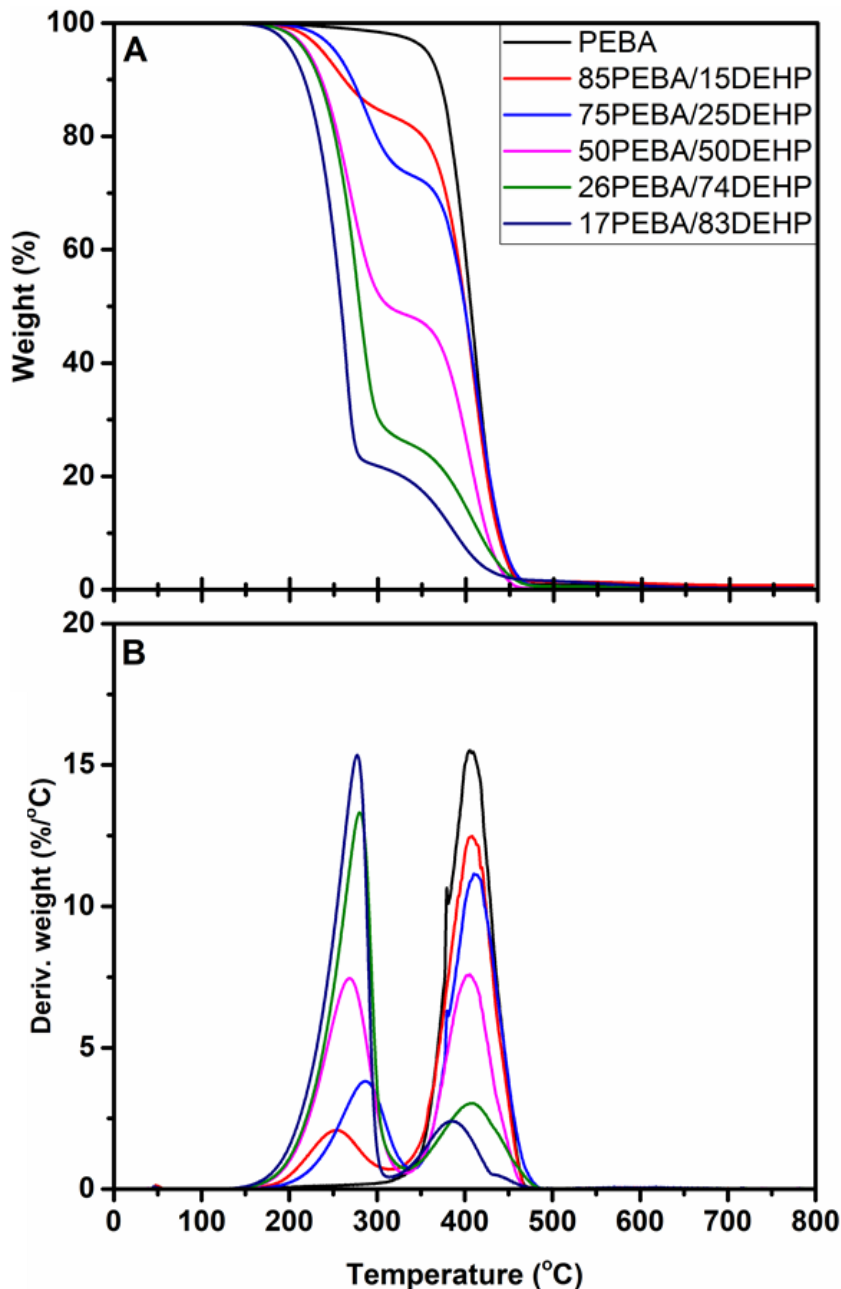


**Figure 3.6** Thermal property analysis of the OLGMs. (A) thermogravimetric analysis(TGA) curves, (B) derivative thermogravimetric (DTG) curves.

The thermal degradation graph of PEBA/DEHP OLGMs in Figure 3.6 (B) shows that the maximum weight loss rates are at 280°C and 440°C, which could be attributed to the degradation of DEHP and PEBA, respectively. As shown in the figure, the DEHP oil starts to degrade at around 150°C and vaporize at 323°C, which agrees with the data reported elsewhere [78]. As DEHP content in membranes increases, the degradation peaks of DEHP become stronger. Once DEHP content surpasses 50wt.%, the degradation peak of DEHP is more prominent than that of PEBA. The

decompositions for PEBA and DHEP can also be seen in Figure 3.6 (A); the first decomposition at 280 °C is attributed to the DEHP oil, while the second decomposition at 440°C is caused by PEBA. It is also observed that an increasing DEHP oil content in the membrane can cause decreases in both initial and second decomposition temperatures, details of which are shown in Table 3.1.

As can be seen from the table, adding 15% oils in PEBA caused a significant drop of initial decomposition temperature from 370 to 280 °C, and the trend then leveled off by adding more oils. The differences in the second decomposition temperatures of membranes are small, which means the oil has little effect on the thermal properties of the PEBA material in the OLGMs. The PEBA/DEHP OLGMs show overall degradation temperatures higher than 240°C, which is attributed to the high degradation temperature of PEBA and low volatility of the DEHP oil. The thermal stability of the prepared OLGMs is sufficient for VOC recovery since the operating temperatures for most of the VOC recovery process are room temperature. Moreover, weight loss in the membranes at 350°C in Figure 3.6 (A) also represents the weight of DEHP oil immobilized in the membrane, and the results of weight loss are summarized in Table 3.1. As can be seen, the results have a good coincidence with the oil content calculated from weight measurement in the previous section. The thermal property analysis by TGC further confirms the accuracy of the weight-based oil content measurement and offers a new method to evaluate the oil content in OLGMs.

**Table 3.1** Results of thermal analysis for OLGMs.

Membrane name	initial decomposition temperature (°C)	2 <sup>nd</sup> decomposition temperature (°C)	Weight lost @350°C (wt.%)
PEBA	370	X	0
85PEBA/15DEHP	280	355	16.04
75PEBA/25DEHP	285	355	25.15
50PEBA/50DEHP	252	350	51.14
26PEBA/74DEHP	253	345	75.80
13PEBA/87DEHP	240	340	83.37

### 3.3.3 Morphology studies of OLGs

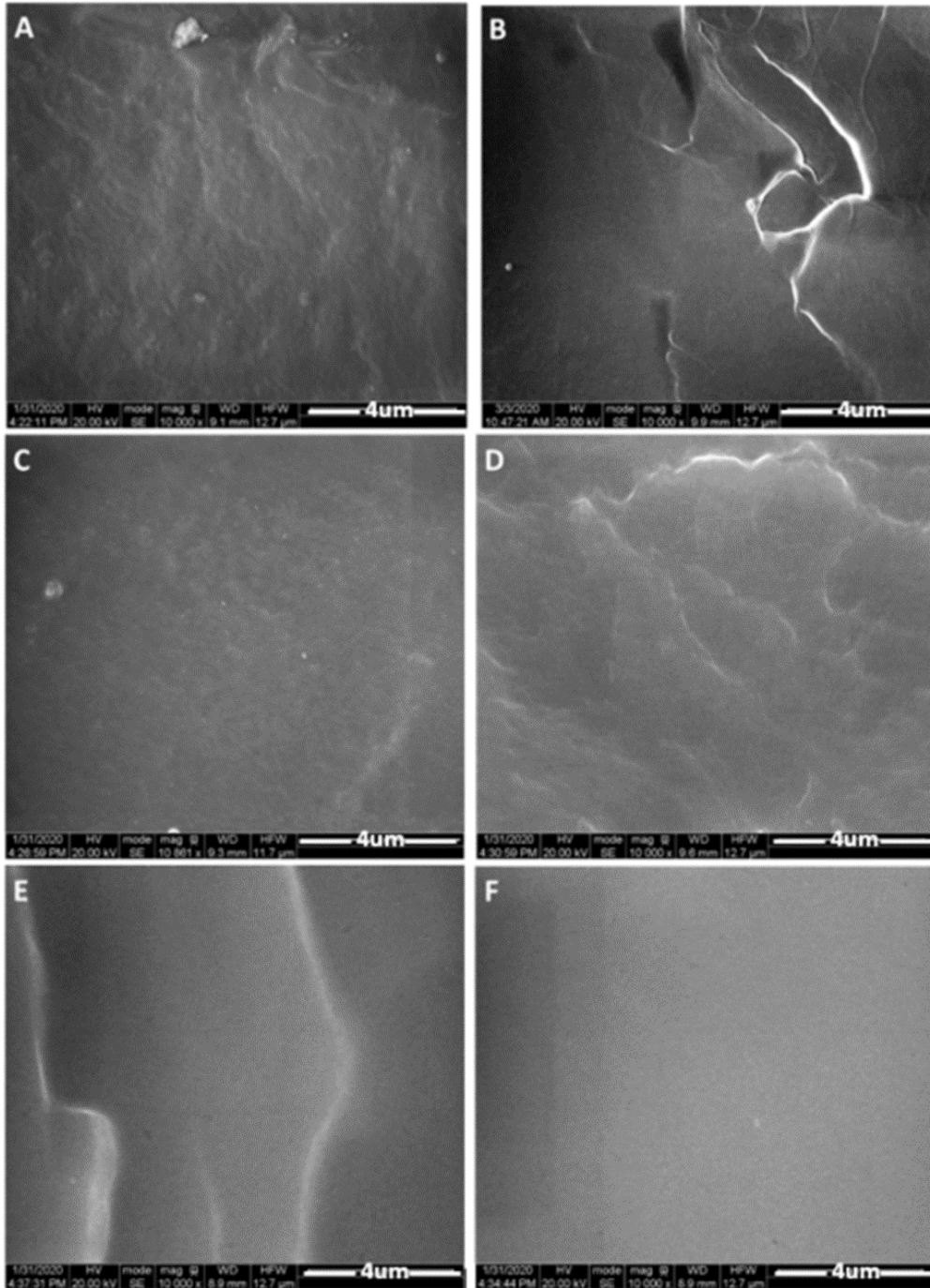


**Figure 3.7** The cross-section SEM image of PEBA/DEHP OLGs. (A) PEBA, (B) 85PEBA/15DEHP, (C) 75PEBA/25DEHP, (D) 50PEBA/50DEHP, (E) 26PEBA/74DEHP, and (F) 17PEBA/83DEHP.

The cross section of the OLGMs are scanned under the SEM, and the images are shown in Figure 3.7. As can be seen, the cross-section of the prepared membrane is dense and homogenous, indicating that PEBA and DEHP oil are well miscible. As the oil content of the DEHP increases in the membrane, the cross-section of the membrane becomes smoother. The physical properties analysis in the previous part proved that DEHP oil was successfully immobilized in OLGMs. Here, these SEM images are evidence that DEHP oils are well dispersed in the PEBA polymer matrix.

### 3.3.4 Mechanical property study

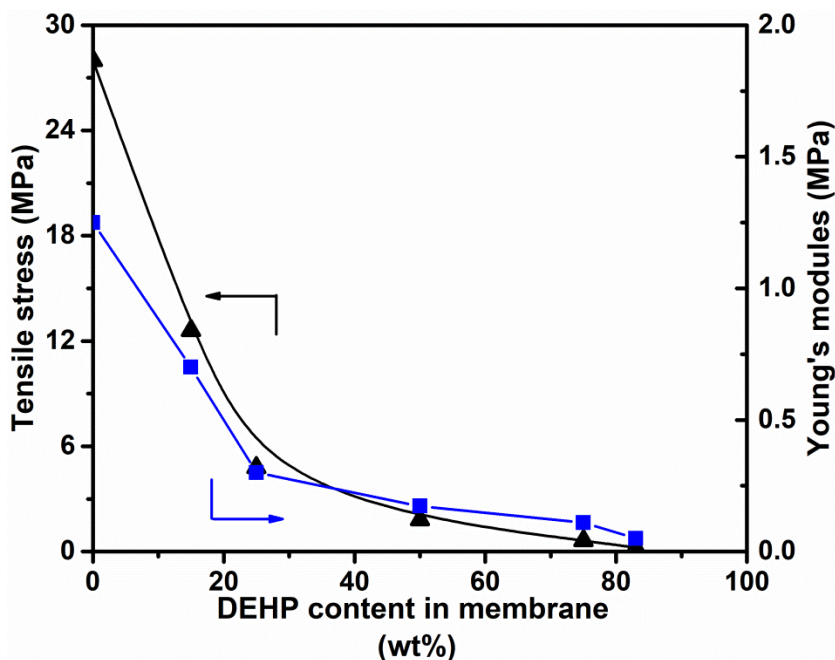


**Figure 3.8** Mechanical properties of the PEBA/DEHP OLGMs.

The mechanical property is one of the most important factors that could be used to evaluate the feasibility of applying the membrane in the industry. In this study, the tensile stress and Young's modulus of the PEBA membrane and PEBA/DEHP OLGMs were measured to evaluate their mechanical properties, and the results are presented in Figure 3.8. Tensile stress indicates the resistance of the material against the deformation. Young's modulus quantifies the relation between the tensile stress and strain, and measures the tensile stiffness when the force is applied to the material. As can be seen, PEBA membrane shows tensile stress of 27 MPa and Young's modulus of 1.3 MPa, which are in agreement with the data in reported literature [79, 80]. It could also be noticed that the tensile stress of the membrane decreases with the increase of DEHP loading. This is expected since the content of PEBA becomes lower when DEHP content in the membrane increases and PEBA acts as the mechanical support in the membrane to immobilize the oil. Moreover, Young's modulus of

the membrane also decreases with the increase of DEHP oil content, indicating the membrane becomes softer with more immobilized DEHP oil [81].

It is worth mentioning that Young's module of the membrane decreases slower than that of the tensile stress. This is because the strain of the membrane also decreases with the increase of DEHP loading. However, the decrease of the strain is slower than that of the tensile stress.

In the pure gas and VOC/N<sub>2</sub> mixture gas separation evaluation, the 17PEBA/83DEHP with tensile stress of 0.2 MPa and Young's module of 0.05 MPa showed no selectivity to the selected gases, and the permeate flux of the membrane was high. This might be attributed to the weak mechanical property caused by the high content of DEHP, which may cause defects on the membrane. Therefore, other five membranes with lower DEHP content, including 26PEBA/74DEHP, 50PEBA/50DEHP, 75PEBA/25DEHP, 85PEBA/15DEHP, and pure PEBA membrane, were selected for the further comprehensive gas permeation evaluation.

### 3.3.5 Effect of oil content in the membrane on gas permeation

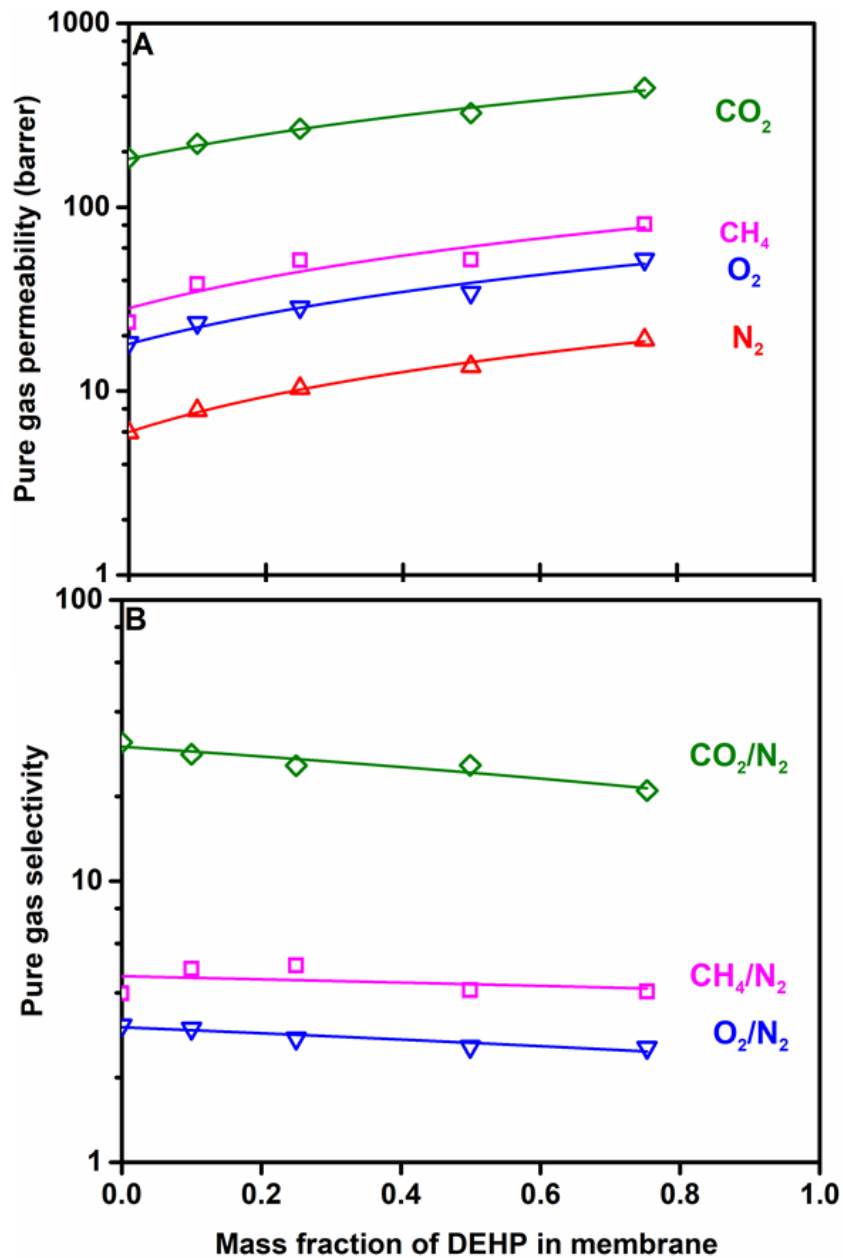


**Figure 3.9** The effect of DEHP content in the membrane on pure gas perm-selectivity. (A) Gas permeability vs. DEHP content, (B) Gas/N<sub>2</sub> selectivity vs. DEHP content.

Nitrogen, oxygen, methane, and carbon dioxide were selected to evaluate the membrane pure gas permeability and gas/nitrogen selectivity, and the results are shown in Figure 3.9. Pure PEBA membrane shows a CO<sub>2</sub> permeability of 180 barrer and good selectivity for CO<sub>2</sub> to nonpolar gases (CO<sub>2</sub>/N<sub>2</sub>=30) because PTMO segments in PEBA have a strong affinity to the quadrupolar carbon

dioxide [82]. As the content of immobilized DEHP oil in the membrane increases, the membrane gas permeability increases. The enhancement of the gas permeability could be explained by the immobilization of DEHP oil in the membrane. DSC measurements demonstrate that the more retained oil in the membrane, the more amorphous the membrane will be, and thus the membrane will have more free volume and be more favorable for the diffusion of small gas molecules. In figure 3.10 (B), as the DEHP content increases in the membrane, the gas/nitrogen selectivity slightly decreases, which is in accordance with typical Robison permeance and selectivity trade-off behavior.

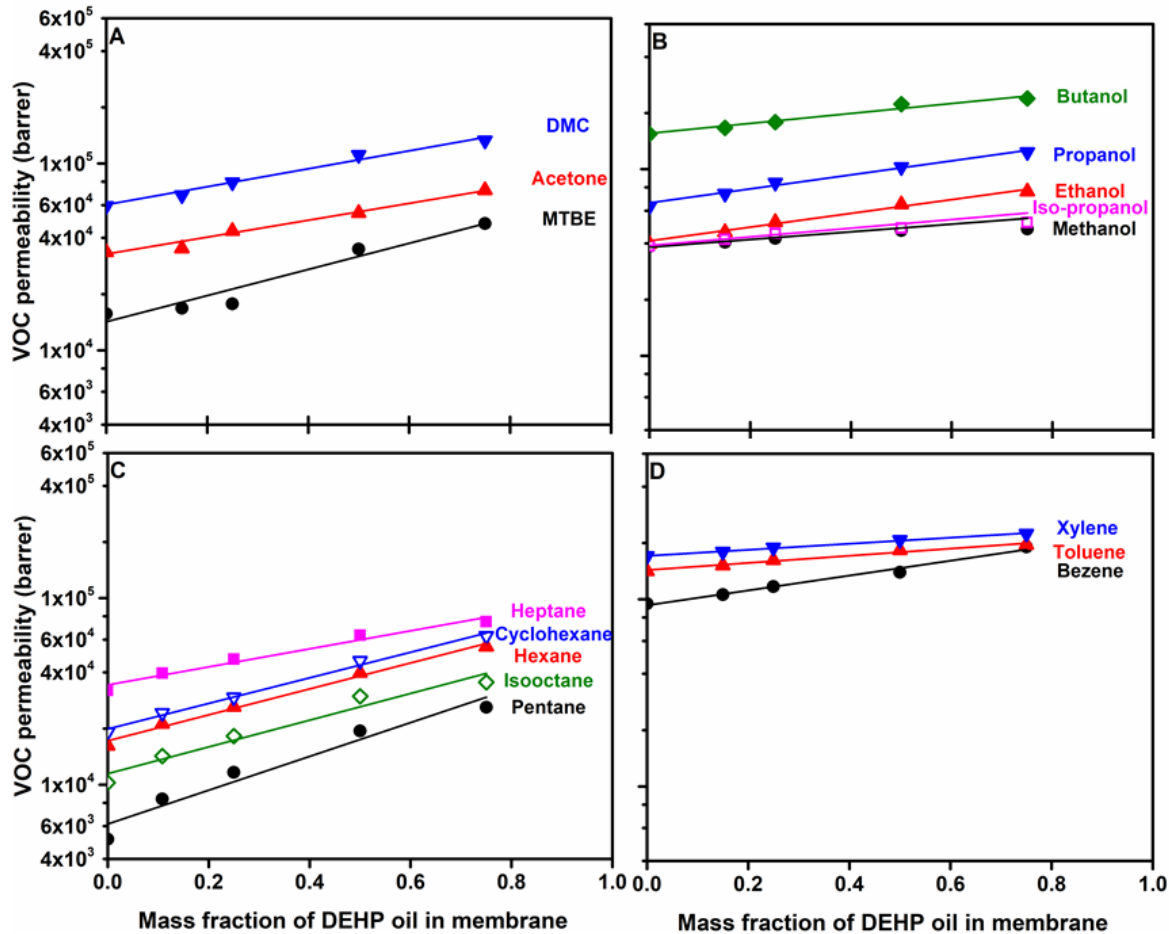


**Figure 3.10** The effect of DEHA content in the membrane on the VOC permeability of the membrane. (A) fuels additives, (B) alcohols, (C) paraffin, (D) aromatic compounds.

The retained DEHP oil could also improve the VOC permeation in the membrane. The VOC permeabilities of the selected five OLGMs were measured at 22°C in binary VOC/N<sub>2</sub> mixtures, in which the VOCs are saturated. Figure 3.10 shows the effect of oil content on the VOC permeability of the membrane. The VOC permeabilities in the membrane were compared based on the categories of VOCs. As can be seen from the Figure, the VOCs permeabilities of the membrane are oil content



dependent. This is because a higher loading of DEHP content in the membrane could make the membrane structure more amorphous, which could increase the diffusivity of VOCs in the membrane. Moreover, more DEHP content could also make the membrane form a stronger affinity to VOCs and thus, increase the sorption of VOCs to the membrane.

Solubility parameters indicate the intensity of the interatomic forces between two molecules, and the difference in solubility parameters could describe the affinity between the polymers or chemical components [83]. Here, the solubility parameters are used to quantify the affinity among PEBA, DEHP, and VOCs and further investigate the effects of the oil content on membrane VOC permeability. As the oil content increases in the membrane, the increase of MTBE permeability is more significant than that of acetone and DMC in the additive group. This is because the solubility parameter of MTBE ( $15.7 \text{ MPa}^{1/2}$ ) [84] is closer to DEHP ( $18.4 \text{ MPa}^{1/2}$ ) [85], while the solubility parameters of acetone ( $20.1 \text{ MPa}^{1/2}$ ) [86] and DMC ( $20.6 \text{ MPa}^{1/2}$ ) [87] are closer to that of PEBA ( $20.3 \text{ MPa}^{1/2}$ ) [88, 89]. Similarly, as the oil content increases in the membrane, the VOC permeability in the paraffin group increases significantly than VOCs in other groups because the solubility parameters of VOCs in the paraffin group ( $14.4 - 16.7 \text{ MPa}^{1/2}$ ) [90] is closer to DEHP than PEBA. On the other hand, the alcohol solubility parameters ( $23.1-29.7 \text{ MPa}^{1/2}$ ) [93, 96, 95] are far from both DEHP and PEBA. The effects of DEHP and PEBA content in the membrane on membrane VOC permeability are small. The solubility parameters ( $18.1 -18.7 \text{ MPa}^{1/2}$ ) [90, 91] of aromatic compounds are similar to those of DEHP and PEBA. The effects of DEHP and PEBA content in the membrane have an equal and counteractive impact on membrane VOC permeability, and thus the VOC permeability increases less significantly than the VOCs from other groups. In conclusion, the affinities of both oil and PEBA to VOCs could affect the VOC permeabilities of the membrane.

Figure 3.11 shows the effect of DEHP content in the membrane on membrane VOC/N<sub>2</sub> selectivity. As can be seen, the VOC/N<sub>2</sub> selectivity of the membrane decreased with the increase of DEHP oil in the membrane. It may be because the diffusion of small gas molecules (N<sub>2</sub>) is enhanced more significantly than big vapor molecules (VOCs) as the structure in the membrane becomes amorphous.

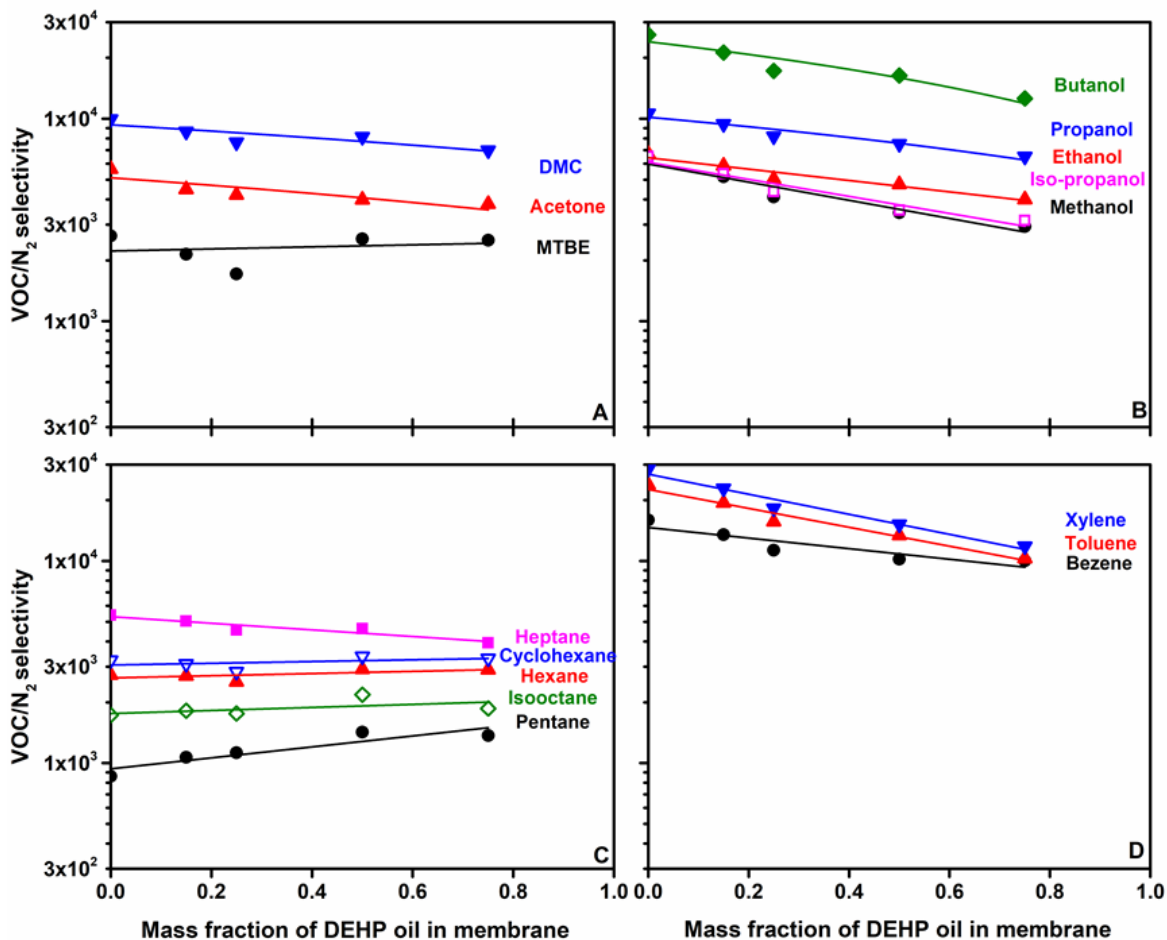


**Figure 3.11** The effect of DEHP content in the membrane on VOC/N<sub>2</sub> selectivity of the membrane. (A) fuel additives, (B) alcohols, (C) paraffin, (D) aromatic compounds.

Table 3.2 summarizes the VOC permeability of reported membranes on VOC/N<sub>2</sub> separation. The discrepancy in the reported permeability for the same VOC is due to the different evaluation methods and test conditions. The VOC permeability of the membranes from works in this Chapter and Chapter 5 were also listed in the table for comparison. The PEBA 2533 shows lower acetone permeability than the PDMS because PA in block copolymer structure in the PEBA constrains the permeation of VOC. The membrane 26PEBA/74DEHP showed the highest permeability for selected VOCs (acetone and ethanol) over the previously reported membranes, demonstrating a promising membrane for VOC permeation.

**Table 3.2** Membrane performance in the literature.

Membrane material	VOC type	Test temperature (°C)	VOC permeability (Barrer)	Reference
PDMS	Acetone	40	10000 ~ 20000	[7]
PDMS	Acetone	28	23275 ~ 45325	[92]
PDMS	Acetone	30	6000 ~ 7000	[93]
PDMS	Acetone	22	66828	Chapter 5
PEBA 2533	Acetone	22	33553	This work
26PEBA/74DEHP	Acetone	22	72046	This work
PDMS	C <sub>2</sub> H <sub>2</sub> Cl <sub>3</sub>	35	20000 ~ 50000	[94]
PDMS/PTMO/PU	Toluene	25	5000 ~ 18000	[30]
PDMS	Ethanol	40	10000 ~ 30000	[7]
PDMS	Ethanol	22	31508	Chapter 5
PDMS/ZIF-X	Ethanol	35	6000 ~ 10000	[95]
26PEBA/74DEHP	Ethanol	22	75992	This work
PVC	Acetone	40	800 ~ 10000	[7]

Membrane 26PEBA/74DHEP, which exhibits the highest VOC permeability and a favorable VOC/N<sub>2</sub> selectivity among the prepared PEBA/DEHP OLGMs, were selected to perform the further systematic VOC/N<sub>2</sub> mixture separation tests. 10 VOCs from the alcohol and paraffin group were chosen to investigate the effect of feed VOC concentration and operation temperature on the VOC/N<sub>2</sub> separation performance of the membrane.

### 3.3.6 Effect of VOC concentration on VOCs permeation

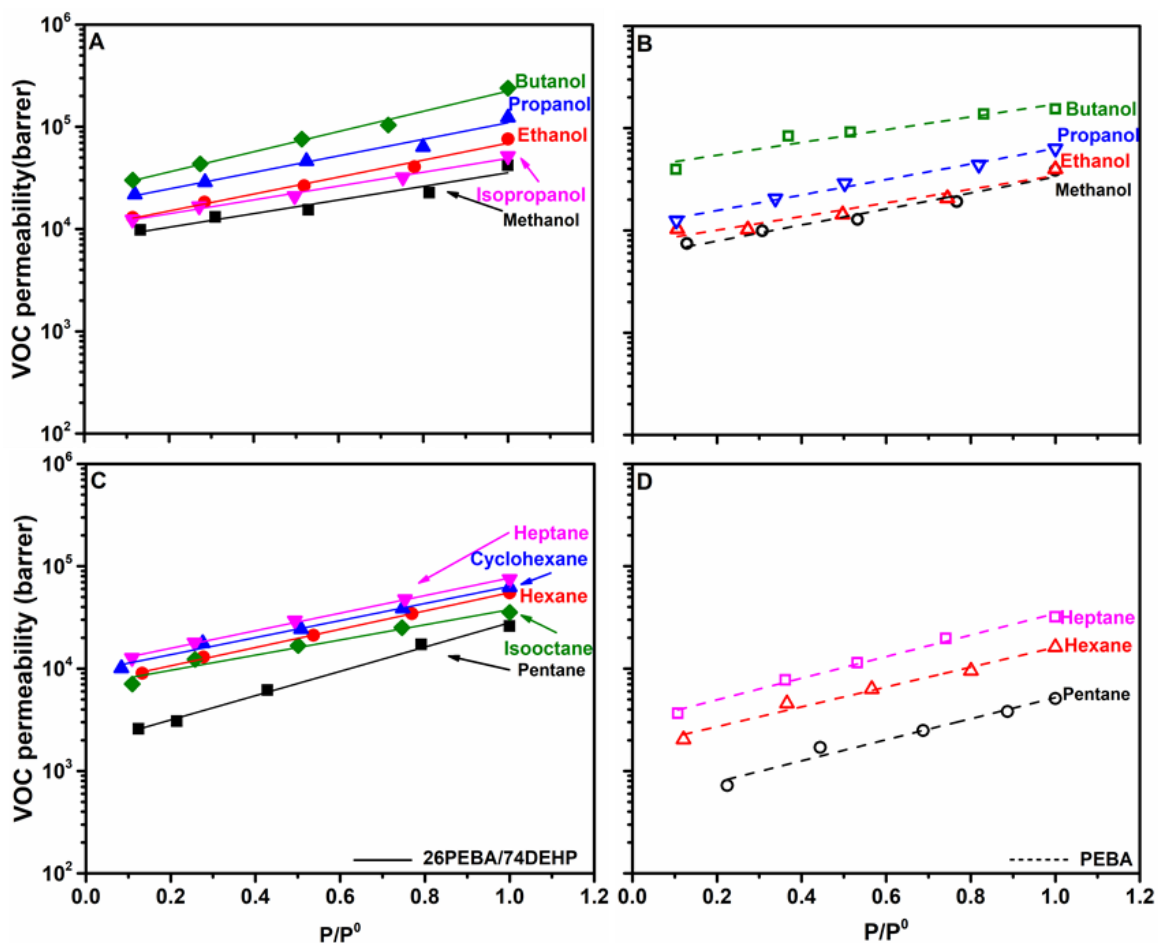


**Figure 3.12** Effect relative vapor pressure ( $P/P^0$ ) on VOC permeability. VOCs permeabilities of 26PEBA/74DEHP membrane are in solid line, VOCs are (A) alcohols and (C) paraffin. VOCs permeabilities of PEBA membrane are in the dashed line, VOCs are (B) alcohols and (D) paraffin.

The VOC/ $N_2$  separation performance of the 26PEBA/74DEHP membrane was evaluated using a mixture with different VOC concentrations. VOCs and their isomers from the alcohol and paraffin group were chosen for evaluation, and PEBA as an oil-free membrane was evaluated for comparison. All evaluations were performed at 22°C. The results in Figure 3.12 were plotted as VOC permeability versus relative pressure ( $P/P_0$ ), where  $P$  is the VOC partial pressure in VOC/ $N_2$  mixture and  $P_0$  is the VOC saturated vapor pressure at 22°C. In Figures 3.12 (B and D), the VOC permeability of the PEBA membrane increases along with the relative pressure. At the same relative pressure, the VOC permeability in PEBA follows the order of methanol  $\approx$  ethanol  $>$  heptane  $>$  hexane, and these results are in agreement with the previous study [96]. As 74 wt.% of DEHP oil was immobilized in the

PEBA, the VOC permeability of the membrane improved dramatically. As indicated in Figures 3.12 (A) and (B), the difference between the methanol and ethanol permeabilities in 26PEBA/74DEHP becomes more obvious than that in PEBA. The permeability is improved significantly for each VOCs in 26PEBA/74DEHP. While comparing the permeabilities of each VOC in 26PEBA/74DEHP, a trend became apparent: as the VOC saturated vapor pressure becomes higher (see Table 3.3), the VOC permeability decreases in the order of butanol > n-propanol > ethanol > methanol in the alcohol group and heptane > hexane > pentane in the paraffin group. Because the saturated vapor pressure measures the condensability and sorption of the vapor [7], a low saturated vapor pressure of VOC implies a favorable condensability and good sorption on the membrane [35]. The reverse proportional dependence of VOC permeability on VOC saturation pressure indicates that sorption dominates the VOC permeation. However, some VOC permeabilities don't follow this trend. For example, isopropanol has lower saturated vapor pressure and permeability than ethanol, and isooctane has lower vapor pressure and permeability than hexane. This is because the VOC molecules with branched chains (e.g., isopropanol and isooctane) will have a bigger size than those with straight-chain (e.g., ethanol and hexane). And the size of the VOC molecules could be indicated by the molar volume, as seen in Table 3.3. Generally, the molecules with bigger molar volume, the molecular size will be bigger, and molecules diffuse slower in the membrane [97]. It indicates besides the sorption of VOC in the membrane, the diffusion of VOCs in the membrane also plays an important role in determining the VOC permeation through the membrane.

**Table 3.3** Saturated vapor pressure at 22°C and molar volume of VOCs at STP.

	<b>Saturated vapor pressure (mmHg)</b>	<b>Molar volume (cm<sup>3</sup>/mole)</b>
Methanol	109	41
Ethanol	50	57
Propanol	17	75
Isopropanol	36	77
Butanol	5	92
Pentane	455	115
Hexane	133	131
Cyclohexane	86	109
Isooctane	44	165
Heptane	39	149

Figure 3.13 and Figure 3.14 show the effects of feed VOC concentration on VOC permeate flux and permeate VOC concentrations for 26PEBA/74DEHP membrane. In Figure 3.14, the permeate flux of VOC grows with an increased feed VOC concentration, and a higher feed concentration leads to a faster growth of the flux. The positive convexity of the curve for VOC in the alcohol group (A) and paraffin group (B) implies that the rise of VOC permeate flux is due to the increased driving force for VOC permeation [34]. In Figure 3.15, the permeate VOC concentration grows with an increased feed VOC concentration. When VOC concentration is higher than 5 mol%, the permeate concentration of most VOCs in the alcohol and paraffin group is more than 90 mol%. The results demonstrated an excellent VOC/N<sub>2</sub> separation performance of 26PEBA/74DEHP OLGm over a wide range of VOC concentrations in the gas stream.

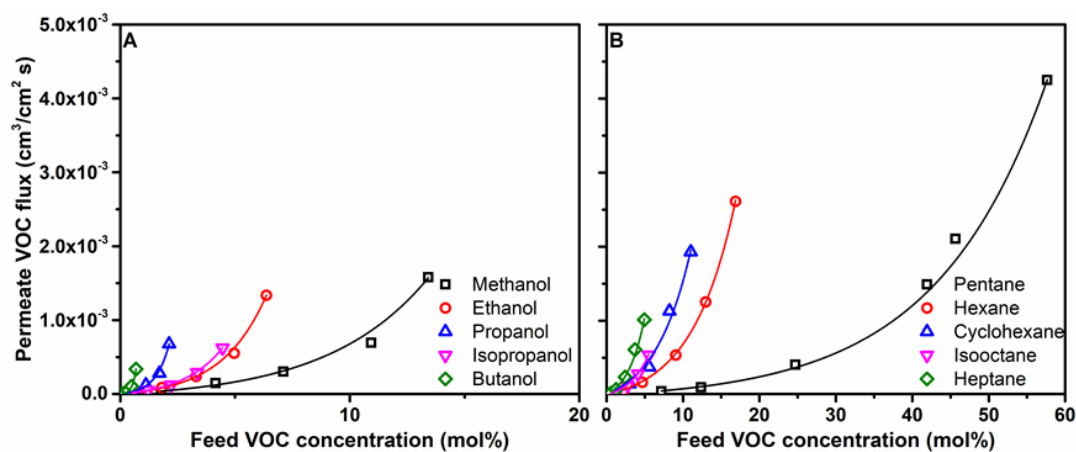


**Figure 3.13** Permeate flux of VOC vs feed VOC concentration, (A) alcohols, and (B) paraffin.

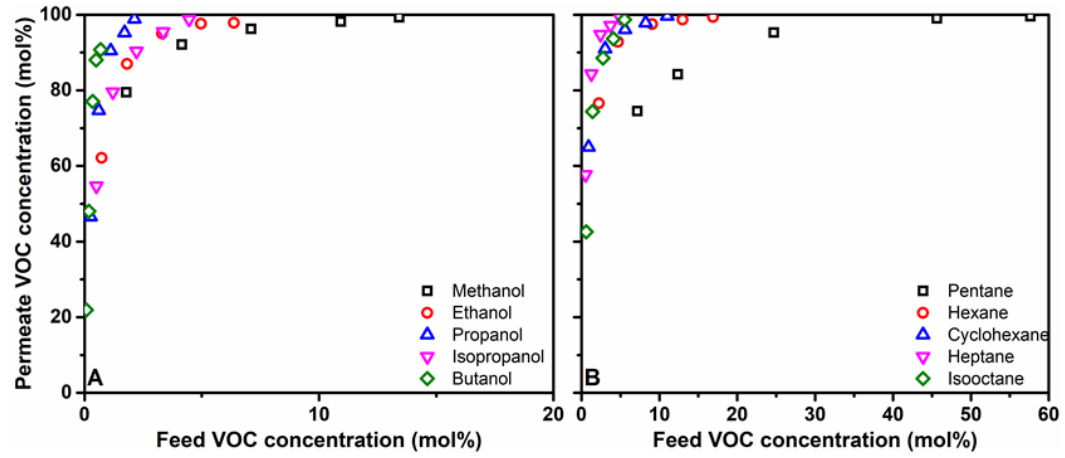


**Figure 3.14** Permeate VOC concentration vs feed VOC concentration, (A) alcohols, and (B) paraffin.

### 3.3.7 Effect of temperature on VOCs permeation

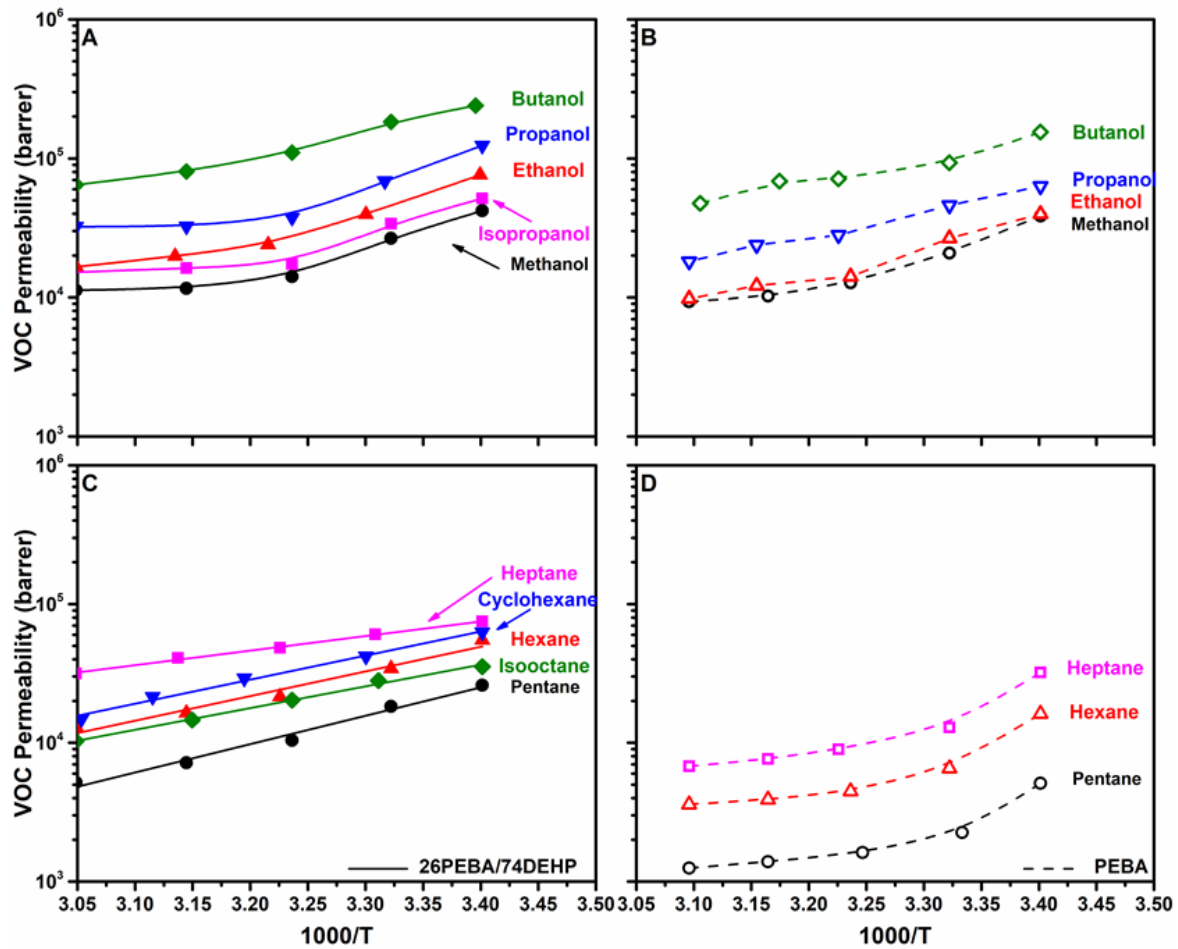


**Figure 3.15** Effect of temperature (1000/T) on VOC permeability. VOCs permeabilities of 26PEBA/74DEHP membrane are in solid line, VOCs are (A) alcohols and (C) paraffin. VOCs permeabilities of PEBA membrane are in the dashed line, VOCs are (B) alcohols and (D) paraffin.

The separation experiments for VOC/N<sub>2</sub> mixture using 26PEBA/74DEHP and PEBA were carried out at temperatures from 22 to 55°C to investigate the effect of operating temperature on the membrane separation performance. The VOC was saturated at 22 °C in the mixture, and the VOC concentration was kept the same as the temperature further increased. VOC compounds and corresponding isomers from the alcohol and paraffin groups were selected as the feed for the evaluation, and the results are shown in Figure 3.15. As can be seen, the VOC permeabilities of membranes have a relationship with the reciprocal of temperature in a semi-log scale. The VOC permeability of the PEBA membrane experiences a significant decrease with the increase of temperature, which is in agreement with other literature [35]. The VOC permeability of 26PEBA/74DEHP at all operating temperatures is improved



significantly compared with pure PEBA membrane attributed to the high loading of DEHP. It can also be found that the temperature has a more significant effect on the permeability of paraffin than alcohol, which could be attributed to the stronger affinity of the paraffin molecules to DHEP oil.

The temperature dependence of paraffin permeability follows the Arrhenius relation as shown in Equation 2.9. The activation energies  $E_p$  for paraffins were negative (Table 3.4), suggesting the temperature has an adverse effect on the permeability of paraffin in the membrane. On the other hand,  $E_p$  could also be considered a sum of the activation energy for diffusion (a kinetic parameter) and the enthalpy change of sorption (a thermodynamic parameter) in the membrane. The activation energy for molecule diffusion in the polymer is generally positive, while the enthalpy change of molecule sorption is usually negative. When the negative enthalpy change of sorption is dominant over the positive activation energy for diffusion, a negative value of  $E_p$  will be derived. Therefore, the negative activation energy in Table 3.4 also suggests that paraffin permeation is dominated by its sorption in the membrane [93]. Moreover, because the activation energy was obtained from the relation of the temperature dependence of the gas permeability, it could also indicate the effect of temperature on the gas permeability. In Table 3.4, the activation energy of paraffin was in the order of Pentane > Hexane > Cyclohexane > Isooctane > Heptane, following the same order as their saturated vapor pressures. It indicates the VOCs with high volatilities are more affected by the temperature compared with the VOCs with low volatilities.

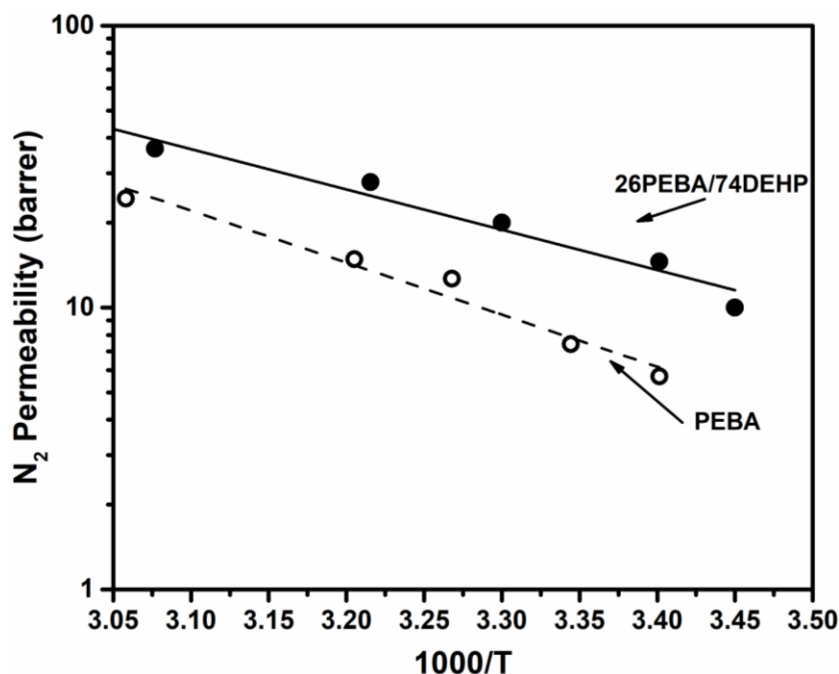


**Figure 3.16** Effect of temperature ( $1000/T$ ) on  $N_2$  permeability. The solid line is for the 26PEBA/74DEHP membrane, and the dashed line is for the PEBA membrane.

**Table 3.4** Activation energy for permeation of VOC and  $N_2$ .

Membrane	Component	The permeation activation energy ( $\text{kJ mol}^{-1}$ )
26PEBA/74DEHP	Pentane	-39.1
	n-Hexane	-34.0
	Cyclohexane	-33.2
	Heptane	-20.0
	Iso-Octane	-29.9
	$N_2$	27.4
PEBA	$N_2$	35.4

Figure 3.16 shows the effect of temperature on nitrogen permeabilities of PEBA and 26PEBA/74DEHP membranes. The nitrogen permeabilities of both membranes increase significantly with temperatures from 22 to 55°C. This is because the permeate molecules are more energetic at a higher temperature, and the thermal motion of the polymer chains in the membrane is also enhanced. As a result, the diffusion of nitrogen through the membrane is favored. In Figure 3.16,

26PEBA/74DEHP exhibits higher nitrogen permeability than the PEBA membrane as DEHP oil enhances the free volume for gas permeation in the membrane. Moreover, the activation energies  $E_p$  for nitrogen of PEBA and 26PEBA/74DEHP membranes were calculated and shown positive value in Table 3.4, indicating that the nitrogen permeation is dominant by its diffusion in the membrane [93].

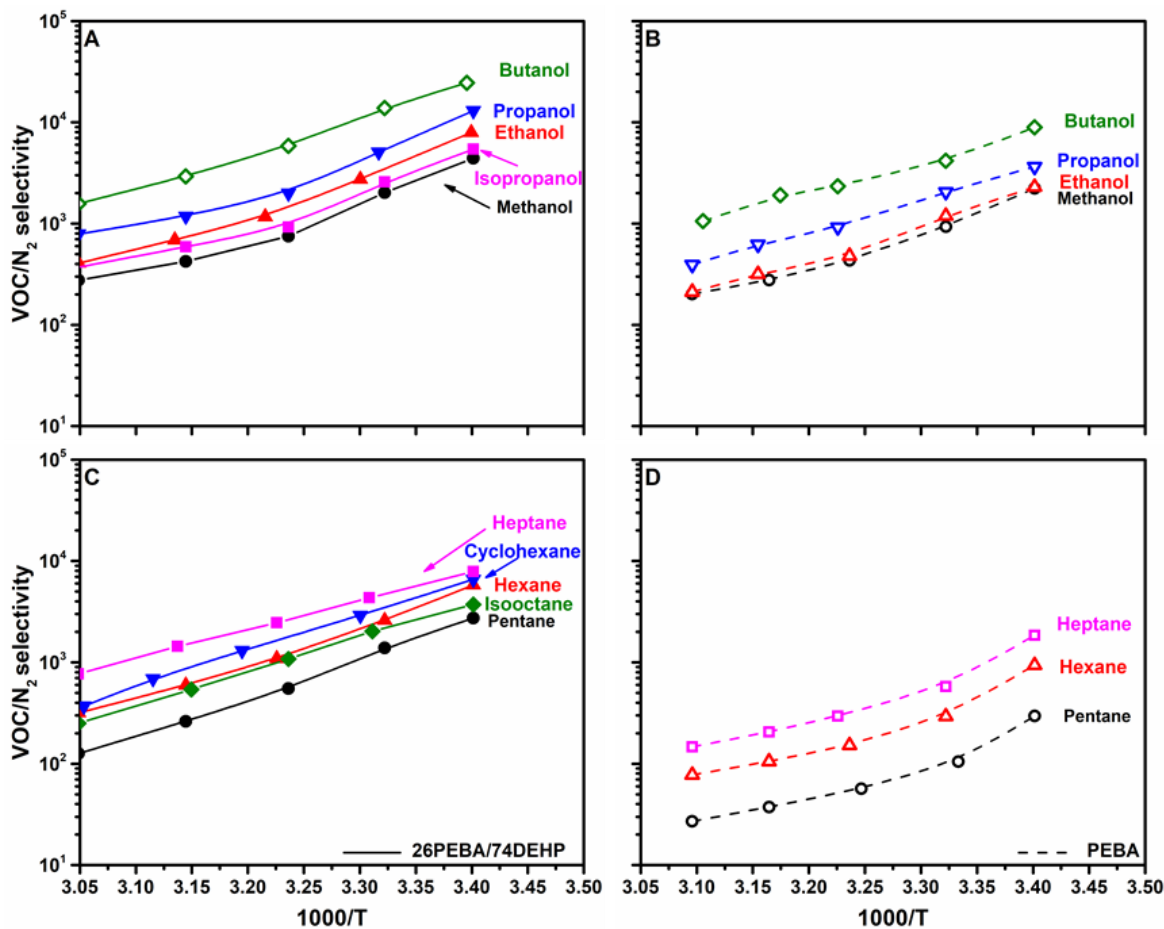


**Figure 3.17** Effect of temperature (1000/T) on VOC/N<sub>2</sub> selectivity. VOC/N<sub>2</sub> selectivity of 26PEBA/74DEHP membrane is in solid line, VOCs are (A) alcohols and (C) paraffin. VOC/N<sub>2</sub> selectivity of PEBA membrane are in the dashed line, VOCs are (B) alcohols and (D) paraffin.

The VOCs/N<sub>2</sub> selectivity of PEBA and 26PEBA/74DEHP membranes at different temperatures are shown in Figure 3.17. As can be seen, the selectivity of the membrane to VOCs and nitrogen decreased with the increase of operating temperature. This suggests that a low operating temperature is more favorable for membrane in VOC/N<sub>2</sub> separation with the aim of high

selectivity. It was also noticed that 26PEBA/74DEHP showed a higher selectivity to VOC than that of pure PEBA membrane under all testing temperatures.

### 3.3.8 Membrane stability

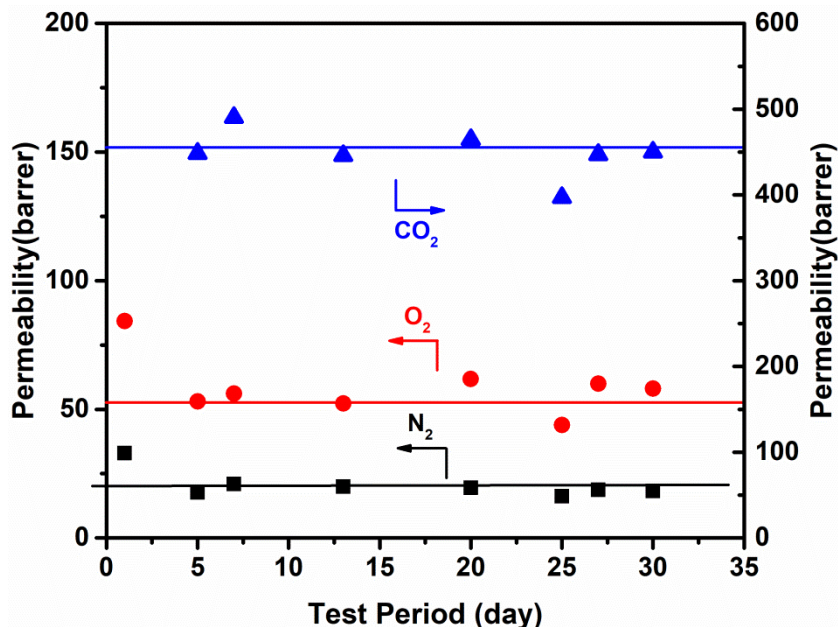


Figure 3.18 Pure gas permeability of 26PEBA/74DEHP membrane.

The stability test for 26PEBA/74DEHP was also carried out. The membrane was applied to the separation of the VOC/N<sub>2</sub> mixture for over 30 days, during which time different operating conditions (i.e., VOC species, feed concentration, operating temperature) were applied. After the experiment for each condition, the pure gas measurement tests, including the permeation tests for carbon dioxide, oxygen, and nitrogen, were performed to check the stability of the membrane, and the results are shown in Figure 3.9. All permeability data in the figure were measured in the pure gas at room temperature with the feed and permeate pressure at 0.4MPa and 1 atm, respectively. As can be seen, The membrane showed excellent stability, and the permeabilities of nitrogen, oxygen, and carbon dioxide were constant at 25 barrers, 50 barrers, and 450 barrers, respectively.

### 3.4 Conclusion

The defect-free oleo gel membrane was prepared through hand casting by immobilizing bis (2-ethylhexyl) phthalate (DEHP) oil into PEBA membranes. Various characterizations, including FTIR, TGA, and SEM were carried out to fully evaluate the physical properties and morphologies of the

prepared membranes. It was shown that the PEBA/DEHP oleo gel membranes became softer and had more amorphous structures than pure PEBA membranes.

In gas permeation evaluations, 16 VOCs from 4 groups, including the fuel additive, alcohol, paraffin, and aromatic compounds, were selected to evaluate VOC/N<sub>2</sub> separation performance on PEBA/DEHP membranes. The selected VOCs and their isomers were tested on the prepared membrane to investigate the VOC permeation. The PEBA/DEHP OLGMs showed excellent permeability for all 16 VOCs. The VOC permeability was proportionally dependent on the DEHP oil content in the membrane, which could be attributed to the amorphous structure in OLGMs and the good affinity of DEHP oil to VOCs. VOCs from alcohol and paraffin groups were selected as representatives to evaluate membrane VOC/N<sub>2</sub> separation performance at different temperatures and VOC concentrations in the feed stream.. The prepared PEBA/DEHP membranes showed excellent stabilities and orders of magnitude higher VOC permeabilities than the PEBA membrane, demonstrating a promising membrane for VOC/N<sub>2</sub> separation.

## Chapter 4

### PEBA/DEHA oleo gel membrane for VOC/N<sub>2</sub> Separation

#### 4.1 Introduction

The power plant and industrial process emissions have been the primary sources of VOC emission according to report released by the US environmental protection agency [98]. The VOC emissions have caused a series of social, healthy, and ecological problems [49, 99, 100]. Many countries and regions have made legislations to combat the issues that arose from the VOC emissions. Technologies, such as carbon adsorption, incineration, biofiltration, combustions, and membrane separation, have been developed to meet the VOC emissions requirements [43, 101, 102]. Membrane separation has been treated as one of the most promising technologies for its advantages of low power consumption, bench integration, environmental friendliness, easy operation, and good VOC recovery performance [5, 19, 53, 95].

The VOC/N<sub>2</sub> separation membranes could be categorized into the VOC rejective membrane [42, 55] and VOC permeative membrane [2, 34]. The VOC rejective membrane is usually made of glassy polymers, such as polyimide. The membrane has a rigid structure to allow small gas molecules to permeate faster than big molecules. The weakness of the polyimide and some other glassy polymers is its low permeate flux and loss of membrane selectivity caused by polymer chain collapse or reorganization during the testing [103-105]. Many efforts have been made to improve membrane separation performance and stability. For example, Ingo et al. developed two triptycene-based polyimides, and the membrane showed excellent separation performance to define the 2015 upper bound limit for O<sub>2</sub>/N<sub>2</sub> separation [106-108]. Jin and Zhou synthesized and applied triphenylene-based polyimides membrane on VOC/N<sub>2</sub> separation, and 99% cyclohexane rejection was observed [42, 43]. However, those membranes showed relatively low or moderate VOC flux, which withdraws the application of the membrane in the industry.

The VOC permeative membrane overcomes the weakness of the low permeate flux observed from the VOC rejective membrane. In the realized industrial VOC recovery process, the membrane can help concentrate VOC in the permeate to increase the feed VOC concentration before the next separation process and make the residue stream meet the air emissions requirement [109, 110]. Polydimethylsiloxane (PDMS) has been widely investigated since the 20th century as a highly VOC/N<sub>2</sub> selective and VOC permeable material [111-119]. The PDMS membrane showed a high VOC permeation rate, but the plasticization in the presence of heavy hydrocarbons may destroy the polymer chain and reduce the membrane selectivity [120, 121]. Poly(ether block amide) (PEBA)

combines the good mechanical property from the polyamide segment and the property of high gas permeation and flexible structure from the polyether segment. The good mechanical property from the polyamide segment helps the PEBA membrane overcome the plasticization phenomena in heavy hydrocarbons. Additionally, the good VOC permeation flux makes PEBA 2533 membrane have excellent potential on VOC/N<sub>2</sub> separations [34, 122, 123].

In this work, the oleo gel membrane was made by immobilizing DEHA oil in the PEBA matrix. The DEHA oil was used here because of its following properties: (i) high boiling points and low volatility; (ii) high sorption coefficient to VOCs [124]. PEBA 2533, as a reliable VOC permeable polymer, successfully retains the DEHA oil in the membrane. The amine and hydroxyl groups could form the hydrogen bonding with the carboxyl group in PEBA [66, 67], thus making PEBA a torsional structure to retain the DEHP oil. The carboxyl group in the DEHA oil could also form the hydrogen bond with the amine and hydroxyl group in PEBA. Additionally, the ether group in DEHA oil may form the hydrogen bond with the hydroxyl group in PEBA, resulting in good oil dispersion and immobilization in the polymer matrix at the molecular level [68]. Moreover, the straight polymer chain in DEHA oil enhances the oil dispersion in the PEBA matrix than the DEHP oil, which has the benzene ring with side chains.

The constitution of high VOC favorable DEHA oil and strong oil supported PEBA matrix result in a stable oleo gel membrane with high VOC permeability. 15 VOCs were selected from four different groups to evaluate VOC permeation property, and they are from alcohols (methanol, ethanol, propanol, and butanol), paraffins (pentane, hexane, cyclohexane, isooctane, and heptane), aromatic compounds (benzene, toluene, and xylene), and fuel additives (methyl tert-butyl ether (MTBE), dimethyl carbonate (DMC), and acetone). Membranes with different DEHA oil content were fabricated and tested to measure VOC permeability and VOC/N<sub>2</sub> selectivity. The effects of feed VOC concentration and the temperature on membrane VOC/N<sub>2</sub> separation performance were evaluated, and the results were furthermore compared with the pristine PEBA membrane. The stability was overseen on the selected membrane in 60 days.

## **4.2 Experiment**

### **4.2.1 Material**

Poly (ether block amide) (PEBA 2533) was the same PEBA used to make PEBA/DEHP membrane in Chapter 3 and acquired from Arkema Inc. (Philadelphia, PA). Bis (2-ethylhexyl) adipate (DEHA) was obtained from Fluka Analytical (Germany). All solvents used in membrane preparation and VOC

separation experiment were reagent grade. The purities of gases used in the permeation experiment were at least 99.9%. The vendors' information for solvents and gases can be found in Section 3.2.1.

#### **4.2.2 Membrane preparation**

PEBA 2533 and DEHA were dissolved in DMAc to make the membrane casting solution, and the ratio of PEBA and DEHA in the casting solutions varied. The solutions were stirred vigorously at 70 °C for 10 hours to be homogenous and then sat in the oven at 70 °C for 12 hours to remove gas bubbles. Afterward, the solution was cast onto a glass plate and dried at 70 °C for 48 hrs.

#### **4.2.3 Permeation experiment**

The permeation experiment set-up has been described in Section 3.24 and shown in Figure 3.1.

#### **4.2.4 Gas permeance measurement**

The Nitrogen permeance in the presence of VOC was measured using the system shown in Figure 3.1. Once closing the valve on the vapor/gas mixer, the membrane was isolated from the feed VOC/N<sub>2</sub> mixture, and the bubble in the bubble flowmeter moved downward due to the gas permeation. The nitrogen permeance could be determined from the speed of the bubble movement. The pure gas permeances of N<sub>2</sub>, O<sub>2</sub>, H<sub>2</sub>, CH<sub>4</sub>, C<sub>2</sub>H<sub>4</sub>, and CO<sub>2</sub>, were measured by keeping feed and permeate pressures at 0.4MPa and 1atm, respectively.

#### **4.2.5 VOC/N<sub>2</sub> separation performance characterization**

The method to determine the VOC permeability of the membrane was introduced in Chapter 3. A set of equations from (3.1) to (3.4) need to be solved.



## 4.3 Result and discussion

### 4.3.1 Characterization of oil content in the membrane

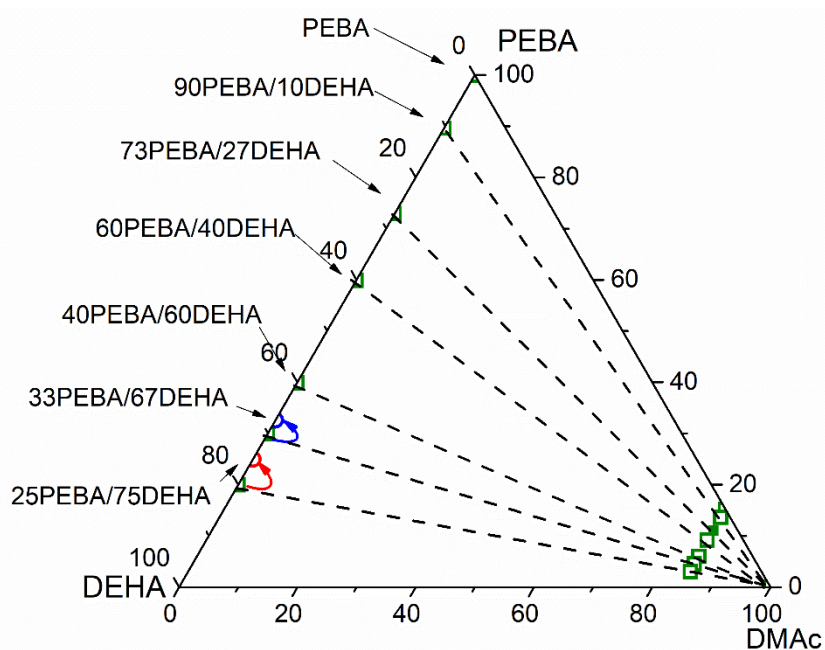


**Figure 4.1** The content of PEBA and DEHA in the membrane casting solution and membranes; PEBA and DEHA content in the membrane are used to name membranes, and names were labeled on the left side of the Figure.

PEBA and DEHA were well blended at different ratios and dissolved in the solvent DMAC; the contents of PEBA and DEHA can be seen from the green points on the right side in Figure 4.1. After DMAC evaporated, the PEBA/DEHA membrane formed. The content of PEBA and DEHA immobilized in the membrane could be seen on the left side in the Figure. During the membrane formation, Some oils saturated out and were observed at the surface of 33PEBA/67DEHA and 25PEBA/75DEHA membranes. As can be seen from the figure, two green points shifted to the points in different colors (red and blue) with lower DEHA content for those two membranes. It should be noted that the amount of saturated and immobilized oil in the membrane could be calculated, and membranes were named based on the content of PEBA and DEHA in the membrane. When comparing the oil contents in the membranes and casting solutions, the amount of oil saturated out of 33PEBA/67DEHA and 25PEBA/75DEHA membranes were respectively 2.6wt.% and 5wt.% out of the total amount of the oil used in membrane fabrications. The amount of oil saturated out from PEBA/DEHA membranes was more than that in PEBA/DEHP membranes. This could be because the

solubility parameter of DEHP [85] is closer to PEBA [89] than DEHA [125], making the DEHA oil is less compatible with PEBA than the DEHP.

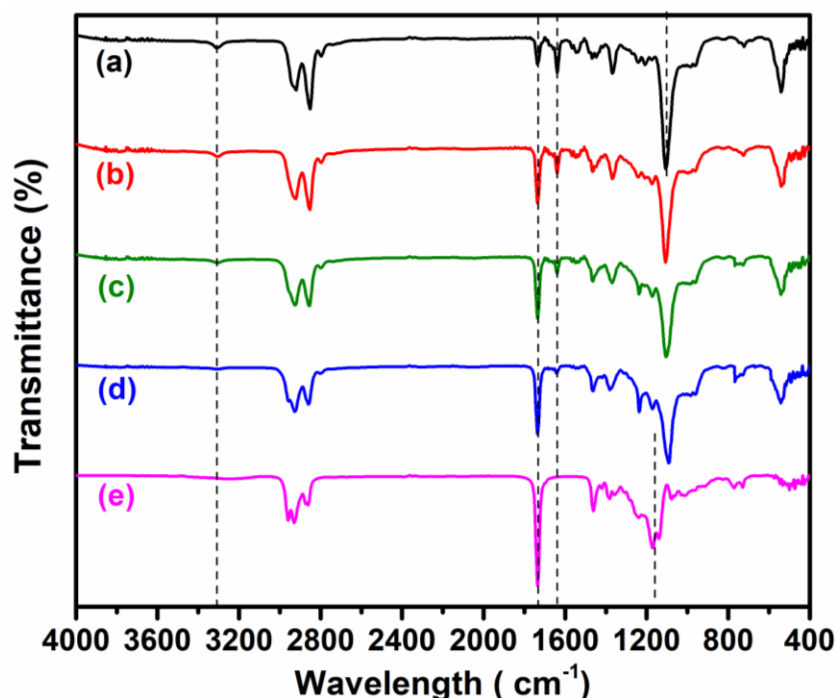


**Figure 4.2** FTIR spectra of PEBA/DEHA oleo gel membranes. (a) PEBA, (b)73PEBA/27DEHA, (c) 40PEBA/60DEHA, (d) 25PEBA/75DEHA and (e) DEHA oil.

PEBA/DEHA membranes were characterized by Fourier transformation infrared spectra (FTIR) (Bruker-VERTEX 70). In Figure 4.2, the FTIR spectra of membranes with different DEHA oil contents were performed in the region of 400–4000  $\text{cm}^{-1}$ . The peaks at around 3299 $\text{cm}^{-1}$ , 1640  $\text{cm}^{-1}$ , and 1735  $\text{cm}^{-1}$  are attributed to the vibrations of (N-H), C=O (in O-C=O), and C=O (in H-N-C=O), respectively. Those peaks in the spectra are attributed to the 20% polyamide segment in PEBA. A strong peak of (C-O-C) at 1110  $\text{cm}^{-1}$  is attributed to an 80% polyether segment in PEBA. As more DEHA oil is immobilized in the PEBA from spectra (a) to (e), the peak of C-O shifts from 1110 to 1150  $\text{cm}^{-1}$ , which suggests that the hydrogen bond forms between the C-O group in DEHA oil and O-H group in PEBA [68]. With an increasing amount of DEHA oil retained in membranes (from spectra a to e), the peaks of (N-H) and (H-N-C=O) gradually weaken and eventually disappear in DEHA spectra because there is no nitrogen compound in the DEHA oil, resulting in the peak of (C=O) in DEHA spectra becoming stronger [126]. The formed hydrogen bonds and peaks changing in the FTIR spectra (from spectra a to e) confirm that DEHA oil is retained in the PEBA polymer matrix, and the

content of DEHA oil retained in membranes increases from 73PEBA/27DEHA (b) membrane to 25PEBA/75DEHA membrane (d).

### 4.3.2 Gas permeation properties in the membrane

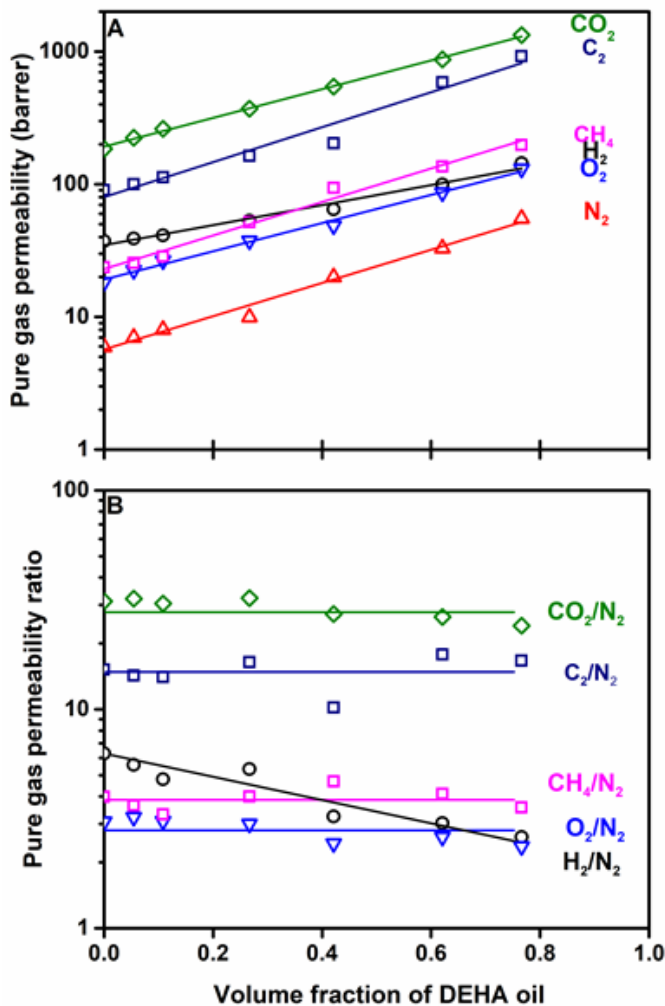


**Figure 4.3** The effect of DEHA content in the membrane on pure gas perm-selectivity. (A) permeability vs. DEHA content, (B) Gas/N<sub>2</sub> selectivity (pure gas permeability ratio) vs. DEHA content.

To understand the gas permeation property in the PEBA/DEHA membranes, six gases, including nitrogen, oxygen, hydrogen, methane, ethane, and carbon dioxide, were selected to evaluate pure gas permeabilities and gas/nitrogen selectivities for the membrane. The pristine PEBA as the DEHA oil-free membrane was also under evaluation, and gas permeabilities in the PEBA membrane are similar to those reported by previous literature [127]. All results were correlated with the volume fraction of

DEHA oil in the membrane, as shown in Figure 4.3. All gas permeabilities increase with the increase of oil content in the membrane. This observation is similar to that in PEBA/DEHP membranes because the free volume of the membrane was enhanced by the oil immobilization in the PEBA matrix (reference is Chapter 3), thereby improving the gas diffusion in the membrane. Additionally, the increase of gas permeabilities are similar, and the pure gas permeability ratios keep constant as the DEHA oil content increases in the membrane. In contrast, hydrogen permeability increases less significantly than other gases, resulting in decreased hydrogen/nitrogen selectivity, as shown in Figure 4.3 (B). This could be because hydrogen has the smallest gas molecules among six gases (kinetic diameter = 2.89 Å) and already has an excellent diffusion in the pristine PEBA [2]. The increasing free volume in the membrane may have a negligible effect on the improvement of hydrogen diffusion in the membrane; however, it may significantly impact the diffusion of other large gas molecules in the membrane, and the impact is at the same extent.

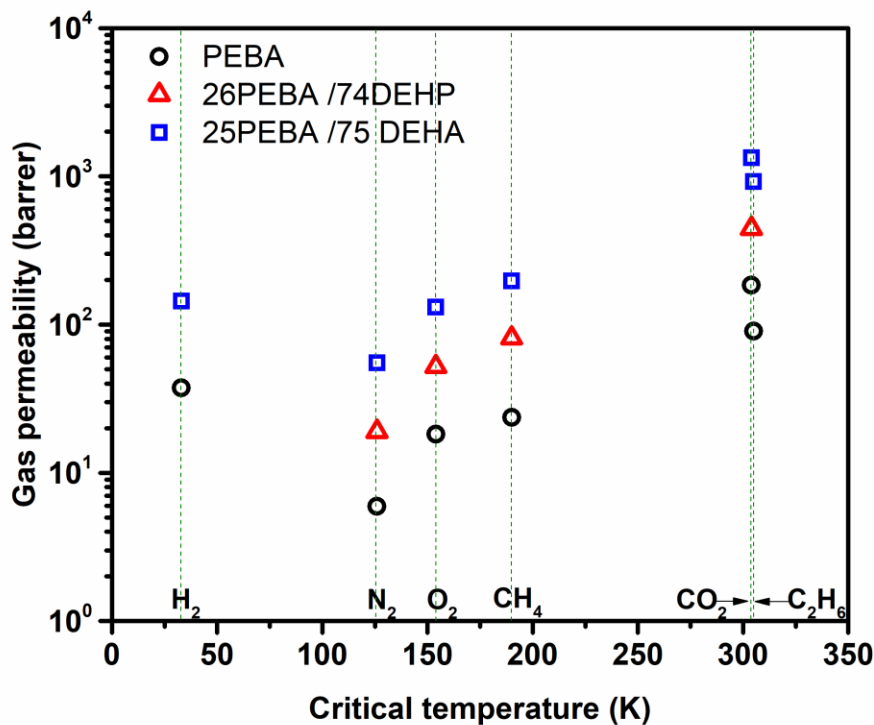


**Figure 4.4** Pure gas permeability of membranes vs. critical temperature of gases. The pure gas permeability of 26PEBA/74DEHP is from Chapter 3.

The permeabilities of non or less condensable gases for the PEBA/DEHA membrane are compared with the PEBA/DEHP (see Chapter 3) and PEBA membrane, as shown in Figure 4.4. All gas permeabilities were plotted as a function of the critical temperature of gas molecules. As the critical

temperature of the gas become higher, the gas becomes more condensable, and the gas permeability of the membrane becomes higher, which means that the sorption of gases in the membrane is more important than diffusion (references are Chapter 3 and 5). In 26PEBA/74DEHP and 25PEBA/75DEHA membranes, the oil content in the membrane is similar, but the gas permeabilities of 25PEBA/75DEHA are higher than the 26PEBA/74DEHP membrane. This means that the gas permeabilities are improved dramatically by immobilizing DEHA oil in the PEBA membrane compared with DEHP oil. The gas permeability improvement may attribute to i) DEHA oil having better sorption to gases than DEHP oil; ii) DEHA oil making the membrane have more free volume than DEHP oil. Moreover, comparing the DEHA and DEHP oils structure, the aromatic ring in the DEHP oil reduces the mobility of molecular chain rotation, which could make the gas diffusion in DEHP oil slower than the DEHA oil [128]. The exceptional high hydrogen permeability out of the trend may attribute to the small hydrogen molecular size (kinetic diameter: hydrogen ( $2.89\text{\AA}$ ) < nitrogen( $3.64\text{\AA}$ )).

In conclusion, the permeation of non or less condensable gases in the PEBA/DEHA OLGMs is affected by both diffusion and sorption. The VOC diffusion may be improved by free volume enhancement caused by DEHA oil immobilization in the PEBA membrane. The sorption is enhanced by the excellent sorption properties of the DEHA oil, and the sorption is dominant in the gas permeation in PEBA/DEHA OLG. The DEHA oil may have better sorption and diffusion to above non or less condensable gases than the DEHP oil, making the gas permeabilities of 25PEBA/75DEHA membrane higher than the 26PEBA/74DEHP membrane.

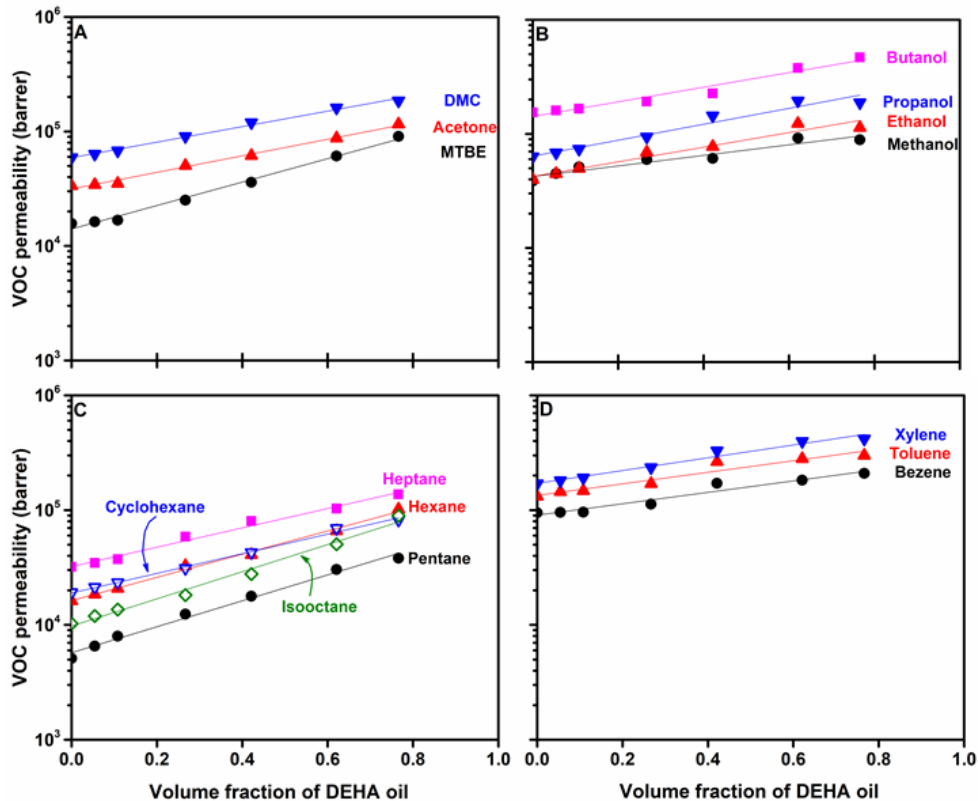


**Figure 4.5** The effect of DEHA oil volumetric content on VOC permeability in the membrane (A) fuel additives, (B) alcohols, (C) paraffin, (D) aromatic compounds.

PEBA/DEHA membranes were evaluated in binary VOC/N<sub>2</sub> mixtures with the different VOCs. The effect of the DEHA oil content on the VOC permeability is shown in Figure 4.5. The VOC permeability increases with an increase of DEHA oil content in the membrane. This could be because i) enhanced free volume of the membrane caused by oil immobilization, which improves the VOCs diffusion in the membrane (reference is in Chapter 3); ii) DEHA oil has a higher sorption coefficient to VOCs than the PEBA.

Moreover, the oil content dependence of membrane VOCs' permeabilities increase at different rates. This could be because of the differences in the affinity of DEHA oil to different VOCs. Hansen solubility parameters (HSP) are physicochemical parameters that could estimate the type of interactive forces responsible for compatibility between materials. They were used here to indicate the affinity of PEBA and DEHA to different VOCs (shown in Table 4.1). As the oil content increases in the membrane, MTBE permeability increases more significantly than acetone and DMC in the fuel additives because the solubility parameter of MTBE is close to DEHA, and the solubility of acetone and DMC is close to the PEBA. The paraffin VOC permeabilities increase more

significantly than VOCs in other groups as the oil content increases in the membrane because the solubility parameter of paraffin VOCs (14.4 – 16.7 MPa<sup>1/2</sup>) is closer to DEHA than PEBA. The alcohol solubility parameters (23.1-29.7 MPa<sup>1/2</sup>) are far from both DEHA and PEBA, and the aromatic solubility parameters (18.2-18.5 MPa<sup>1/2</sup>) are close to both DEHA and PEBA. The effect of DEHA content in the membrane on VOC permeability improvement is either small or similar to the effect of PEBA content in the membrane. Therefore, the permeabilities of VOCs in alcohols and aromatic compounds increase less significantly as oil content increases in the membrane.

**Table 4.1** Solubility parameters for components in the membrane and VOCs.

Type	Component name	Solubility parameter (MPa <sup>1/2</sup> )	Reference
Membrane part	PEBA	19.5-20.3	[88], [89]
	DEHA	17.6	[125]
VOC (fuel additives)	MTBE	15.7	[84, 86, 87]
	Acetone	20.1	
	DMC	20.6	
VOC (Alcohols)	Methanol	29.7	[86, 129]
	Ethanol	26.6	
	Propanol	23.1	
	Butanol	23.1	
VOC (Paraffins)	Pentane	14.4	[90]
	Hexane	14.9	
	Cyclohexane	16.7	
	Heptane	15.3	
	Iso-Octane	14.2	
VOC (Aromatic compounds)	Benzene	18.7	[90, 91]
	Toluene	18.2	
	Xylene	18.1-18.2	

Additionally, the VOC permeabilities increase linearly as oil content increases in the membrane. In homogeneous blend membranes, mixing rules which describe the relationship between the gas permeation property and component volume fraction in the membrane have been developed from the activated state and free volume theories of transport [130]. A few empirical equations were developed

for predicting the gas permeability of the membrane [131]. The logarithmic relationship between VOC permeabilities and DEHA oil content in the membrane (shown in Figure 4.5) could be well illustrated by Equation 4.1 for miscible blends:

$$\ln P_b = \phi_1 \ln P_1 + \phi_2 \ln P_2 \quad (4.1)$$

where  $P_b$ ,  $P_1$  and  $P_2$  are gas permeabilities in the homogeneous blend, pure polymer and dispersed polymer, respectively, and  $\phi_1$  and  $\phi_2$  are the volume fraction of the matrix polymer and dispersed polymer in the blended membrane, respectively. In this work,  $P_1$  and  $P_2$  represent VOC permeabilities of the pristine Pebax and DEHA oil. The VOC permeabilities of the PEBA/DEHA membrane and PEBA membrane are known and measured in the experiment. The VOC permeabilities of DEHA oil are unknown and could be solved by the equation. The VOC permeabilities of DEHA oil were calculated and compared with the data of pristine PEBA, PEBA/DEHP membrane, and PEBA membrane, as shown in Figure 4.6.

In Figure 4.6, the calculated VOC permeabilities of DEHA oil are overall two orders of magnitude higher than the PEBA membrane, which means that the DEHA oil makes a significant contribution to the VOC permeability improvement in PEBA/DEHA OLGMs. As the critical temperature of VOCs increases and VOCs become more condensable, DEHA oil shows higher VOC permeability in each VOC group. For example, DMC > acetone > MTBE in the fuel additives, butanol > propanol > ethanol > methanol in the alcohols, heptane > hexane > pentane in the paraffin, and xylene > toluene > benzene in the aromatic compounds. The VOC permeability of cyclohexane and isooctane is off the trend. It may be caused by the effect of size and shape of VOC molecules on their diffusion in the membrane [132] that the isomer with the side chain has a bigger size and diffuses slower than the straight-chained molecule. The VOC permeability of DEHA oil is overall proportional to VOC critical temperatures, which means good sorption properties of DEHA oil to VOCs and especially for VOCs with high critical temperatures. It also indicates that sorption is more important than the diffusion for gas permeation in the DEHA oil. The sorption property of the oil to VOCs is essential for oleo gel membrane development.

The VOC permeabilities of the 25PEBA/75DEHA membrane and 26PEBA/74DEHP membrane are compared, as shown in Figure 4.6. The VOC permeabilities of 25PEBA/75DEHA membrane and 26PEBA/74DEHP membrane are similar to their permeabilities comparison in non or less condensable gases (shown in Figure 4.4). The oil content in 25PEBA/75DEHA membrane is similar to 26PEBA/74DEHP membrane, but 25PEBA/75DEHA membrane shows overall higher VOC permeabilities than the 26PEBA/74DEHP membrane, which could be the fact that DEHA oil shows higher solubility to VOCs than the DEHP oil. This coincides with the literature that the DEHA has an overall higher sorption coefficient to VOCs than DEHP [133].



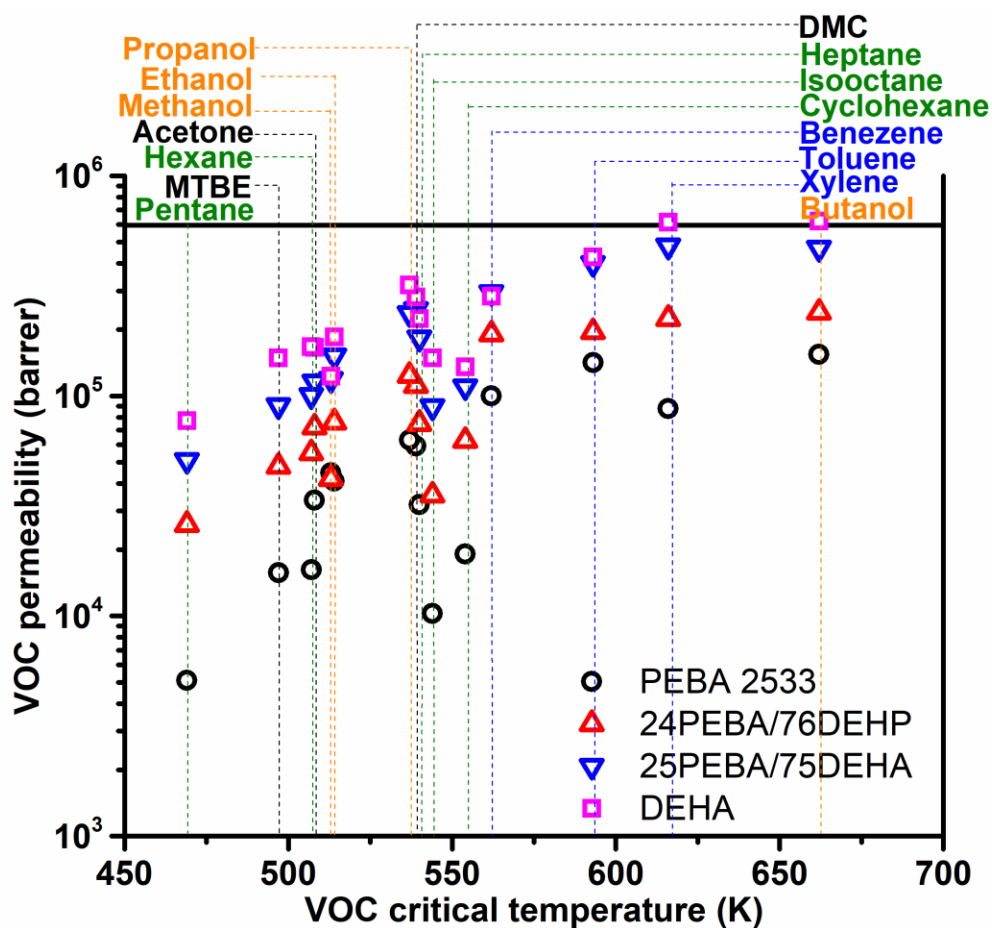
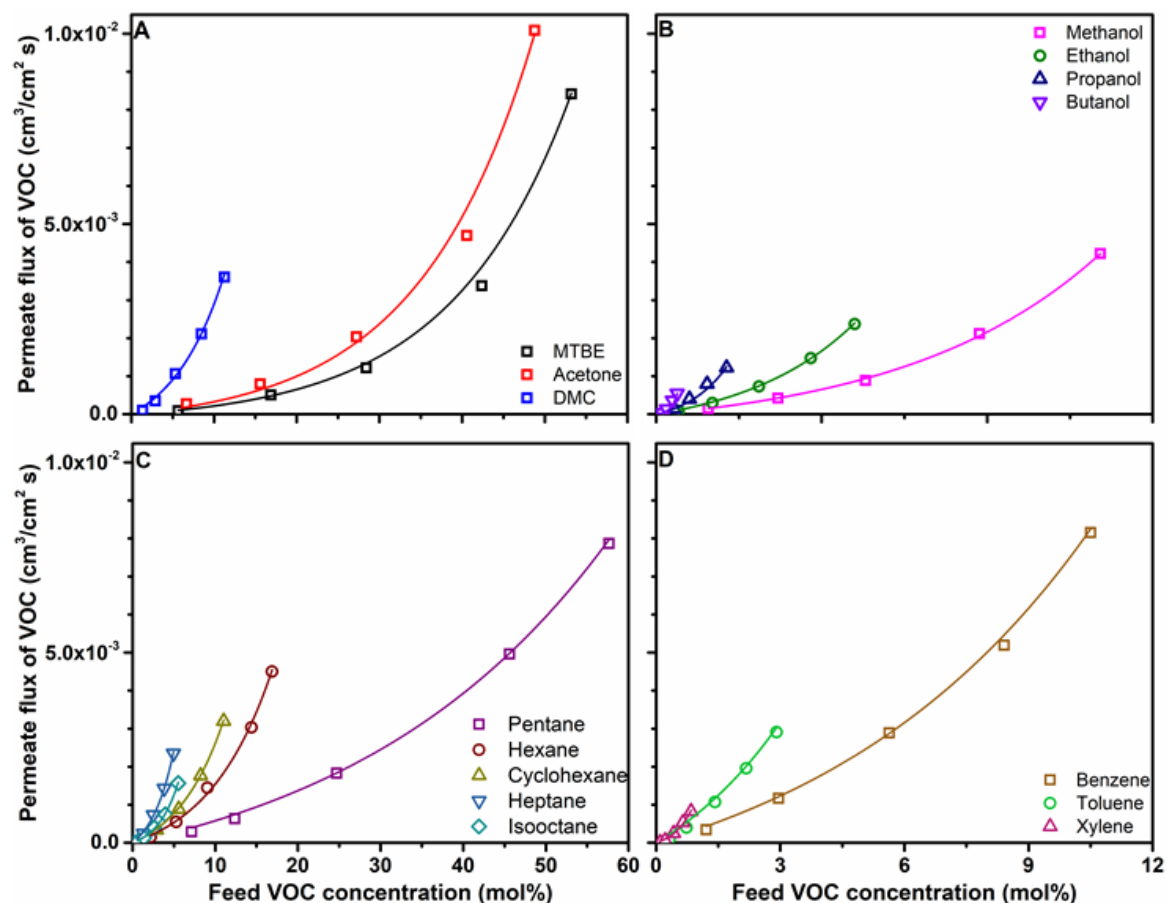


Figure 4.6 VOC permeability vs. critical temperature of VOCs. VOC permeabilities of 26PEBA /74DEHP membrane are from Chapter 3.

25PEBA/75DEHA shows the highest VOC permeability in PEBA/DEHA OLGMs, and it was selected to continue further systematic separation performance evaluations in VOC/N<sub>2</sub> mixtures. VOCs from four groups, including the fuel additives, alcohols, paraffin, and aromatic compounds, were selected for investigating the effect of feed VOC concentration and operation temperature on the VOC/N<sub>2</sub> separation performance of the membrane. The pristine PEBA membrane was tested at conditions as well, and its VOC/N<sub>2</sub> separation performance was compared with the 25PEBA/75DEHA membrane.

### 4.3.3 Effect of VOC concentration



**Figure 4.7** VOC permeate flux vs. feed VOC concentration. (A) fuel additives, (B) alcohols, (C) paraffin, and (D) aromatic compounds.

The effect of feed VOC concentration on the VOC/N<sub>2</sub> separation performance of 25PEBA/75DEHA membrane was investigated under 22°C in a binary VOC/N<sub>2</sub> mixture with a selection of 15 VOCs. Figure 4.7 shows the effects of feed VOC concentrations on the VOC permeate flux. As the feed VOC concentration increases, the VOC flux increases more than proportionally. This means that the increased VOC permeation flux was not only due to the improved driving force for permeation, but the permeability of the membrane to the VOCs was also enhanced at higher feed VOC concentration [34].

Based on the experimental results shown in Figure 4.7, a semi-empirical relation was attempted to correlate VOC permeation flux with operating conditions. Similar approaches have been widely used in the study of mass transfer in pervaporation processes [134, 135]. At steady state, the VOC permeation flux,  $Q_{VOC}$ , can be described by the Fick's law,

$$Q_{VOC} = -D_{VOC} \frac{dC_{VOC}}{dL} \quad (4.2)$$

where  $D_{VOC}$  and  $C_{VOC}$  are the diffusivity coefficient of VOC and feed VOC concentration, respectively. Assume that the VOC diffusivity exponentially depends on the feed VOC concentration.

$$D_{VOC} = D_0 \exp(\emptyset C_{VOC}) \quad (4.3)$$

where  $D_0$  is a constant and  $\emptyset$  measure the concentration dependence of VOC diffusivity. Then integrating Equation (4.2) gives:

$$Q_{VOC} = \frac{D_0}{\emptyset L} [\exp(\emptyset C_F) - \exp(\emptyset C_P)] \quad (4.4)$$

where  $L$  is the membrane thickness,  $C_F$  and  $C_P$  are VOC concentration on the feed and permeate sides of the membrane, respectively. Assuming the equilibrium partition coefficient is independent of the feed VOC concentration, then it gives  $C_F = \omega P_F x$  and  $C_P = \omega P_P y$ . When the vacuum was applied to the permeate side,  $C_P \approx 0$ , Equation (4.4) can be simplified as:

$$Q_{VOC} = \frac{D_0}{\emptyset L} [\exp(\emptyset \omega P_F x) - 1] \quad (4.5)$$

**Table 4.2** Parameters from the correlation between permeate VOC flux and the feed VOC concentration.

	$D_0/\emptyset$ (cm <sup>3</sup> /cm s)	$\omega\emptyset$ (kPa <sup>-1</sup> )	R <sup>2</sup>
Methyl tert-butyl ether	8.25E-06	1.47E-03	0.99433
Acetone	1.25E-05	1.48E-03	0.99104
Dimethyl carbonate	2.63E-05	3.39E-03	0.99692
Methanol	2.12E-05	1.72E-03	0.99948
Ethanol	2.13E-05	2.98E-03	0.99937
Propanol	1.16E-05	9.10E-03	0.97805
Butanol	5.39E-07	5.28E-02	0.91815
Pentane	5.03E-05	3.57E-04	0.99917
Hexane	2.04E-05	1.39E-03	0.99726
Cyclohexane	1.74E-05	2.03E-03	0.99956
Heptane	2.14E-05	3.62E-03	0.99862
Iso-Octane	8.58E-06	3.78E-03	0.99857
Benzene	7.88E-05	1.68E-03	0.99768
Toluene	9.60E-05	3.06E-03	0.9882
Xylene	5.96E-06	2.44E-02	0.99071

Equation (4.5) was fitted to the experimental data of VOC flux at different feed VOC concentrations (shown in Figure 4.7), and the trend lines are generated in the same Figure. The equation fits the experimental data well, with a correlation coefficient of higher than 0.99 (shown in Table 4.2). The parameters of  $\frac{D_0}{\phi}$  and  $\phi\omega$  for each VOC were determined, and they are presented in Table 4.2.

Parameter  $\frac{D_0}{\phi}$  and  $\phi\omega$  consider the feed gas composition effect on gas diffusion and sorption. By using the parameters of  $\frac{D_0}{\phi}$  and  $\phi\omega$ , the VOCs permeability can be expressed as:

$$Permeability_{VOC} = \frac{D_0/\phi}{P_F x} [\exp(\phi\omega P_F x) - 1] \quad (4.6)$$

Using the parameters ( $\frac{D_0}{\phi}$ ) and ( $\phi\omega$ ) in Table 4.2, the calculated permeabilities are shown as solid lines in Figure 4.8. The excellent alignment between the calculated permeability and the experimental data justifies that the semi-empirical correlation is useful to predict the VOC/N<sub>2</sub> separation performance of the PEBA/DEHA OLGMs. Moreover, Figure 4.8 shows that the membrane has a high VOC permeability at high feed VOC concentrations, confirming the convex curve of VOC permeates flux in Figure 4.7. At a given feed VOC concentration, the membrane showed higher permeabilities to more condensable VOCs. It followed the trend of DMC > MTBE and acetone (fuel additives), butanol > propanol > ethanol > methanol (alcohols), heptane > hexane > pentane (paraffin) and xylene > toluene > benzene (aromatic compounds). The results are consistent with the previous analysis.

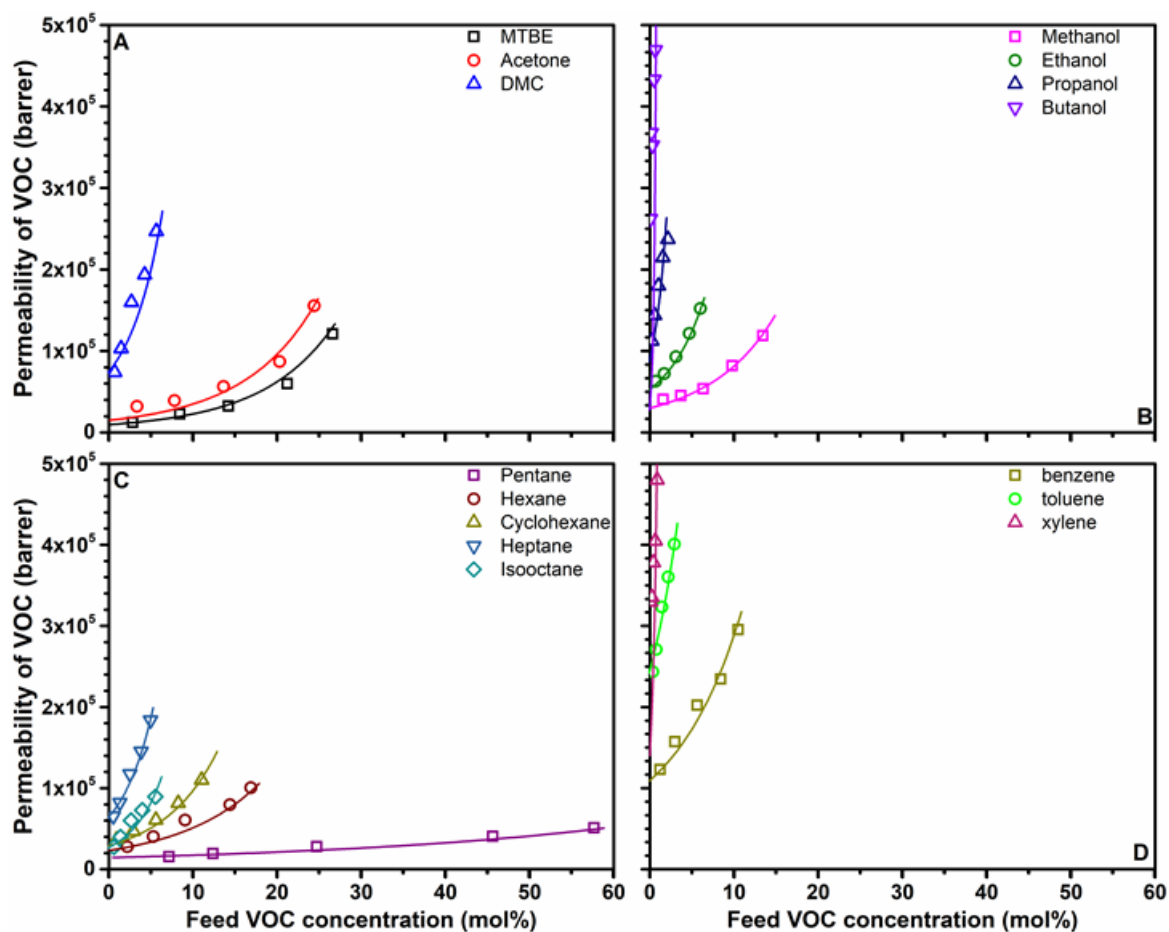


**Figure 4.8** VOC permeability vs. feed VOC concentration. (A) fuel additives, (B) alcohols, (C) paraffin, (D) aromatic compounds. The solid lines are obtained from the equation correlation, and the symbols are experimental data.

Figure 4.9 shows permeate VOC concentration as a function of feed VOC concentration. As the feed VOC concentration increases, the VOC concentration in the permeate increases as well. At a VOC concentration of higher than 2.5 mol%, a permeate VOC concentration of over 90 mol% is achieved, demonstrating the excellent VOC/N<sub>2</sub> separation performance for all 15 VOCs in the 75PEBA/25DEHA membrane.

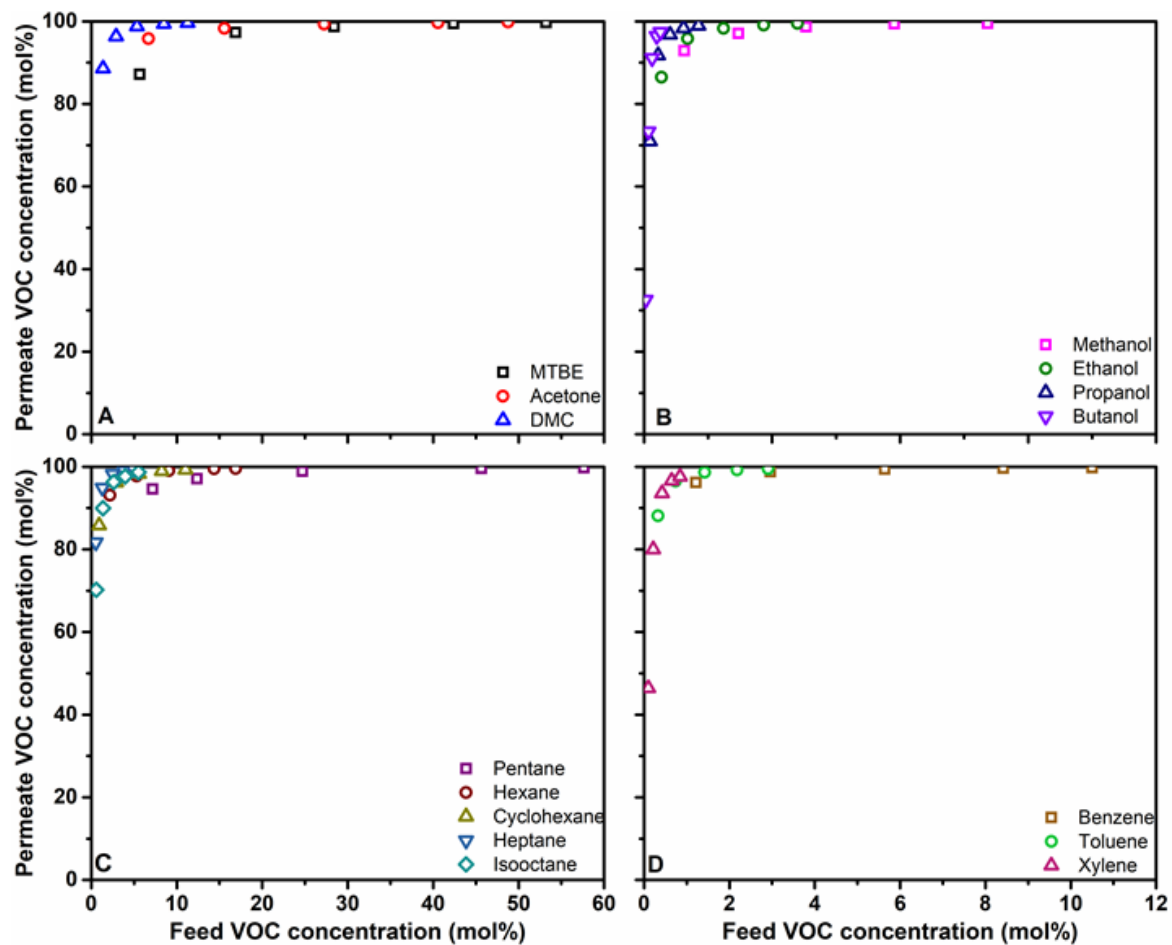


**Figure 4.9** Permeate VOC concentration vs. feed VOC concentration. (A) fuel additives, (B) alcohols, (C) paraffin, and (D) aromatic compounds.

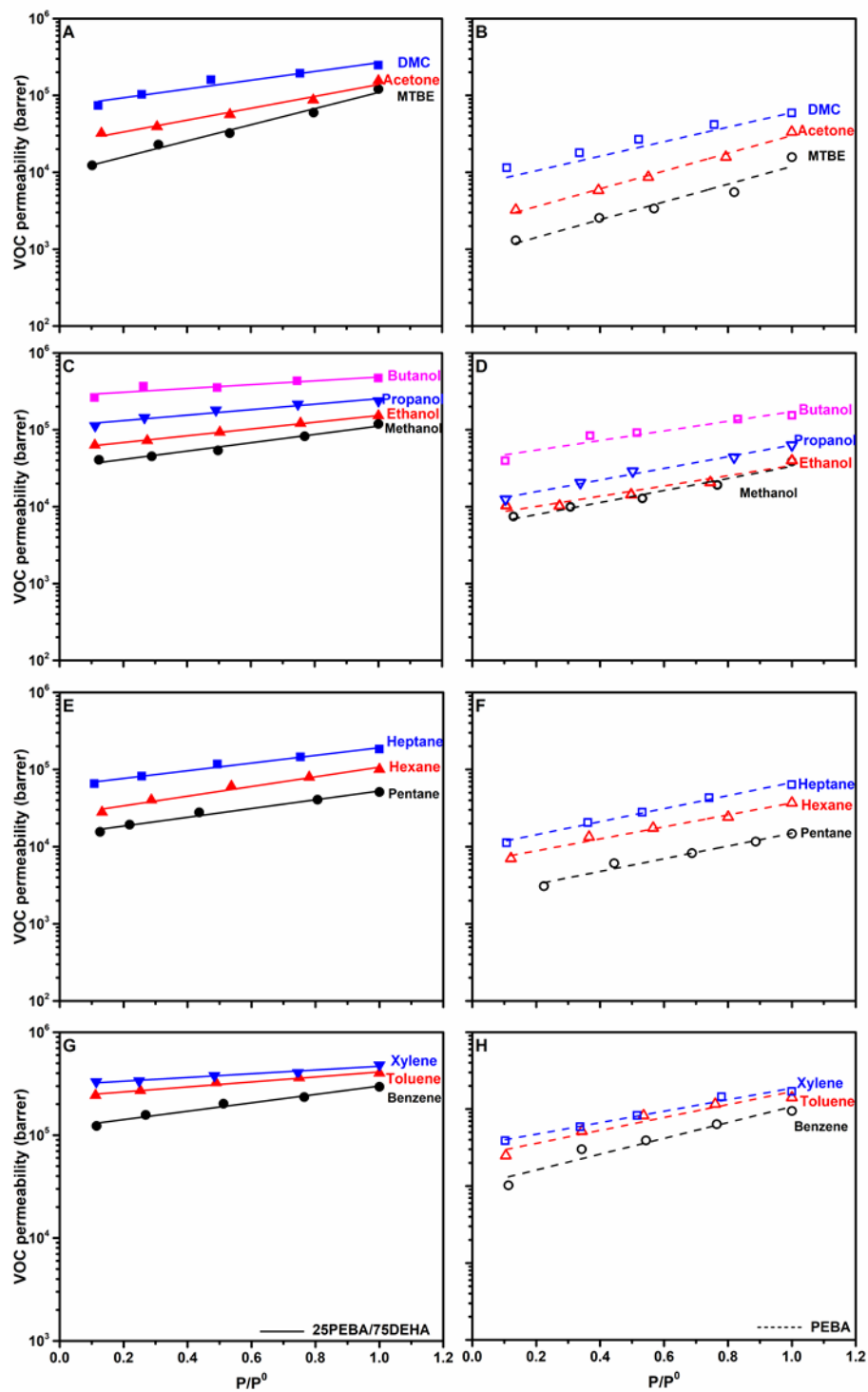


**Figure 4.10** VOC permeability comparison between 25PEBA/75DEHA and PEBA membranes.  $P/P^0$  (VOC relative volatility) is defined as VOC vapor pressure to its saturation vapor pressure. Fuel additives: (A)&(B); Alcohols:(C)&(D); Paraffins:(E)&(F); Aromatic compounds:(G)&(H).

To investigate the VOC/N<sub>2</sub> separation performance improvement of 25PEBA/75DEHA membrane at different feed VOC concentrations, the performance of the pristine PEBA membrane was evaluated at 22°C, and the results were compared with 25PEBA/75DEHA membrane. Figure 4.10 shows the effects of feed VOC concentration on VOC permeability of the membranes, where the VOC feed concentration was represented by the relative pressure ( $P/P^0$ ) ( $P$  and  $P^0$  represent the VOC partial pressure in binary VOC/N<sub>2</sub> mixture and the VOC saturated vapor pressure at 22°C, respectively). Saturated vapor pressure indicates the degree of condensability and sorption of the vapor [7]. It should be noted that the effects of condensability and sorption of different VOCs on VOCs permeability were neglected by comparing the VOC permeability in the function of VOC relative pressure in the feed. Therefore, the VOC relative pressure dependence of the membrane VOC permeability is increasing linearly upward. As relative pressure increases, the VOC permeabilities of both PEBA and 25PEBA/75DEHA membrane increase, which is consistent with the results obtained from the previous work of the PEBA/DEHP membrane. However, the increase of VOC permeabilities in the 25PEBA/75DEHA membrane was less significant than the PEBA membrane and 26PEBA/74DEHP membrane (DHEP oil content in the membrane is 76wt.%). It suggests that the high VOC partial pressure in the VOC/N<sub>2</sub> mixture has less impact on the VOC permeabilities of the PEBA/DEHA membrane than the PEBA and PEBA/DEHP membrane. This might be because the immobilization of the DEHA oil in the PEBA decreases the effects of VOC exposure and high feed VOC concentration on the VOC permeabilities of the membrane.

As 75 wt.% of DEHA oil is immobilized in the PEBA, the VOC permeabilities of the alcohol (shown in Figure 4.10 (C)) and paraffin (shown in Figure 4.10 (E)) are improved an order of magnitude higher than the PEBA membrane. A similar VOC permeability improvement was observed with 26PEBA/74DEHP membrane in Chapter 3. The similarity of VOC/N<sub>2</sub> separation performance improvement for alcohol and paraffin VOCs between 26PEBA/74DEHP and 25PEBA/75DEHA membrane confirms VOCs permeation behavior in PEBA based OLGs at different VOC partial pressure in the VOC/N<sub>2</sub> mixture. In Figure 4.10 (C) and (D), the difference in VOC permeability between methanol and ethanol for 25PEBA/75DEHA membrane becomes more prominent than PEBA, which might be that the sorption coefficient difference between methanol and ethanol in DEHA oil become more obvious than PEBA.

The permeabilities of VOCs from the groups of fuel additives and aromatic compounds for the 25PEBA/75DEHA membrane are shown in Figures 4.10 (A) & (G). Similar to the permeabilities of alcohol and paraffin VOCs, the VOC permeabilities are improved in orders of magnitude higher than the PEBA membrane. As the VOC saturated vapor pressure (shown in Table 4.3) becomes higher, the VOC permeability follows the order of DMC > Acetone > MTBE for the fuel additives group and



xylene> toluene> benzene for the aromatic group. The trends of VOC permeability for the fuel additives and aromatic compounds are the same as the alcohol and paraffin permeabilities in 25PEBA/DEHA and 26PEBA/74DEHP membranes. Because the saturated vapor pressure represents the condensability and solubility of the vapor [7], a low saturated vapor pressure of the VOC implies easy condensability and good sorption in the membrane [35]. The molar volume of the VOCs could indicate their molecular sizes. The small VOC molecule usually has a low molar volume (shown in Table 4.3) and a high diffusivity [2]. Based on the solution diffusion model, both solubility and diffusivity affect VOC permeation. The 25PEBA/75DEHA membrane shows high VOC permeability for VOC with low saturated pressure and high molar volume, suggesting that the sorption predominates VOC permeation in the membrane.

**Table 4.3** Saturated vapor pressure at 22°C and molar volume of VOCs at STP.

	Saturated vapor pressure (mmHg)	Molar volume (cm <sup>3</sup> /mole)
MTBE	220	119
Acetone	202	73
DMC	47	61
Methanol	109	41
Ethanol	50	57
Propanol	17	75
Isopropanol	36	77
Butanol	5	92
Pentane	455	115
Hexane	133	131
Cyclohexane	86	109
Isooctane	44	165
Heptane	39	149
Benzene	87	89
Toluene	24	107
Xylene	7.2	124

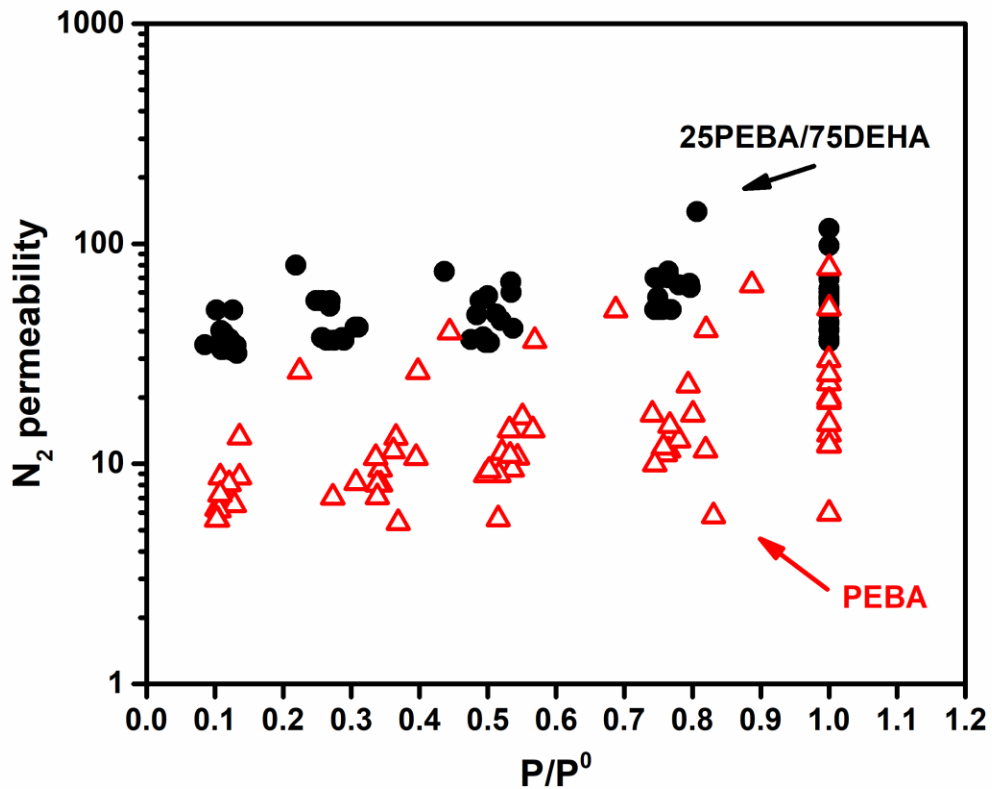


**Figure 4.11** N<sub>2</sub> permeability in 25PEBA/75DEHA and PEBA membranes. P/P<sup>0</sup> is VOC relative pressure.

The nitrogen permeability in PEBA and 25PEBA/75DEHA membranes was evaluated at 22°C immediately after the membrane exposing to VOC/N<sub>2</sub> mixture with different VOC concentrations. The nitrogen permeability was plotted in the function of VOC concentrations. To keep the analysis constant with previous one, the VOC concentrations were indicated by VOC relative pressure (P/P<sup>0</sup>), as shown in Figure 4.11. The nitrogen permeabilities in the PEBA membrane increase as VOC relative pressure increases. This is because the free volume of the membrane increases with an increase of the VOC concentration in the mixture. The nitrogen permeabilities in PEBA vary significantly at a given feed VOC concentration, and such variations become more apparent as feed VOC concentration increases. It means that different types of VOCs, as well as the high VOC concentration in the VOC/N<sub>2</sub> mixture, have a significant effect on the free volume of the PEBA membrane, causing the variation of the N<sub>2</sub> permeabilities (see Figure 4.11). As a comparison, the variation of N<sub>2</sub> permeability in 25PEBA/75DEHA membrane at certain relative pressure was less

significant than the PEBA membrane. Additionally, the nitrogen permeability in 25PEBA/75DEHA membrane increases less significantly than in the PEBA membrane as the VOC relative pressure increases. It means that the 25PEBA/75DEHA membrane structure is barely affected by different types of VOCs and feed VOC concentrations. Therefore, DEHA oil immobilized into the PEBA helps decrease the effects of different types of VOCs and high feed VOC concentration on membrane structure and reduces the variation of  $N_2$  permeabilities compared to the PEBA membrane.

The VOC/ $N_2$  selectivities of 25PEBA/75DEHA and PEBA membranes are shown in Figure 4.12. The VOC/ $N_2$  selectivities increase as the  $P/P^0$  increase. The feed VOC relative pressure dependence of VOC/ $N_2$  selectivity in the 25PEBA/75DEHA membrane was as linear as its trend in VOC permeability (see Figure 4.10). In contrast, the selectivity trends of VOC/ $N_2$  in the PEBA membrane were not linear because the effects of different VOCs and high feed VOC concentrations make significant variations in nitrogen permeabilities with different VOC relative pressure.

Moreover, the 25PEBA/75DEHA membrane shows a higher VOC/ $N_2$  selectivity, especially for condensable VOCs. The overall VOC/ $N_2$  selectivity of the 25PEBA/75DEHA membrane is higher than the PEBA membrane.

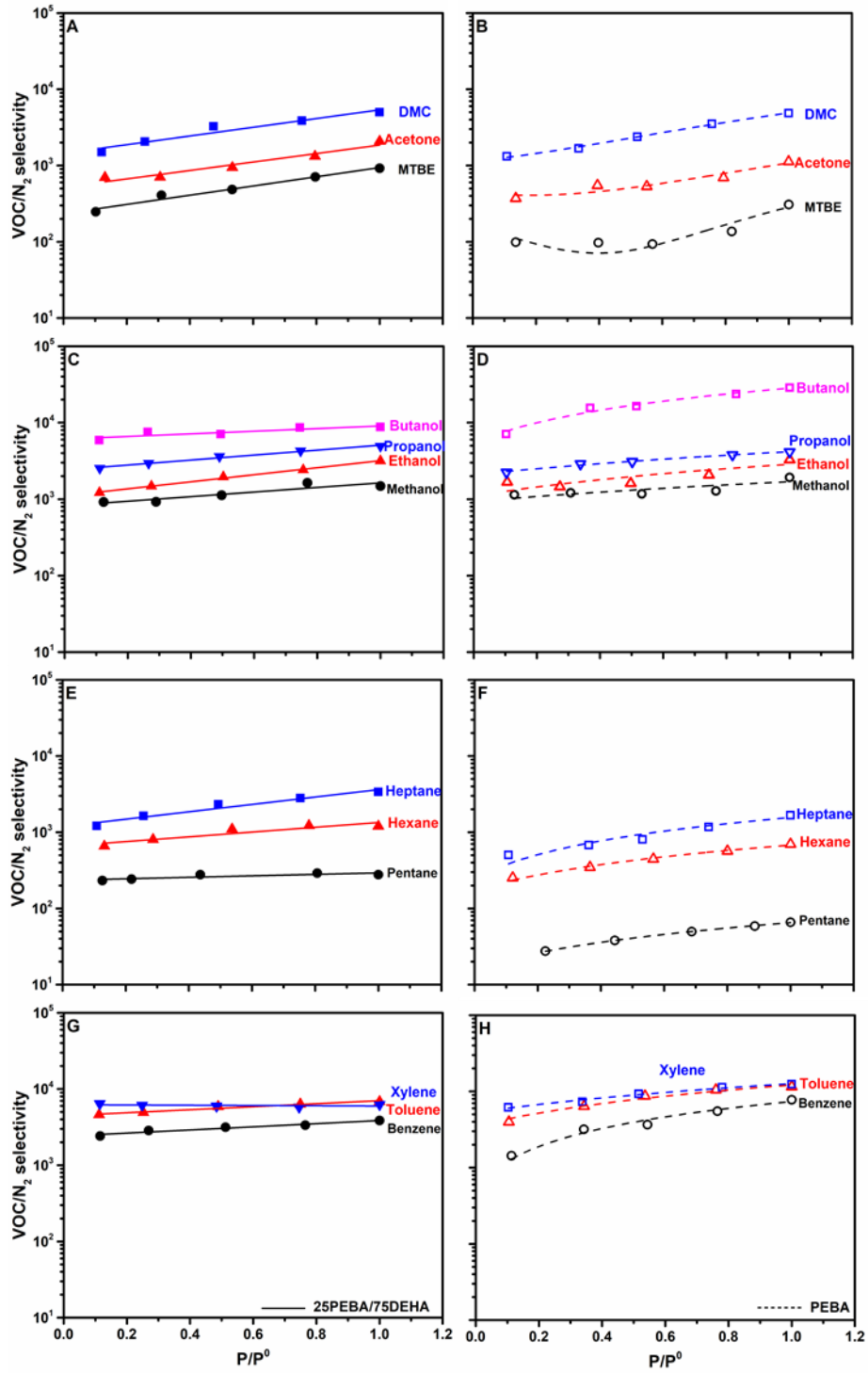


**Figure 4.12** VOC/N<sub>2</sub> comparison between 25PEBA/75DEHA and PEBA membranes.  $P/P^0$  is VOC relative volatility. Fuel additives: (A)&(B); Alcohols:(C)&(D); Paraffins:(E)&(F); Aromatic compounds:(G)&(H).

#### 4.3.4 Effect of temperature

The effects of temperature on membrane VOC/N<sub>2</sub> separation performance were evaluated at temperatures ranging from 22°C to 50°C. The VOC concentrations in the feed stream are shown in Table 4.4. Both membranes of 25PEBA/75DEHA and PEBA were tested under this condition.

**Table 4.4** Feed VOC concentrations in feed stream with binary VOC/N<sub>2</sub>.

	VOC concentration (%)
Methyl tert-butyl ether (MTBE)	26.6
Acetone	24.4
Dimethyl carbonate (DMC)	5.5
Methanol	12.7
Ethanol	5.8
n-Propanol	1.9
n-Butanol	0.6
Pentane	56.6
n-Hexane	15.9
Cyclohexane	10.5
Heptane	5.0
Iso-Octane	5.3
Benzene	10.5
Toluene	2.9
Xylene	0.84

Figure 4.13 shows the membrane VOC permeability as a function of reciprocal temperature in a semi-logarithm scale. The permeabilities of 15 VOCs for the 25PEBA/75DEHA and PEBA membranes are respectively shown in Figures (A), (C), (E), (G) and (B), (D), (F), (H). More VOCs were used to evaluate VOC/N<sub>2</sub> separation performance for membranes compared with the works in Chapter 3. The effect of temperature on VOC permeability is similar to the previously reported result in Chapter 3 that all VOC permeabilities of both 25PEBA/75DEHA and PEBA membranes decrease as the temperature increases, and the VOC permeability of the PEBA membrane shows the convex curve as the temperature changes. When 75wt.% DEHA oil present in the PEBA matrix, the membrane VOC permeability at all operating temperatures improves. The curve of VOC permeability

vs.  $1000/T$  for 25PEBA/75DEHA membrane is straight linear and follows the Arrhenius equation, which makes the VOC permeabilities of the PEBA/DEHA membrane at different temperatures more predictable than PEBA and PEBA/DEHP membranes, which doesn't follow the Arrhenius equation.

The VOC activation energies for the 25PEBA/75DEHA membrane obtained from the slope of the straight line in Figure 4.13 are shown in Table 4.5. The negative VOC activation energy suggests that VOC permeability is more dependent on the sorption of VOC than the diffusion in the membrane [93], which has been explained in Chapter 3. Additionally, as the saturated vapor pressures of VOCs (Table 3.3) become higher, the VOCs become more volatile, the activation energy for VOC permeation (Table 4.5) follows the same order of volatility as MTBE  $\approx$  acetone > DMC, methanol > ethanol > propanol > butanol and benzene > toluene > xylene, which indicates that the effect of temperature on membrane permeability becomes more significant as VOC become more volatile.

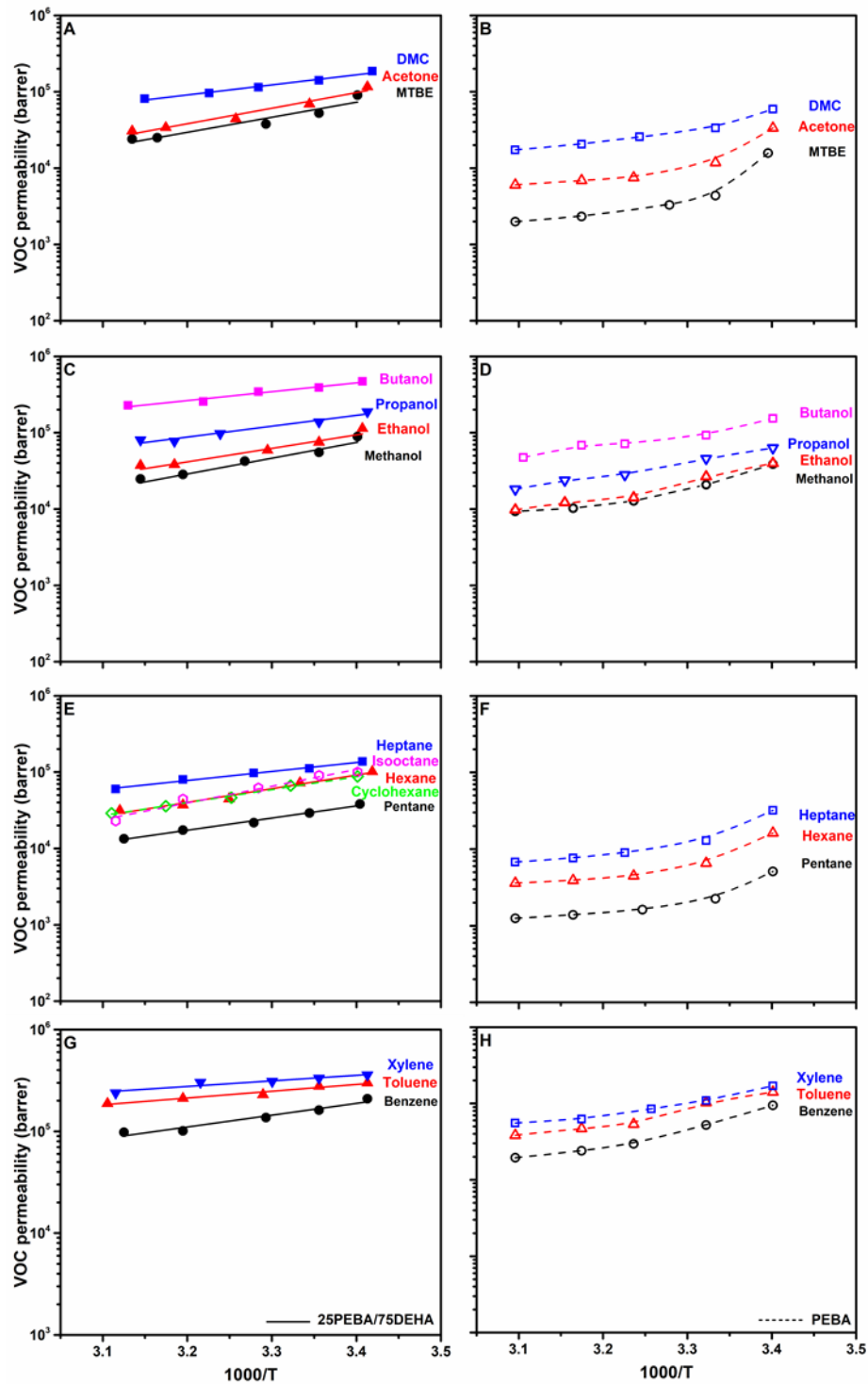


**Figure 4.13** Effect of temperature ( $1000/T$ ) on VOC permeability. VOCs permeabilities of 25PEAB/75DEHA membrane and PEBA membrane are in solid line and dashed line, respectively. Fuel additives: (A)&(B); Alcohols:(C)&(D); Paraffins:(E)&(F); Aromatic compounds:(G)&(H).

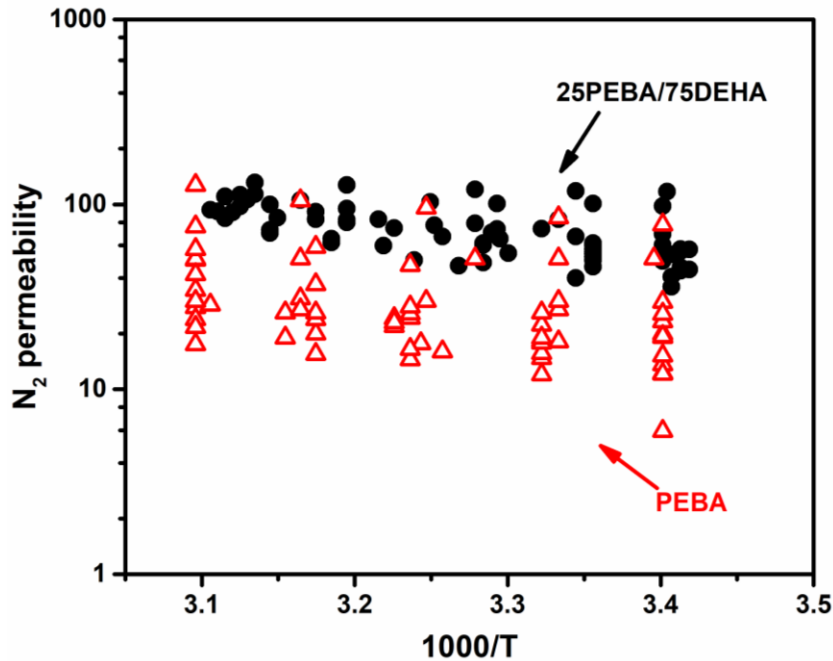


**Figure 4.14** N<sub>2</sub> Permeability at different temperatures.

Figure 4.14 shows the temperature dependence of nitrogen permeabilities for PEBA and 25PEBA/75DEHA membranes. The nitrogen permeability increases as temperature increases for both membranes because the thermal motion of the polymer chain is enhanced, and the free volume of the membrane increases [136]. At a specific temperature, the nitrogen permeability of PEBA has a more extensive range than the 25PEBA/75DEHA membrane. This could be because the VOCs significantly affect membrane structure in PEBA membrane but barely affect 25PEBA/75DEHA membrane.

The nitrogen activation energies for 25PEBA/75DEHA and PEBA are positive (Table 4.5), indicating that the diffusion aspect is more critical in nitrogen permeation. And the nitrogen activation energy for 25PEBA/75DEHA is overall lower than the PEBA membrane, which also shows evidence that the effect of temperature on the nitrogen permeation in the PEBA/DEHA membrane is less significant than the PEBA membrane.



**Table 4.5** Activation energy for permeation of VOC and N<sub>2</sub>.

		The permeation activation energy		
		(kJ mol <sup>-1</sup> )		
		PEBA25/DEHA75		PEBA
		VOC	N <sub>2</sub>	N <sub>2</sub>
Fuel additive	MTBE/N <sub>2</sub>	-37.8	3.7	7.7
	Acetone/N <sub>2</sub>	-39.0	15.4	7.43
	DMC/N <sub>2</sub>	-25.3	16.7	13
Alcohol	Methanol/N <sub>2</sub>	-39.6	14.8	14.4
	Ethanol/N <sub>2</sub>	-33.9	13.3	14.8
	n-Propanol/N <sub>2</sub>	-27.3	8.3	17.7
	n-Butanol/N <sub>2</sub>	-22.2	10.2	18.8
paraffin	Pentane/N <sub>2</sub>	-30.5	5.2	11.5
	n-Hexane/N <sub>2</sub>	-46.9	6.7	12.4
	Cyclohexane/N <sub>2</sub>	-21.0	6.9	10.2
	Heptane/N <sub>2</sub>	-46.2	16.1	11.3
	Iso-Octane/N <sub>2</sub>	-27.3	13.2	10.9
Aromatic compound	Benzene/N <sub>2</sub>	-43.5	18.0	17.6
	Toluene/N <sub>2</sub>	-32.6	17.0	6.5
	Xylene/N <sub>2</sub>	-31.2	15.6	15.1

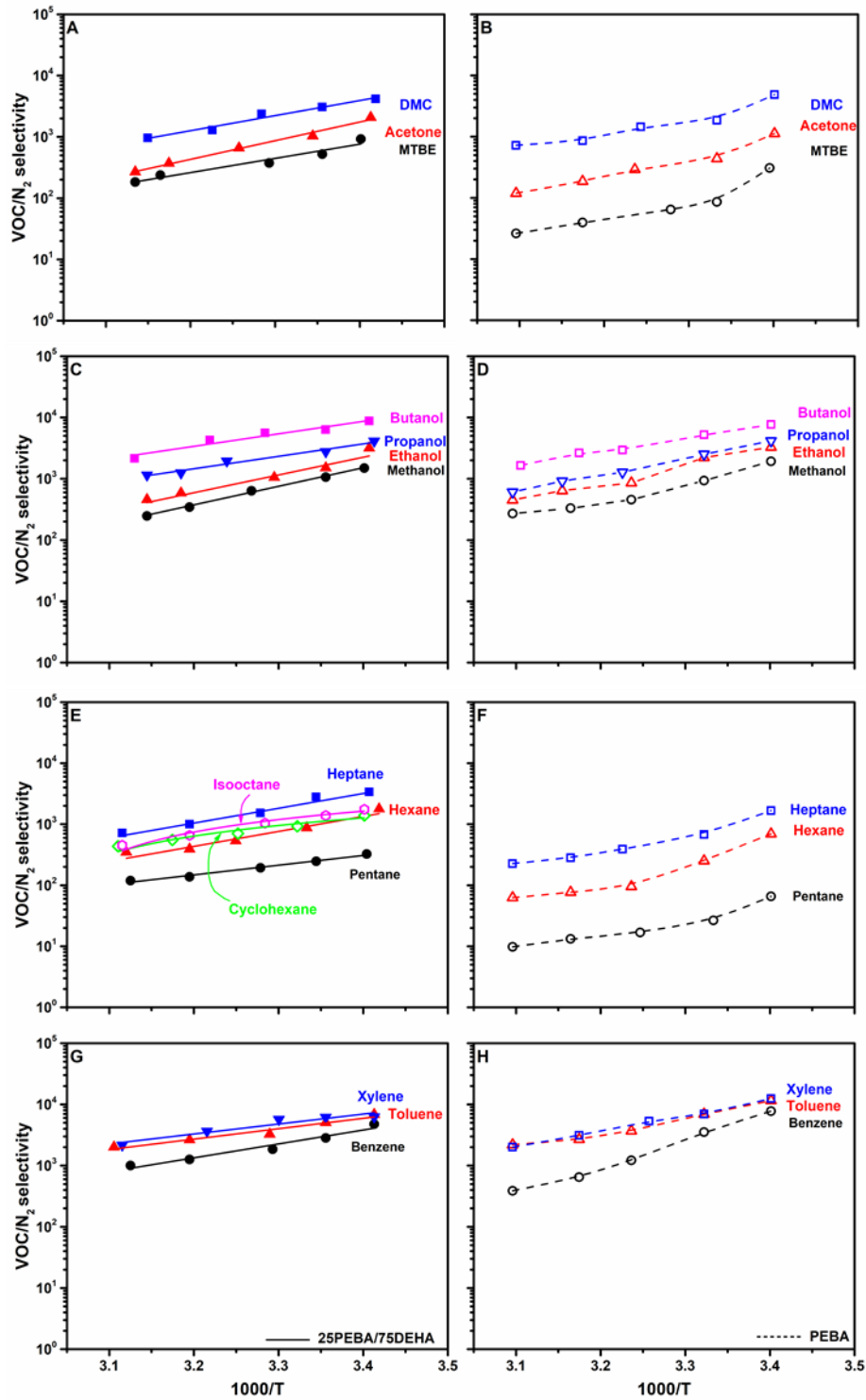


**Figure 4.15** Effect of temperature ( $1000/T$ ) on VOC/N<sub>2</sub> selectivity. VOC/N<sub>2</sub> selectivity of 25PEAB/75DEHA membrane and PEBA membrane are in solid line and dashed line, respectively. Fuel additives: (A)&(B); Alcohols:(C)&(D); Paraffin:(E)&(F); Aromatic compounds:(G)&(H).

VOC/N<sub>2</sub> selectivity at different temperatures for PEBA and 25PEAB/75DEHA membranes are shown in Figure 4.15. The VOCs/N<sub>2</sub> selectivity increases as the temperature decrease. And 25PEBA/75DEHA membrane shows an order of magnitude higher VOCs/N<sub>2</sub> selectivity than the PEBA membrane at all evaluated temperatures.

#### 4.3.5 Membrane stability

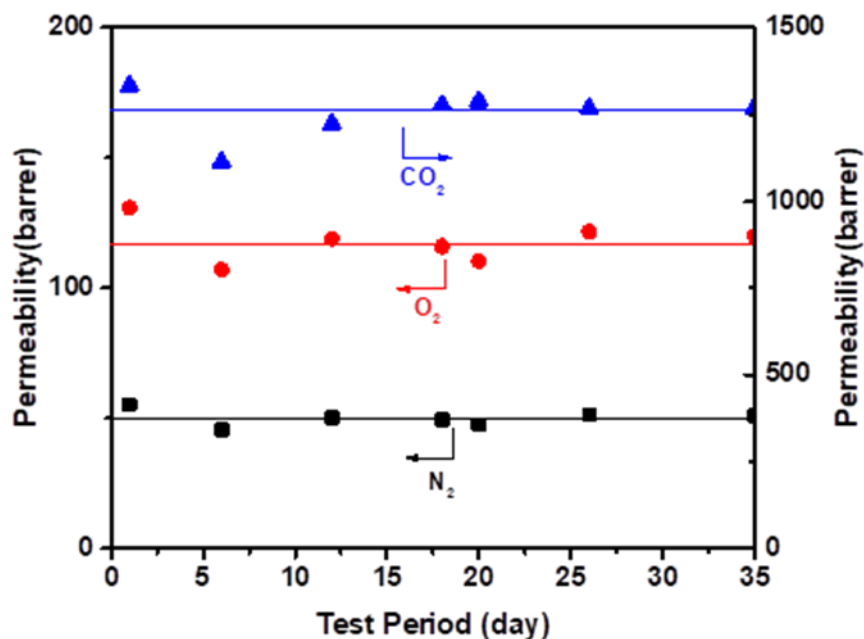


**Figure 4.16** Membrane stability evaluation by measuring the pure gas performance of the membrane in the 60 days.

The 25PEAB/75DEHA membrane was selected for a long-term stability test (35 days). The membrane was tested in VOC/N<sub>2</sub> mixtures with different VOCs, feed VOC concentrations, and temperatures. After a period of VOC/N<sub>2</sub> mixed gas testing, the pure gases test with carbon dioxide, oxygen, and nitrogen was conducted to confirm the membrane stability. Figure 4.16 shows the permeabilities of gases (CO<sub>2</sub>, O<sub>2</sub>, and N<sub>2</sub>) measured at room temperature with a feed pressure at 0.4MPa and permeate pressure at 1 atm. The membrane showed excellent stability with a permeability of 50 barrers to nitrogen, 120 barrers to oxygen, and 1300 barrers to carbon dioxide.

#### 4.4 Conclusion

The homogeneous PEBA/DEHA OLGMs were successfully prepared. Compared with the DEHP oil, the lower infinity of PEBA to DEHA oil makes the DEHA prone to saturation than the DEHP oil during the membrane formation. However, DEHA could still be well immobilized in the PEBA, and

75wt.% of DEHA oil was immobilized in the PEBA/DEHA membrane, which may mainly rely on the hydrogen bonding between the DEHA and the PEBA.

The evaluation of gas separation on PEBA/DEHA OLGMs was performed with six pure gases and fifteen binary VOC/N<sub>2</sub> mixtures, which proved its excellent gas permeation property. The VOC/N<sub>2</sub> separation performance of the PEBA/DEHA OLGMs was better than the PEBA membrane because of the DEHA oil immobilization in the membrane and good solubility of the VOCs in the membrane materials (e.g., PEBA and DEHA). Moreover, the VOC permeabilities of the PEBA/DEHA OLGMs are dependent on the content of DEHA oil in the membrane, and the permeabilities of DEHA oil to VOCs were calculated based on the miscible blending rules in this work.

During the binary VOC/N<sub>2</sub> mixed gas test, the 25PEBA/75DEHA OLGGM showed better VOC permeability at the lower temperature and higher feed VOC concentration. The temperature dependence of VOC permeability of the membrane followed the Arrhenius equation and made the VOC permeability more predictable at different temperatures. The nitrogen permeabilities were measured after the membrane was exposed in VOCs with various feed concentrations, demonstrating that the structure in 25PEBA/75DEHA OLGGM was less affected by VOCs and high feed VOC concentration than that in PEBA. Additionally, the membrane was stable during 35 days test at the various conditions. It was concluded that the membrane stability in VOC exposure could be improved significantly by DEHA oil immobilization, which gave the membrane great potential to be applied in VOC removal and VOC enrichment at high feed VOC concentration.

## Chapter 5

### PDMS/DEHA oleo gel membrane for VOC/N<sub>2</sub> separation

#### 5.1 Introduction

The social, health and ecological problems caused by VOC emissions have drawn attention in many countries [49, 99, 100]. United States Environmental Protection Agency (US-EPA) has treated the VOC as major pollutants and hazardous air pollutants (HAPs) [52]. Similar legislation has also been set by many other countries and regions to prevent VOC emission. Membrane separation has advantages of low energy consumption, no regeneration requirement, and compact equipment is getting attention to apply on VOC removal [5, 19, 110, 137].

The oleo gel membrane (OLGM) was developed in previous work to improve the VOC permeability of the PEBA membrane. The oils which have low volatility and high VOC permeability are immobilized in the PEBA matrix. The PEBA/DEHP (Bis(2-ethylhexyl) phthalate) oleo gel membrane has been developed, and the membrane showed significant VOC permeability improvement than the PEBA membrane (Chapter 3). The VOC permeability was further improved by developing the PEBA/DEHA membrane since the VOC permeability (Chapter 4) and VOC sorption coefficients [133] in DEHA (Bis (2-ethylhexyl) adipate) oil are higher than the DEHP oil. The VOC permeability in the PEBA-based oleo gel membrane increased with the oil content increase in the membrane. The highest content of the DEHA oil that could be immobilized in the PEBA matrix is 75wt.%, which means that PEBA, as the oil retainer, limits the oil to be further immobilized in the membrane.

To further improve the oil immobilization in the polymer, a polymer with an amorphous structure and more free volume will be needed. PDMS as a good candidate was selected. The DEHA oil, which has excellent VOC permeabilities, was immobilized in the PDMS. And the PDMS/DEHA OLGM was developed in this work. The OLGMs were fabricated by making the PDMS crosslinked at various degrees. Moreover, Different contents of DEHA oil were also immobilized in a standard crosslinked PDMS to fabricate the OLGMs. The VOC permeability and VOC/N<sub>2</sub> selectivity of all OLGMs were evaluated. 15 VOCs from four groups were selected to assess VOC/N<sub>2</sub> separation performance: alcohols (methanol, ethanol, propanol, and butanol); paraffin (pentane, hexane, cyclohexane, isooctane, and heptane); aromatic compounds (benzene, toluene, and xylene); and fuel additives (methyl tert-butyl ether (MTBE), dimethyl carbonate (DMC), and acetone). The PDMS(SC)-60/DEHA-40 membrane showed the highest VOC permeabilities in PDMS/DEHA OLGMs and was selected to assess its VOC/N<sub>2</sub> separation performance at various feed VOC

concentrations and temperatures. The membrane showed excellent VOC/N<sub>2</sub> separation performance and was stable in two months test period.

## **5.2 Experiment**

### **5.2.1 Material**

Polydimethylsiloxane (RTV655, General Electrics) was purchased from Toshiba Silicones (Tokyo, Japan), and it consisted of an elastomer base (part A) and a curing agent (part B). Bis (2-ethylhexyl) adipate (DEHA) was obtained from Fluka Analytical (Germany). The purity of gases used in the permeation experiment was at least 99.9%; The organic solvents used to generate VOCs in the vapor/gas permeation tests were at reagent grade. The supplier of the gas and VOCs were introduced in Chapter 3.

### **5.2.2 Membrane preparation**

The membrane casting solution was formulated by dissolving part A and part B of PDMS with DEHA oil in cyclohexane; the total content of PDMS and DEHA in the membrane casting solution was 10wt.%. In addition to the conventionally used part A to part B ratio of 10:1, a less amount of part B was also used to reduce the degree of crosslinking in the PDMS. Table 5.1 lists the formulation of membrane casting solutions. The casting solution was blended at room temperature for 14 hrs to be homogeneous and then cast onto a glass plate, following by evaporation of the solvent for 12hrs in the fume hood. The membrane was subjected to heat treatment in an oven at 75°C for 12hrs to allow full crosslinking of PDMS. The resulting membranes were dense and homogeneous. The thickness of all membranes was controlled to be approximately 250 μm. For convenience, the membrane names in Table 5.1 are used to describe the membrane in the following discussion.

**Table 5.1** The composition of the membrane casting solution.

#	Membrane name	Membrane casting solution composition	
		Crosslinker content (part A to B mass ratio)	PDMS to DEHA mass ratio (wt.%)
1	PDMS(SC)		100/0
2	PDMS(SC)-95/DEHA-5		95/5
3	PDMS(SC)-90/DEHA-10	A/B=10/1	90/10
4	PDMS(SC)-75/DEHA-25	Standard crosslinking	75/25
5	PDMS(SC)-60/DEHA-40		60/40
6	PDMS(SC)-50/DEHA-50		50/50
7	PDMS(LC)-60/DEHA-40	A/B=20/1 lower crosslinking	60/40
8	PDMS(LLC)-60/DEHA-40	A/B=30/1 Lower crosslinking	60/40

Note: The total content of PDMS and DEHA in membrane casting solution is 10 wt.%.

### 5.2.3 Contact angle, SEM, microscope, and mechanical properties

The contact angle was measured by the contact angle meters (Tantec CAM-PLUS). The cross-sections of PDMS/DEHA membranes were examined using scanning electron microscopy (SEM, LEO FESEM 1530). The membrane cross-sections were fractured in liquid nitrogen and sputtering coated with gold. The surface morphology of membranes was characterized using the Zeiss LSM 710 confocal microscope. Fourier transformation infrared spectra (FTIR) was characterized by Bruker-VERTEX 70. The mechanical properties of membranes were determined using an Instron 4465 tensile and compression tester equipped with Bluehill software. The tensile strain  $\varepsilon$  (mm/mm), tensile stress  $\delta$  (MPa), and young's modules  $E$  (MPa) were evaluated and the brief introduction was in Chapter 3.

### 5.2.4 Permeation experiment

The permeation experiment set-up has been described in section 3.24 and shown in Figure 3.1.

### 5.2.5 Nitrogen permeance measurement

The nitrogen permeance measurement and permeance calculation were introduced in section 4.2.4 in Chapter 4.

### 5.2.6 VOC/N<sub>2</sub> separation performance characterization

The method to determine VOC permeability was introduced in section 3.26 in Chapter 3. A set of equations from (3.1) to (3.4) need to be solved.

## 5.3 Result and discussion

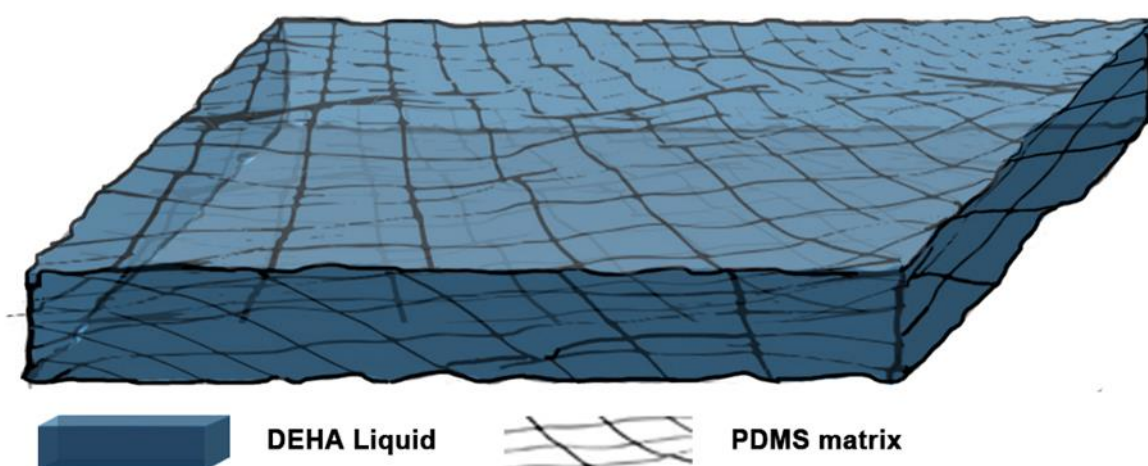


**Figure 5.1** Schematic diagram of DEHA oil randomly dispersed in the PDMS matrix.

A schematic diagram of the PDMS/DEHA membrane is shown in Figure 5.1. DEHA as a non-volatile liquid oil that was embedded in the PDMS matrix. Once the membrane was formed, DEHA oil was locked in the PDMS network. To investigate the amount of DEHA oil that can be retained in the PDMS network, PDMS was crosslinking at a conventional A/B ratio of 10/1, and DEHA oil contents varied in the membrane (refer to membrane 2 to membrane 6 in Table 5.1). The PDMS(SC)-50/DEHA-50 is too delicate to form the membrane, and it was not used in any evaluation and characterization in this work. To further improve the membrane ability to retain the DEHA oil, PDMS with the reduced crosslinking degree at A/B ratios of 20/1 and 30/1 were fabricated; meanwhile, a constant DEHA content in the membrane was maintained. The resultant membranes were denoted as membrane PDMS(LC)-60/DEHA-40 and membrane PDMS(LLC)-60/DEHA-40. PDMS(LLC)-60/DEHA-40 was found to be too fragile to form a free-standing membrane, while PDMS(LC)-



60/DEHA-40 could form free-standing membranes. Therefore, the VOC/N<sub>2</sub> permeation test was only performed on the latter membrane. The VOC/N<sub>2</sub> separation performance of the membrane was compared with the membrane PDMS(SC)-60/DEHA-40 in this work.

### 5.3.1 Membrane characterization

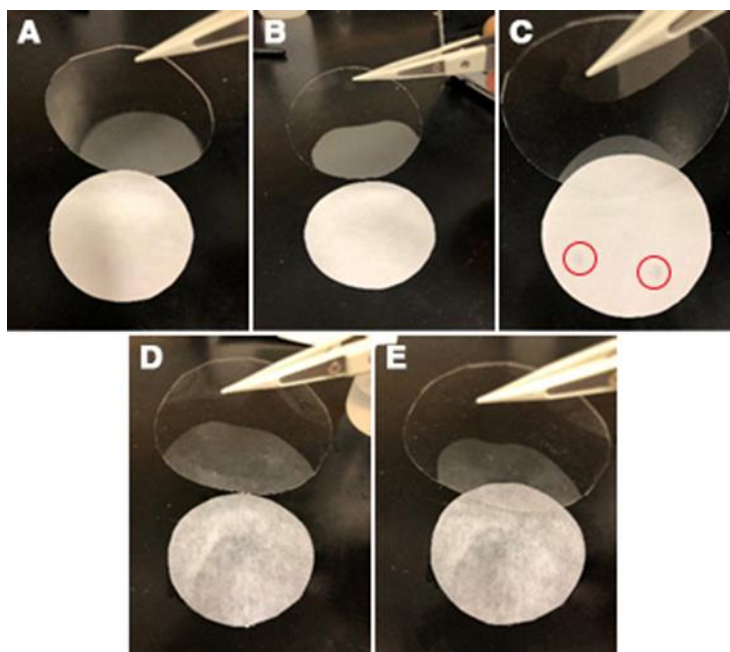


**Figure 5.2** Image of standard crosslinked PDMS/DEHA membranes and the papers underneath: (A) PDMS(SC), (B) PDMS(SC)-95/DEHA-5, (C) PDMS(SC)-90/DEHA-10, (D) PDMS(SC)-75/DEHA-25, (E) PDMS(SC)-60/DEHA-40.

The pictures of standard crosslinked PDMS/DEHA membranes are shown in Figure 5.2. They were all transparent and homogenous. Both sides of the membranes were placed on a sheet of paper to remove the DEHA oils saturated out on the membrane surface and further determine the amount of DEHA oil retained in the PDMS matrix.

No oil stains were found on the paper when contacting PDMS(SC) and PDMS(SC)-95/DEHA-5 membranes, as shown in Figure 5.2 (A) and (B). Two spots of oil imprint (red circles marked) were observed on the paper when contacting PDMS(SC)-90/DEHA-10, as shown in Figure 5.2 (C). More oil stains were found on the papers when contacting PDMS(SC)75/DEHA-25 (Figure 5.2 (D)), and this becomes more significant for PDMS(SC)-60/DEHA-40 (Figure 5.2 (E)).

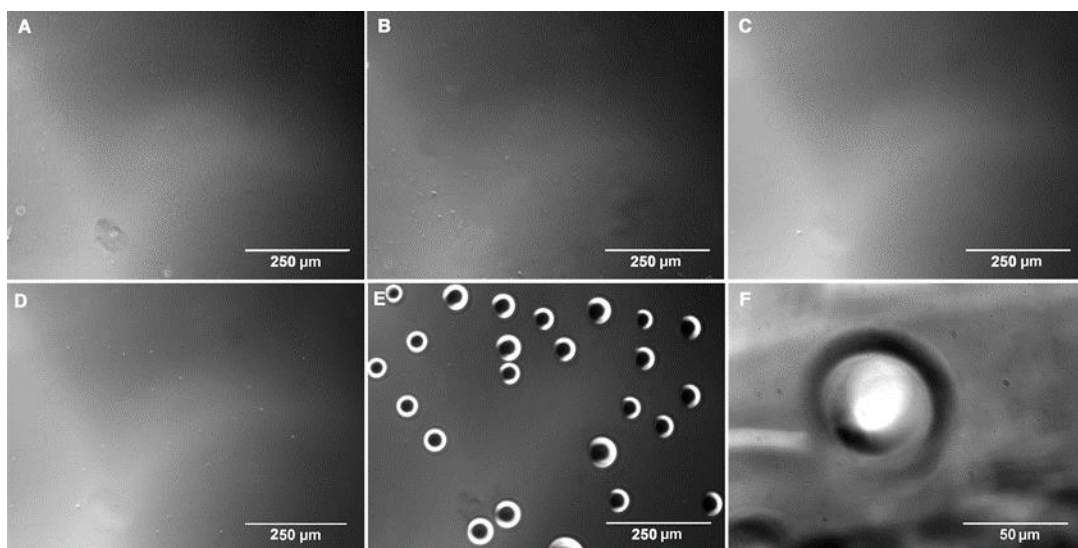


**Figure 5.3** Membrane surface image scanned under Microscopic: (A) PDMS(SC), (B) PDMS(SC)-90/DEHA-10, (C) PDMS(SC)-75/DEHA-25, (D) PDMS(SC)-60/DEHA-40(non-dripping area), (E) PDMS(SC)-60/DEHA-40(dripping area), (F) enlarged scan of the DEHA liquid droplet on image (E).

To better look into and confirm the phenomena of oil saturation on the membrane surface, some membranes were further examined under a microscope after fabrication without oil removal by papers. Four membranes (i.e., PDMS(SC), PDMS(SC)-90/DEHA-10, PDMS(SC)-75/DEHA-25, and PDMS(SC)-60/DEHA-40) were selected, and the images are shown in Figure 5.3. It shows that the surfaces of PDMS(SC), PDMS(SC)-90/DEHA-10, and PDMS(SC)-75/DEHA-25 were flat, and no clear oil droplets were observed on the membrane surface. For PDMS(SC)-60/DEHA-40 in Figure 5.3 (E), some parts of the membrane are similar to the other membranes shown in Figure 5.3 (A)- (C) that there are no oil drippings were observed on the membrane surface. Meanwhile, some oil drippings were observed on the rest part of the membrane surface with the diameter at 50um, as shown in the enlarged image in Figure 5.3 (F). Although no clear oil drippings were detected on membrane surfaces under the microscope for PDMS(SC)-90/DEHA-10 and PDMS(SC)-75/DEHA-25, some “oily” feelings for PDMS(SC)-90/DEHA-10, and more for PDMS(SC)-75/DEHA-25 could be felt when touched with hands. It means that the DEHA oil was uniformly distributed on the surface of the membranes PDMS(SC)-90/DEHA-10 and PDMS(SC)-75/DEHA-25, but the oil could not form the drippings on membranes surfaces.

In summary, PDMS and DEHA have very similar solubility parameters ( PDMS=16.4 [138] and DEHA =16.7 [90]) and could be well blended in cyclohexane to form a homogeneous membrane

casting solution. After solvent evaporation and PDMS crosslinked, a certain amount of oil is excluded from the membrane if the amount of DEHA was over-retained in the PDMS matrix. Thus, more DEHA oil in the membrane casting solution, more over-saturated oil may be observed on the membrane surface after membrane formation. The contact angle of DEHA oil on the PDMS(SC) membrane was measured and shown a value of  $40^\circ$ . It means that the PDMS is oleophilic to the DEHA oil, and the contact angle is big enough for the DEHA oil droplet formed and observed on the membrane surface in Figure 5.3 (F) and (E).

To quantify the DEHA oil immobilized in membranes, the excess oil on the membrane surface was wiped out, the weights of the membrane were measured before and after oil removal. The relative weights of after/before oil removal for membranes are shown in Figure 5.4(A), and the contents of oil immobilized in the membrane are shown in Figure 5.4(B). Both figures are generated as the function of the oil content in the membrane casting solutions. The membrane name was also labeled on the X-axis to their respective membrane casting solution. In Figure 5.4 (A), the membrane relative weight decreases as the oil content increase in the membrane casting solution. It means that the more DEHA oil in the membrane casting solution, the more oil was excluded from the membrane due to saturation of oil in the membrane, which agrees with the observations from previous surface characterizations. The actual DEHA content in the membrane was then calculated based on oil retained in the membrane, and the results are shown in Figure 3.5 (B). As the DEHA content increases in the membrane casting solution, the immobilized oil content in the membrane increases, but the content of the immobilized oil in the membrane could be less than that in the membrane casting solutions.

In previously reported PEBA/DEHA OLGs, there was no oil saturation observed in the membrane which was fabricated by the casting solution with 40 wt.% of the oil. The oil is more easily immobilized in the PEBA than the PDMS. It could be because the NH and OH groups in PEBA are good hydrogen bond donors, and they have an H atom with electropositivities [139]. C=O groups in DEHA are good hydrogen bond acceptors with free electrons/high electronegativity to give to the H atom [67]. The DEHA oil is retained in the PEBA matrix, and hydrogen bonding forms between the PEBA and DEHA stabilize the oil immobilization in PEBA. However, PDMS does not contain hydrogen bond donors, the electrons on Si-O-Si are more tightly held, and the interaction with DEHA would be weaker than the PEBA. There would be electrostatic forces between PDMS and DEHA in the OLG, but these are weaker than hydrogen bonds. The DEHA oil in PDMS can only rely on the capability of the PDMS for oil immobilization.

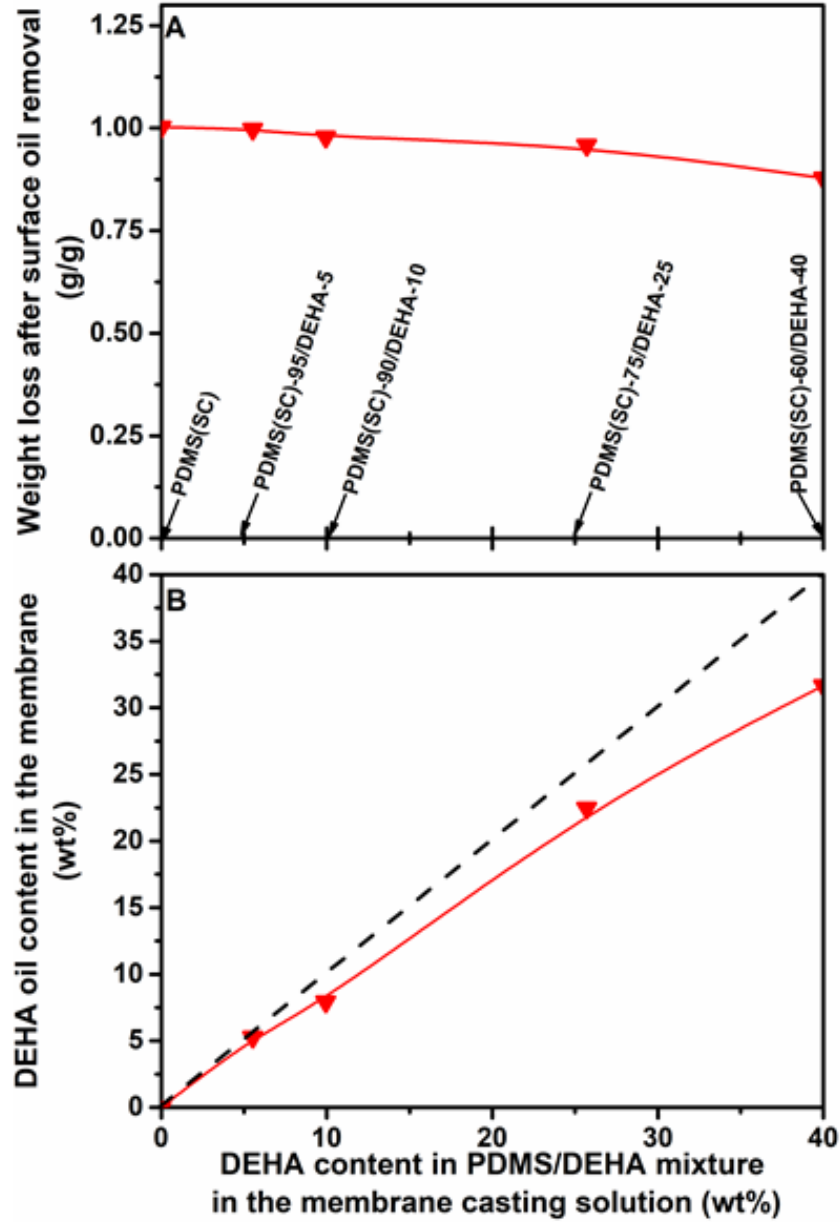


**Figure 5.4** (A) membrane weight loss after oil removal vs. DEHA content in PDMS/DEHA mixture in the membrane casting solution. (B) DEHA oil content in the membrane vs. DEHA content in PDMS/DEHA mixture in the membrane casting solution. The membrane weight loss after oil removal is normalized by the initial membrane weight before oil removal.

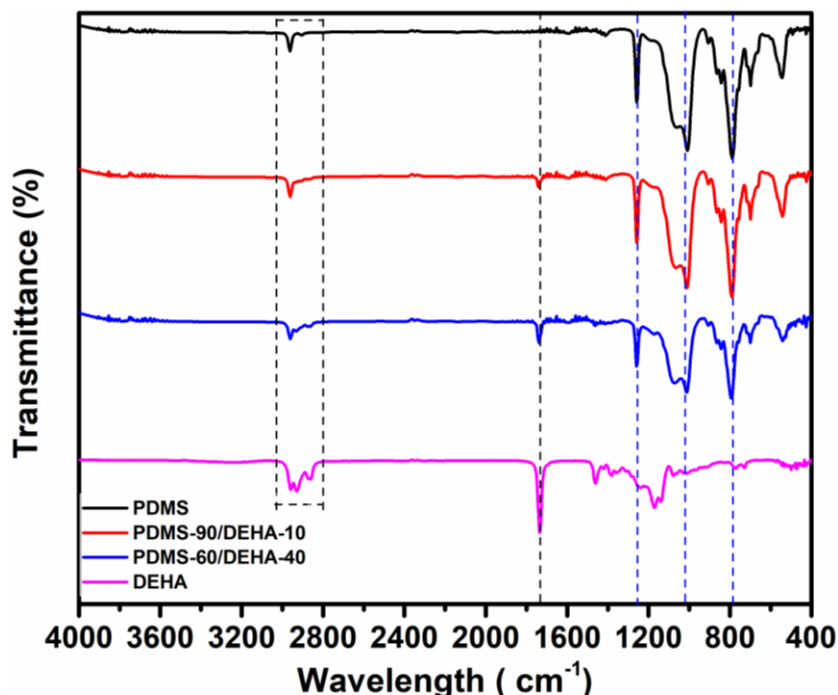


**Figure 5.5** FTIR spectra of PDMS and PDMS/DEHA OLGMs. The blue dash line indicates the peaks from the PDMS, and the black dash line shows the peaks from the DEHA.

The DEHA oil content in the membrane was characterized by Fourier transformation infrared spectra (FTIR), and the spectra are shown in Figure 5.5. The absorption band at  $1024\text{ cm}^{-1}$  is assigned to Si-O-Si [140]. The absorption band at  $1260\text{ cm}^{-1}$  and  $795\text{ cm}^{-1}$  are assigned to Si-CH<sub>3</sub> [141]. As more DEHA oil is retained in membranes, the PDMS content in the membrane becomes less, and the silicone-related band in the PDMS becomes weak and finally disappears in the DEHA oil. In contrast, as the DEHA oil content increases in the membrane, the peak of (C=O) at  $1739\text{ cm}^{-1}$  [142] and peaks in the carboxyl region ( $2850\sim 3000\text{ cm}^{-1}$ ) [143] for DEHA becomes stronger. In conclusion, the FTIR verifies that DEHA oil is retained in the PDMS polymer matrix, and the content of DEHA oil retained in membranes could be proved to increase as the spectra move from PDMS to DEHA oil. Moreover, no peak shifting was found in the spectra of PDMS/DEHA OLGMs, which means there is no hydrogen bond forming between the PDMS and the DEHA, and the interaction of the DEHA oil in the PDMS matrix is weak. This could explain that the DEHA oil is easily saturated from the PDMS than the PEBA during the membrane fabrication, which is consistent with the observation in the membrane weight measurement.

The mechanical properties of the standard crosslinked PDMS and PDMS/DEHA membranes were evaluated. Tensile stress and Young's modulus are common parameters to characterize membrane

mechanical properties and were investigated in this work. The results are shown in Figure 5.6. PDMS(SC) shows its Young's modulus at 1.71 MPa, which is in the range of 1.16 to 2.18 MPa as reported in the literature [144, 145]. When the content of DEHA oil in the membrane increases from 0 to 33 wt%, the tensile stress of the membrane decreases 75%, which is lower than the 89% decrease in PEBA based OLGMS (Chapter 3). The effect of the oil immobilization on the mechanical properties of PDMS based OLGMS is less than PEBA based OLGMS. This is because PEBA as a copolymer consists of polyamide and polyether blocks. The polyamide block provides mechanical strength to the polymer and makes the tensile stress stronger than the silicone rubber. The tensile strength and Young's module decrease as the oil content increases in the membrane. It means the membrane becomes more flexible and softer, and the PDMS matrix becomes more loosely packed with more DEHA oil retained, which is expected to improve the gas permeabilities in the membrane. However, the negative side effect on the mechanical strength of the membrane caused by too much oil immobilized in the membrane will limit the membrane application in the industry.

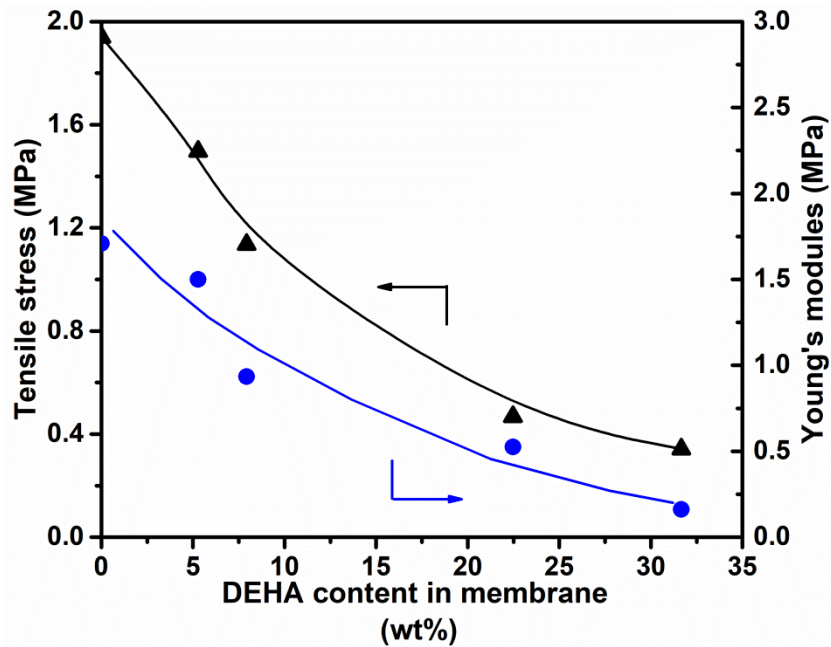


**Figure 5.6** Mechanical properties of the PDMS/DEHA OLGMS.

The standard crosslinked PDMS/DEHA OLGMS were subjected to gas and vapor permeation tests after oil was removed from the surface of the membrane.

### 5.3.2 Effect of oil content in membranes on gas permeation

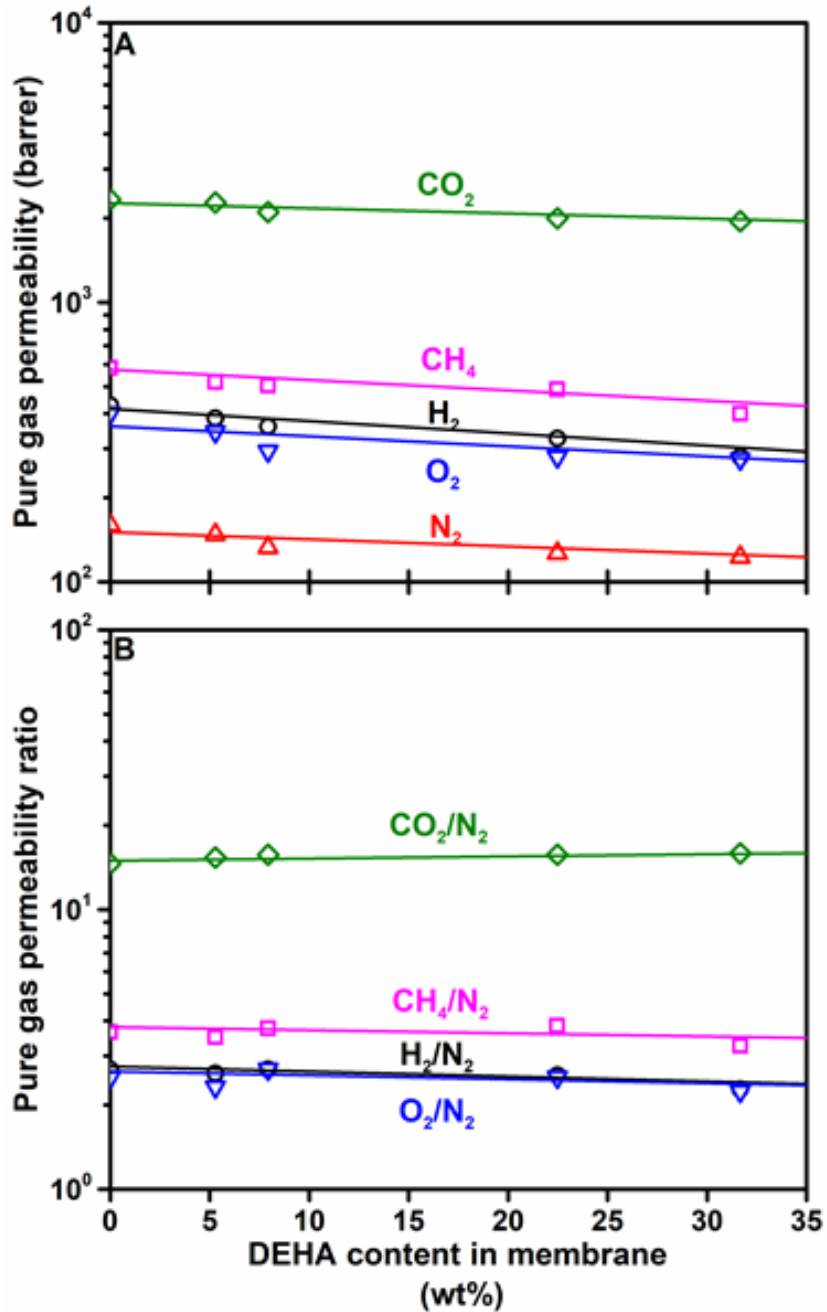


**Figure 5.7** The effect of DEHA oil content in the standard cross-linked OLGMs on pure gas permeability and pure gas permeability ratio (selectivity).

Five gases (nitrogen, oxygen, hydrogen, methane, and carbon dioxide) were selected to evaluate gas permeabilities for standard crosslinked OLGMs. Gas permeabilities and pure gas permeability ratio (gas/nitrogen selectivities) are shown in Figure 5.7. The oil-free PDMS membrane (DEHA content is

0) shows a nitrogen permeability of 160 barrer with the selectivity of  $O_2/N_2$  2.5 and  $CO_2/N_2$  14.6. This membrane has a slightly lower nitrogen permeability and higher gas/ $N_2$  selectivity than the previously reported PDMS membrane [146, 147]. As the DEHA content in the membrane increases, the membrane permeability to all five gases slightly decreases, while these changes are within 10%, and gases/nitrogen selectivity are kept constant. Therefore, different contents of DEHA in the membrane barely affect the gas permeability of the PDMS-based oleo gel membrane, and DEHA oil may have similar permeabilities to the PDMS for those tested gases.

### 5.3.3 Effect of oil content in membranes on VOC permeation

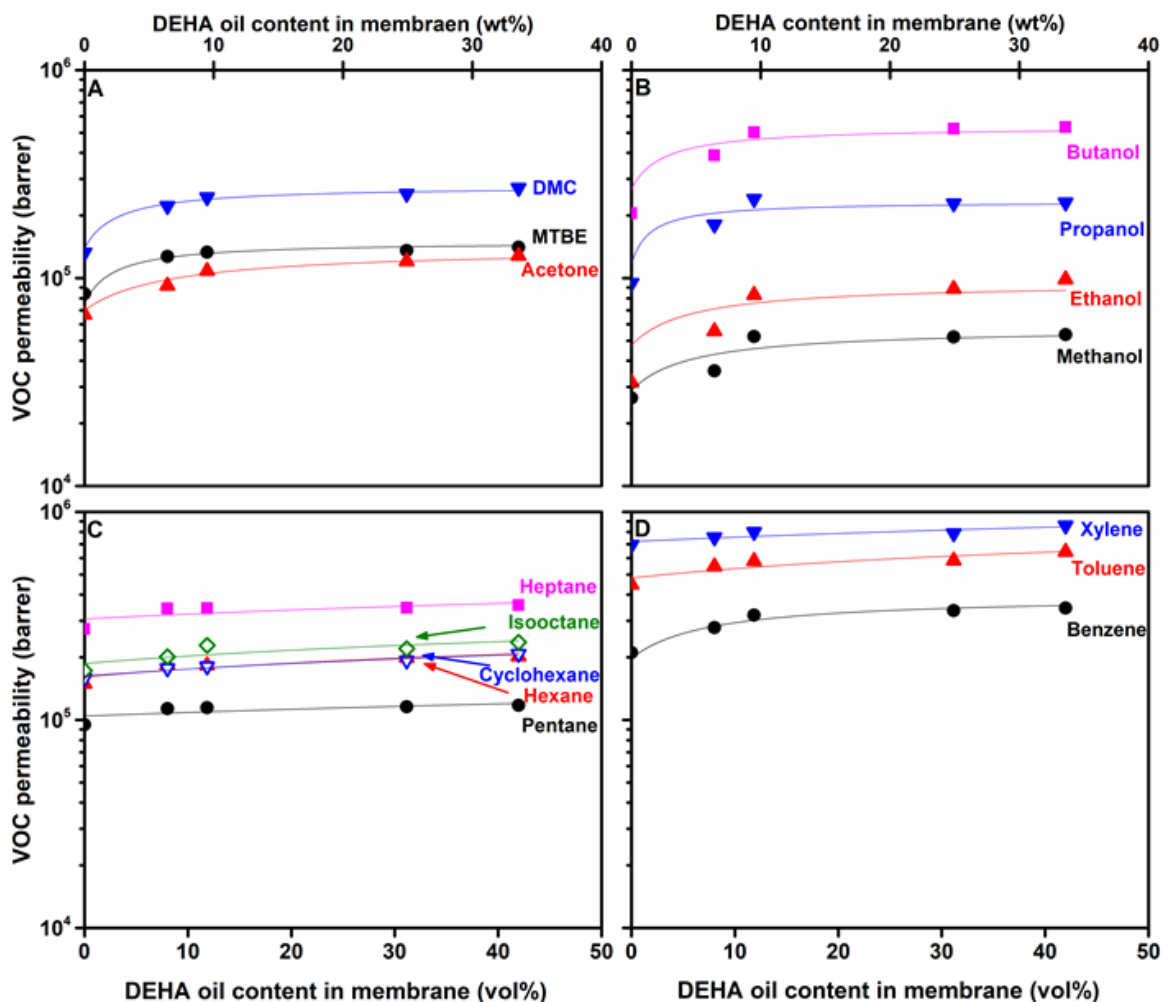


**Figure 5.8** The effect of DEHA content in the standard cross-linked membrane on membrane VOC permeability. (A) fuel additives, (B) alcohols, (C) paraffin, (D) aromatic compounds. Top X-axis: DEHA oil content is in wt%. Bottom X-axis: DEHA oil content is in vol%.



The VOC permeabilities of the standard crosslinked OLGMs were measured at 22°C in binary VOC/N<sub>2</sub> mixtures with VOC saturated. The effect of the DEHA content in the membrane on the permeabilities of four types of VOCs (fuel additives, alcohols, paraffin, and aromatic compounds) is correspondingly shown in Figure 5.8 (A–D). The permeabilities of all 15 VOCs increase as the oil content increases in the membrane from 0 to 8 wt.%. A further rise in DEHA content from 8 to 32 wt.% does not affect the VOC permeability. This trend is very similar to the description of the Maxwell equation in polymer blending rules [130, 131]. Therefore, the relationship between VOC permeability and DEHA oil content in the membrane was attempted to fit into the Maxwell equation [148], as shown in Equation 5.1 below:

$$P_b = P_c \left[ \frac{P_d + 2P_c - 2\phi V_d(P_c - P_d)}{P_d + 2P_c - \phi V_d(P_c - P_d)} \right] \quad (5.1)$$

DEHA oil was treated as the discontinuous phase, and PDMS was treated as the continuous phase to fit the equation. Where  $P_b$ ,  $P_c$  and  $P_d$  are gas permeabilities of the polymer blend, continuous phase, and discontinuous phase, respectively. Here,  $P_b$ ,  $P_c$  and  $P_d$  are the VOC permeability of standard crosslinked PDMS/DEHA membrane, pristine PDMS, and DEHA oil, respectively.  $V_d$  is the volume fraction of the discontinuous phase (DEHA oil) in the polymer blend. Because the density for both PDMS and DEHA oil changes in the membrane formation,  $\phi$  as the correction factor converting the oil mass fraction in the membrane to the volumetric one, was considered in Equation 5.1.

Equation 5.1 was fitted to the experimental data, and the trend lines are shown in Figure 5.8. Most of the trend lines were well fitted to the experimental data, with correlation coefficients higher than 0.80 listed in Table 5.2. The Maxwell equation can describe the relationship between the VOC permeabilities and oil content in the membrane, which may be because of the low interaction between the DEHA oil and the PDMS. The VOC permeabilities of PDMS and DEHA oil could be calculated from the correlated Maxwell equation. The experimental VOC permeabilities of PDMS and the reported VOC permeabilities of DEHA oil (Chapter 4) were plotted for comparison in the figures as well. The VOC permeability generated from the equation correlation has a range, shown as the error bar in the figure. The VOC permeabilities of the PDMS from the equation correlation and experiment are shown in Figure 5.9(A). They are in line with each other and have negligible differences. The VOC permeabilities of DEHA oil from the equation correlations of Maxwell (this work) and miscible blending (Chapter 4) are shown in Figure 5.9(B). There are differences in VOC permeabilities of DEHA oil from different equation correlations. It may be due to the bad equation correlations on experimental permeabilities of some VOCs (e.g., methanol, ethanol, pentane, heptane, and isooctane) for PDMS/DEHA OLGMs. On the other hand, when DEHA oil is immobilized in the polymers, the free volume and polymer chain distribution in polymers could be changed, and those changes in

PEBA and PDMS could be different. It could affect the VOC permeabilities in OLGMs, furthermore affect the calculated VOC permeabilities of DEHA oil obtained from the OLGMs made in different polymers (e.g., PEBA and PDMS).

**Table 5.2** fitting coefficient in maxwell equation correlation.

VOC compound	R <sup>2</sup>
Methyl tert-butyl ether	0.936
Acetone	0.969
Dimethyl carbonate	0.984
Methanol	0.829
Ethanol	0.770
Propanol	0.872
Butanol	0.882
Pentane	0.537
Hexane	0.817
Cyclohexane	0.955
Heptane	0.531
Iso-Octane	0.687
Benzene	0.942
Toluene	0.808
Xylene	0.768

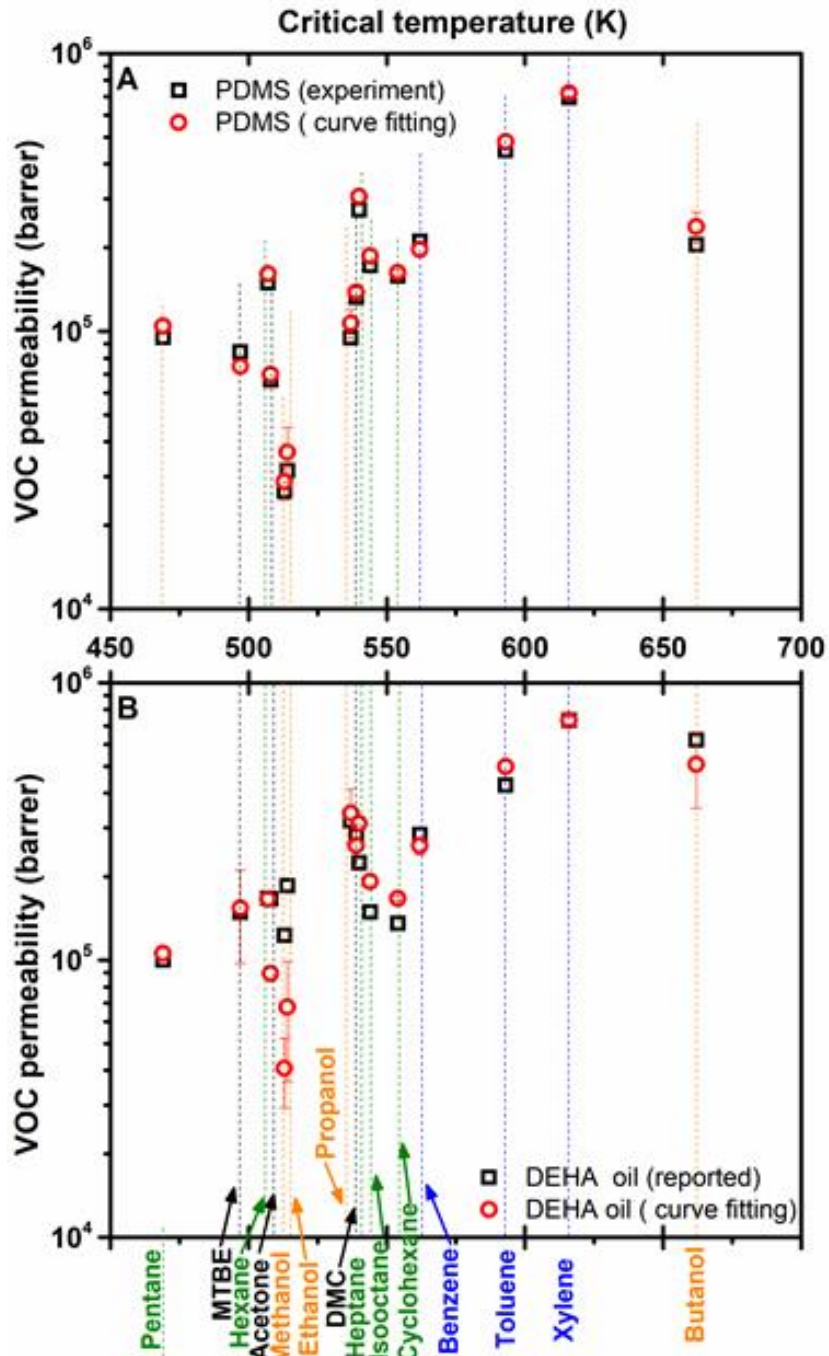


**Figure 5.9** The VOC permeability of PDMS and DEHA. The VOC permeabilities of PDMS (curve fitting) and DEHA oil (curve fitting) were generated from the maxwell equation correlation. The VOC permeabilities of the PDMS (experiment) were measured in work. The VOC permeabilities of DEHA oil (reported) were generated from the miscible blending equation and reported in Chapter 4.

Figure 5.9 (B) shows that most VOC permeabilities in DEHA oil between this work and previous work in Chapter 4 are within 10%, and the difference is small. The agreement between the correlated VOC permeabilities from this work and Chapter 4 confirms the feasibility of measuring the VOC permeability of the oil by calculating the oil permeability in a blended oleo gel membrane through correlating the polymer blending equation to the experimental data.

#### **5.3.4 Effects of base/curing ratio (A: B) on vapor permeation**

To improve the capability of the membrane for retaining the DEHA oil, PDMS/DEHA OLGMs with less crosslinked PDMS matrix were prepared. Unfortunately, the saturated oil was observed on the membrane surface of PDMS(LC)-60/DEHA-40 as well. The oil content immobilized in standard crosslinked PDMS and less crosslinked PDMS was measured and calculated, and they are similar to each other. It appears to suggest that the PDMS network with a lower degree of crosslinking did not help the oil retention in the membrane. Figure 5.10 shows the VOC/N<sub>2</sub> separation performance of membrane PDMS(SC)-60/DEHA-40 and membrane PDMS(LC)-60/DEHA-40. Both membranes were tested in the same condition as described in section 5.2.2. Three membrane samples from different membrane batches were used in testing. The results in Figure 5.10 are the averaged values. The VOC permeability and VOC/N<sub>2</sub> selectivity are plotted versus the critical temperatures of the VOC compounds.

In general, VOCs with higher critical temperatures tend to be more condensable and higher perm selective to VOC/N<sub>2</sub>. For easy comparison, the different groups of VOCs were color-coded in Figure 5.10. It is shown that the permselectivities of both membranes, PDMS(SC)-60/DEHA-40 and PDMS(LC)-60/DEHA-40, were in the order of butanol > propanol > ethanol > methanol for alcohols, heptane > hexane > pentane for paraffin and xylene > toluene > benzene for aromatic compounds.

Reduced crosslinking PDMS may lead to more defects on the membrane, making the membrane PDMS(SC)-60/DEHA-40 shows an overall better VOC/N<sub>2</sub> separation performance than membrane PDMS(LC)-60/DEHA-40. Therefore, the conventional A to B ratio of 10:1 used for PDMS was considered appropriate at the current stage.

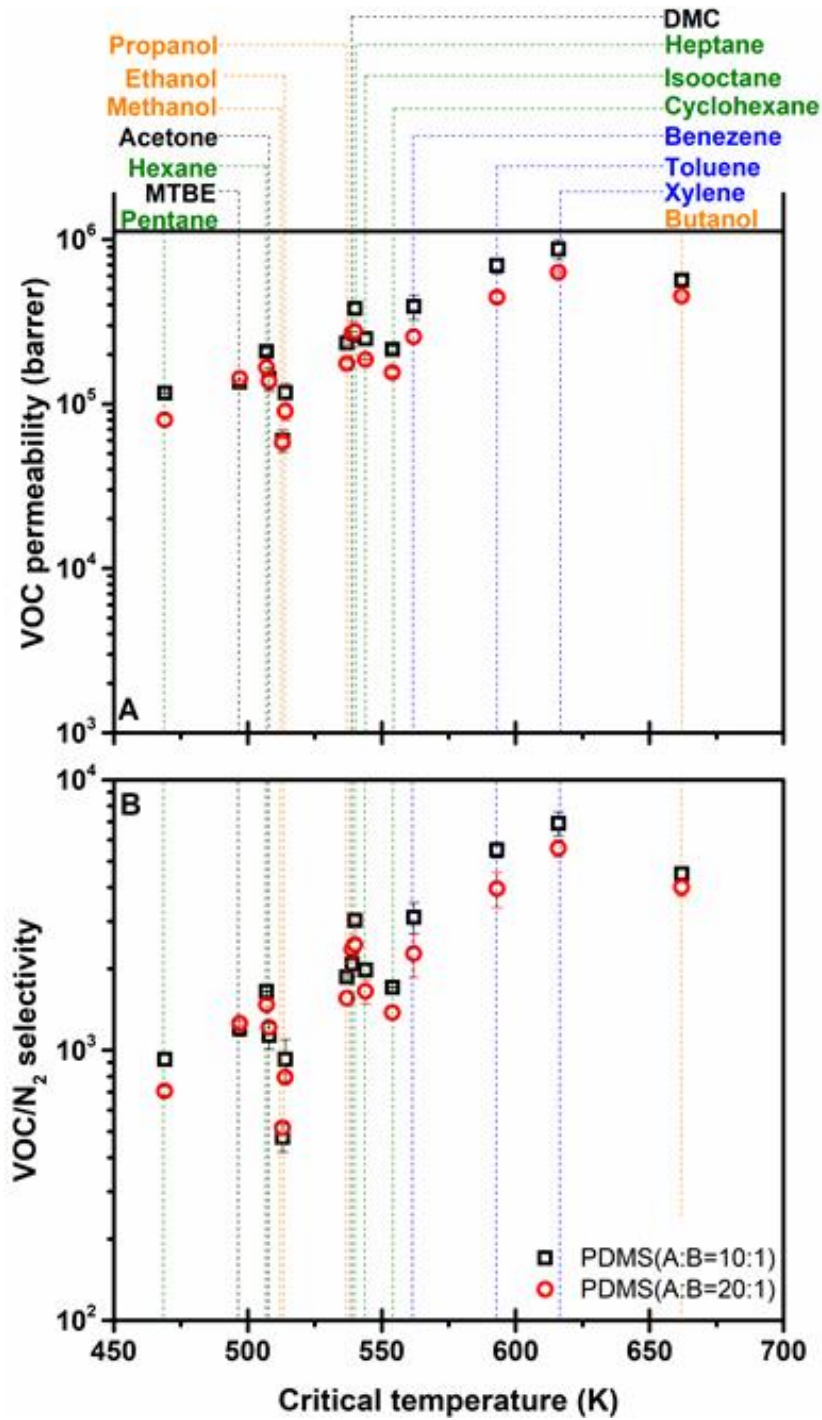


**Figure 5.10** Membrane perm selectivity vs VOC critical temperature.  $\blacksquare$  : membrane PDMS(SC)-60/DEHA-40;  $\bullet$  : membrane PDMS(LC)-60/DEHA-40.

In Figure 5.11, the VOC permeabilities of membrane PDMS(SC)-60/DEHA-40 are compared with the other reported oleo gel membrane, PEBA-25/DEHA-75, at the same test conditions. The VOC

permeabilities of pristine PEBA and PDMS tested at the same condition are also shown in the figure. The oil content in membrane PEBA-25/DEHA-75 is 75 wt.%. Even though the content of the oil immobilized in PEBA-25/DEHA-75 is more than that in PDMS(SC)-60/DEHA-40, the PDMS(SC)-60/DEHA-40 shows higher VOC permeabilities than the PEBA-25/DEHA-75 except for methanol and ethanol. This is because the VOC permeabilities of PDMS are significantly higher than the PEBA. PEBA shows higher permeabilities for methanol and ethanol than the PDMS, making the permeabilities of those two VOC compounds in PEBA-25/DEHA-75 higher than those in PDMS(SC)-60/DEHA-40. Therefore, the VOC permeabilities of the oleo gel membrane are not only affected by the oil content immobilized in the membrane but also strongly dependent on the VOC permeabilities of the polymeric matrix (e.g., PDMS) to immobilize the oil.

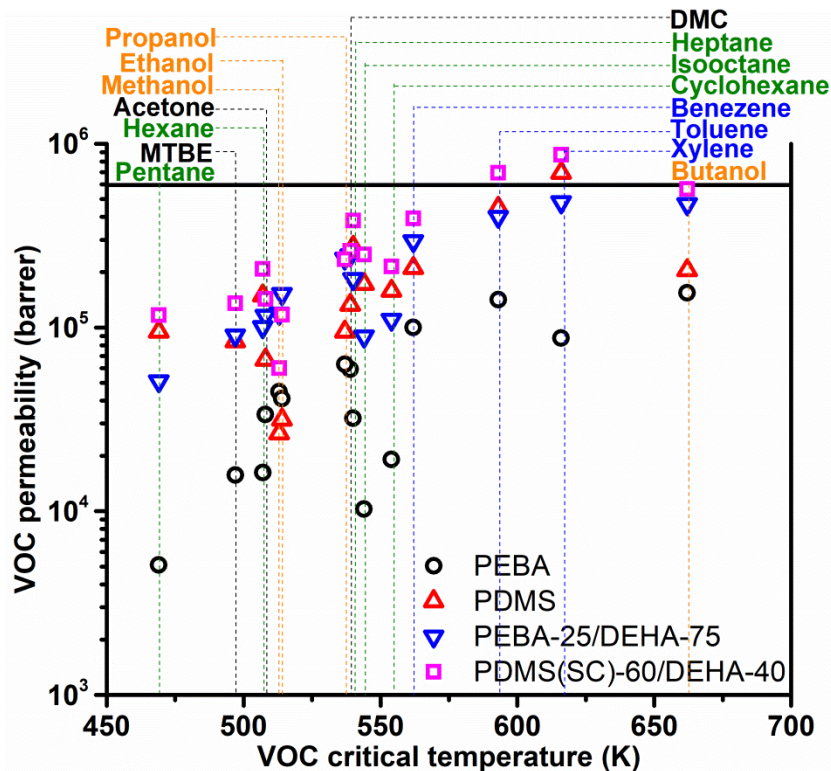


**Figure 5.11** VOC permeability comparison among the membranes. The data of PDMS and PDMS(SC)-60/DEHA-40 are from this work. The data of PEBA and PEBA-25/DEHA-75 are from Chapter 4.

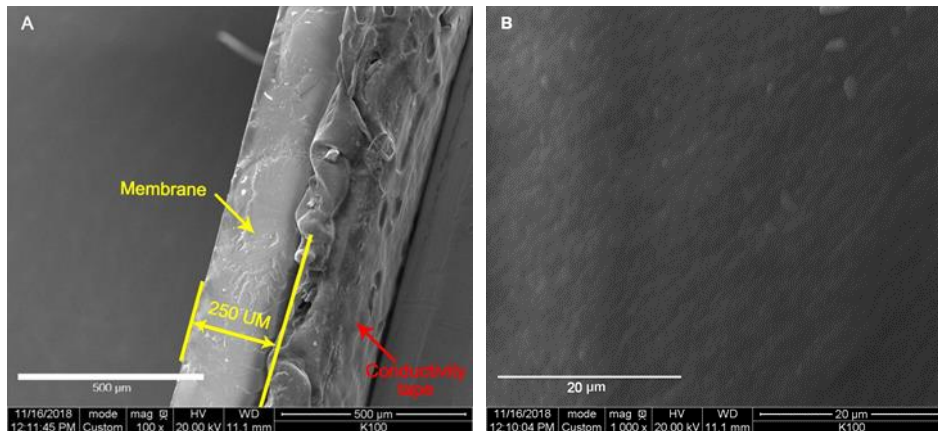


**Figure 5.12** SEM images of membrane PDMS(SC)-60/DEHA-40. (A) Cross-section, (B) Enlarged cross-section.

Figure 5.12 shows the SEM image of the cross-sections of membrane PDMS(SC)-60/DEHA-40. The membrane had a thickness of about 250μm, which matches the thickness measured by the micrometer. The enlarged scan in Figure 5.12 (B) shows the membrane was dense and defect-free. Because membrane PDMS(SC)-60/DEHA-40 shows the best VOC/N<sub>2</sub> separation performance among all fabricated PDMS/DEHA OLGMs, it was selected for the following systematic evaluation of VOC/N<sub>2</sub> separation.

### 5.3.5 Effect of feed VOC concentration

It was reported that concentration polarization might take place for VOC separation using a PDMS-based membrane [94]. To avoid concentration polarization, pre-experiments were performed to choose an appropriate feed flow rate for VOC/N<sub>2</sub> separation. A feed flow rate as high as 500 sccm was used in the present work. A further increase in the feed flow rate did not change the membrane permeate flux, indicating the concentration polarization was insignificant.

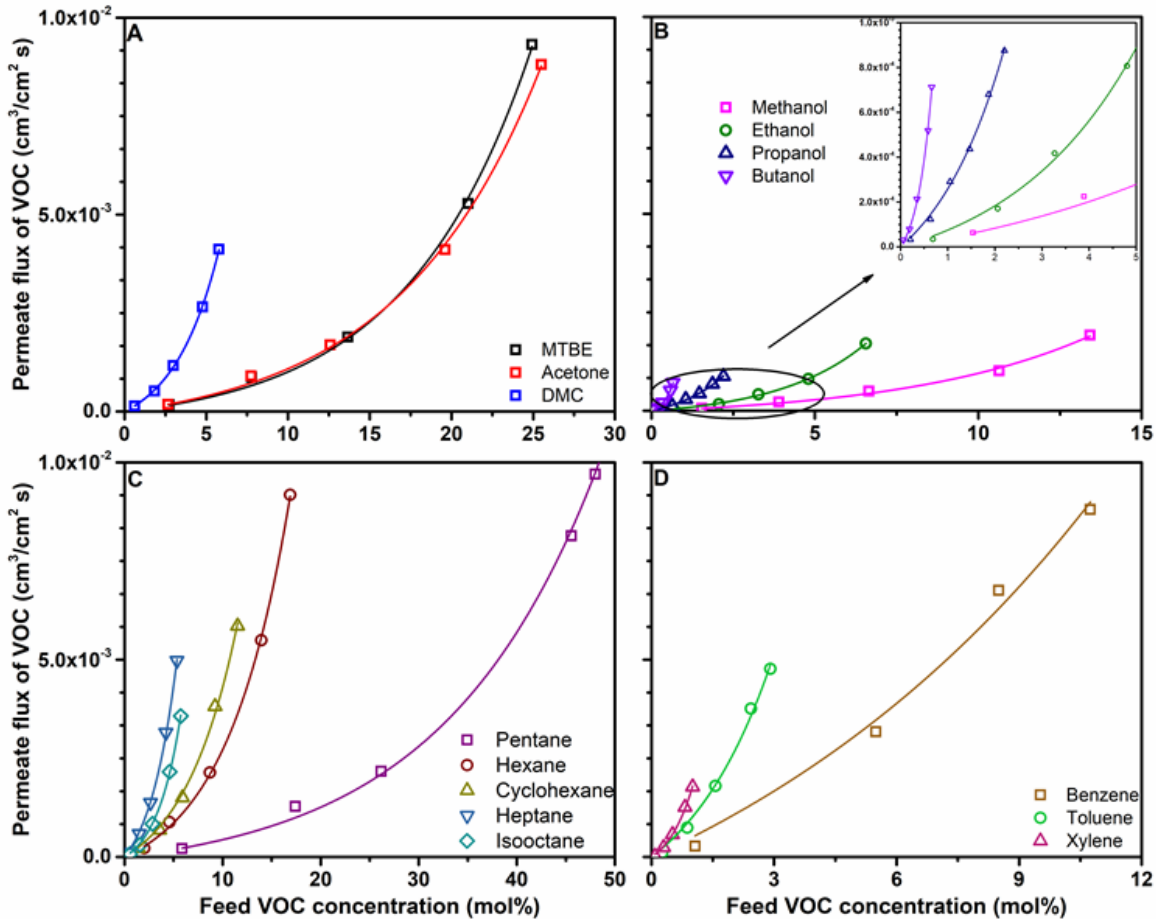


**Figure 5.13** VOC permeate flux vs feed VOC concentration. (A) fuel additives, (B) alcohols, (C) paraffin, (D) aromatic compounds.

The permeation of binary VOC/ $\text{N}_2$  mixtures in the PDMS(SC)-60/DEHA-40 membrane was studied at 22°C at different feed VOC concentrations. The permeation fluxes of VOCs are shown in Figure 5.13. As the feed VOC concentration increased, the VOC flux increased more than proportionally. It means that the increased VOC permeation flux was not only due to the increased driving force for permeation, and the membrane permeability to the VOCs was also enhanced at higher feed VOC concentration.

Based on the experimental results in Figure 5.13, a semi-empirical relation was attempted to correlate VOC permeate flux with operating conditions. Similar approaches have been widely used in the study of mass transfer in pervaporation processes [134, 135]. At steady state, the VOC permeation flux,  $Q_{VOC}$ , can be described by the Fick's law, and a series of equation could be generated for correlation of membrane separation performance and operation parameters. The details are introduced in section 4.33. By applying Equation (4.5) to fit the experimental data of VOC flux at different feed



VOC concentrations, the trend lines are generated and shown in Figure 5.13. The equation fits the experimental data well, with a correlation coefficient of higher than 0.99. The parameters  $\frac{D_0}{\phi}$  and  $\phi\omega$  for each VOC were determined, and they are presented in Table 5.3.

**Table 5.3** Parameters from the correlation between permeate VOC flux and the feed VOC concentration.

	$D_0/\phi$ (cm <sup>3</sup> /cm s)	$\omega\phi$ (kPa <sup>-1</sup> )	R <sup>2</sup>
Methyl tert-butyl ether	$1.05 \times 10^{-5}$	$1.29 \times 10^{-3}$	0.999
Acetone	$1.43 \times 10^{-5}$	$1.12 \times 10^{-3}$	0.999
Dimethyl carbonate	$1.64 \times 10^{-5}$	$3.57 \times 10^{-3}$	1.000
Methanol	$5.51 \times 10^{-6}$	$1.74 \times 10^{-3}$	0.995
Ethanol	$4.70 \times 10^{-6}$	$3.63 \times 10^{-3}$	0.999
Propanol	$8.21 \times 10^{-6}$	$6.24 \times 10^{-3}$	0.997
Butanol	$2.91 \times 10^{-6}$	$3.07 \times 10^{-2}$	0.999
Pentane	$1.40 \times 10^{-5}$	$6.22 \times 10^{-4}$	1.000
Hexane	$2.12 \times 10^{-5}$	$1.51 \times 10^{-3}$	0.999
Cyclohexane	$2.39 \times 10^{-5}$	$1.78 \times 10^{-3}$	0.997
Heptane	$2.60 \times 10^{-5}$	$3.43 \times 10^{-3}$	0.999
Iso-Octane	$1.10 \times 10^{-5}$	$4.00 \times 10^{-3}$	0.999
Benzene	$5.72 \times 10^{-4}$	$1.78 \times 10^{-3}$	0.991
Toluene	$4.19 \times 10^{-5}$	$5.55 \times 10^{-3}$	0.995
Xylene	$8.95 \times 10^{-6}$	$2.57 \times 10^{-2}$	0.998

Parameter  $\frac{D_0}{\phi}$  and  $\phi\omega$  consider the feed gas composition effect on gas diffusion and sorption. To better understand the permeation mechanism of the PDMS/DEHA OLGMs, these two parameters were plotted in function of mole volume and critical temperatures, respectively, as shown in Figure 5.14.

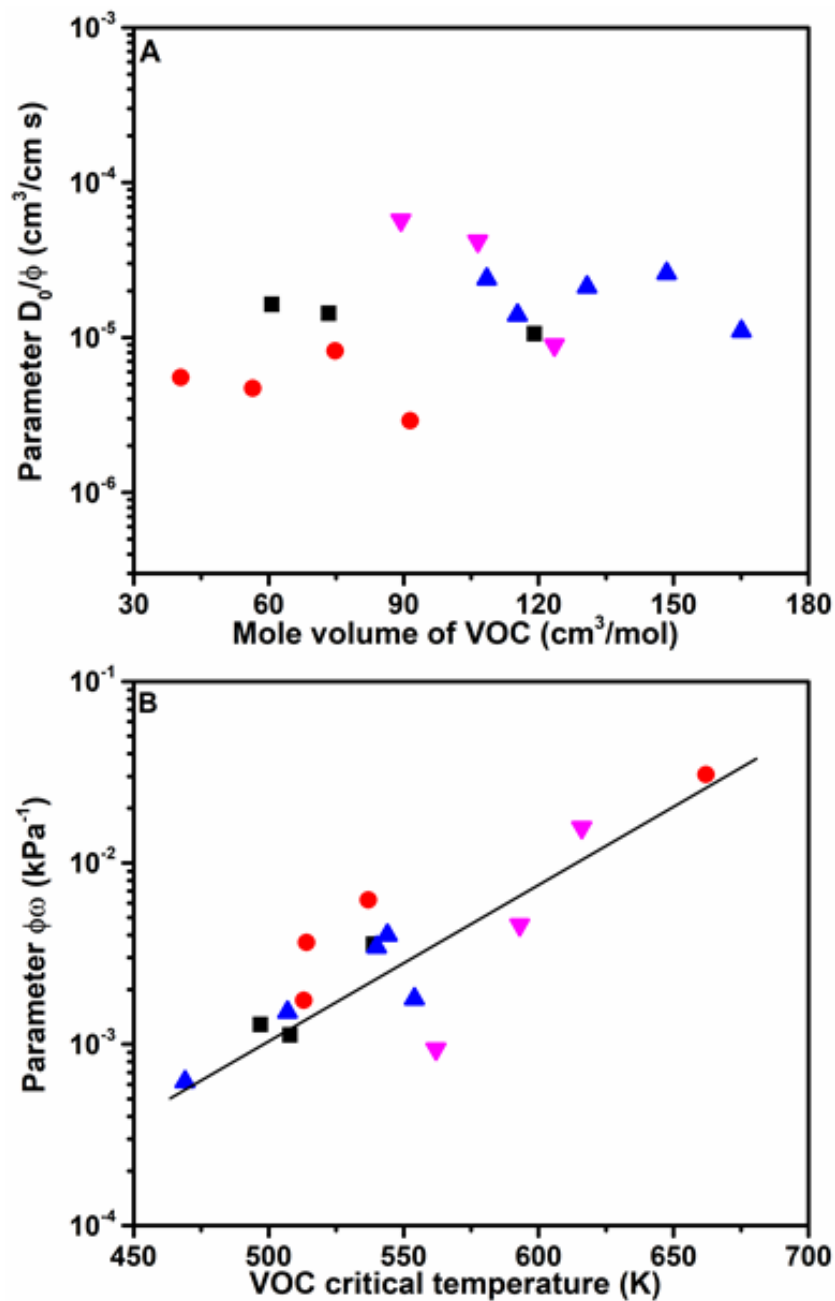


**Figure 5.14** The relationship of Parameters ( $\frac{D_0}{\phi}$ ) and ( $\phi\omega$ ) to mole volume and critical temperatures of the VOCs. Four types of VOCs are color-coded, as shown in above Figure and Table 5.4.

**Table 5.4** The supplementary table for Figure 5.14.

Supplementary table of Figure 5.14 [149]				
VOCs type	Mark in figure	VOCs name	Mole volume (cm <sup>3</sup> /mol)	Critical temperature (K)
Fuel additives	■	MTBE	119	497
		Acetone	73	508
		DMC	61	539
Alcohols	●	Methanol	41	513
		Ethanol	57	514
		Propanol	75	537
		Butanol	92	662
Paraffins	▲	Pentane	115	469
		Hexane	131	507
		Cyclohexane	109	554
		Heptane	149	540
		Iso-Octane	165	544
Aromatic compounds	▼	Benzene	89	562
		Toluene	107	593
		Xylene	124	616

Figure 5.14 (A) shows the changes of the parameter ( $D_0/\delta$ ) are affected by the mole volume of the VOC. Generally, as the VOC molecular size becomes bigger, the value of ( $D_0/\delta$ ) is lower. However, no clear trend was found in the figure; the parameters ( $D_0/\delta$ ) are more randomly distributed at  $10^{-5}$  (cm<sup>3</sup>/cm s). This could be that feed gas composition has effects on gas diffusion, or the gas diffusion coefficient for each VOC compound is similar to each other in the membrane.

Figure 5.14 (B) shows the parameter ( $\phi\omega$ ) versus the critical temperature of the VOCs. It is shown that values of the parameters are in the order of butanol>propanol>ethanol>methanol for alcohols, heptane>hexane>pentane for paraffin, and xylene>toluene>benzene for aromatic compounds. In each VOC group, VOCs with higher critical temperatures are more condensable, and they have higher values of ( $\phi\omega$ ). The overall trend for all VOCs is the same as the one in each VOC category. It suggests that the effect of feed VOC concentration on VOC sorption permeation is not significant. The parameters ( $\phi\omega$ ) of the VOCs from the alcohol group are higher than the VOCs from other groups at the given VOC critical temperature, indicates the VOC from the alcohol group has higher

sorption to the membrane than VOCs in other groups, presumably due to the good affinity of polar alcohol molecules to the membrane.

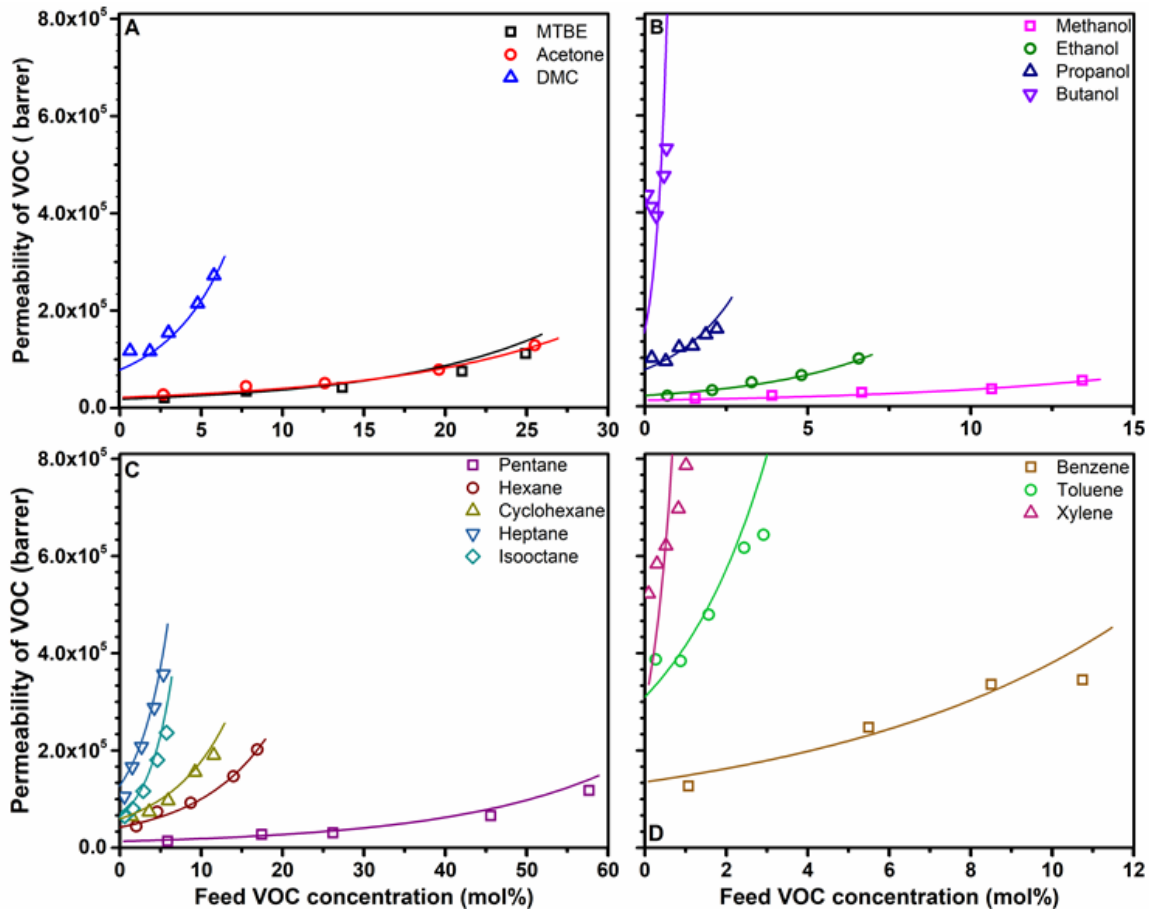


**Figure 5.15** VOC permeability vs. feed VOC concentration. (A) fuel additives, (B) alcohols, (C) paraffin, (D) aromatic compounds. The solid lines are obtained from the equation correlation. The symbols are experimental data.

Using the parameters ( $\frac{D_0}{\phi}$ ) and ( $\phi\omega$ ) in Table 5.3, the calculated permeabilities are shown as solid lines in Figure 5.15 (The details of the calculation were introduced in section 4.3.3). The agreement between the calculated permeability and the experimental data justifies that the semi-empirical correlation is useful to predict the separation performance of the OLGMs. Moreover, Figure 5.15 shows that the membrane has a higher VOC permeability at higher feed VOC concentrations, confirming the convex curve of VOC permeates flux in Figure 5.13. At a given feed VOC concentration, the membrane showed higher permeabilities to more condensable VOCs. The VOC permeabilities followed the trend of  $DMC > MTBE$  and acetone (fuel additives),

butanol>propanol>ethanol>methanol (alcohols), heptane>hexane>pentane (paraffin) and xylene>toluene>benzene (aromatic compounds).

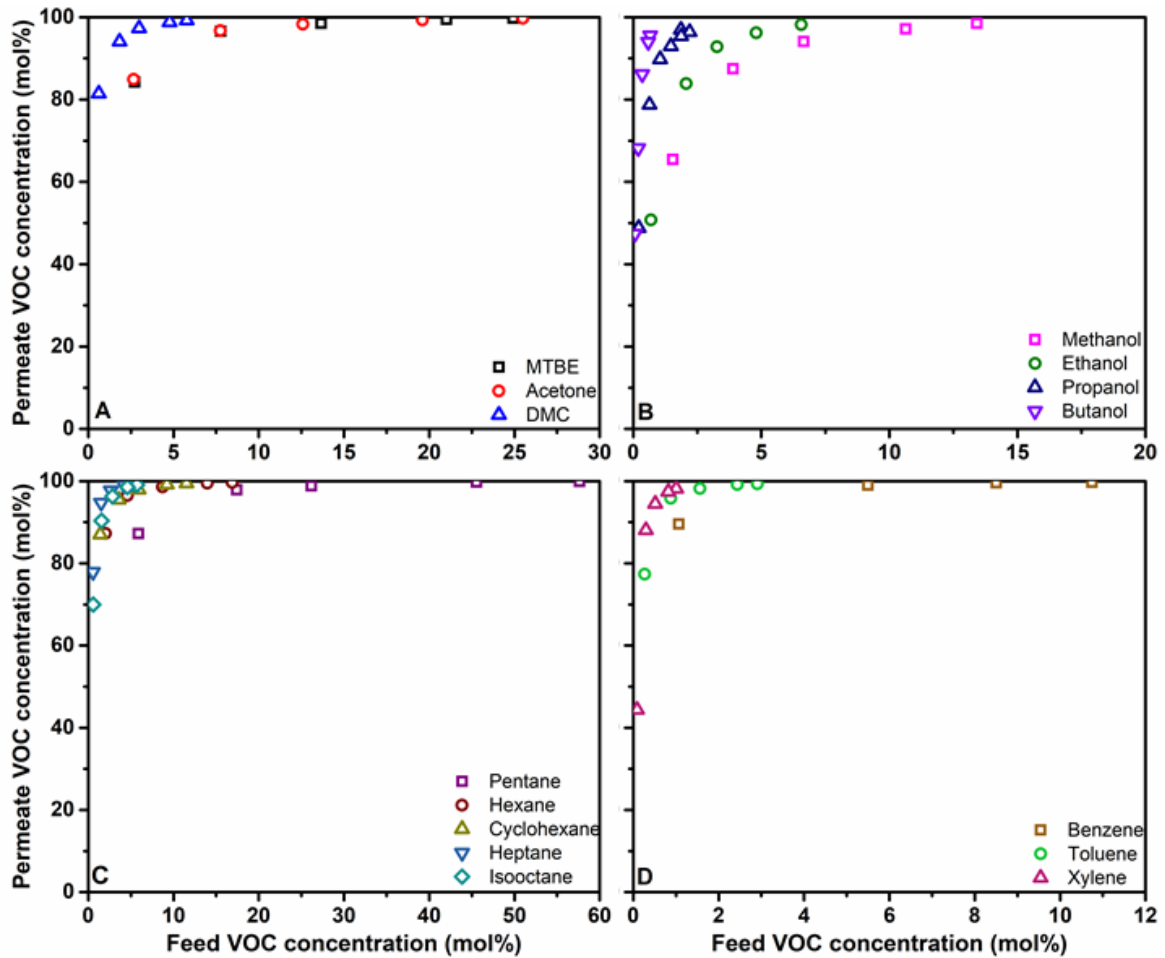


**Figure 5.16** Permeate VOC concentration vs. feed VOC concentration. (A) fuel additives, (B) alcohols, (C) paraffin, (D) aromatic compounds.

Figure 5.16 shows permeate VOC concentration as a function of feed VOC concentration. As the feed VOC concentration increases, the VOC concentration in the permeate increases as well. At a VOC concentration higher than 2.5 mol%, a permeate VOC concentration of over 90 mol% is achieved. It demonstrates that the PDMS/DEHA OLGMs have excellent VOC/N<sub>2</sub> separation performance for all 15 VOCs.

### 5.3.6 Effect of temperature

The effects of temperature on the membrane performance for binary VOC/N<sub>2</sub> separation were evaluated at temperatures ranging from 10°C to 40°C at VOC concentrations shown in Table 5.5.

**Table 5.5** Feed VOC concentrations used in determining temperature effects on VOC/N<sub>2</sub> separation performance of the membrane.

	VOC concentration (%)
Methyl tert-butyl ether	14.5
Acetone	12.9
Dimethyl carbonate	3.0
Methanol	6.5
Ethanol	3.1
n-Propanol	1.0
n-Butanol	0.3
Pentane	25.5
n-Hexane	8.5
Cyclohexane	5.4
Heptane	2.5
Iso-Octane	2.7
Benzene	5.5
Toluene	1.5
Xylene	0.5

VOC permeabilities of the membrane at different temperatures are shown in Figure 5.17. VOC permeabilities decrease as the temperature increase for all 15 VOCs, suggesting the exothermic nature of the sorption process and the dominating effect of sorption in VOCs permeation [93]. The membrane shows the different temperature dependence of permeability for four types of VOCs. The permeability of alcohol is significantly affected by temperature, followed by paraffin and other VOCs (aromatic compounds and fuel additives).

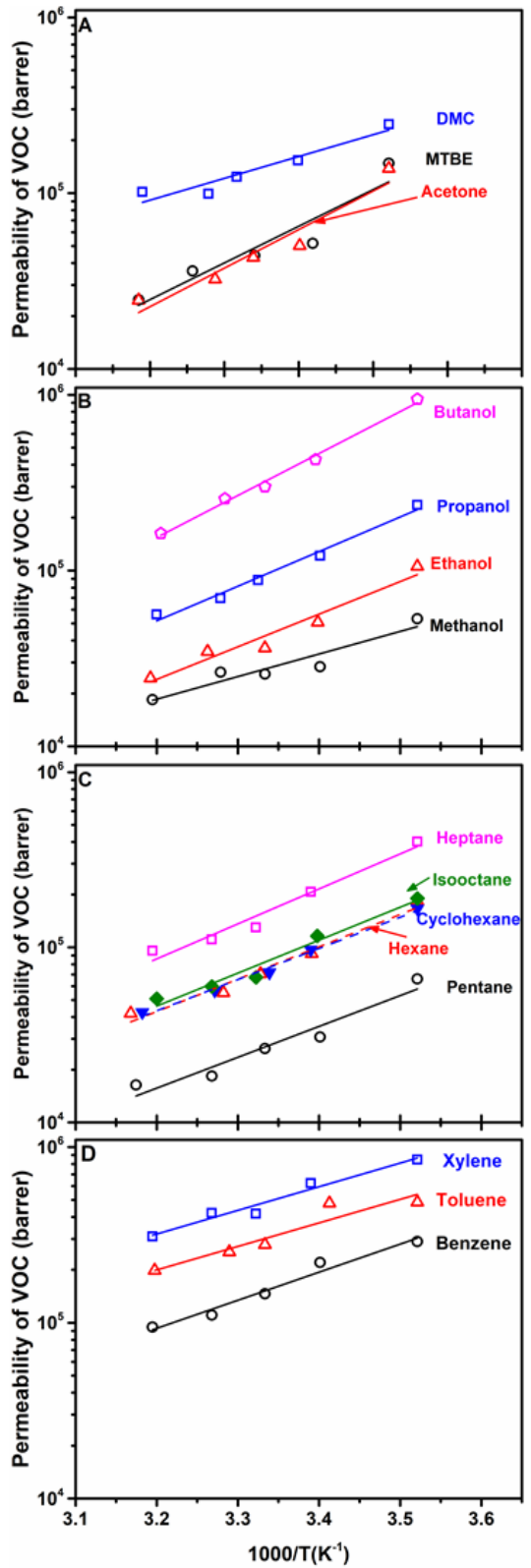


**Figure 5.17** Permeability of VOCs vs.  $1000/T$ . (A) fuel additives, (B) alcohols, (C) paraffin, (D) aromatic compounds.

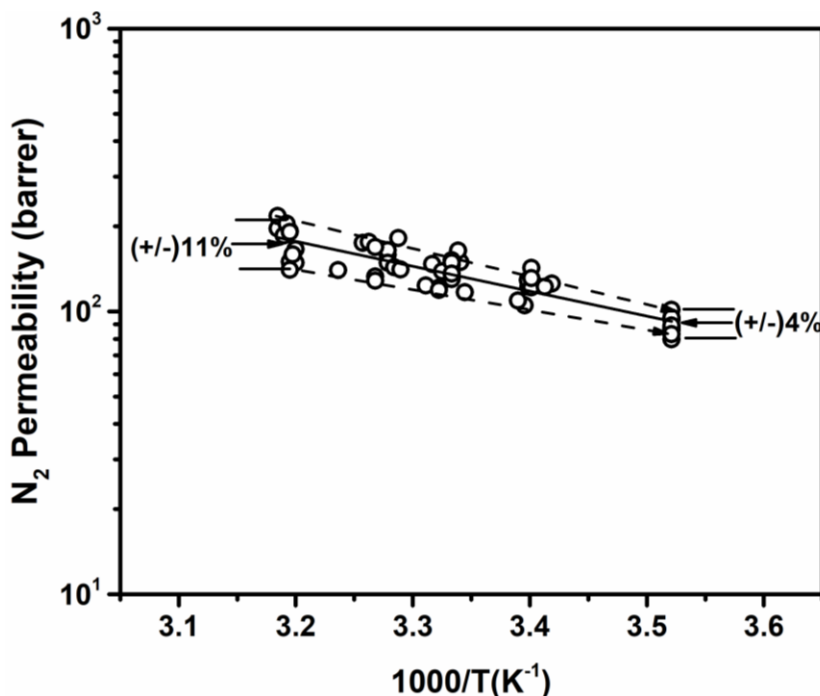


**Figure 5.18** N<sub>2</sub> Permeability at different temperatures.

Figure 5.18 shows the nitrogen permeability at different temperatures. The nitrogen permeability was evaluated immediately after the VOC/N<sub>2</sub> mixed gas test. The pure nitrogen data at elevated feed pressure and nitrogen permeability at sub-atmospheric permeate pressure are all shown in the figure. The nitrogen permeability increases as temperature increases. This could be explained by the fact that nitrogen, as an inert gas, has negligible interaction with the membrane material, but nitrogen permeation could be affected by membrane structure; at higher temperatures, the membrane has more free volume, resulting in higher nitrogen permeability [136]. The difference in nitrogen permeability in the presence of different VOCs at low temperatures is  $\pm 4\%$ , at high temperatures is  $\pm 11\%$ . Because the difference in nitrogen permeabilities is small, the pure nitrogen permeability was used to calculate the VOC/N<sub>2</sub> selectivity of the membrane. The conclusion is consistent with what was proved in Chapter 4 that there was little change in nitrogen permeabilities in the presence of different VOCs at variable pressures and temperatures. Therefore, pure nitrogen permeability was valid for calculating VOC/N<sub>2</sub> separation performance for OLGMs.

Figures 5.17 and 5.18 show the temperature dependence of VOC and nitrogen permeabilities, and they followed the Arrhenius relation, which was described by Equation 2.9. The activation energies for VOC and nitrogen permeation are shown in Table 5.5 and could indicate the effect of temperature on the permeabilities of VOCs and nitrogen. The negative VOC activation energy values imply that



VOC permeability is dominated by sorption in the membrane [93]. As VOC becomes more condensable, VOC activation energy in the alcohol group changes the most. The VOC permeability of alcohol is affected by temperature more significantly than other VOCs. Nitrogen has positive activation energy, indicating that the diffusion aspect is more important in nitrogen permeation than the sorption. The activation energy for both VOCs and nitrogen is at the same order of magnitude as other silicone rubber-based membranes [27, 150].

**Table 5.6** Activation energy for permeation of VOC and N<sub>2</sub>.

		The permeation activation energy (kJ mol <sup>-1</sup> )	
		VOC	N <sub>2</sub>
Fuel additive	Methyl tert-butyl ether/N <sub>2</sub>	-39.9	16.8
	Acetone/N <sub>2</sub>	-42.0	17.5
	Dimethyl carbonate/N <sub>2</sub>	-23.8	18.1
Alcohol	Methanol/N <sub>2</sub>	-24.6	19.2
	Ethanol/N <sub>2</sub>	-35.5	20.1
	n-Propanol/N <sub>2</sub>	-37.7	13.7
	n-Butanol/N <sub>2</sub>	-45.7	16.7
paraffin	Pentane/N <sub>2</sub>	-33.7	17.5
	n-Hexane/N <sub>2</sub>	-35.4	17.0
	Cyclohexane/N <sub>2</sub>	-34.0	17.2
	Heptane/N <sub>2</sub>	-38.2	22.6
	Iso-Octane/N <sub>2</sub>	-36.0	12.4
Aromatic	Benzene/N <sub>2</sub>	-30.6	13.9
	Toluene/N <sub>2</sub>	-28.1	17.4
	Xylene/N <sub>2</sub>	-25.8	13.8

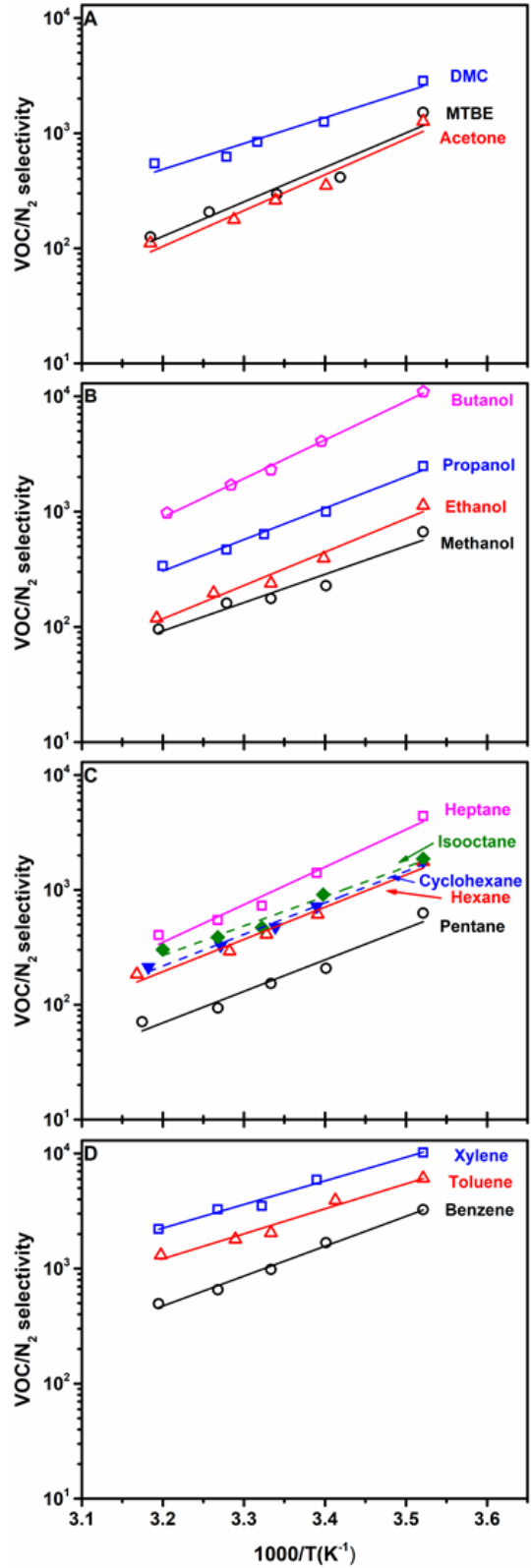


**Figure 5.19** VOC/N<sub>2</sub> selectivity vs. 1000/T. (A) fuel additives, (B) alcohols, (C) paraffin, (D) aromatic compounds.

Nitrogen permeability increases and VOC permeability drops with an increase in temperature, resulting in decreased VOCs/N<sub>2</sub> selectivities, as shown in Figure 5.19. The membrane still shows very high VOC/N<sub>2</sub> selectivity, especially for more condensable VOCs. For example, butanol/N<sub>2</sub> selectivity changes from 1000 at 40°C to 10000 at 10°C, and xylene/N<sub>2</sub> selectivity is 1000 at 40°C, and it was increased to 10000 at 10°C. Because the PDMS(SC)-60/DEHA-40 shows high VOC permeability and VOC/N<sub>2</sub> selectivity at low temperatures, low operating temperatures are favorable to the separation process.

### 5.3.7 Membrane stability

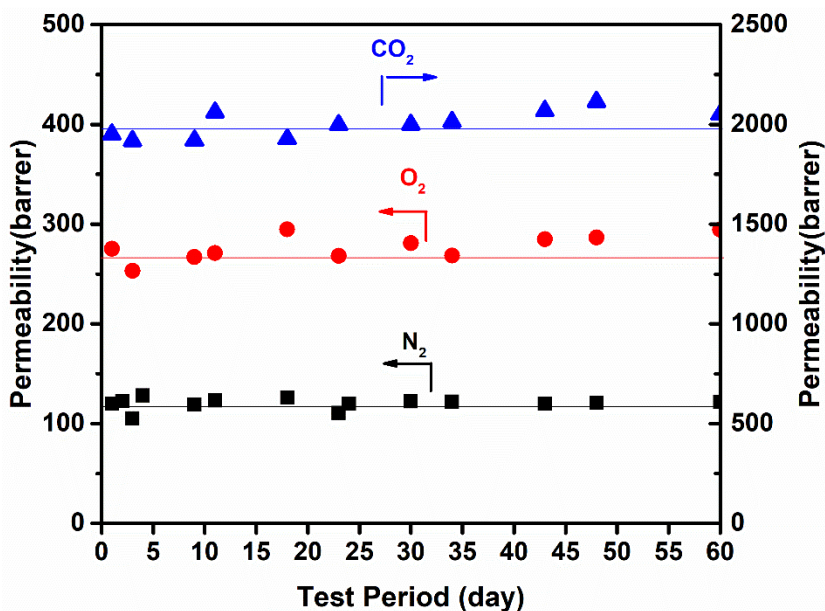


**Figure 5.20** Membrane stability evaluation by measuring the pure gas performance of the membrane in the 60 days.

The PDMS(SC)-60/DEHA-40 membrane was selected for a long-term stability test (60 days). The membrane was tested in VOC/N<sub>2</sub> mixtures with VOCs at various feed VOC concentrations and temperatures. After each VOC/N<sub>2</sub> mixed gas test, a pure gas test with carbon dioxide, oxygen, and nitrogen was conducted to confirm whether the membrane was stable. Figure 5.20 shows the gas (CO<sub>2</sub>, O<sub>2</sub>, and N<sub>2</sub>) measured at room temperature with a feed pressure of 0.4MPa and permeate pressure at 1atm. The membrane showed excellent stability with a permeability of 120 barrers to nitrogen, 270 barrers to oxygen, and 2000 barrers to carbon dioxide.

## 5.4 Conclusion

The DEHA oil has been successfully gelled into the crosslinked PDMS. PDMS/DEHA OLGMs were developed in this work. Less crosslinked PDMS was proved to be not helpful for DEHA oil immobilization in the OLG. Standard crosslinking was then used to fabricate the PDMS/DEHA OLGs and the 32wt.% was proved to be the maximum amount of oil content that could be immobilized in the membrane. The standard crosslinked OLG shows better VOCs permeabilities than the less crosslinked OLG. The systematic gas separation performance evaluations were performed on standard crosslinked OLGs. 15 different VOCs selected from the categories of fuel additives, alcohols, paraffin, and aromatic compounds were used to evaluate the VOC/N<sub>2</sub> separation of OLGs. The membrane VOC/N<sub>2</sub> separation performance at different feed VOC concentrations and temperatures were tested on membrane PDMS(SC)-60/DEHA-40. The membrane performance for VOC/N<sub>2</sub> separation was improved significantly than the traditional PDMS membranes and previously reported PEBA/DEHA and PEBA/DEHP OLGs. The membrane shows the permeate VOC concentration of over 90 mol% at a feed VOC concentration higher than 2.5 mol% for all 15 VOCs. The VOC/N<sub>2</sub> separation performance was investigated at temperatures as low as 10°C. At lower temperatures and higher feed VOC concentrations, the membrane shows better VOC/N<sub>2</sub> separation performance. The VOC/N<sub>2</sub> selectivity for butanol and xylene at 10°C is as high as 10000. Therefore, a low operating temperature is favorable to VOC separation. The membrane also showed good stabilities without significant change in gas permeabilities of the membrane over two months.

## Chapter 6

### Supported liquid membrane for VOC/N<sub>2</sub> separation

#### 6.1 Introduction

Volatile organic compounds (VOCs) are organic chemicals with high vapor pressures at room temperature and are harmful to human health and the natural environment. Many of them are treated as hazardous and priority air pollutants by the United States Environmental Protection Agency (US-EPA) [52]. VOC removal from waste gas is an urgent issue for preservation of air environment and human well-being. Membrane separation as a promising process for VOC removal has attracted increasing attention from the industry and researchers due to its low energy consumption, no regeneration requirement, and compact equipment [5, 19, 110, 137].

PDMS is a polymer widely used in the membrane preparation for VOC removal. For instance, Liu et al. [27] developed a PDMS hollow fiber membrane for chloroform/N<sub>2</sub> separation, and Majumdar et al. [28, 29] obtained a 95% VOC recovery rate in a pilot-scale study using PDMS-based membranes. However, the VOC/N<sub>2</sub> or VOC/air selectivity of the PDMS membrane is always lower than its ideal selectivity due to membrane swelling caused by VOCs adsorption [30]. By contrast, PEBA is an alternative polymer to PDMS and consists of rubbery polyether segments and glassy polyamide segments. The polyamide segments in PEBA could refrain the membrane from swelling by the adsorbed VOCs. Liu et al. [35] reported that PEBA-based hollow fiber membranes effectively recovered gasoline vapors from nitrogen. Rezac et al. [151] and Liu et al. [34] have proved the competitive VOC/N<sub>2</sub> separation performance of PEBA membrane to silicone rubber membrane at variable operating conditions. However, the VOC permeabilities of PEBA were much lower than the PDMS membrane (Chapter 5).

The OLGMs made by the mixture of polymers (e.g., PEBA and PDMS) and oils (e.g., DEHP and DEHA) were developed (Chapters 1 to 4). The intrinsic performance of the OLGMs on VOC/N<sub>2</sub> separation was comprehensively investigated, which showed a significant VOC/N<sub>2</sub> separation performance improvement compared to the traditional polymer membrane (e.g., PEBA and PDMS). However, the mechanical property of OLGMs is a main limitation during the separation process since there is no substrate to resist the operation pressure for the soft OLGMs. The liquid oil contained by OLGMs is also an unstable factor in the VOC/N<sub>2</sub> separation process. Therefore, the supported liquid membrane and supported oleo gel membrane were developed in this work to promote the feasible application of the oil and OLGMs in the membrane separation process.

In this study, we report a simple method to fabricate an efficient and stable PDMS/SO based supported liquid membrane for VOC/N<sub>2</sub> separation by immobilizing oil or oleo gel into the membrane substrate. Previous studies showed that Bis (2-ethylhexyl) adipate (DEHA) /PDMS oleo gel membranes have high VOC permeance and VOC/N<sub>2</sub> selectivity. However, DEHA has a small molecule viscosity at around 12cp, which is too low to be retained in the PS membrane support [152]. Therefore, silicone oil 200 was selected to fabricate the supported liquid membrane because it is a macromolecule with high viscosity and also an excellent absorbent to various VOCs [156]. Thus, the SO based supported liquid membrane was fabricated by retaining the SO in the PS membrane pore. The viscous SO was expected to improve the stability and separation performance of the supported liquid membrane [76]. The separation performance and instability of the SO based supported liquid membrane were investigated and compared to silicone rubber membrane using a binary VOC/N<sub>2</sub> mixture. However, the membrane was still not stable in some specific VOC environments (e.g., DMC, benzene, hexane). To further improve the membrane stability and achieve better retention of SO in the membrane pores, the SO was blended with the PDMS to make the oleo gel, and the crosslinked PDMS was expected to act as the “nest” bridged in the membrane pores to retain the SO.

The intrinsic properties of PDMS/SO oleo gel on VOC/N<sub>2</sub> separation were investigated to evaluate the feasibility of PDMS/SO oleo gel as the membrane selective layer. Thus, the oleo gel membranes (OLGMs) were prepared and the different PDMS/SO weight ratios were applied to investigate the effect of SO content on VOC/N<sub>2</sub> separation of the membrane. The VOC permeability and VOC/N<sub>2</sub> selectivity were measured on PDMS/SO OLGM. 15 VOCs from four groups were selected to assess the separation performance: alcohols (methanol, ethanol, propanol, and butanol); paraffin (pentane, hexane, cyclohexane, isooctane, and heptane); aromatic compounds (benzene, toluene, and xylene); and fuel additives (methyl tert-butyl ether (MTBE), dimethyl carbonate (DMC), and acetone).

Additionally, the PDMS/SO oleo gel was one-side coated on the PTFE membranes to fill up the pores of the membrane to fabricate PDMS/SO supported oleo gel membranes. The PTFE membrane substrate has excellent mechanical and chemical stability, which may further improve the membrane stability and increase the retained SO in the membrane pores. Therefore, the PDMS/SO based supported oleo gel membrane was expected to have the following advantages: i) The membrane designed by the combination of PDMS/SO oleo gel and PTFE membrane, as membrane selective and support layer, respectively, has excellent stability in the variable VOCs environment; ii) PDMS/SO oleo gel acting as the selective layer exhibits better VOC/N<sub>2</sub> separation performance than the silicone rubber membrane. iii) the crosslinked PDMS can help the immobilization of SO in both the polymer matrix and the PTFE membrane pores; In conclusion, the PDMS/SO based supported oleo gel

membrane shows reliable stability and better VOC/N<sub>2</sub> separation performance and provides a promising candidate for the practical application of VOC/N<sub>2</sub> separation.

## 6.2 Experiment

### 6.2.1 Materials

The gases and chemicals used in this work were the same as those used in Chapter 5. Ultrafiltration (UF) Polysulfone (PS)-35 membrane from Nanostone Water Inc was used as the substrate to prepare SO-based supported liquid membrane. PMX Silicone 200 (silicone oil) was supplied by the Univar Company. Microfiltration (MF) PTFE membrane was used as the substrate to prepare SO-based supported OLM.

### 6.2.2 Membrane preparation

#### Preparation of SO based supported liquid membrane

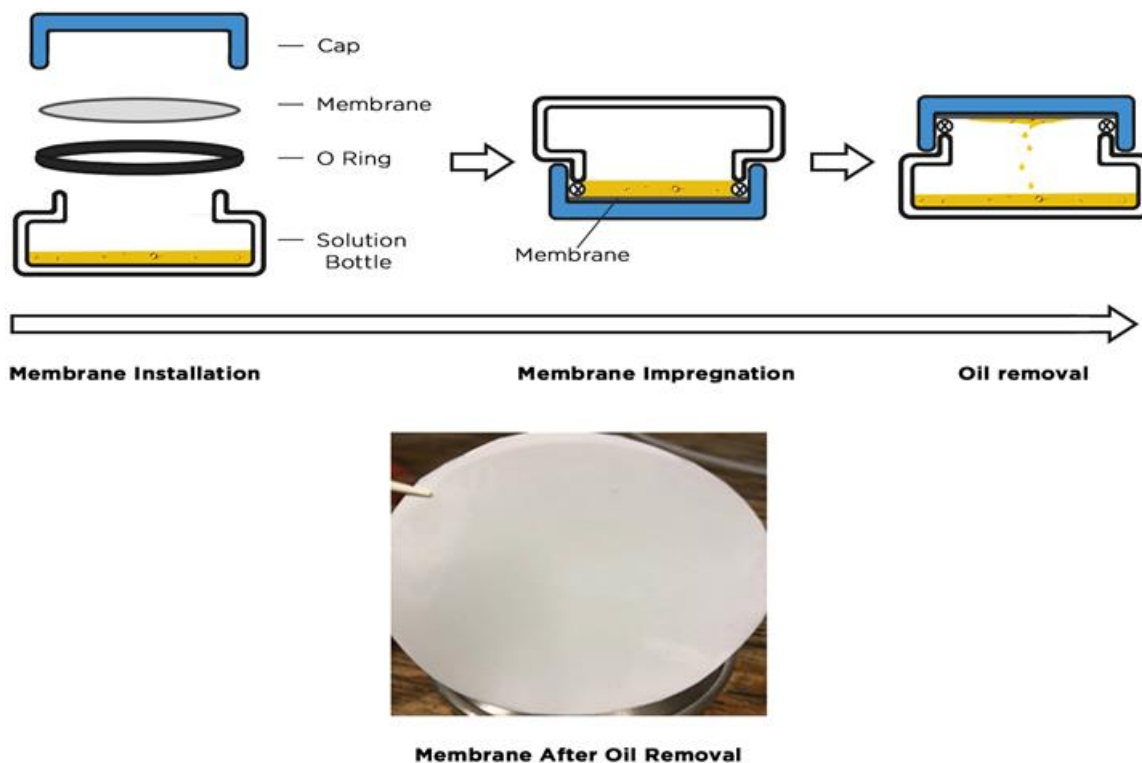


**Figure 6.1** The process of making SO based supported liquid membrane.

The preparation process of SO based supported liquid membranes is shown in Figure 6.1. The SO solution was poured into a wide-mouth bottle, and a PS membrane was mounted using a cap with the PS layer facing the SO solution. The wide-mouth bottle was placed upside down to allow the SO to penetrate the membrane under interfacial force. The placement lasted two hours to ensure that the membrane pores were completely filled with SO. Then, the wide-mouth bottle was inverted to remove the excess SO until no oil dripped out from the membrane. As seen in Figure 6.1, the prepared membrane is uniform and looks like an “oily paper”.

### Preparation of PDMS/SO OLG

The membrane casting solution was prepared by dissolving PDMS oligomer kits (part A and part B in the standard ratio of 10:1) and SO in cyclohexane at room temperature for 14 hrs. The total silicon content (i.e., PDMS + silicone oil) remained at 10 wt.%, while the amount of PDMS/SO changed with different mass ratios. The casting solution compositions and the according membrane designations are specified in Table 6.1. Afterward, the PDMS/SO solution was cast onto a glass plate, followed by thorough solvent vaporization. The glass plate was in an oven at 75°C for 12hrs for PDMS membrane crosslink. Thus, a dense membrane with the thickness of ~250 μm was obtained.

**Table 6.1** The composition of the membrane casting solution.

#	Membranes	Membrane casting solution composition
		PDMS to SO mass ratio
1	PDMS	100:0
2	PDMS-97.5/SO-2.5	97.5:2.5
3	PDMS-95/SO-5	95:5
4	PDMS-90/SO-10	90:10
5	PDMS-75/SO-25	75:25
6	PDMS-60/SO-40	60:40

### Preparation of PDMS/SO supported oleo gel membrane

The casting solutions were prepared with the same protocol in the previous section. The casting solution compositions and the according membrane designations are specified in Table 6.2. The PDMS/SO supported oleo gel membrane was prepared by coating the oleo gel on one side of the PTFE membrane. Then, after removing the residue solution on the membrane surface, the obtained



membrane was crosslinked in an oven at 75°C for 12hrs to enhance the membrane stability and lock the SO in membrane pores. Thus, the PDMS/SO supported oleo gel membrane was thus obtained.

**Table 6.2** The composition of the membrane casting solution.

#	Membranes	Membrane casting solution composition
		PDMS to SO mass ratio
1	PDMS-50/SO-50	50:50
2	PDMS-40/SO-60	40:60

### 6.2.3 Membrane characterization

The surface and cross-sections of membranes were scanned by SEM LEO FESEM 1530 with EDX Pegasus 1200 integrated EDX/OIM and Raith/Nabity electron beam writer. The oil on membrane surfaces was viewed under the Zeiss LSM 710 confocal microscope. The mechanical properties of membranes were measured by an Instron 4465 tensile and compression tester equipped with Bluehill software, and the detailed procedures have been described in Chapter 3.

### 6.2.4 Permeation experiment

The membrane test setup, procedures, and membrane permeability determination have been introduced in Chapter 3. It was noted that the nitrogen permeability measured in VOC/N<sub>2</sub> mixture was very close to pure nitrogen permeability. Therefore, pure nitrogen permeability was used to evaluate the VOC/N<sub>2</sub> separation performance.

## 6.3 Result and discussion

### 6.3.1 SO based supported liquid membrane

Chapter 6 developed a simple way to fabricate an efficient and stable SO based supported liquid membrane. It is noted that good compatibility among materials was an important factor in preparing a high-performance membrane. Thus, the contact angle was measured by dropping SO on the PS membrane surface to evaluate the material compatibility, and then a low contact angle (17°) was observed. The result indicates that SO can wet the membrane surface once SO contacts the PS membranes and fill up the pores in the PS membrane immediately. On this basis, an anticipated

schematic diagram of the SO-based supported liquid membrane was shown in Figure 6.2 (A). Especially, a thin SO layer was formed on the membrane surface, and SO occupied the void space in the support paper and PS microporous layer. The surface and cross-section of the membrane were scanned by SEM to verify the formation of SO layer.

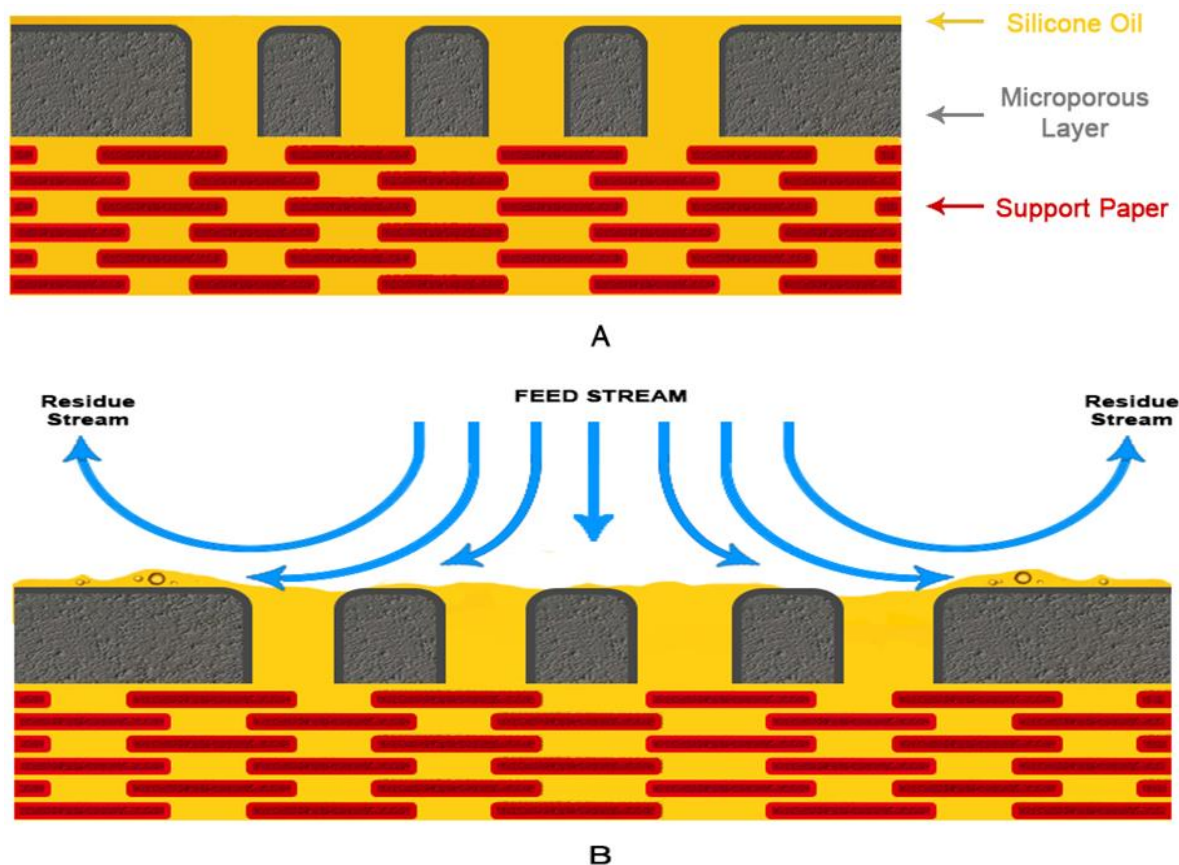


**Figure 6.2** Schematic diagram of SO-based supported liquid membrane: (A) oil-filled membrane; (B) membrane under the gas flow.

The surface morphologies of both the PS membrane and the SO-supported liquid membrane were presented by SEM in Figures 6.3. As for the PS membrane, the pores can be observed all over the membrane surface, and the microporous structure looks even more significant with a higher magnified scan (Figure 6.3 (A) and (B)). The diameter of membrane pores is measured at around 20nm. Those pores are well distributed on the surface of the PS membrane, and some of them are connected by tiny cracks. After the SO wetting the PS membrane surface, the cracks on the membrane surface become obviously less than before. This might be attributed to the oil, which acts as a lubricant and fills up the cracks on the membrane surface.

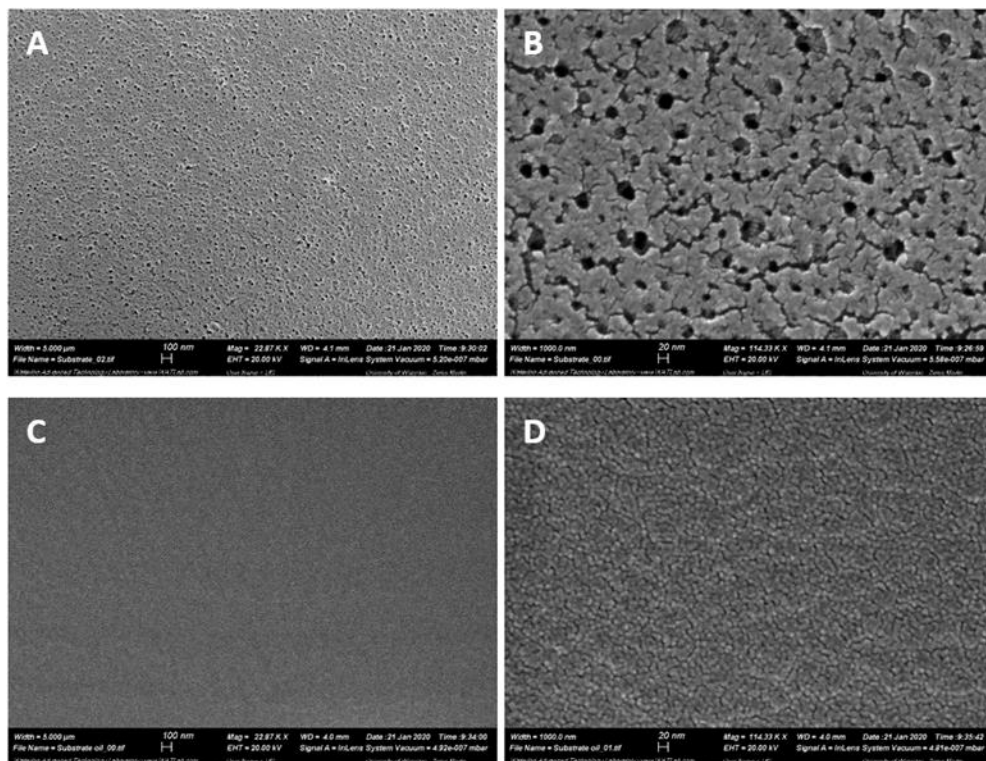


**Figure 6.3** The surface SEM image of PS membrane (image A and B) and SO-based supported liquid membrane (image C & D), which was scanned at different magnification: (A) and (C) were at 22KX; (B) and (D) were at 115KX.

The cross-section of the membranes was further scanned to view the internal structure of the membrane. The PS separation layer and nonwoven fabric support paper can be observed as shown in Figure 6.4 (A). Figure 6.4(B) shows the close-up scan of the PS layer, and the thickness of the PS layer is measured at around 30um. As the scan multiplier increases, the microporous structures of the PS layer are clearly viewed in Figure 6.4 (C).

The overview image of the SO-based supported liquid membrane was shown in Figure 6.4 (D), in which the texture of the nonwoven fabric in support paper becomes blurred, indicating that the SO has completely covered the PS membrane surface/pores, even permeated into the nonwoven fabric support layer. Figure 6.4 (E) and (F) show similar results that the micropores in the PS layer disappear, and the pores are fully filled with oil.

The cross-sections of the PS layer before and after the oil impregnation were also analyzed by SEM-EDX. The corresponding EDX spectra are shown on the right-hand side of Figure 6.5. The

spectra of compounds C, O, S and Si were detected in the pristine PS membrane, as shown in Figure 6.5 (A). Among them, the Si signal with high intensity was detected after SO impregnation (Figure 6.5 (B)), which confirms that SO is immobilized in the PS membrane from the chemical aspect. Thus, the SO-based supported liquid membrane was successfully fabricated.

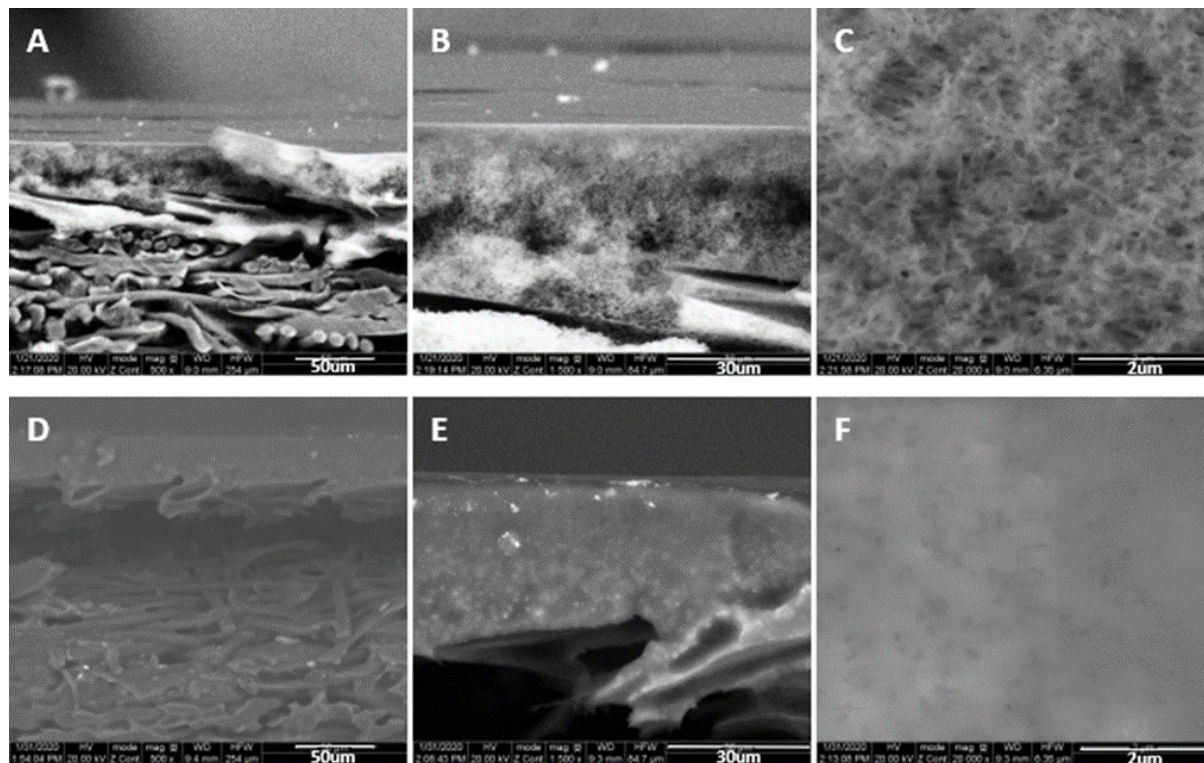


**Figure 6.4** The cross-section SEM image of PS membrane (image A, B & C) and SO-based supported liquid membrane (image D, E & F), which was scanned at different magnification: (A) and (D) were at 500X; (B) and (E) were at 1500X; (C) and (F) were at 20,000X.

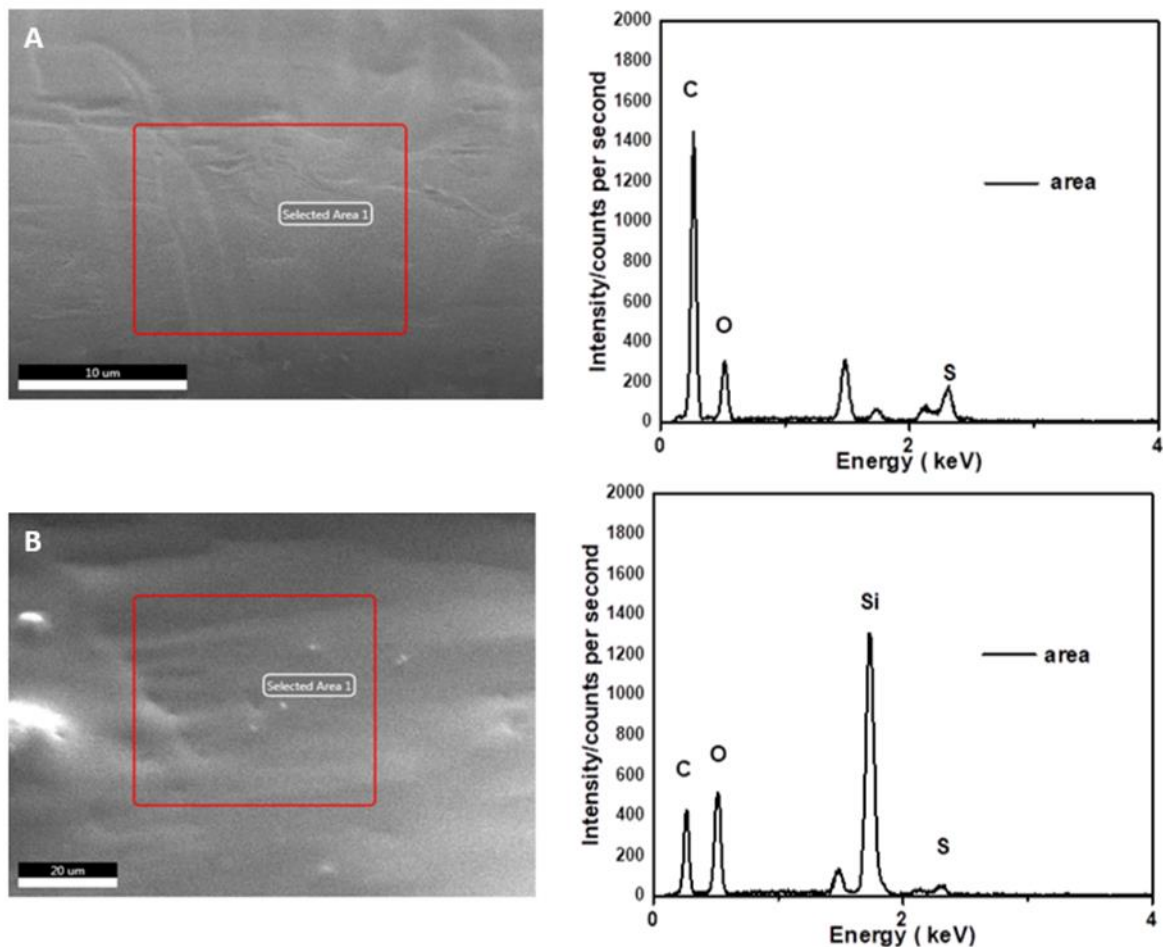


**Figure 6.5** SEM-EDX analysis performed on the cross-section of PS membrane. The SEM image with the EDX scanning area is on the left, and the corresponding EDX spectra are on the right hand. (A) PS membrane and (B) SO-based supported liquid membrane. EDX analysis was performed at an accelerating voltage of 20.0 kV using a silicon drift detector.

The pure gas separation performance of PS membrane and SO based supported liquid membrane were tested, and the results are shown in Table 6.3. By impregnation of SO in the pores of PS membrane, the SO based supported liquid membrane shows lower permeance but higher gas/N<sub>2</sub> selectivity than the PS membrane. The gas selectivity of the SO based supported liquid membrane is consistent with the result of dense PDMS membranes presented in the previous section and reported in previous literature [146, 147]. Compared with the crosslinking process during the conventional PDMS membrane preparation, the SO based supported liquid membrane is relatively easy to prepare as well as maintains the similar gas/N<sub>2</sub> selectivity, demonstrating its potential to replace the conventional PDMS membrane for gas separation.

**Table 6.3** pure gas separation performance of SO based supported liquid membrane.

	Permeance (GPU)		Ideal selectivity	
	PS membrane	liquid membrane	PS membrane	liquid membrane
N <sub>2</sub>	320	0.30		
O <sub>2</sub>	280	0.66	O <sub>2</sub> /N <sub>2</sub>	0.9
CO <sub>2</sub>	280	3.36	CO <sub>2</sub> /N <sub>2</sub>	11.2

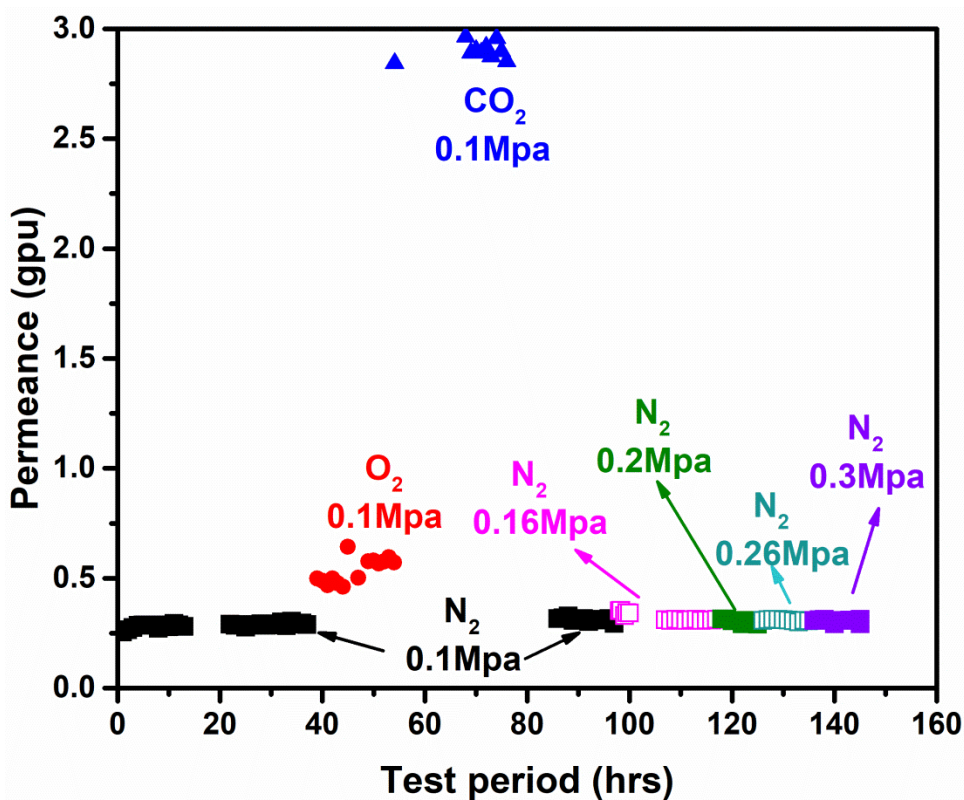


**Figure 6.6** Pure gas permeance of SO based supported liquid membrane.

The membrane stability under the operation pressure was evaluated by the continuous pure gas test at room temperature for 150hrs, and the results were shown in Figure 6.6. At the beginning of the test, nitrogen was used for flushing the membrane for a period of time to ensure the membrane achieved a steady state, and then the data of nitrogen, oxygen, and carbon dioxide were collected, respectively. As seen in Figure 6.6, the SO based supported liquid membrane exhibits relatively constant permeance for all of the gases within 150hrs. Among them, the nitrogen permeance, which was measured at 0.1-0.3MPa, shows independence with the operation pressure. The result is consistent

with other reported silicone rubber membranes [146, 153] and indicates that the SO is immobilized in membrane pores, and the membrane is stable under the pressure of 0.3MPa.

The membrane was further tested with the VOC/N<sub>2</sub> mixtures containing methanol, ethanol, propanol, and butanol. The SO based supported liquid membrane exhibits a similar VOCs/N<sub>2</sub> separation performance compared to the dense PDMS membrane and even the slightly higher selectivity for methanol, ethanol, and butanol (Table 6.4). Therefore, the SO based supported liquid membrane provides an alternative option for the application of PDMS membrane in VOC/N<sub>2</sub> separation.

**Table 6.4** VOCs/N<sub>2</sub> selectivity of SO-based supported liquid membrane vs. PDMS membrane.

VOCs type	VOCs/N <sub>2</sub> selectivity	
	Liquid membrane	PMDS membrane
Methanol	180	165
Ethanol	280	220
Propanol	577	596
Butanol	1973	1723

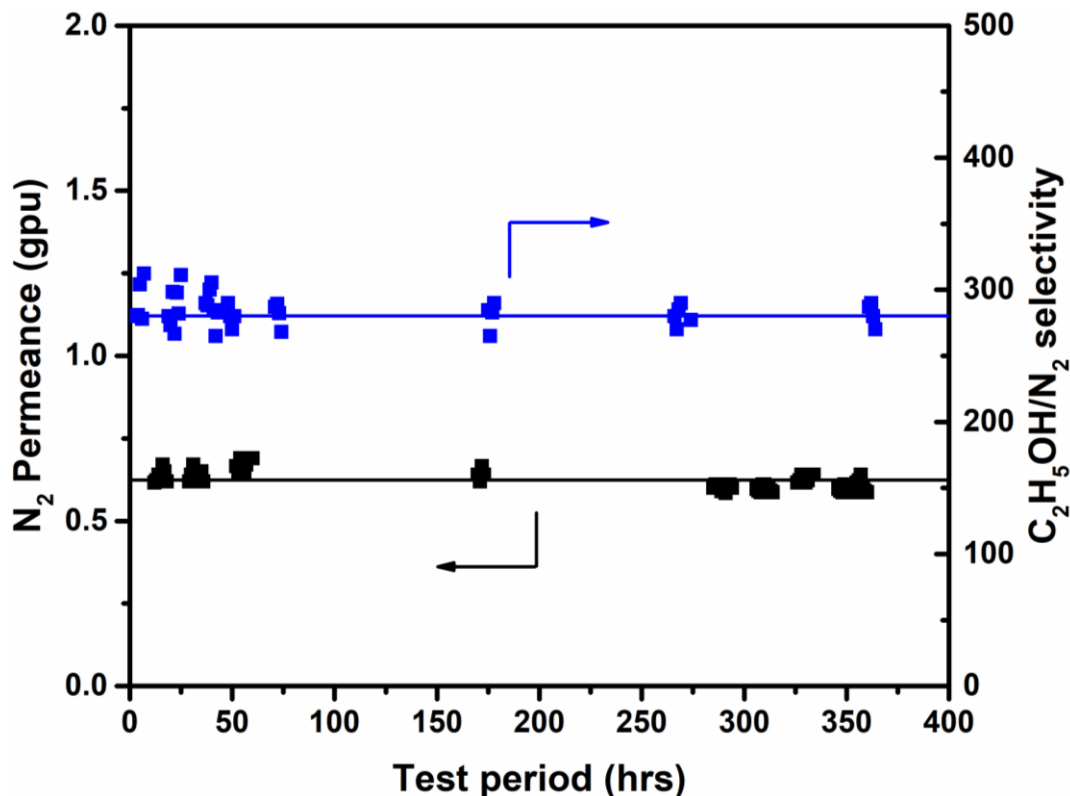


**Figure 6.7** The stability of SO-supported liquid membrane in long-term VOCs permeation test.

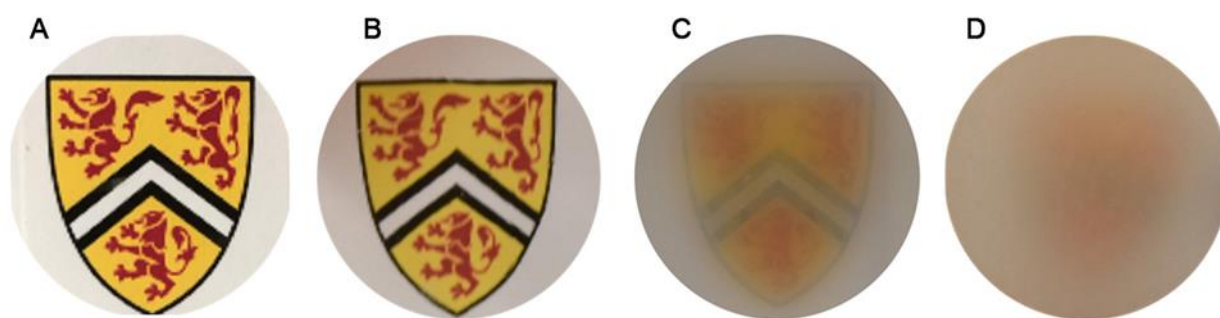
Ethanol/N<sub>2</sub> mixtures were applied to further verify the membrane stability through a 350 hrs continuous permeation test. The pure nitrogen permeance was measured periodically during the continuous permeation test. Both nitrogen permeance and ethanol/N<sub>2</sub> selectivity were constant (shown in Figure 6.7), indicating the membrane was stable for the separation of the alcohol and N<sub>2</sub>.

The SO based supported liquid membrane was also evaluated in binary VOC/N<sub>2</sub> mixture with the VOC other than those from the alcohol group. However, the VOC permeance of the membrane was continuously increasing, and VOC/N<sub>2</sub> selectivity was continuously dropping for separating these VOCs, i.e., DMC, pentane, and benzene, from nitrogen over a prolonged period, which means that the membrane was unstable in such VOCs environment. The instability could be explained by: 1) PS membrane becomes unstable when exposed to specific VOCs. 2) the unstable PS membrane weakens the retention of the SO in the membrane pores.



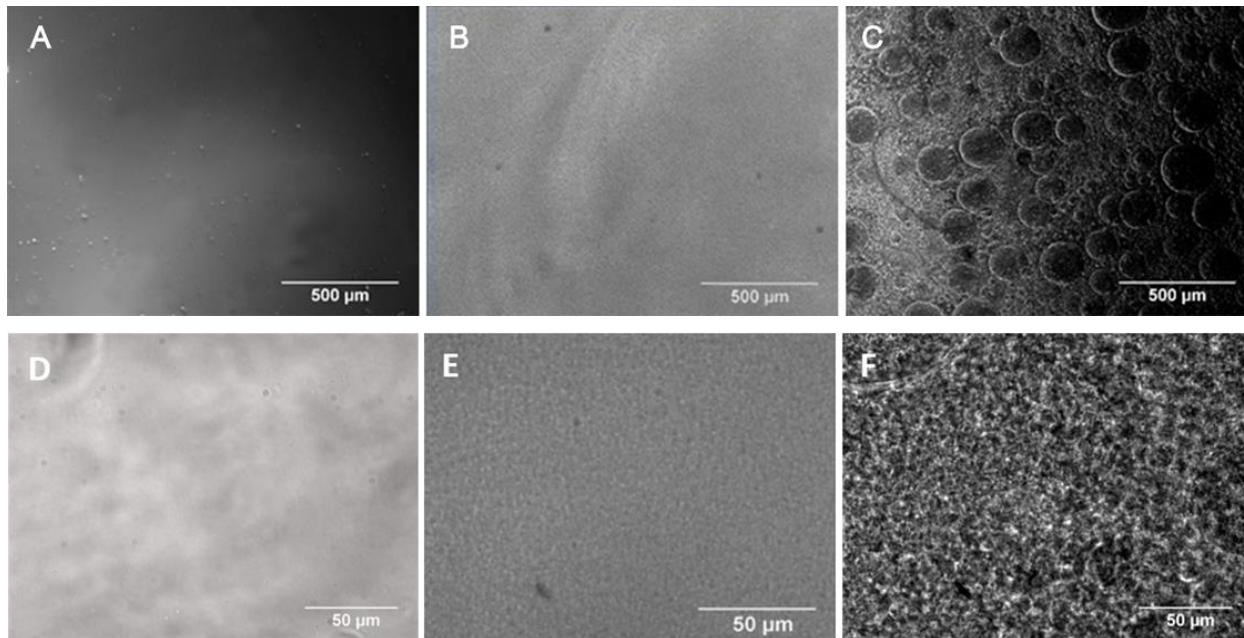
### 6.3.2 PDMS/SO oleo gel membrane

PDMS membrane was proved to be stable when exposed to various VOCs. Thus, we selected PDMS to immobilize the SO in its polymer matrix to improve the SO stability in the membrane pores. The SO was blended with the PDMS, and the blended PDMS/SO solution was used for filling up into the pores of the membrane substrate. Once PDMS was crosslinked, SO could be “locked” in the PDMS network to form the oleo gel. The crosslinked PDMS was expected to form the “bird nests” in the pores of the membrane to retain the SO. In this part, the pristine oleo gel was made to investigate its intrinsic performance to separate VOC/N<sub>2</sub>. The resultant oleo gel was named PDMS/SO OLG. The resultant oleo gel was named PDMS/SO OLG.



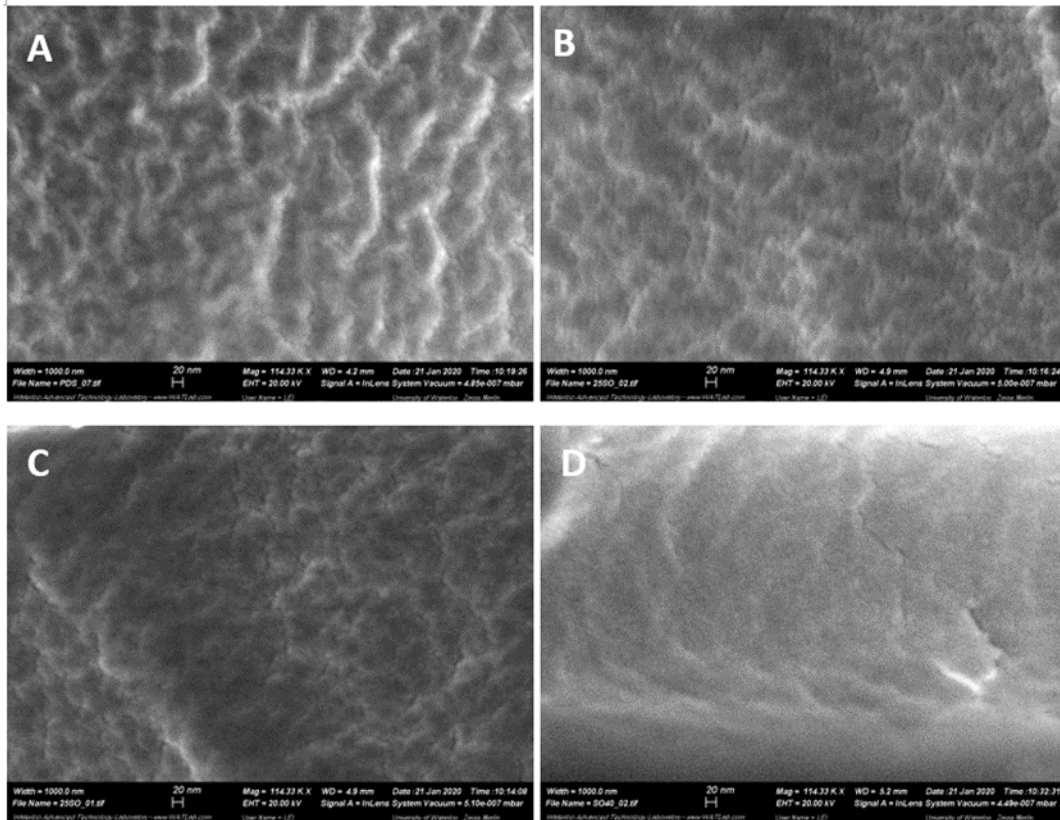
**Figure 6.8** The image of PDMS/SO oleo gel membrane. (A) PDMS, (B) PDMS-90/SO-10, (C) PDMS-75/SO-25, (D) PDMS-60/SO-40.

Figure 6.8 shows the picture of PDMS/SO OLGs, including PDMS, PDMS-90/SO-10, PDMS-75/SO-25, and PDMS-60/SO-40. To better illustrate their transparencies, the University of Waterloo badge was placed below the membranes. The PDMS and PDMS-90/SO-10 (shown as (A) and (B) in Figure 6.8) are transparent, and no silicone oil was found on the surface of the membrane. In Figure 6.8 (C), a small amount of oil was found on the membrane surface, and the membrane looked translucent. As more oil was retained in the oleo gel membrane, more oil was found on the membrane surface, and the membrane became opaque, as shown in Figure 6.8 (D).



**Figure 6.9** Microscopic images of SO oleo gel membrane at different magnifications. PDMS-90/SO-10 membrane:(A) and (D); PDMS-75/SO-25 membrane:(B) and (E); PDMS-60/SO-40 membrane: (C) and (F).

The surfaces of PDMS-90/SO-10, PDMS-75/SO-25, and PDMS-60/SO-40 were examined under the microscope, as shown in Figure 6.9. In Figure 6.9 (A) and (D), the surface of PDMS-90/SO-10 is flat, and no difference can be identified in comparison with the PDMS membrane (the microscopic images of the PDMS membrane were shown in Figure 5.3 (A) in Chapter 5). As can be seen from the images, the surface of PDMS-75/SO-25 is significantly rougher than that of PDMS-90/SO-10. Besides, some oil droplets could be observed on the membrane surface in Figure 6.9 (C), as some oil may saturate out and remain on the membrane surface. When magnifying the surface area of the PDMS-60/SO-40 membrane without oil droplet (shown in Figure 6.9 (F)), the observed membrane surface is even rougher than PDMS-75/SO-25. Thus, it could be concluded that the membrane surface tends to become rougher with the increase of SO content in the membrane.



**Figure 6.10** The cross-section SEM image of PDMS/SO OLGMs: (A) PDMS, (B) PDMS-90/SO-10, (C) PDMS-75/SO-25 and (D) PDMS-60/SO-40.

The cross-section of PDMS/SO OLGMs is also scanned under the SEM and presented in Figure 6.10. The cross-section of the oil-free PDMS membrane is textured. However, as the oil SO content increases in the membrane, the cross-section of membranes becomes smoother. It coincides with the observation on PEBA/DEHP membrane in Chapter 4, which indicates oils are well dispersed in the PDMS polymer matrix, and the as-prepared OLGMs are dense and non-porous membranes.

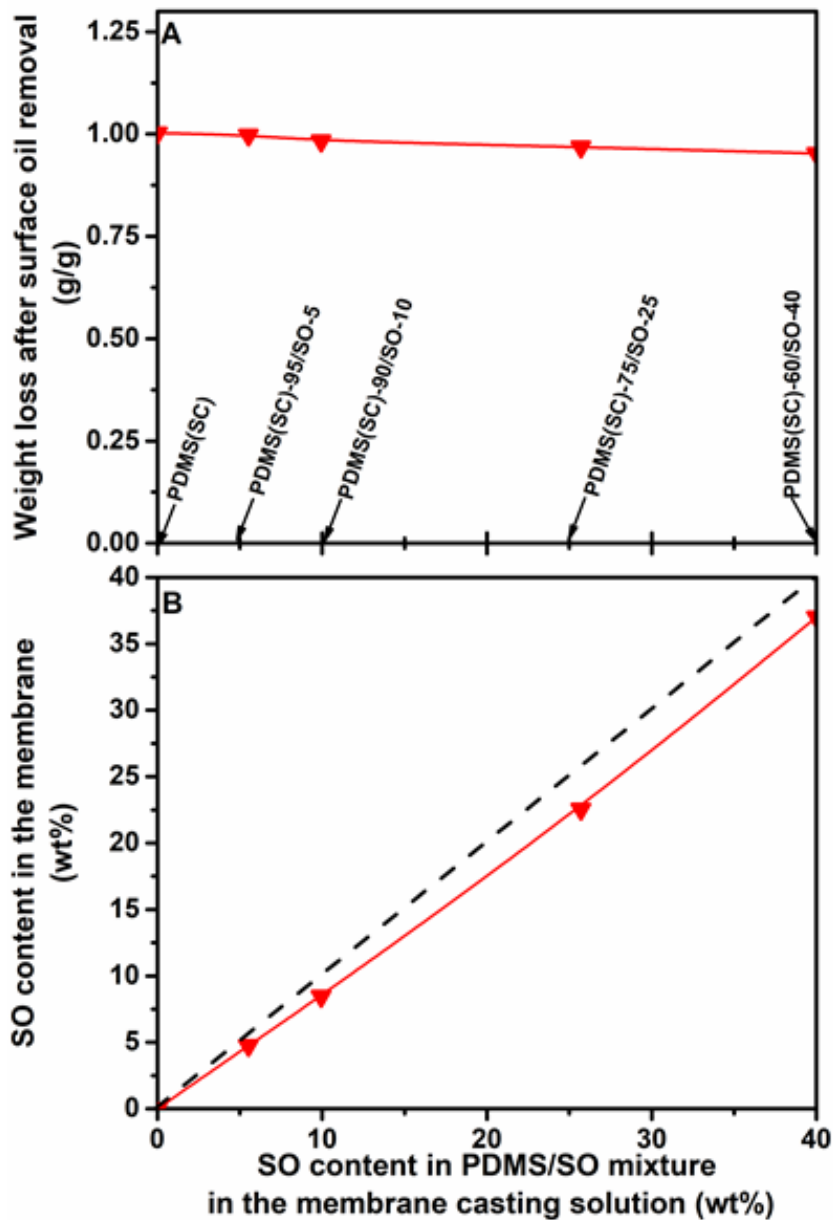


**Figure 6.11** (A) The membrane weight vs. SO content in PDMS/SO mixture in the membrane casting solution. (B) SO content in the membrane vs. SO content in PDMS/SO mixture in the membrane casting solution. The membrane weight in Figure (A) is the membrane weight after oil removal on the membrane surface to the membrane weight before oil removal.

Figure 6.11 (A) shows the membrane weight after removing the excess oil relative to the initial membrane weight. The more SO in the membrane casting solution, the more oil was saturated out of the membrane. The actual SO content in the membrane was then calculated based on oil retained in

the membrane, and the results are shown in Figure 6.11 (B). It could be concluded from Figure (A&B) that more oil is immobilized in the membrane with the increased SO content of the casting solution. The results are coincident with the observation in membrane surface characterization.

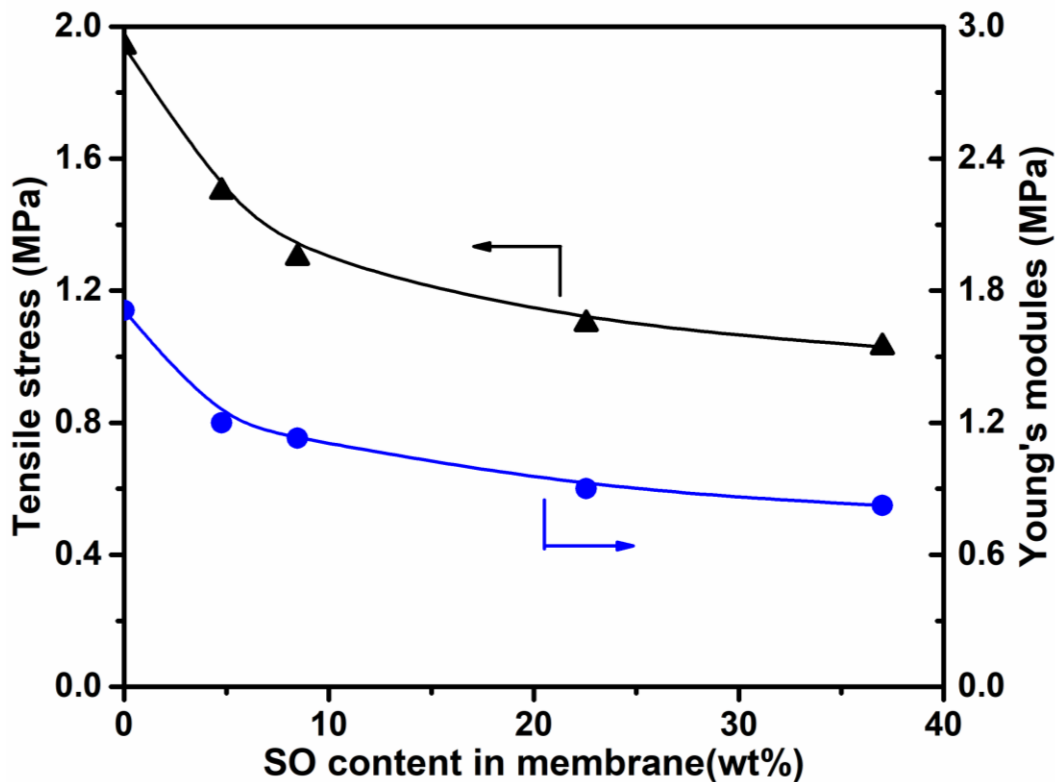


Figure 6.12 Mechanical properties of PDMS/SO OLGMs.

The mechanical properties were evaluated for PDMS, PDMS-90/SO-10, PDMS-75/SO-25, and PDMS-60/SO-40, as shown in Figure 6.12. As the oil content in the membrane increased, the tensile stress and Young's modulus decreased, indicating that the membrane containing more oil tends to be softer and mechanically weaker, which agrees with the previous studies on PDMS/DEHA membrane in Chapter 5.

### 6.3.2.1 Effect of SO on gas permeation

To investigate the effect of SO in PDMS/SO OLGm, five gases (nitrogen, oxygen, hydrogen, methane, and carbon dioxide) were selected to measure the pure gas permeability of the membranes, and the results are shown in Figure 6.13. With the increased SO content in PDMS/SO OLGm, only

the permeability of hydrogen has a tiny decrease, while the permeability of other gases increased slightly.

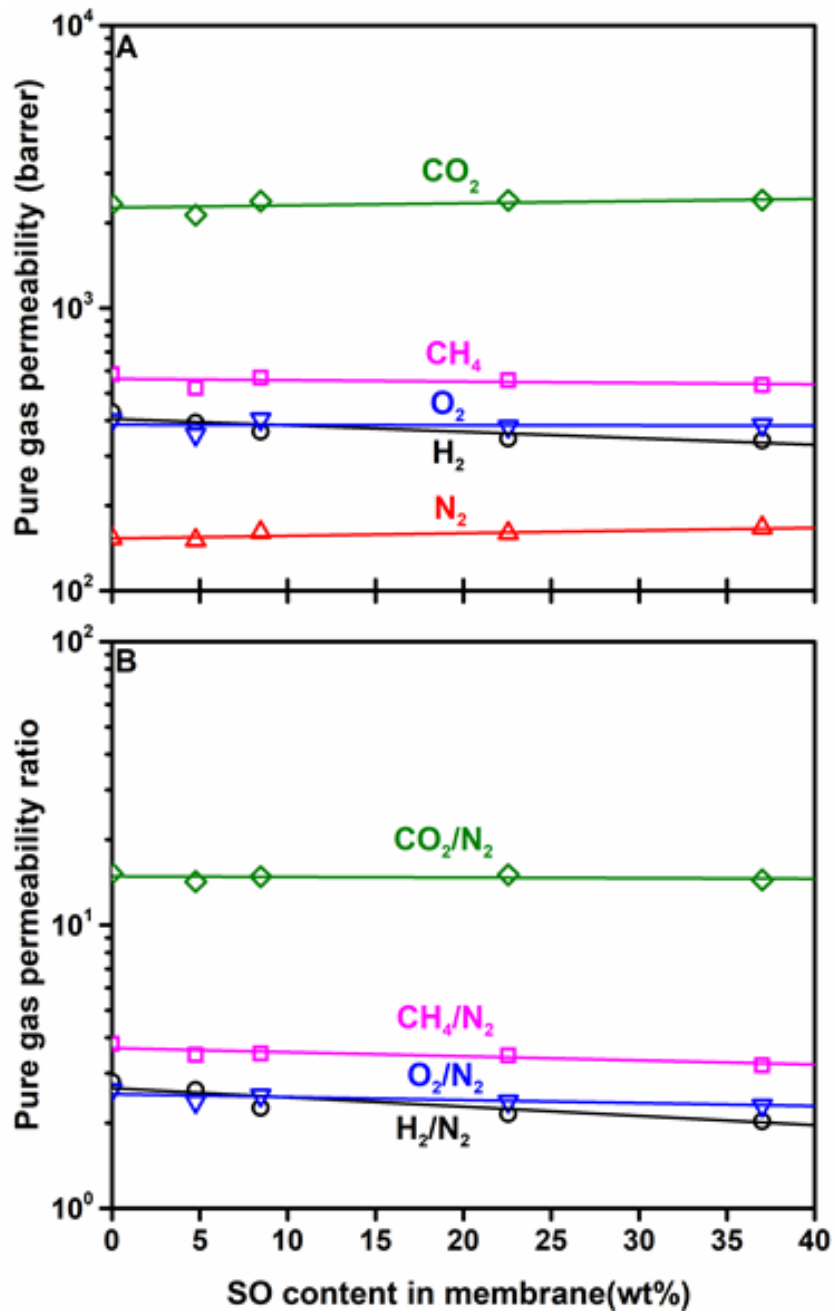
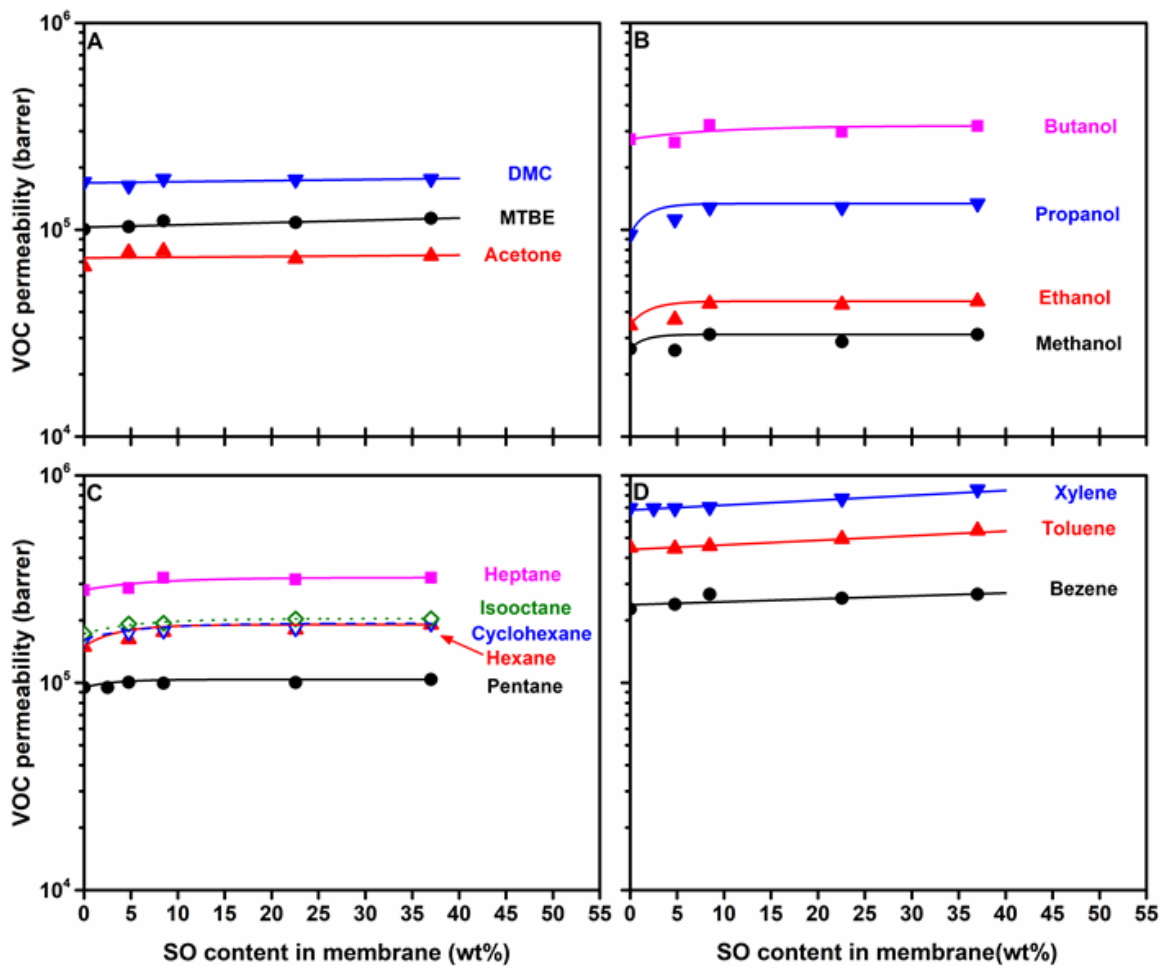


Figure 6.13 The effect of SO content on membrane perm-selectivity.

### 6.3.2.2 Effect of SO content on vapor permeation

The vapor permeation was carried out with 15 kinds of VOC components in binary VOC/N<sub>2</sub> mixtures, in which the VOCs are the form of saturated vapors. The VOC permeability of the membranes with different SO contents were measured, as shown in Figure 6.14. With the increased SO content in PDMS/SO OLG, the VOC permeability of the membrane increases. This means that the SO possesses a relatively higher VOC permeable ability than the PDMS polymer, which is consistent with the results in pure gas measurement.



**Figure 6.14** The effect of SO content in the membrane on VOCs permeability of the membrane. (A) fuel additives, (B) alcohols, (C) paraffin, (D) aromatic compounds.

### 6.3.2.3 Effect of feed VOC concentration

To further investigate the permeation mechanism and membrane performance, additional tests with different feed VOC concentrations were conducted for the PDMS/SO OLG and PDMS-75/SO-25. Based on the results in Chapter 5, an appropriate feed flow rate (less than 500 ml/min) was applied to eliminate the concentration polarization effect.

The permeation of binary VOC/N<sub>2</sub> mixtures with different VOC concentrations through the membrane was studied at 22°C. The relationships between the permeation flux of VOCs and feed VOC concentrations are shown in Figure 6.15. As the feed VOC concentration increased, the VOC flux was greater than the proportional increase, resulting in a convex curve. This trend is similar to the behavior of PDMS/DEHA membranes studied in Chapter 5, indicating that for the PDMS-based OLGs, the VOC flux could be improved by a high VOC concentration. Besides, the membrane was more permeable to condensable VOCs, such as DMC, butanol, heptane and xylene, indicating the sorption effect plays an important role in VOC permeation.

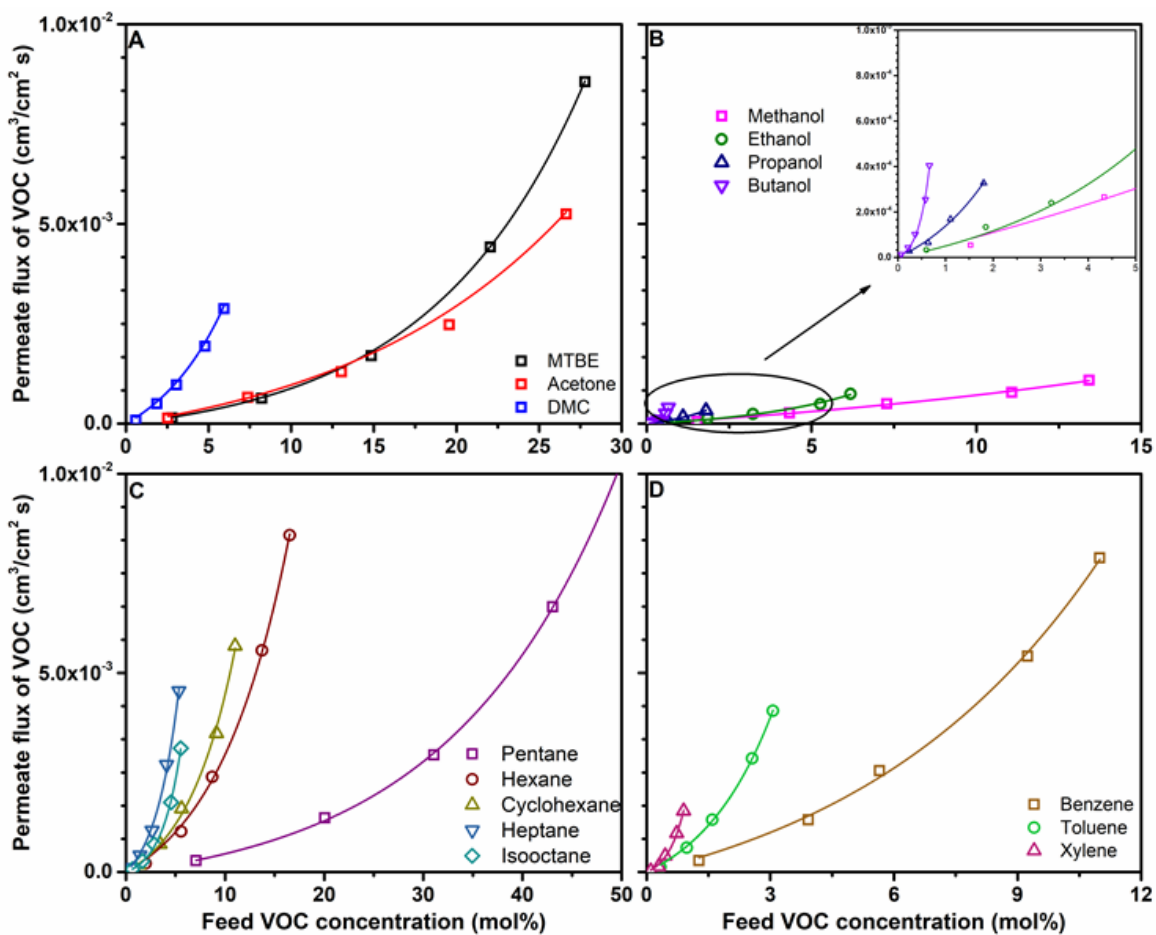


**Figure 6.15** VOC permeate flux vs feed VOC concentration. (A) fuel additives, (B) alcohols, (C) paraffin, (D) aromatic compounds.



The quantities of parameter  $\frac{D_0}{\phi}$  and  $\phi\omega$  were used to measure the feed gas composition effects on gas diffusion and sorption. The semi-empirical relation was attempted to correlate the permeate VOC flux at different feed VOC concentrations. The details have been described in Chapter 5. The values of  $\frac{D_0}{\phi}$  and  $\phi\omega$  are listed in Table 6.5. The high correlation coefficients of more than 0.99 confirm the good fit of the equation to experimental data.

**Table 6.5** Parameters from the correlation between the permeate VOC flux and the feed VOC concentration.

	$D_0/\phi$ (cm <sup>3</sup> /cm s)	$\omega\phi$ (kPa <sup>-1</sup> )	R <sup>2</sup>
Methyl tert-butyl ether	$1.12 \times 10^{-5}$	$1.07 \times 10^{-3}$	0.999
Acetone	$2.27 \times 10^{-5}$	$7.13 \times 10^{-4}$	0.991
Dimethyl carbonate	$2.51 \times 10^{-5}$	$2.28 \times 10^{-3}$	0.994
Methanol	$2.08 \times 10^{-5}$	$6.08 \times 10^{-4}$	0.993
Ethanol	$3.79 \times 10^{-6}$	$2.81 \times 10^{-3}$	0.990
n-Propanol	$4.06 \times 10^{-6}$	$5.86 \times 10^{-3}$	0.992
n-Butanol	$6.15 \times 10^{-7}$	$3.8 \times 10^{-2}$	0.995
Pentane	$1.39 \times 10^{-5}$	$5.89 \times 10^{-4}$	0.999
n-Hexane	$2.59 \times 10^{-5}$	$1.33 \times 10^{-3}$	0.999
Cyclohexane	$1.71 \times 10^{-5}$	$1.97 \times 10^{-3}$	0.997
Heptane	$1.49 \times 10^{-5}$	$3.70 \times 10^{-3}$	0.997
Iso-Octane	$4.66 \times 10^{-6}$	$4.95 \times 10^{-3}$	0.998
Benzene	$3.85 \times 10^{-5}$	$1.50 \times 10^{-3}$	0.998
Toluene	$2.20 \times 10^{-5}$	$5.24 \times 10^{-3}$	0.999
Xylene	$4.48 \times 10^{-6}$	$2.08 \times 10^{-2}$	0.996

The relationship between parameters and VOC properties was plotted in Figure 6.16. Figure 6.16 (A) shows the values of the parameter ( $\frac{D_0}{\phi}$ ) for different VOCs vs. the mole volume of the VOC. It can be found that large VOC molecule has small  $\frac{D_0}{\phi}$  for comparison within the VOC group (e.g. DMC > acetone > MTBE in the fuel additive; Methanol > ethanol > propanol > butanol in the alcohol; Pentane > hexane > heptane in the paraffin and Benzene > toluene > xylene in aromatic compounds.).

However, parameters ( $\frac{D_0}{\phi}$ ) for all VOCs are randomly distributed around  $10^{-5}$  ( $\text{cm}^3/\text{cm s}$ ), which means that the VOC concentration has a substantial effect on the diffusion process of VOC molecules. It could also mean that diffusion cannot make a difference for VOCs permeation in the membrane.

Figure 6.16 (B) shows the values of the parameter ( $\phi\omega$ ) for VOCs at a different critical temperature. The trend in this figure follows that the VOC with higher critical temperature is more condensable and has a higher value of the parameter( $\phi\omega$ ). Moreover, the VOCs within each group also follow the same trend (e.g., Butanol > propanol> ethanol> methanol in alcohol; heptane> hexane> pentane in the paraffin and Xylene> toluene> benzene in aromatic compounds). It indicates that the sorption process dominates the VOCs permeation through the membrane over the diffusion process.

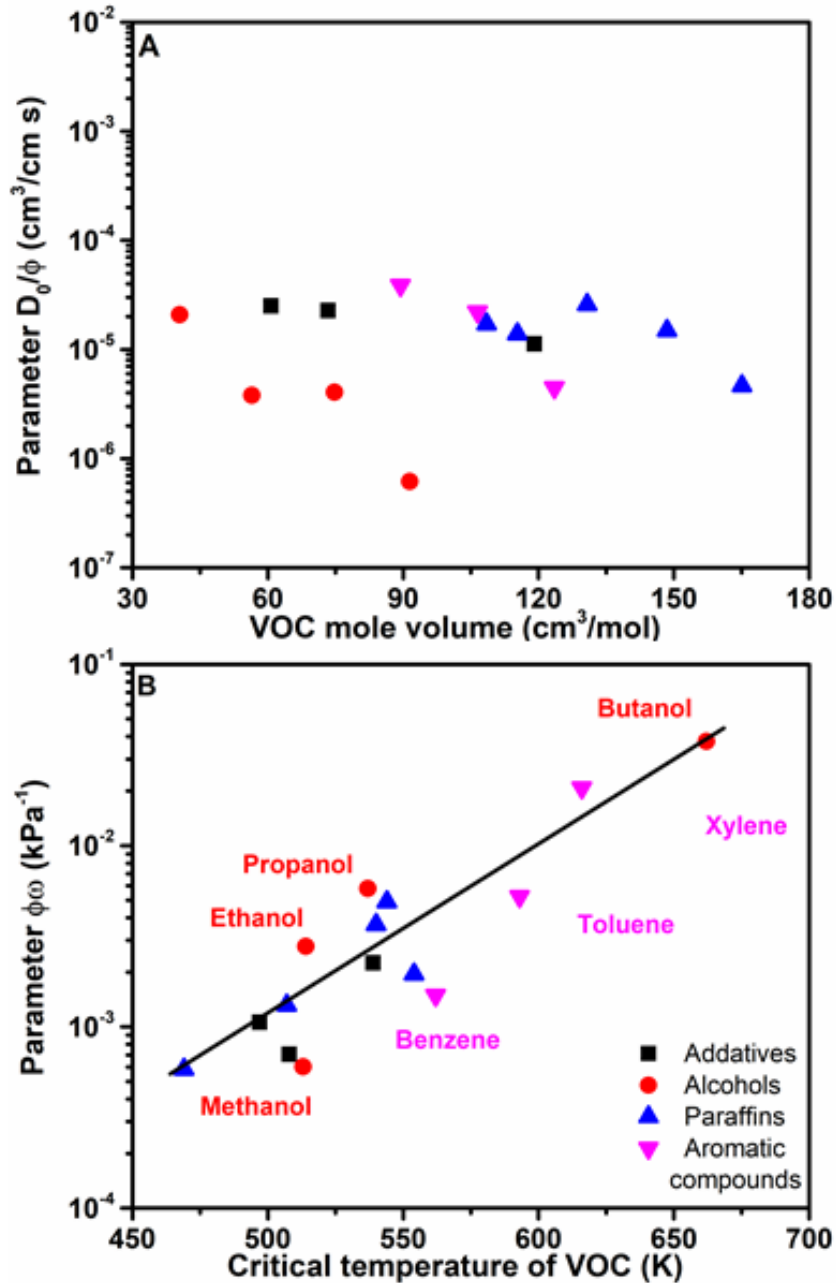


**Figure 6.16** Relationship between parameters and VOC physical properties. (A) parameters ( $D_0/\phi$ ) -critical temperature of VOCs, (B) parameters ( $\phi\omega$ ) -boiling points.

By using the parameters ( $\frac{D_0}{\phi}$ ) and ( $\phi\omega$ ) in Table 6.5, the calculated permeability is shown in Figure 6.17. The good agreement between the calculated permeability and experimental data confirms that the semi-empirical correlation is useful to predict the separation performance of the PDMS/SO

OLGM. The data in Figure 6.17 shows that the permeabilities of PDMS/SO membrane increase with the feed concentration of VOCs, which is consistent with the VOC permeation tests (Figure 6.15).

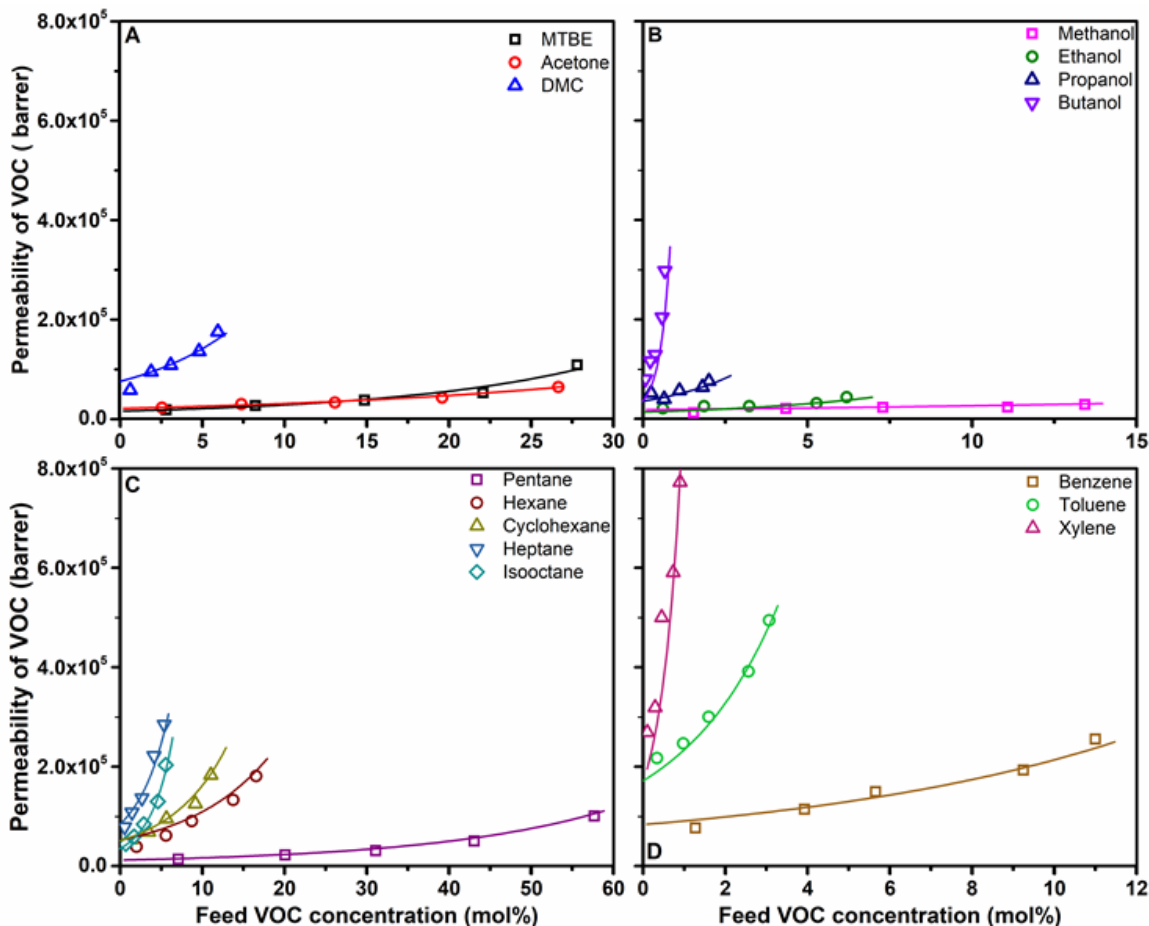


**Figure 6.17** VOC permeability vs. feed VOC concentration. (A) fuel additives, (B) alcohols, (C) paraffin, (D) aromatic compounds.

The VOC concentration in the permeate side was measured for binary VOC/N<sub>2</sub> separation, as seen in Figure 6.18. As the feed VOC concentration increased, the VOC concentration in the permeate increased as well. When feed VOC concentration exceeds 5 mol%, the VOC purity in the permeate will be more than 80 mol%, which demonstrates an excellent VOC/N<sub>2</sub> separation performance of the PDMS/SO OLGMs.

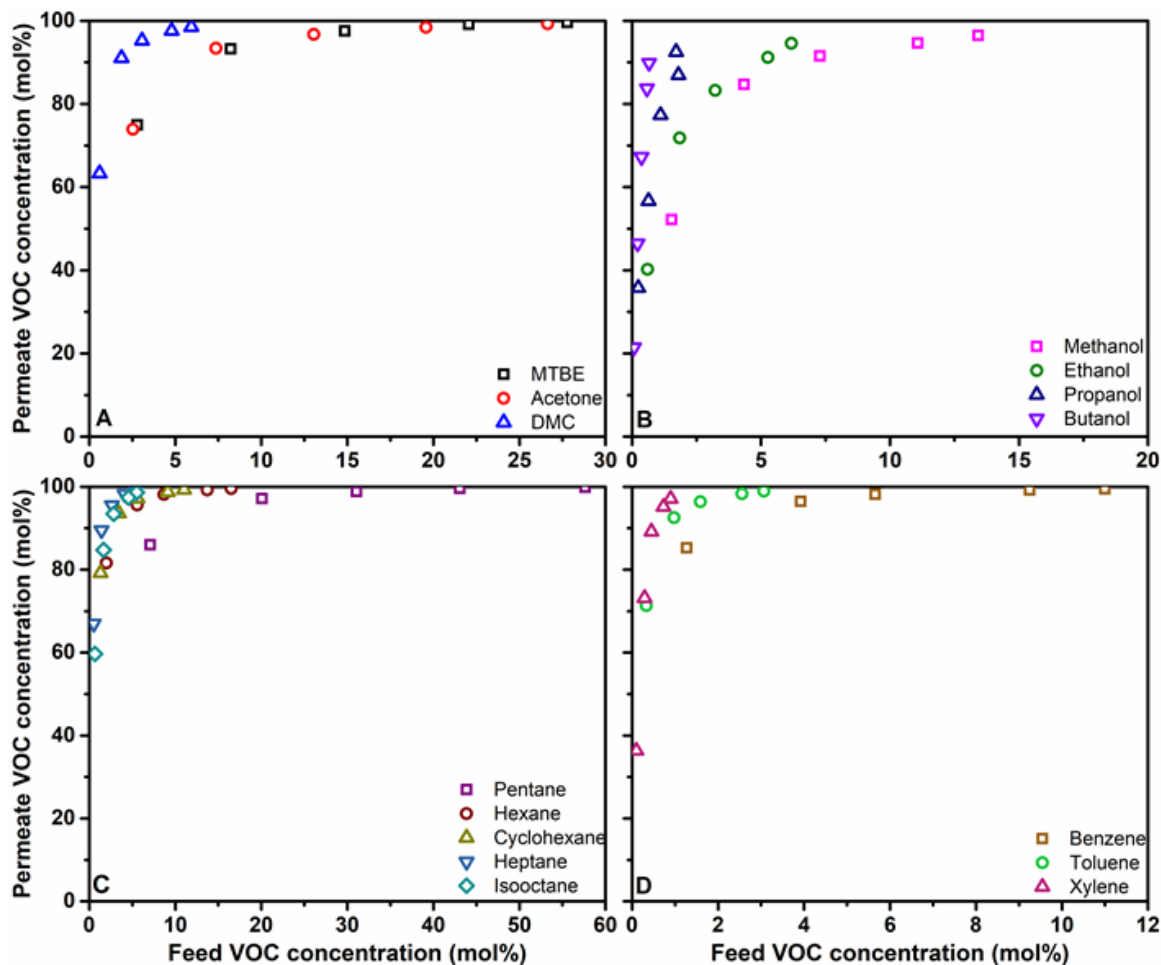


**Figure 6.18** Permeate VOC concentration vs feed VOC concentration. (A) fuel additives, (B) alcohols, (C) paraffin, (D) aromatic compounds.

### 6.3.2.4 Membrane stability

The PDMS-75/SO-25 membrane was selected for a long stability test over 27 days in various VOC/N<sub>2</sub> mixtures. After the VOC/N<sub>2</sub> mixture test, the pure gas permeability of carbon dioxide, oxygen, and nitrogen were measured again to see if there were any changes in the membrane stability. The pure gas permeability is measured at room temperature with feed gas at 0.4MPa and permeate pressure at 1atm, and the results are shown in Figure 6.19. The membrane showed excellent stability, and the membrane permeability was constant at 160 barrers for nitrogen, 380 barrers for oxygen, and 2250 barrers for carbon dioxide.

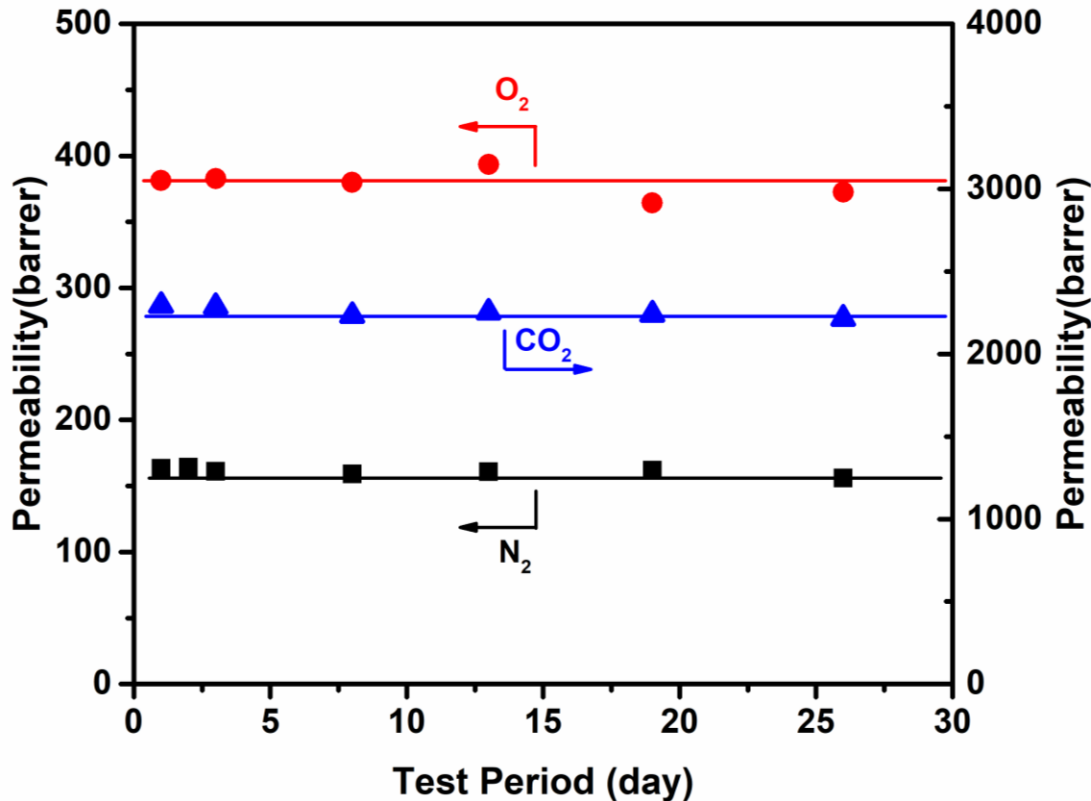


**Figure 6.19** The pure gas permeability of PDMS-75/SO-25 membrane measured over 27 days.

In conclusion, the dense PDMS/SO OLG was prepared by immobilizing the SO in the PDMS membrane matrix. 15 different VOCs were used to investigate the intrinsic property of the membrane on VOC/N<sub>2</sub> separation. The membrane shows competitive VOC/N<sub>2</sub> separation performance to the PDMS membrane, and the membrane is stable during the long-term stability tests. Therefore, immobilization of PDMS/SO oleo gel in the membrane substrate may be a better option than that of SO for the fabrication of supported liquid membrane.

### 6.3.3 PDMS/SO based supported oleo gel membrane

For the concern about the instability of the SO-based support liquid membrane caused by polysulfone (PS) instability in specific VOCs, the microfiltration (MF) PTFE membrane was chosen as the substrate because of its excellent chemical resistance [154]. However, the MF PTFE membrane has a larger pore size than the PS, and it is hard to retain the SO in it. A certain amount of PDMS was blended with the SO to increase the solution viscosity and the blended PDMS/SO would be better immobilized in the membrane than the only SO. Once the PDMS was crosslinked, SO was expected to be immobilized in membrane pores, as illustrated in Figure 6.20. Besides, the PDMS/SO OLGs

were proved to have excellent stability in various VOC/N<sub>2</sub> exposure in the previous test. The crosslinked PDMS/SO may also help the SO immobilize in the pores of the MF PTFE membrane and enhance the stability of the immobilized SO in specific VOC environments.

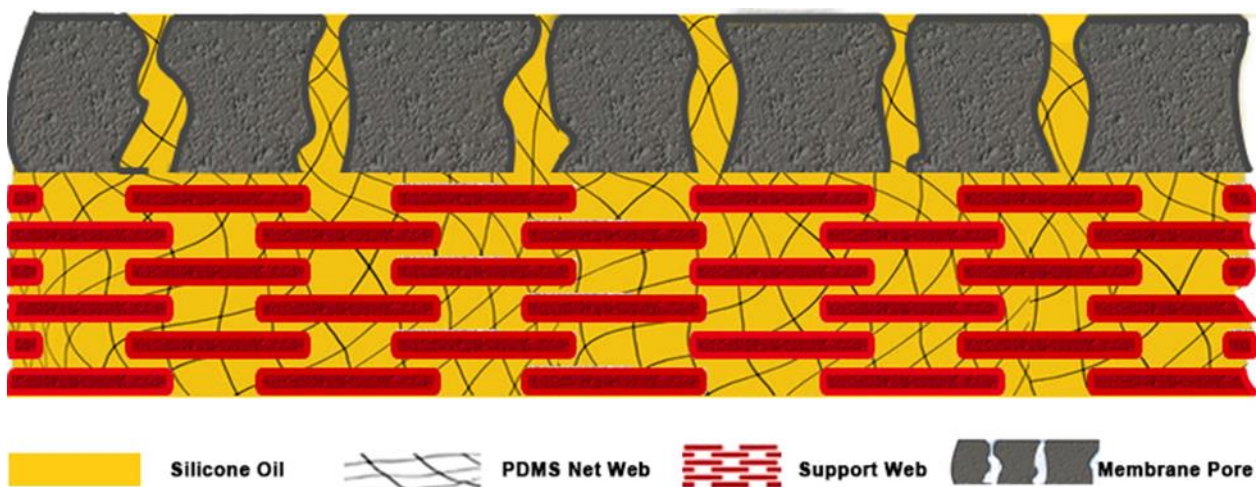


**Figure 6.20** The schematic diagram of the PDMS/SO supported oleo gel membrane.

In a previous investigation on the PDMS/SO OLGs, the result showed that VOC/N<sub>2</sub> separation performance is contingent on the SO content in the membrane, and the membrane that contains the highest SO content exhibits the best separation performance. In the preparation of the supported oleo gel membrane, the membrane with higher SO content, such as PDMS-50/SO-50 and PDMS-40/SO-60, was fabricated, expecting that more SO could be immobilized in the membrane by the crosslinking PDMS nest in the PTFE membrane pores. Unfortunately, some tiny defects and cracks appear on the membrane prepared with the ratio of PDMS-40/SO-60. While with the ratio of the PDMS-50/SO-50, a defect-free membrane can be fabricated. Thus, the PDMS-50/SO-50 was subjected to mechanical property evaluation, SEM scanning and binary VOC/N<sub>2</sub> separation performance evaluation.

**Table 6.6 Mechanical properties of membranes**

Items	PDMS/SO film	PDMS-50/SO-50
Max load (N)	1.9~2.4	78
Tensile stress (MPa)	1.5~1.9	156
Young's module (MPa)	0.8~1.8	870

The mechanical performance of PDMS-50/SO-50 supported oleo gel membrane was evaluated, and the results were compared with the PMDS/SO membrane as in Table 6.6. Obviously, the mechanical performance of the PDMS/SO supported oleo gel membrane is much better than the PDMS/SO homogenous membrane. The reason is that the PDMS/SO supported oleo gel membrane is supported by nonwoven fabrics and PTFE layer, which own the significantly solid mechanical strength. And the robust mechanical performance can ensure the supported oleo gel membrane is much more resistant to the harsh industrial operation environment than the previously developed OLMGs.

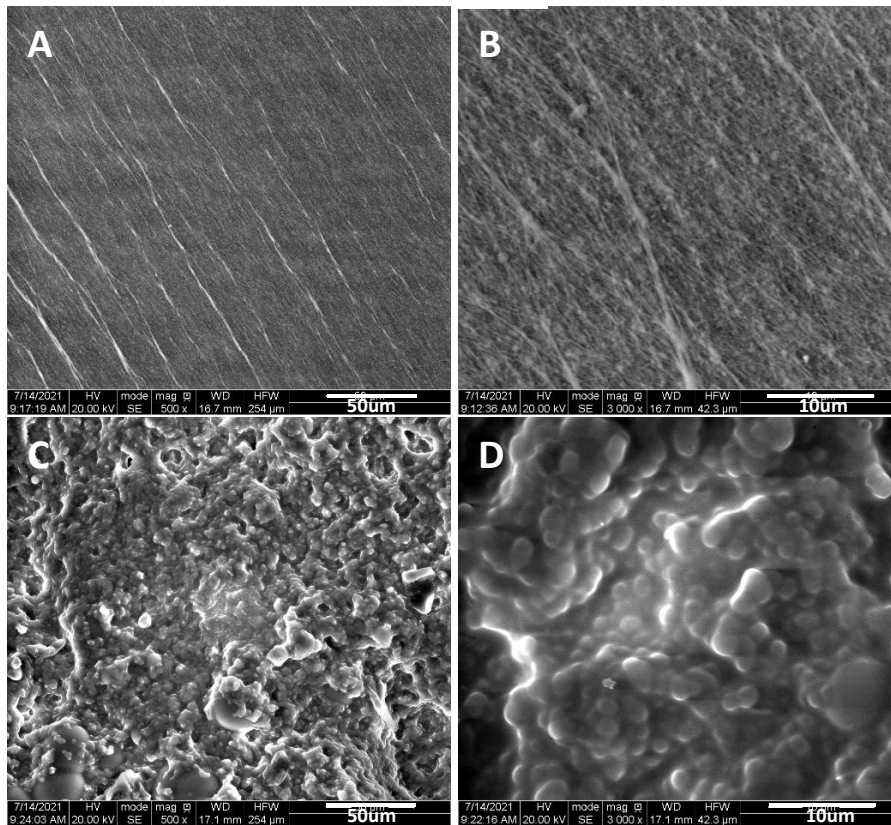


**Figure 6.21** The surface SEM image of PTFE membrane (image A and B) and PDMS-50/SO-50 supported oleo gel membrane (image C & D), which was scanned at different magnification: (A) and (C) were at 500X; (B) and (D) were at 3000X.

The SEM tests for the surface of PTFE membrane and PDMS-50/SO-50 supported oleo gel membrane was carried out, and the results were presented in Figure 6.21. As seen in Figure 6.21 (A), the PTFE membrane possesses a flat and smooth membrane surface; with a higher magnified scan, the uniform micropores can be observed all over the membrane surface (Figure 6.21(B)). After



coating the PDMS/SO oleo gel in the PTFE, the microporous structure on the PTFE membrane surface was disappeared instead by the irregular particle morphology, indicating that the membrane was filled up and covered by the oleo gel (Figure 6.21 (C) and (D)). Because of the high SO content in PDMS/SO oleo gel, the membrane surface is rough, and it is similar to the surface image of the PDMS/SO oleo gel with high SO content in Figure 6.9.

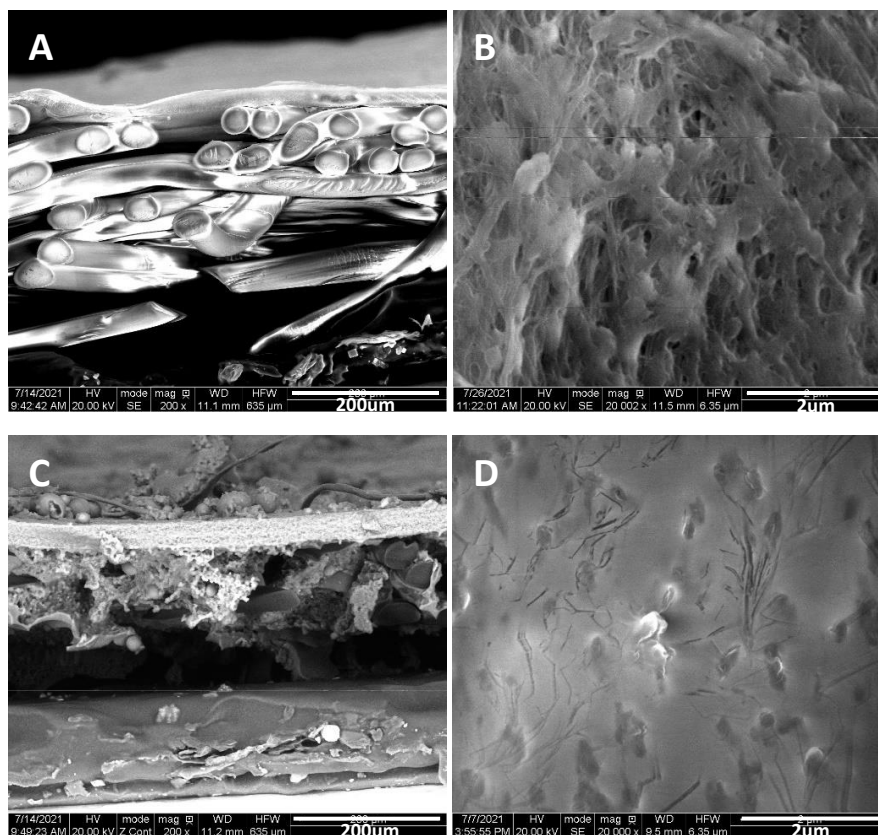


**Figure 6.22** The cross-section SEM image of PTFE membrane (image A and B ) and PDMS-50/SO-50 supported oleo gel membrane (image C and D), which was scanned at different magnification: (A) and (C) were at 200X; (B) and (D) were at 20,000X.

The cross-section images of the PTFE membrane and the PDMS-50/SO-50 supported oleo gel membrane were presented in Figure 6.22. As seen in Figure 6.22 (A) and (B), a thin PTFE layer can be observed above the nonwoven fabric support paper, and the zoomed-in image of the PTFE layer illustrates its microporous structures. In Figure 6.22 (C), the PDMS/SO oleo gel could be observed above and below the PTFE layer, and also, part of the oleo gel is attached to the nonwoven fabric below the PTFE layer. The distribution of oleo gel demonstrated that the SO penetrated through the PTFE layer and filled up some gaps in the nonwoven fabric. The PTFE layer in the supported oleo gel membrane was further observed under higher magnification; as seen in Figure 6.22 (D), the

PDMS/SO oleo gel completely filled up micropores in the PTFE layer, and the membrane is dense and defect-free. The image of Figure 6.22 (D) looks blurred, which is similar to the observation on the SEM image of SO based supported oil liquid membrane in Figure 6.9, indicating that the SO oil has successfully been retained by the crosslinked oleo gel nest and the PTFE membrane micropores.

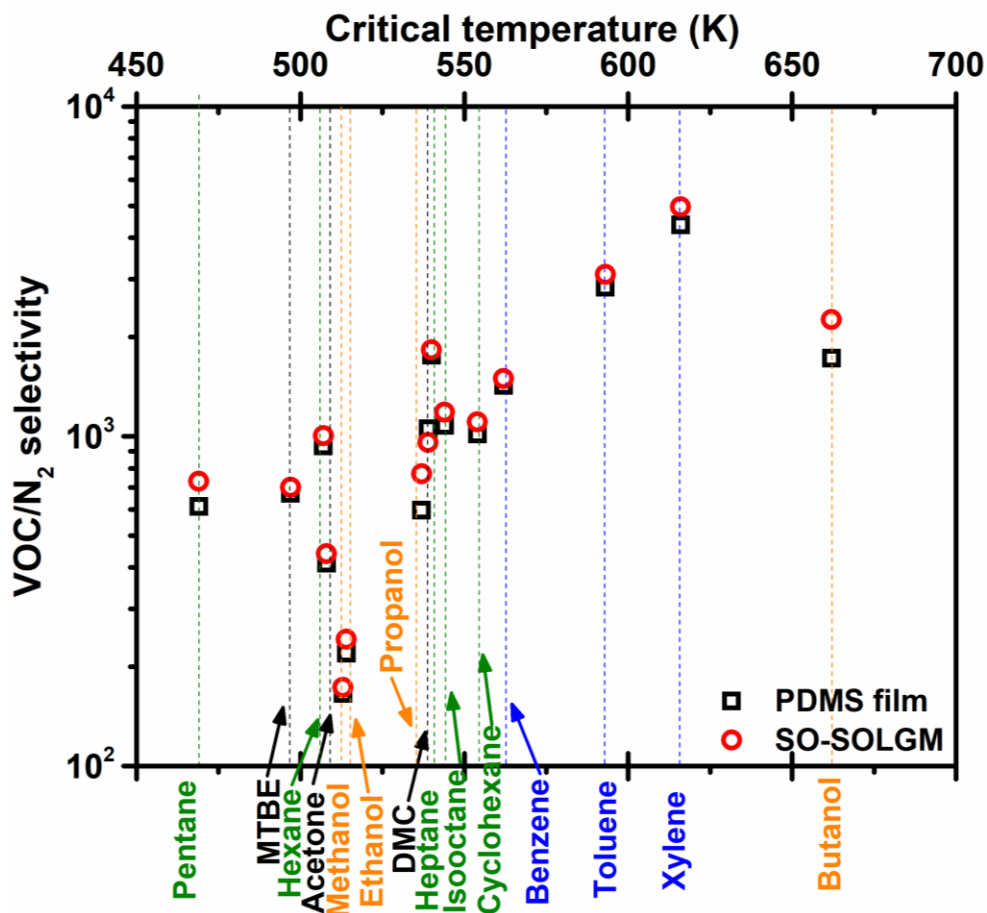


**Figure 6.23** The comparison of VOC/N<sub>2</sub> separation performance between SO-SOLGM (supported oleo gel membrane) and PDMS dense membrane. The comparison is in terms of VOC/N<sub>2</sub> selectivity vs VOCs' critical temperature. VOCs in different categories are labeled with different colors: fuel additive-black, alcohol-orange, paraffin-green, aromatic-blue. ■ PDMS dense membrane; ● : PDMS-50/SO-50 supported oleo gel membrane (SO-SOLGM).

The PDMS-50/SO-50 supported oleo gel membrane was tested at 22°C using 15 VOCs with its saturated vapor state in a binary VOC/N<sub>2</sub> mixture. The VOC/N<sub>2</sub> selectivity of the PDMS-50/SO-50 membrane is shown in Figure 6.23, and the VOC/N<sub>2</sub> selectivity of the pristine PDMS membrane from

Chapter 5 was also presented for comparison. The PDMS-50/SO-50 showed a slightly higher VOC/N<sub>2</sub> selectivity than the PDMS membrane.

The membrane was continuously tested for over 100hrs with 15 various VOC/N<sub>2</sub> mixtures. The tests of binary ethanol/N<sub>2</sub> mixtures and pure nitrogen were carried out every 20 hours during the long-term test to confirm the membrane stability. As seen in Figure 6.24, the nitrogen permeance of the membrane was maintained at 0.45 gpu, and the ethanol/N<sub>2</sub> selectivity was maintained at 240. These results verify the excellent stability of the PDMS-50/SO-50 membrane.

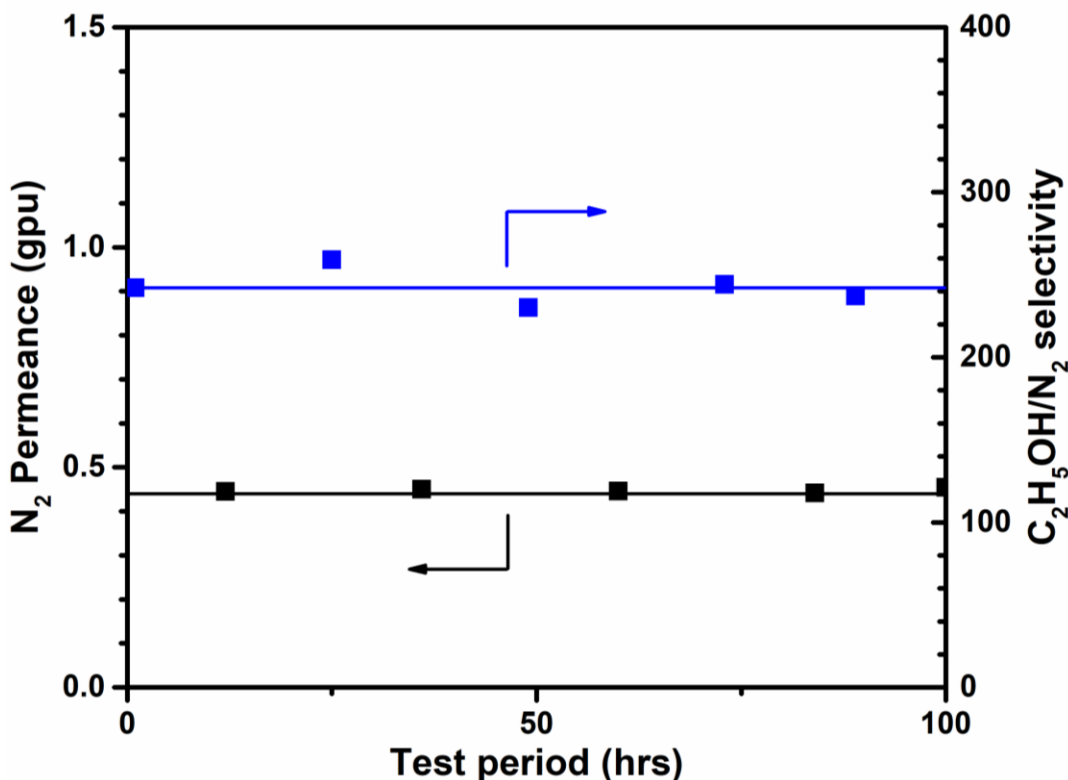


**Figure 6.24** The stability of PDMS-50/SO-50 supported oleo gel membrane.

## 6.4 Conclusion

In this study, a supported liquid membrane was firstly fabricated by filling the SO in the pores of the PS membrane. The membrane exhibited a favorable VOC/N<sub>2</sub> selectivity compared to the silicone rubber membrane and good stability for the alcohol/N<sub>2</sub> mixtures. However, the membrane was found unstable in some specific VOC environments (e.g., DMC, benzene, and hexane), which could be attributed to the instability of the PS membrane substrate and SO in the substrate. To solve this

problem, we designed a PMDS/SO based supported oleo gel membrane with PTFE membrane as substrate. The PMDS/SO oleo gel layer would increase the SO content retained in the membrane because of the crosslinking PDMS nest would enhance the stability of the immobilized SO in the membrane under VOC exposure. The PTFE membrane was selected as membrane substrate because of its good mechanical strength and chemical resistance property. Firstly, a series of tests, including separation performance and membrane stability, were carried out for PDMS/SO OLGm to ensure the availability of the oleo gel layer for VOC/N<sub>2</sub> separation. The results showed that the VOC/N<sub>2</sub> permselectivity of PDMS/SO OLGm increased with the SO content in the membrane. The membrane showed slightly higher VOC permeability and VOC/N<sub>2</sub> selectivity for all the 15 VOCs than oil-free PDMS membrane, and reliable membrane stability was well demonstrated in the 30-day test using various VOCs as feeds. On the basis of these results, the PDMS/SO based supported oleo gel membrane (PDMS-50/SO-50) was prepared; it showed stronger mechanical properties than the previously developed oleo gel membrane. The PDMS-50/SO-50 showed a higher VOC/N<sub>2</sub> selectivity than the PDMS membrane in the permeation test of 15 different VOCs. And the membrane was proved stable in continuously testing for over 100hrs, which demonstrated its prospective application on VOC/N<sub>2</sub> separation. Additionally, the PDMS as an immobilizer successfully reinforced the SO retained in the pores of the substrate, which may be used in the investigation of oil immobilization for developing new supported oleo gel membranes with higher VOC/N<sub>2</sub> separation performance.

## Chapter 7

### General conclusion, contributions and recommendations

#### 7.1 General conclusions and contributions

Different types of oleophilic membranes, including the oleo gel liquid membrane (OLGM), support oil liquid membrane, and support oleo gel liquid membrane, were developed in this work. All the membranes were comprehensively evaluated at different operating conditions to investigate the VOC permeation behavior in the prepared membranes. Five non or less condensable gases (e.g., N<sub>2</sub>, H<sub>2</sub>, CO<sub>2</sub>, CH<sub>4</sub>, and O<sub>2</sub>) and more than 15 VOCs from groups of fuel additives, alcohols, paraffin, and aromatic compounds were used as feeds to evaluate the gas permeation performance in the membranes. The following is the conclusion drawn from this research, and the contribution to original research is behind it:

1. The DEHA and DEHP oil, which has higher diffusion and sorption coefficient to VOCs than the polymers PEBA and PDMS, was immobilized in the polymer for the first time. And the oleo gel membrane was innovatively developed and applied to VOC/N<sub>2</sub> separation. The oleo gel membranes were made into films to investigate the intrinsic membrane performance on VOC/N<sub>2</sub> separation (VOCs permeabilities and VOC/N<sub>2</sub> selectivities). This is critical and will benefit the development of relevant oleophilic composite membranes. Four oleo gels, including PEBA/DEHP, PEBA/DEHA, PDMS/DEHA and PDMS/SO, were fabricated in this work. Oleo gel membranes of PEBA/DEHP, PEBA/DEHA, PDMS/DEHA developed in this work showed dramatically higher VOCs permeabilities than polymeric membranes (e.g., PEBA and PDMS) currently adopted in the industry for VOC/N<sub>2</sub> separation. And the VOCs permeabilities of the membranes are in order of PEBA/DEHA > PEBA/DEHP > PEBA and PDMS/DEHA > PDMS/SO > PDMS.
2. The VOC permeation mechanism in OLGMs was investigated. The mechanism of VOC and N<sub>2</sub> permeation was well demonstrated by studying membrane separation performance on VOC/N<sub>2</sub> separation at different feed VOC concentrations and temperatures. The VOC and N<sub>2</sub> permeation in the membrane follows the sorption diffusion model, and the sorption was found to be dominant over diffusion in the VOC permeation in the membranes.
3. This work detailly investigated the effects of oil and polymer contents in the membrane on membrane VOC/N<sub>2</sub> separation performance. The content of DEHA and DEHP oil retained in the PEBA reached as high as 75wt.%. However, the content of the DEHA oil in the PDMS reached only up to 32wt.%, and even the PDMS has more free volume than the PEBA. It may

be because DEHA (or DEHP) could form hydrogen bonding with PEBA, but not with PDMS. The VOC permeability of the membrane was proportional dependent on the oil content in the membrane, and the PDMS/DEHA OLGGM showed the overall higher VOC permeabilities than PEBA based OLGGMs. Because the PDMS has higher VOCs permeabilities than PEBA, and the polymer for oil immobilization in the membrane also plays significant effects on VOC permeation.

4. A facile way to calculate the VOC permeabilities in oils was firstly developed in this work. Typically, the diffusion coefficient and sorption coefficient of the VOCs in the oil could be determined from the gas sorption kinetics [155]. The permeability of the VOCs could then be calculated by multiplying the diffusivity coefficient and sorption coefficient. In this work, the experimental VOC permeability of OLGGM was employed in the empirical equations from the polymer blending rules. The VOC permeabilities in oils could be directly calculated, which is more convenient than the determination by the gas sorption kinetics.
5. An efficient and straightforward method was developed in this work to fabricate the oil liquid membrane and supported oleo gel membranes, and the membranes were successfully fabricated for VOC/N<sub>2</sub> separation. The membranes were simply made by wetting the membrane surface with oil or oleo gel, and the oil was then retained in the pores of the membrane by the capillary forces. Because the PDMS based oleo gel is more viscous than the liquid oil and oleo gel could form the polymeric web in the membrane pores after PDMS based oleo gel becomes cross-linked. Therefore, the PDMS based oleo gel could be better retained in the membrane pores than the liquid oil, making the SO-based supported oleo gel membrane more robust and stable in the environment with the various VOCs than the oily liquid membrane.

## **7.2 Recommendations for future work**

### **7.2.1 Investigation of VOC diffusivity and solubility in the membrane**

The permeability indicates the intrinsic property of gas or vapor permeation in the membrane. To understand the VOC permeation in the OLGGM, the VOC permeability was investigated from different aspects, including the effect from the oil content in the membrane, feed VOC concentrations, and the operating temperatures. The VOC permeation in the OLGGM was proved to follow the solution diffusion model

However, the quantity contributions from sorption and diffusion to VOC permeability of the membrane were unknown. The determination of the sorption and diffusion coefficients are suggested

in future work to quantitatively understand the contribution from sorption and diffusion to VOC permeation in OLGMs.

The sorption coefficient  $S_i$  is described in the equation below, which was also introduced in Chapter 2.  $C_i$  and  $p_i$  could be measured at the different conditions [92].

$$C_i = S_i \times p_i$$

Because the permeability data was known in this work, the diffusion coefficient could be obtained by the below equation, which was introduced in Chapter 2 as well.

$$P = D \times S$$

### **7.2.2 Development of supported oleo gel membrane**

The PDMS/SO supported oleo gel membrane was developed in Chapter 6. The membrane was stable in various VOCs but only showed slightly higher VOC/N<sub>2</sub> separation performance to silicone rubber membrane. To further improve the VOC/N<sub>2</sub> separation performance of the supported oleo gel membrane, oils with better VOC permeability are suggested to replace the SO in the supported oleo gel membrane. The DEHP and DEHA, which showed higher calculated VOC permeability in this work, might be applied to replace the SO in the membrane. Other oils that may have better VOC permeability than DEHP and DEHA oils are also worth an investigation. The PTFE substrate used in fabricating the supported oleo gel membrane in this work has big pores, which may not be the optimum option for oil immobilization. Therefore, the investigation of alternative membrane substrates is also suggested in future work.

### **7.2.3 Development of oleo gel hollow fiber membranes**

The OLGMs were developed using various oils and oil immobilizers. All OLGMs fabricated in this study showed competitive VOC/N<sub>2</sub> separation performance to the polymers that are currently used in the industry for membrane fabrication (e.g., PDMS and PEBA). Additionally, the supported oleo gel membrane prepared in this work was in the form of the flat sheet membrane. Hollow fiber membranes have several advantages over flat sheet membranes, including self-supporting characteristics, high surface-to-volume ratio, high packing density, and ease to scale up [156]. A thin layer of the PDMS/DEHA oleo gel could be either cast on a hollow fiber substrate or immobilized in a hollow fiber substrate. Therefore, the way to make the hollow fiber membranes could be studied further along with the mode for gas introduction in the hollow fiber membrane. The gas introduction modes to be considered include shell-side feed and bore-side feed. Flow configurations for hollow fiber

membrane operation, including counter-current, co-current and counter-/co-current, will also be worthy of investigation.

#### **7.2.4 Separation at the high stage cut (recovery)**

The OLGMs and their relevant composite membranes reported in this work for VOC/N<sub>2</sub> separation were carried out at the low stage cut to keep the VOC concentration in the residue stream same to the feed stream, to avoid the concentration polarization. However, the membrane will be operated at the high stage cut in reality. Evaluating the VOC purity and flux in the permeate stream versus the stage cut from an engineering standpoint is suggested in future works.



## Bibliography

- [1] P.K. Tewari, Membrane Technology, in: Nanocomposite Membrane Technology, CRC Press, 2015, pp. 1-68.
- [2] R.W. Baker, Membrane Technology and Applications, 3rd ed., A John Wiley & Sons, Ltd., 2012.
- [3] Market report: global membrane filtration market, in, 2018, pp. 582.
- [4] H. Strathmann, Membrane separation processes: current relevance and future opportunities, *AIChE J.*, 47 (2001) 1077-1087.
- [5] R.W. Baker, Recent developments in membrane vapour separation systems, *Membr. Technol.*, 114 (2002) 9-12.
- [6] P.S. Monkasa, Atmospheric composition change – global and regional air quality, *Atmos. Environ.*, 43 (2009) 5268–5350.
- [7] R.W. Baker, N. Yoshioka, J.M. Mohr, A.J. Khan, Separation of organic vapors from air, *J. Membr. Sci.*, 31 (1987) 259-271.
- [8] E.H. Kim, T.P. Lyon, Strategic environmental disclosure: evidence from the DOE's voluntary greenhouse gas registry, *J. Environ. Econ. Manage.*, 61 (2011) 311-326.
- [9] D.T. Allen, Emissions from oil and gas operations in the united states and their air quality implications, *J. Air Waste Manage. Assoc.*, 66 (2016) 549-575.
- [10] I. Manisalidis, E. Stavropoulou, A. Stavropoulos, E. Bezirtzoglou, Environmental and health impacts of air pollution: a review, *Front. Public Health*, 8 (2020) 14.
- [11] J. Lelieveld, J.S. Evans, M. Fnais, D. Giannadaki, A. Pozzer, The contribution of outdoor air pollution sources to premature mortality on a global scale, *Nature*, 525 (2015) 367-371.
- [12] W.R. Stockwell, C.V. Lawson, E. Saunders, W.S. Goliff, A review of tropospheric atmospheric chemistry and gas-phase chemical mechanisms for air quality modeling, *Atmosphere*, 3 (2012) 1-32.
- [13] F.I. Khan, A. Kr. Ghoshal, Removal of volatile organic compounds from polluted air, *J. Loss Prev. Process Ind.*, 13 (2000) 527-545.
- [14] E.N. Ruddy, L.A. Carroll, Select the best VOC control strategy, *Chem. Eng. Prog.*, 89 (1993) 28-35.
- [15] V. Sivasubramanian, Environmental sustainability using green technologies, CRC Press, 2016.
- [16] D.M. D'Alessandro, B. Smit, J.R. Long, Carbon dioxide capture: prospects for new materials, *Angew. Chem. Int. Ed.*, 49 (2010) 6058-6082.
- [17] A.R. Millward, O.M. Yaghi, Metal–organic frameworks with exceptionally high capacity for storage of carbon dioxide at room temperature, *JACS*, 127 (2005) 17998-17999.
- [18] S. Vicki, J. Kaschemekat, M.L. Jacobs, D.D. Dortmund, Membrane systems offer a new way to recover volatile organic air pollutants, *Chem. Eng. J.*, 101 (1994) 92.
- [19] R. Baker, Recent developments in membrane vapour separation systems, *Membr. Technol.*, 1999 (1999) 9-12.
- [20] J.G. Wijmans, R.W. Baker, The solution-diffusion model: a review, *J. Membr. Sci.*, 107 (1995) 1-21.
- [21] H. Lin, B.D. Freeman, Materials selection guidelines for membranes that remove CO<sub>2</sub> from gas mixtures, *J. Mol. Struct.*, 739 (2005) 57-74.
- [22] N. Du, H.B. Park, M.M. Dal-Cin, M.D. Guiver, Advances in high permeability polymeric membrane materials for CO<sub>2</sub> separations, *Energy&Environmental Science* 5(2012) 7306-7322.
- [23] D.R. Lide, CRC handbook of chemistry and physics, CRC press, 2004.
- [24] M.V. Chandak, Y.S. Lin, W. Ji, R.J. Higgins, Sorption and diffusion of volatile organic compounds in polydimethylsiloxane membranes, *J. Appl. Polym. Sci.*, 67 (1998) 165-175.
- [25] H. Paul, C.Philipsen, F.J. Gerner, H. Strathmann, Removal of organic vapors from air by selective membrane permeation, *J. Membr. Sci.*, 36 (1988) 363-372.

- [26] A. Fouda, J. Bai, S.Q. Zhang, O. Kutowy, T. Matsuura, Membrane separation of low volatile organic compounds by pervaporation and vapor permeation, *Desalination*, 90 (1993) 209-233.
- [27] S. Liu, W.K. Teo, X. Tan, K.Li, Preparation of PDMS<sub>vi</sub>-Al<sub>2</sub>O<sub>3</sub> composite hollow fibre membranes for VOC recovery from waste gas streams, *Sep. Purif. Technol.*, 46 (2005) 110-117.
- [28] S. Majumdar, D. Bhaumik, K.K. Sirkar, Performance of commercial-size plasmapolymerized PDMS-coated hollow fiber modules in removing VOCs from N<sub>2</sub>/air, *J. Membr. Sci.*, 214 (2003) 323-330.
- [29] D. Bhaumik, S. Majumdar, K.K. Sirkar, Pilot-plant and laboratory studies on vapor permeation removal of VOCs from waste gas using silicone-coated hollow fibers, *J. Membr. Sci.*, 167 (2000) 107-122.
- [30] H.B. Park, Y.M. Lee, Separation of toluene/nitrogen through segmented polyurethane and polyurethane urea membranes with different soft segments, *J. Membr. Sci.*, 197 (2002) 283-296.
- [31] G.M. Dennis, G. O'Brien, Poly (ether block amide) resins: bridging the gap between thermoplastics and rubbers, in: 158th technical meeting, Cincinnati, OH, 2000.
- [32] M.E. Rezac, T. John, P.H. Pfromm, Effect of copolymer composition on the solubility and diffusivity of water and methanol in a series of polyether amide, *J. Appl. Polym. Sci.*, 65 (1998) 1983-1993.
- [33] J. Chen, X. Feng, A. Penlidis, Gas permeation through Poly(ether - b - amide) (PEBAX 2533) block copolymer membranes, *Sep. Sci. Technol.*, 39 (2005) 149-164.
- [34] L. Liu, A. Chakma, X. Feng, D. Lawless, Separation of VOCs from N<sub>2</sub> using poly(ether block amide) membranes, *Can. J. Chem. Eng.*, 87 (2009) 456-465.
- [35] Y. Liu, X. Feng, D. Lawless, Separation of gasoline vapor from nitrogen by hollow fiber composite membranes for VOC emission control, *J. Membr. Sci.*, 271 (2006) 114-124.
- [36] P.M. Budd, B.S. Ghanem, S. Makhseed, N.B. McKeown, K.J. Msayib, C.E. Tattershall, Polymers of intrinsic microporosity (PIMs): robust, solution-processable, organic nanoporous materials, *Chem. Commun.*, (2004) 230-231.
- [37] S.M. Meckler, J.E. Bachman, B.P. Robertson, C. Zhu, J.R. Long, B.A. Helms, Thermally rearranged polymer membranes containing tröger's base units have exceptional performance for air separations, *Angew. Chem. Int. Ed.*, 57 (2018) 4912-4916.
- [38] M.D. Guiver, Y.M. Lee, Polymer rigidity improves microporous membranes, *Science*, 339 (2013) 284-285.
- [39] X. Feng, S. Sourirajan, F.H. Tezel, T. Matsuura, B.A. Farnand, Separation of volatile organic compound/nitrogen mixtures by polymeric membranes, *Ind. Eng. Chem. Res.*, 32 (1993) 533-539.
- [40] S. Deng, A. Sourirajan, T. Matsuura, B. Farnand, Study of volatile hydrocarbon emission control by an aromatic poly(ether imide) membrane, *Ind. Eng. Chem. Res.*, 34 (1995) 4494-4500.
- [41] X. Feng, S. Sourirajan, H. Tezel, T. Matsuura, Separation of organic vapor from air by aromatic polyimide membranes, *J. Appl. Polym. Sci.*, 43 (1991) 1071-1079.
- [42] H. Zhou, F. Tao, Q. Liu, C. Zong, W. Yang, X. Cao, W. Jin, N. Xu, Microporous polyamide membranes for molecular sieving of nitrogen from volatile organic compounds, *Angew. Chem. Int. Ed.*, 56 (2017) 5755-5759.
- [43] C. Zhang, X. Gao, J. Qin, Q. Guo, H. Zhou, W. Jin, Microporous polyimide VOC-rejective membrane for the separation of nitrogen/VOC mixture, *J. Hazard. Mater.*, 402 (2021) 123817.
- [44] M. Matsumoto, Y. Inomoto, K. Kondo, Selective separation of aromatic hydrocarbons through supported liquid membranes based on ionic liquids, *J. Membr. Sci.*, 246 (2005) 77-81.
- [45] M. Teramoto, Y. Sakaida, S.S. Fu, N. Ohnishi, H. Matsuyama, T. Maki, T. Fukui, K. Arai, An attempt for the stabilization of supported liquid membrane, *Sep. Purif. Technol.*, 21 (2000) 137-144.
- [46] R.D. Noble, D.L. Gin, Perspective on ionic liquids and ionic liquid membranes, *J. Membr. Sci.*, 369 (2011) 1-4.
- [47] F. Zhang, W. Sun, J. Liu, W. Zhang, Z. Ren, Extraction separation of toluene/cyclohexane with hollow fiber supported ionic liquid membrane, *Korean J. Chem. Eng.*, 31 (2014) 1049-1056.

- [48] T.P. Thuy Pham, C.W. Cho, Y.S. Yun, Environmental fate and toxicity of ionic liquids: a review, *Water Res.*, 44 (2010) 352-372.
- [49] M.J.Salar-García, V.M.Ortiz-Martínez, F.J.Hernández-Fernández, A.P.d.l. Ríos, J.Quesada-Medina, Ionic liquid technology to recover volatile organic compounds (VOCs), *J. Hazard. Mater.*, 321 (2017) 484-499.
- [50] A. Noda, M. Watanabe, Highly conductive polymer electrolytes prepared by in situ polymerization of vinyl monomers in room temperature molten salts, *Electrochim. Acta*, 45 (2000) 1265-1270.
- [51] J. Wijmans, Membrane system for recovery of volatile organic compounds from remediation off-gases, in, *Membrane Technology and Research, Inc.(US)*, 2003.
- [52] Z. Rahme, R. Zytner, R. Corsi, M. Madani-Isfahani, Predicting oxygen uptake and VOC emissions at enclosed drop structures, *J. Environ. Eng.*, 123 (1997) 47-53.
- [53] P.R. Donald, Y. P.Yuri, Polymeric gas separation membranes, 1st ed., CRC Press, 1994.
- [54] I. Blume, J.G. Wijmans, R.W. Baker, The separation of dissolved organics from water by pervaporation, *J. Membr. Sci.*, 49 (1989) 253-286.
- [55] I. Pinnau, L.G. Toy, Transport of organic vapor through poly(1-trimethylsilyl-propyne), *J. Membr. Sci.*, 116 (1996) 199-209.
- [56] B. Ozturk, C. Kuru, H. Aykac, S. Kaya, VOC separation using immobilized liquid membranes impregnated with oils, *Sep. Purif. Technol.*, 153 (2015) 1-6.
- [57] B.D. Freeman, Basis of permeability/selectivity tradeoff relations in polymeric gas separation membranes, *Macromolecules*, 32 (1999) 375-380.
- [58] L.M. Robeson, Correlation of separation factor versus permeability for polymeric membranes, *J. Membr. Sci.*, 62 (1991) 165-185.
- [59] R.M. Palou, N.V. Likhanov, O.O. Xometl, Supported ionic liquid membranes for separations of gases and liquids: an overview, *Pet. Chem.*, 54 (2014) 595-607.
- [60] L. Cui, S. Gao, X. Song, L. Huang, H. Dong, J. Liu, F. Chen, S. Yu, Preparation and characterization of chitosan membranes, *RSC Adv.*, 8 (2018) 28433-28439.
- [61] M. Chakraborty, D. Dobaría, P.A. Parikh, The separation of aromatic hydrocarbons through a supported ionic liquid membrane, *Pet. Sci. Technol.*, 30 (2012) 2504-2516.
- [62] T. Uragami, E. Fukuyama, T. Miyata, Selective removal of dilute benzene from water by poly(methyl methacrylate)-graft-poly(dimethylsiloxane) membranes containing hydrophobic ionic liquid by pervaporation, *J. Membr. Sci.*, 510 (2016) 131-140.
- [63] A. Ito, G. Sui, N. Yamanouchi, VOC vapor permeation through a liquid membrane using triethylene glycols, *Desalination*, 234 (2008) 270-277.
- [64] I. Béchohra, A. Couvert, A. Amrane, Absorption and biodegradation of toluene: optimization of its initial concentration and the biodegradable non-aqueous phase liquid volume fraction, *Int. Biodeterior. Biodegrad.*, 104 (2015) 350-355.
- [65] J.H. Kim, S.H. Kim, C.H. Lee, J.W. Nah, A. Hahn, DEHP migration behavior from excessively plasticized PVC sheets, *Bull. Korean Chem. Soc.*, 24 (2003) 345-349.
- [66] T. Wu, N. Wang, J. Li, L. Wang, W. Zhang, G. Zhang, S. Ji, Tubular thermal crosslinked-PEBA/ceramic membrane for aromatic/aliphatic pervaporation, *J. Membr. Sci.*, 486 (2015) 1-9.
- [67] D.A. Admond, D.J.W. Grant, Hydrogen bonding in sulfonamides, *J. Pharm. Sci.*, 90 (2001) 2058-2077.
- [68] N.L. Le, Y. Wang, T.S. Chung, Pebax/POSS mixed matrix membranes for ethanol recovery from aqueous solutions via pervaporation, *J. Membr. Sci.*, 379 (2011) 174-183.
- [69] N. Kambia, A. Farce, K. Belarbi, B. Gressier, M. Luyckx, P. Chavatte, T. Dine, Docking study: PPARs interaction with the selected alternative plasticizers to di(2-ethylhexyl) phthalate, *J. Enzyme Inhib. Med. Chem.*, 31 (2016) 448-455.
- [70] ISO16000-6, Volatile organic compounds in air analysis, (1989).
- [71] S. Armstrong, B. Freeman, A. Hiltner, E. Baer, Gas permeability of melt-processed poly(ether block amide) copolymers and the effects of orientation, *Polymer*, 53 (2012) 1383-1392.

- [72] A. Ghadimi, T. Mohammadi, N. Kasiri, A novel chemical surface modification for the fabrication of PEBA/SiO<sub>2</sub> nanocomposite membranes to separate CO<sub>2</sub> from syngas and natural gas streams, *Ind. Eng. Chem. Res.*, 53 (2014) 17476-17486.
- [73] L. Dong, C. Zhang, Y. Bai, D. Shi, X. Li, H. Zhang, M. Chen, High-performance PEBA2533-functional MMT mixed matrix membrane containing high-speed facilitated transport channels for CO<sub>2</sub>/N<sub>2</sub> separation, *ACS Sustainable Chem. Eng.*, 4 (2016) 3486-3496.
- [74] A. Ghadimi, M. Amirilargani, T. Mohammadi, N. Kasiri, B. Sadatnia, Preparation of alloyed poly(ether block amide)/poly(ethylene glycol diacrylate) membranes for separation of CO<sub>2</sub>/H<sub>2</sub> (syngas application), *J. Membr. Sci.*, 458 (2014) 14-26.
- [75] M. Rajamanikyam, V. Vadlapudi, S.P. Parvathaneni, D. Koude, S. Prabhakar, S. Misra, R. Amanchy, S. Upadhyayula, *Brevibacterium mcbrellneri* that cause cytotoxicity and cell cycle arrest, *EXCLI J.*, 16 (2017) 375-387.
- [76] L. Dong, Y. Sun, C. Zhang, D. Han, Y. Bai, M. Chen, Efficient CO<sub>2</sub> capture by metallo-supramolecular polymers as fillers to fabricate a polymeric blend membrane, *RSC Adv.*, 5 (2015) 67658-67661.
- [77] A. Xenopoulos, B. Wunderlich, Thermodynamic properties of liquid and semicrystalline linear aliphatic polyamides, *J. Polym. Sci., Part B: Polym. Phys.*, 28 (1990) 2271-2290.
- [78] K. Aouachria, G. Quintard, V. Massardier-Nageotte, N. Belhaneche-Bensemra, The effect of di(-2-ethyl hexyl) phthalate (DEHP) as plasticizer on the thermal and mechanical properties of PVC/PMMA blends, *Polímeros*, 24 (2014) 428-433.
- [79] X. Zhang, T. Zhang, Y. Wang, J. Li, C. Liu, N. Li, J. Liao, Mixed-matrix membranes based on Zn/Ni-ZIF-8-PEBA for high performance CO<sub>2</sub> separation, *J. Membr. Sci.*, 560 (2018) 38-46.
- [80] J. Gu, X. Zhang, Y. Bai, L. Yang, C. Zhang, Y. Sun, ZSM-5 filled polyether block amide membranes for separating EA from aqueous solution by pervaporation, *J International Journal of Polymer Science*, 2013 (2013) 760156.
- [81] J.A. Brydson, *Plastics materials*, Elsevier, 1999.
- [82] J.H. Kim, S.Y. Ha, Y.M. Lee, Gas permeation of poly(amide-6-b-ethylene oxide) copolymer, *J. Membr. Sci.*, 190 (2001) 179-193.
- [83] G. Kung, L.Y. Jiang, Y. Wang, T.S. Chung, Asymmetric hollow fibers by polyimide and polybenzimidazole blends for toluene/iso-octane separation, *J. Membr. Sci.*, 360 (2010) 303-314.
- [84] S. Zereshki, A. Figoli, S.S. Madaeni, S. Simone, M. Esmailinezhad, E. Drioli, Pervaporation separation of MeOH/MTBE mixtures with modified PEEK membrane: effect of operating conditions, *J. Membr. Sci.*, 371 (2011) 1-9.
- [85] C.M. Hansen, *Hansen solubility parameters: a user's handbook*, CRC press, 2007.
- [86] J.C. Arnold, Environmental effects on crack growth in polymers, in: I. Milne, R.O. Ritchie, B. Karihaloo (Eds.) *Comprehensive structural integrity*, Pergamon, Oxford, 2003, pp. 281-319.
- [87] L. Wang, J. Li, Y. Lin, C. Chen, Separation of dimethyl carbonate/methanol mixtures by pervaporation with poly(acrylic acid)/poly(vinyl alcohol) blend membranes, *J. Membr. Sci.*, 305 (2007) 238-246.
- [88] G. Clarizia, P. Bernardo, G. Gorrasi, D. Zampino, S.C. Carroccio, Influence of the preparation method and photo-oxidation treatment on the thermal and gas transport properties of dense films based on a poly(ether-block-amide) copolymer, *Materials (Basel)*, 11 (2018) 1326.
- [89] K. Liu, C.J. Fang, Z.Q. Li, M. Young, Separation of thiophene/n-heptane mixtures using PEBAX/PVDF-composited membranes via pervaporation, *J. Membr. Sci.*, 451 (2014) 24-31.
- [90] L. Lin, Y. Kong, G. Wang, H. Qu, J. Yang, D. Shi, Selection and crosslinking modification of membrane material for FCC gasoline desulfurization, *J. Membr. Sci.*, 285 (2006) 144-151.
- [91] H.R. Mortaheb, F. Ghaemmaghami, B. Mokhtarani, A review on removal of sulfur components from gasoline by pervaporation, *Chem. Eng. Res. Des.*, 90 (2012) 409-432.
- [92] A. Singh, B.D. Freeman, I. Pinnau, Pure and mixed gas acetone/nitrogen permeation properties of polydimethylsiloxane [PDMS], *J. Polym. Sci., Part B: Polym. Phys.*, 36 (1998) 289-301.

- [93] W. Yang, H. Zhou, C. Zong, Y. Li, W. Jin, Study on membrane performance in vapor permeation of VOC/N<sub>2</sub> mixtures via modified constant volume/variable pressure method, *Sep. Purif. Technol.*, 200 (2018) 273-283.
- [94] C.K. Yeom, S.H. Lee, J.M. Lee, H.Y. Song, Modeling and evaluation of boundary layer resistance at feed in the permeation of VOC/N<sub>2</sub> mixtures through PDMS membrane, *J. Membr. Sci.*, 204 (2002) 303-322.
- [95] F. Şahin, B. Topuz, H. Kalıpçılar, ZIF filled PDMS mixed matrix membranes for separation of solvent vapors from nitrogen, *J. Membr. Sci.*, 598 (2020) 117792.
- [96] Y. Cen, C. Staudt-Bickel, R.N. Lichtenthaler, Sorption properties of organic solvents in PEBA membranes, *J. Membr. Sci.*, 206 (2002) 341-349.
- [97] S. Ebnesajjad, Chemical properties of fluoropolymers, in: *Fluoroplastics (second edition)*, William Andrew Publishing, Oxford, 2015, pp. 432-474.
- [98] Volatile organic compounds emissions, in: *Report on the Environment*, US Environmental Protection Agency, 2014.
- [99] K. Zeng, Z. Wang, D. Wang, C. Wang, J. Yu, G. Wu, Q. Zhang, X. Li, C. Zhang, X.S. Zhao, Three-dimensionally ordered macroporous MnSmOx composite oxides for propane combustion: modification effect of Sm dopant, *Catal. Today*, 376 (2020) 211-221.
- [100] C. Della Pina, M.A. De Gregorio, L. Clerici, P. Dellavedova, E. Falletta, Polyaniline (PANI): an innovative support for sampling and removal of VOCs in air matrices, *J. Hazard. Mater.*, 344 (2018) 308-315.
- [101] C. Zhang, H. Cao, C. Wang, M. He, W. Zhan, Y. Guo, Catalytic mechanism and pathways of 1, 2-dichloropropane oxidation over LaMnO<sub>3</sub> perovskite: An experimental and DFT study, *J. Hazard. Mater.*, 402 (2021) 123473.
- [102] C. Yang, H. Qian, X. Li, Y. Cheng, H. He, G. Zeng, J. Xi, Simultaneous removal of multicomponent VOCs in biofilters, *Trends Biotechnol.*, 36 (2018) 673-685.
- [103] A. Bos, I.G.M. Pünt, M. Wessling, H. Strathmann, Plasticization-resistant glassy polyimide membranes for CO<sub>2</sub>/CO separations, *Sep. Purif. Technol.*, 14 (1998) 27-39.
- [104] S. Kanehashi, T. Nakagawa, K. Nagai, X. Duthie, S. Kentish, G. Stevens, Effects of carbon dioxide-induced plasticization on the gas transport properties of glassy polyimide membranes, *J. Membr. Sci.*, 298 (2007) 147-155.
- [105] J.D. Wind, D.R. Paul, W.J. Koros, Natural gas permeation in polyimide membranes, *J. Membr. Sci.*, 228 (2004) 227-236.
- [106] R. Swaidan, B. Ghanem, M. Al-Saeedi, E. Litwiller, I. Pinnau, Role of intrachain rigidity in the plasticization of intrinsically microporous triptycene-based polyimide membranes in mixed-gas CO<sub>2</sub>/CH<sub>4</sub> separations, *Macromolecules*, 47 (2014) 7453-7462.
- [107] R. Swaidan, B. Ghanem, I. Pinnau, Fine-tuned intrinsically ultramicroporous polymers redefine the permeability/selectivity upper bounds of membrane-based air and hydrogen separations, *ACS Macro Lett.*, 4 (2015) 947-951.
- [108] B.S. Ghanem, R. Swaidan, E. Litwiller, I. Pinnau, Ultra-microporous triptycene-based polyimide membranes for high-performance gas separation, *Adv. Mater.*, 26 (2014) 3688-3692.
- [109] B. Belaisaoui, Y. Le Moullec, E. Favre, Energy efficiency of a hybrid membrane/condensation process for VOC (volatile organic compounds) recovery from air: a generic approach, *Energy*, 95 (2016) 291-302.
- [110] R.W. Baker, B.T. Low, Gas separation membrane materials: a perspective, *Macromolecules*, 47 (2014) 6999-7013.
- [111] D. Lin, Z. Ding, L. Liu, R. Ma, Experimental study of vapor permeation of C<sub>5</sub>C<sub>7</sub> alkane through PDMS membrane, *Chem. Eng. Res. Des.*, 90 (2012) 2023-2033.
- [112] V.V. Zhmakin, V.V. Teplyakov, The evaluation of the C<sub>1</sub>-C<sub>4</sub> hydrocarbon permeability parameters in the thin film composite membranes, *Sep. Purif. Technol.*, 186 (2017) 145-155.
- [113] W.I. Sohn, D.H. Ryu, S.J. Oh, J.K. Koo, A study on the development of composite membranes for the separation of organic vapors, *J. Membr. Sci.*, 175 (2000) 163-170.

- [114] S.H. Choi, J.H. Kim, S.B. Lee, Sorption and permeation behaviors of a series of olefins and nitrogen through PDMS membranes, *J. Membr. Sci.*, 299 (2007) 54-62.
- [115] S.J. Lue, W.W. Chen, S.Y. Wu, L.D. Wang, C.H. Kuo, Vapor permeation modeling of multi-component systems using a poly(dimethylsiloxane) membrane, *J. Membr. Sci.*, 311 (2008) 380-389.
- [116] G. Obuskovic, S. Majumdar, K.K. Sirkar, Highly VOC-selective hollow fiber membranes for separation by vapor permeation, *J. Membr. Sci.*, 217 (2003) 99-116.
- [117] I. Pinnau, Z. He, Pure- and mixed-gas permeation properties of polydimethylsiloxane for hydrocarbon/methane and hydrocarbon/hydrogen separation, *J. Membr. Sci.*, 244 (2004) 227-233.
- [118] Y. Shi, C.M. Burns, X. Feng, Poly(dimethyl siloxane) thin film composite membranes for propylene separation from nitrogen, *J. Membr. Sci.*, 282 (2006) 115-123.
- [119] M. Shokrian, M. Sadrzadeh, T. Mohammadi, C<sub>3</sub>H<sub>8</sub> separation from CH<sub>4</sub> and H<sub>2</sub> using a synthesized PDMS membrane: experimental and neural network modeling, *J. Membr. Sci.*, 346 (2010) 59-70.
- [120] H. Asghar, A. Ilyas, Z. Tahir, X. Li, A.L. Khan, Fluorinated and sulfonated poly (ether ether ketone) and matrimid blend membranes for CO<sub>2</sub> separation, *Sep. Purif. Technol.*, 203 (2018) 233-241.
- [121] M.S. Suleman, K.K. Lau, Y.F. Yeong, Plasticization and Swelling in Polymeric Membranes in CO<sub>2</sub> Removal from Natural Gas, *Chem. Eng. Technol.*, 39 (2016) 1604-1616.
- [122] L. Liu, A. Chakma, X. Feng, A novel method of preparing ultrathin poly(ether block amide) membranes, *J. Membr. Sci.*, 235 (2004) 43-52.
- [123] L. Liu, A. Chakma, X. Feng, CO<sub>2</sub>/N<sub>2</sub> separation by poly(ether block amide) thin film hollow fiber composite membranes, *Ind. Eng. Chem. Res.*, 44 (2005) 6874-6882.
- [124] F. Heymes, P. Manno-Demoustier, F. Charbit, J.L. Fanlo, P. Moulin, A new efficient absorption liquid to treat exhaust air loaded with toluene, *Chem. Eng. J.*, 115 (2006) 225-231.
- [125] C.M. Hansen, Polymer additives and solubility parameters, *Prog. Org. Coat.*, 51 (2004) 109-112.
- [126] X. Han, D. Liu, Di(2-ethylhexyl) adipate (DEHA) detection in antarctic krill (*euphasia superba* dana), *Polar Res.*, 37 (2018) 1457395.
- [127] L. Martínez-Izquierdo, M. Malankowska, J. Sánchez-Laínez, C. Téllez, J. Coronas, Poly(ether-block-amide) copolymer membrane for CO<sub>2</sub>/N<sub>2</sub> separation: the influence of the casting solution concentration on its morphology, thermal properties and gas separation performance, *R. Soc. Open Sci.*, 6 190866.
- [128] R.J. Young, P.A. Lovell, Introduction to polymers, CRC press, 2011.
- [129] C.M. Hansen, The three dimensional solubility parameter and solvent diffusion coefficient, Danish technical press, 1967.
- [130] D.R. Paul, Gas transport in homogeneous multicomponent polymers, *J. Membr. Sci.*, 18 (1984) 75-86.
- [131] L.M. Robeson, Polymer blends in membrane transport processes, *Ind. Eng. Chem. Res.*, 49 (2010) 11859-11865.
- [132] Y.M. Sun, C.H. Wu, A. Lin, Permeation and sorption properties of benzene, cyclohexane, and n-hexane vapors in poly [bis (2, 2, 2-trifluoroethoxy) phosphazene](PTFEP) membranes, *Polymer*, 47 (2006) 602-610.
- [133] R. Hadjoudj, H. Monnier, C. Roizard, F. Lapique, Absorption of chlorinated VOCs in high-boiling solvents: determination of henry's law constants and infinite dilution activity coefficients, *Ind. Eng. Chem. Res.*, 43 (2004) 2238-2246.
- [134] X. Feng, R.Y.M. Huang, Liquid separation by pervaporation: a review, *Ind. Eng. Chem. Res.*, 36 (1997) 1048-1066.
- [135] L. Li, A. Chakam, X. Feng, Propylene separation from nitrogen by poly(ether block amide) composite membrane, *J. Membr. Sci.*, 279 (2006) 645-654.
- [136] C.K. Yeom, S.H. Lee, H.Y. Song, J.M. Lee, Vapor permeations of a series of VOCs/N<sub>2</sub> mixtures through PDMS membrane, *J. Membr. Sci.*, 198 (2002) 129-143.

- [137] M.M. Qiu, S.T. Hwang, Continuous vapor-gas separation with a porous membrane permeation system, *J. Membr. Sci.*, 59 (1991) 53-72.
- [138] X. Su, B. Shi, L. Wang, Investigation on three-dimensional solubility parameters for explanation and prediction of swelling degree of polydimethylsiloxane pervaporation membranes, *J. Macromol. Sci. Part B-Phys.*, 54 (2015) 1248-1258.
- [139] J. Schwöbel, R.U. Ebert, R. Kühne, G. Schüürmann, Modeling the H bond donor strength of -OH, -NH, and -CH sites by local molecular parameters, *J. Comput. Chem.*, 30 (2009) 1454-1464.
- [140] G.Q. Lai, S.M. Xing, Synthesis technology and application of silicon product, Second ed., Chemical industry publishing, Beijing, 2013.
- [141] M. Xia, T. Yang, S. Chen, G. Yuan, Fabrication of superhydrophobic eucalyptus wood surface with self-cleaning performance in air and oil environment and high durability, *Colloid Interface Sci. Commun.*, 36 (2020) 100264.
- [142] L. Coltro, J.B. Pitta, E. Madaleno, Performance evaluation of new plasticizers for stretch PVC films, *Polym. Test.*, 32 (2013) 272-278.
- [143] I.I. Kabir, Y. Fu, N. De Souza, J.C. Baena, A.C.Y. Yuen, W. Yang, J. Mata, Z. Peng, G.H. Yeoh, PDMS/MWCNT nanocomposite films for underwater sound absorption applications, *J. Mater. Sci.*, 55 (2020) 5048-5063.
- [144] H.X. Rao, F.N. Liu, Z.Y. Zhang, Preparation and oxygen/nitrogen permeability of PDMS crosslinked membrane and PDMS/tetraethoxysilicone hybrid membrane, *J. Membr. Sci.*, 303 (2007) 132-139.
- [145] D. Zhou, Y. Zhong, J. Yang, J. Qi, Y. Zhuo, Y. Sha, Preparation and application of PDMS/PES composite membrane in separating light hydrocarbon components from drilling mud, *J. Membr. Sci.*, 566 (2018) 231-238.
- [146] T.C. Merkel, V.I. Bondar, K. Nagai, B.D. Freeman, I. Pinnau, Gas sorption, diffusion, and permeation in poly(dimethylsiloxane), *J. Polym. Sci., Part B: Polym. Phys.*, 38 (2000) 415-434.
- [147] C.Z. Liang, W.F. Yong, T.-S. Chung, High-performance composite hollow fiber membrane for flue gas and air separations, *J. Membr. Sci.*, 541 (2017) 367-377.
- [148] L.M. Robeson, A. Noshay, M. Matzner, C.N. Merriam, Physical property characteristics of polysulfone/poly-(dimethylsiloxane) block copolymers, *Angew. Makromol. Chem.*, 29 (1973) 47-62.
- [149] D.R. Lide, *CRC Hand Book of Chemistry and Physics*, 83rd ed., CRC Press, 2002-2003.
- [150] C.K. Yeom, S.H. Lee, H.Y. Song, J.M. Lee, A characterization of concentration polarization in a boundary layer in the permeation of VOCs/N<sub>2</sub> mixtures through PDMS membrane, *J. Membr. Sci.*, 205 (2002) 155-174.
- [151] M.E. Rezac, T. John, P.H. Pfromm, Effect of copolymer composition on the solubility and diffusivity of water and methanol in a series of polyether amides, *J. Appl. Polym. Sci.*, 65 (1997) 1983-1993.
- [152] L. De Lorenzi, M. Fermeglia, G. Torriano, Density, kinematic viscosity, and refractive index for bis (2-ethylhexyl) adipate, tris (2-ethylhexyl) trimellitate, and diisononyl phthalate, *J. Chem. Eng. Data*, 43 (1998) 183-186.
- [153] S.A. Stern, V.M. Shah, B.J. Hardy, Structure-permeability relationships in silicone polymers, *J. Polym. Sci., Part B: Polym. Phys.*, 25 (1987) 1263-1298.
- [154] G.M. Shi, T.S. Chung, Teflon AF2400/polyethylene membranes for organic solvent nanofiltration (OSN), *J. Membr. Sci.*, 602 (2020) 117972.
- [155] G.S. Park, J. Crank, *Diffusion in polymers*, Academic Press, 1968.
- [156] J.M.S. Henis, M.K. Tripodi, The developing technology of gas separating membranes, *Science*, 220 (1983) 11-17.

## Appendix A Sample calculation

### A.1 Sample calculations for pure gas permeation

#### Pure gas permeability

Membrane: 25PEBA/75DEHA

Membrane area (A): 20.4 cm<sup>2</sup>

Membrane thickness (L): 0.021cm

Temperature (T): 295.15 K

Ambient pressure ( $p_0$ ): 76.3 cm Hg

Feed gas pressure ( $p_{feed}$ ): 376.3 cm Hg

Permeate pressure ( $p_{perm}$ ): 76.3 cm Hg

Permeate flow rate of N<sub>2</sub> (J): 0.0016 cm<sup>3</sup>/s

$$J = V/t$$

$$= 0.1 \text{ cm}^3 / 63.6 \text{ s}$$

$$= 0.0016 \text{ cm}^3/\text{s}$$

The permeability of N<sub>2</sub>:

$$\begin{aligned} P_{N_2} &= \frac{J \times L}{\Delta P \times A} = \frac{J \times L}{(p_{feed} - p_{perm}) \times A} \times \frac{273.15 \text{ K}}{295.15 \text{ K}} \times \frac{76.3 \text{ cm Hg}}{76.3 \text{ cm Hg}} \\ &= \frac{0.0016 \text{ cm}^3/\text{s} \times 0.021 \text{ cm}}{(376.3 \text{ cm Hg} - 76.3 \text{ cm Hg}) \times 20.4 \text{ cm}^2} \times \frac{273.15 \text{ K}}{295.15 \text{ K}} \times \frac{76.3 \text{ cm Hg}}{76.3 \text{ cm Hg}} \\ &= 50.8 \times 10^{-10} \frac{\text{cm}^3 (\text{STP}) \text{ cm}}{\text{cm}^2 \text{ s cm Hg}} \\ &= 50.8 \text{ Barrer} \end{aligned}$$

The permeability of CO<sub>2</sub> and other gases could also be calculated in the same way.

$$P_{CO_2} = 1268 \text{ Barrer}$$



### Ideal gas selectivity

The ideal gas selectivity of CO<sub>2</sub>/ N<sub>2</sub> is the ratio of the permeability between the CO<sub>2</sub> and N<sub>2</sub>:

$$\begin{aligned}\alpha_{CO_2/N_2} &= \frac{P_{CO_2}}{P_{N_2}} \\ &= \frac{1268 \text{ Barrer}}{50.8 \text{ Barrer}} \\ &= 26.9\end{aligned}$$

## A.2 Sample calculations for mixed gas permeation

### VOC permeability

Gas mixture: methanol/N<sub>2</sub>

Membrane: 25PEBA/75DEHA

Membrane area (A): 20.4 cm<sup>2</sup>

Membrane thickness (L): 0.021cm

Operation temperature (T): 295.15 K

Ambient pressure (p<sub>0</sub>): 76.3 cm Hg

Feed mixture pressure (p<sub>feed</sub>): 76.3 cm Hg

Permeate mixture pressure (p<sub>perm</sub>): 0.14 cm Hg

Methanol concentration in the feed (X): 14.16 mol%

Methanol molecular weight: 32 g/mole

Nitrogen molecular weight: 14 g/mole

Methanol permeate flux in the permeate (Q<sub>methanol</sub>): 6.27 × 10<sup>-6</sup> g/ cm<sup>2</sup> s

$$\begin{aligned}Q_{methanol} &= \frac{W_{voc}}{tS} \\ &= \frac{0.187 \text{ g}}{1461 \text{ s} \times 20.4 \text{ cm}^2} \\ &= 6.27 \times 10^{-6} \text{ g/ cm}^2 \text{ s}\end{aligned}$$

$$P_{methanol} = \frac{Q_{voc}L}{M_{VOC} (P_F X - P_P Y)} \quad (3.2)$$

$$Y = \frac{Q_{VOC} M_{N_2}}{Q_{VOC} M_{N_2} + Q_{N_2} M_{VOC}} \quad (3.3)$$

$$P_{N_2} = \frac{Q_{N_2} L}{M_{N_2} [P_F(1-X) - P_P(1-Y)]} \quad (3.4)$$

$N_2$  Permeability measured followed by the membrane exposed to methanol is 49.4 Barrer.

There are three unknown parameters in Equations from (3.2) to (3.4). They are methanol permeability ( $P_{methanol}$ ), methanol concentration in the permeate (Y) and nitrogen permeate flux ( $Q_{N_2}$ ). The results by solving the equations above are listed below.

Methanol permeability ( $P_{methanol}$ ): 87339 Barrer

Methanol concentration in the permeate (Y): 99.58 mole%

Nitrogen flux in the permeate ( $Q_{N_2}$ ):  $1.15 \times 10^{-8}$  g/cm<sup>2</sup> s

### VOC/ $N_2$ selectivity

The selectivity of methanol/  $N_2$  is the ratio of the permeability between the methanol and  $N_2$ :

$$\begin{aligned} \alpha_{methanol/N_2} &= \frac{P_{methanol}}{P_{N_2}} \\ &= \frac{87339 \text{ Barrer}}{49.4 \text{ Barrer}} \\ &= 1768 \end{aligned}$$

### A.3 Sample calculations for experimental errors

Membrane: 25PEBA/75DEHA

Operation temperature (T): 295.15 K

Feed mixture pressure ( $p_{feed}$ ): 76.3 cm Hg

Permeate mixture pressure ( $p_{perm}$ ): 0.14 cm Hg

Methanol concentration in the feed (X): 14.16 mol%

The permeability of methanol was tested at the same condition three times, which are 87339, 80780 and 82137 Barrer, respectively.

The average value of methanol permeability:

$$P_{methanol} = \frac{87339 + 80780 + 82137}{3} = 83419 \text{ Barrer}$$

The standard deviation (SD) is:

$$SD_{methanol} = \frac{(87339-83419)^2+(80780-83419)^2+(82137-83419)^2}{3-1} = 2827 \text{ Barrer}$$

The relative standard deviation (RSD) is:

$$RSD_{methanol} = \frac{2827}{83419} \times 100\% = 3.39\%$$

The RSD in methanol permeability for 25PEBA/75DEHA is 3.39%, which is an acceptable error. The errors for other data reported in this work could also be calculated in this method.